USAID | PAKISTAN
FROM THE AMERICAN PEOPLE

Kurram Tangi Dam Construction

Supplemental Report on Seismic Hazard
Final Report

December 2013
This publication was produced for review by the
United States Agency for International Development.
It was prepared by MWH under contract number AID-391-C-13-00002

This Page Left Blank Intentionally

Map to Kurram Tangi Dam Project Documents

Shown below is the suite of documents submitted to USAID under Contract AID-391-C-13-00002 for the KTDP. This report is shaded in red in order to show its relationship to the full set of documentation.

ENVIRONMENTAL ASSESSMENT	
	VOLUME I: MAIN REPORT
	VOLUME II: PROJECT ECONOMIC BENEFITS
	VOLUME III: MAPS
ENVIRONMENTAL MITIGATION AND MONITORING PLAN	
	MAIN REPORT
	ANNEX I: HEALTH AND SAFETY PLAN FRAMEWORK
	ANNEX II: WATERSHED MANAGEMENT PLAN
	ANNEX III: WASTE MANAGEMENT PLAN
	ANNEX IV: FISHERIES MANAGEMENT PLAN
	ANNEX V: EMERGENCY PREPAREDNESS PLAN
	ANNEX VI: INSTRUMENTATION AND MONITORING PLAN
LAND ACQUISITION AND RESETTLEMENT	
	RESETTLEMENT POLICY FRAMEWORK
	RESETTLEMENT ACTION PLAN (COMPONENT I)
CULTURAL HERITAGE PRESERVATION PLAN	
VULNERABLE TRIBES PLAN	
GENDER PLAN	
KEY SUPPORTING TECHNICAL REPORTS	
	SUPPLEMENTAL REPORT ON GEOLOGY
	SUPPLEMENTAL REPORT ON GEOTECHNICAL ASPECTS
	SUPPLEMENTAL REPORT ON SEISMIC HAZARD
	SUPPLEMENTAL REPORT ON HYDROLOGY
	SUPPLEMENTAL REPORT ON CLIMATE CHANGE

All documents may be read as stand-alone documents, but the reader should be aware of the full set of documents available. Any one document may reference other documents in the suite in order to avoid duplication.

This Page Left Blank Intentionally

Kurram Tangi Dam Construction
Supplemental Report on Seismic Hazard

USAID Environmental Assessment of Kurram Tangi Dam Construction
Contract Number: AID-391-C-13-00002
From MWH Americas, Inc.
To USAID/Pakistan Energy Office
December 2013
Author: MWH Americas, Inc.

The author's views expressed in this publication do not necessarily reflect the views of the United States Agency for International Development or the United States Government.

This Page Left Blank Intentionally

List of Acronyms

Acronym	Term
AOI	Area of Influence
DSHA	Deterministic Seismic Hazard Analysis
GMPE	Ground Motion Prediction Equation
HAZ	(Computer code)
ICOLD	International Commission on Large Dams
ISC	International Seismological Centre
KTDP	Kurram Tangi Dam Project
MBT	Main Boundary Thrust
MCE	Maximum Credible Earthquake
MDE	Maximum Design Event
MKT	Main Karakoram Thrust
MMT	Main Mantle Thrust
MWH	MWH Global, Inc. or MWH, Inc.
NESPAK	National Engineering Services Pakistan
NGA	Next Generation of Ground-Motion Attenuation Models
NNE-WSW	North northeast- West southwest
NORSAR	Norwegian Seismic Array
OBE	Operating Basis Earthquake
PC	Planning Commission
PEER	Pacific Earthquake Engineering Research Center
PGA	Peak Ground Acceleration
PSHA	Probabilistic Seismic Hazard Analysis
RTS	Reservoir Triggered Seismicity
SEE	Safety Evaluation Earthquake
SHAKE	(A computer software for earthquake response analysis)
SRT	Salt Range Thrust
USCOLD	United States Commission on Large Dams
USGS	United States Geological Survey
WAPDA	Water and Power Development Authority

This Page Left Blank Intentionally

Seismic Hazard
Table of Contents

EXECUTIVE SUMMARY **1**
1 INTRODUCTION **1-1**
2 DATA SOURCES **2-1**
3 EVALUATION OF QUALITY AND RECENCY OF DATA **3-1**
4 BRIEF SUMMARY OF THE SUBJECT MATTER FINDINGS/SITUATION **4-1**
5 BACKGROUND AND PURPOSE **5-1**
6 SEISMOTECTONIC SETTING AND HISTORICAL EARTHQUAKES **6-1**
6.1 Regional Tectonics and Stratigraphy 6-1
6.2 Significant Historic Earthquakes 6-1
6.3 Catalog 6-2
6.4 Review of Prior Studies 6-4
6.5 Purpose of Analyses 6-4
7 SEISMIC SOURCE CHARACTERIZATION **7-1**
7.1 Crustal Fault Sources 7-1
7.1.1 Kurram Thrust 7-1
7.1.2 Karak Thrust 7-1
7.1.3 Murree Fault (MBT) 7-1
7.1.4 Kalabagh Fault 7-2
7.1.5 Bhittani Thrust 7-2
7.1.6 Khisor Thrust 7-2
7.1.7 Surghar Range Thrust 7-2
7.1.8 Panjal Thrust 7-3
7.1.9 Chaman Fault 7-3
7.2 Areal Sources 7-3
7.2.1 Zone 1 7-3
7.2.2 Zone 2 7-4
7.2.3 Zone 3 7-4
7.2.4 Zone 4 7-4
7.2.5 Zone 6 7-4
7.2.6 Zone 8 7-4
7.2.7 Zone 11 7-4
7.2.8 Zone 12 NEW 7-4
7.3 Gridded Seismicity 7-4
8 PROBABILISTIC SEISMIC HAZARD ANALYSIS (PSHA) **8-1**
8.1 PSHA Code and Methodology 8-1
8.2 PSHA Source Characterization 8-1
8.2.1 Fault Sources 8-1
8.2.2 Areal Sources 8-2

8.2.3 Deep Continental Source Zones 8-4
8.3 PSHA Ground Motion Prediction Equations 8-4
8.3.1 Crustal Seismicity 8-4
8.3.2 Deep Events 8-4
8.4 Other PSHA Parameters 8-5
8.5 PSHA Results 8-5
8.5.1 Kurram Tangi Main Dam 8-5
8.5.1.1 Kurram Tangi Dam Site - Deaggregation 8-6
8.5.2 Kaitu Weir 8-7
8.5.2.1 Kaitu Weir - Deaggregation 8-7
8.5.3 Weir II 8-7
8.5.3.1 Weir II - Deaggregation 8-8
8.5.4 Weir III 8-8
8.5.4.1 Weir III - Deaggregation 8-9
8.6 Comparison to other Studies 8-9
9 DETERMINISTIC SEISMIC HAZARD ANALYSIS (DSHA) 9-1
9.1 DSHA Methodology 9-1
9.2 DSHA Inputs 9-1
9.3 DSHA Results 9-2
10 RESERVOIR TRIGGERED SEISMICITY (RTS) 10-1
10.1 Characteristics of Reservoir-Triggered Seismicity 10-1
10.2 RTS Empirical Calculations 10-2
10.2.1 Single Attribute Analysis 10-3
10.2.2 Multi-Attribute Analysis 10-3
10.2.3 Conclusions on Reservoir-Triggered Seismicity 10-3
11 CONCLUSIONS AND RECOMMENDATIONS FOR DESIGN BASIS EARTHQUAKE 11-1
11.1 Discussion on Recommended Design Criteria 11-1
11.1.1 Safety Evaluation Earthquake 11-1
11.1.2 Operating Basis Earthquake 11-1
11.1.3 475 Year Return Event or Local Building Code 11-2
11.2 Evaluation of Design Criteria 11-2
12 LIMITATIONS AND RECOMMENDATIONS FOR ADDITIONAL STUDIES 12-1
13 REFERENCES 13-1

List of Tables

Table ES-1: List of Project Features and Recommended Design Criteria.....ES-1
Table 2-1:Data Sources 2-1
Table 2-2: Data Sources Identified but not yet Available..... 2-1
Table 2-3:Contacts who aided in Gathering of Project Data..... 2-2
Table 6-1:Catalog of events greater than M_w 6.0..... 6-3
Table 8-1: Fault Parameters 8-2
Table 8-2:Catalog Completeness Values..... 8-2
Table 8-3:Areal Sources used in the PSHA 8-3
Table 8-4: Ground Motion Prediction Equations used in the PSHA for Crustal Faults 8-4
Table 8-5: Ground Motion Prediction Equations used in the PSHA for Deep Continental Earthquakes 8-5
Table 8-6: Mean Probabilistic Ground Motion (g, freefield) for Kurram Tangi Dam Site..... 8-6
Table 8-7: Deaggregation Results for Dam Site 8-6
Table 8-8: Mean Probabilistic Ground Motion (g, free field) for Kaitu Weir..... 8-7
Table 8-9: Mean Probabilistic Ground Motion (g, freefield) for Weir II 8-7
Table 8-10: Mean Probabilistic Ground Motion (g, freefield) for Weir III..... 8-8
Table 8-11: Deaggregation Results for Weir III 8-9
Table 9-1: Faults considered in Deterministic Seismic Hazard Analysis 9-1
Table 9-2: PGA for Deterministic Assessment 9-2
Table 10-1: Definitions for Reservoir Attribute States..... 10-2
Table 10-2: Single Attribute Analysis – Conditional Probability of RTS Given Only One Attribute 10-3
Table 11-1: List of Project Features and Recommended Design Criteria 11-2

LIST OF PLATES

Plate 1: Project Features
Plate 2: Plate Tectonic Setting of the Project Region
Plate 3: Tectonic Map of the Western Himalaya
Plate 4: Structural Map of Bannu Basin, Kohat and Potwar Plateaus

LIST OF FIGURES

Figure 1: Active Faults within 50 km of the Project Site
Figure 2: Areal Source Zones
Figure 3: Catalog Completeness - Stepp Plot
Figure 4: Gutenberg-Richter Relationship – Zones 1-4, 6, 8, 11 and 12NEW
Figure 5: Gutenberg-Richter Relationship – Zones 1
Figure 6: Gutenberg-Richter Relationship – Zones 2
Figure 7: Gutenberg-Richter Relationship – Zones 3
Figure 8: Gutenberg-Richter Relationship – Zones 4
Figure 9: Gutenberg-Richter Relationship – Zones 6
Figure 10: Gutenberg-Richter Relationship – Zones 8
Figure 11: Gutenberg-Richter Relationship – Zones 11
Figure 12: Gutenberg-Richter Relationship – Zones 12NEW
Figure 13: Comparison of Different Ground Motion Prediction Equations with the Pakistan Model (Magnitude 6.4)
Figure 14: Main Dam - Seismic Source Contributions to Median Peak Horizontal Acceleration Hazard
Figure 15: Main Dam - Seismic Source Contributions to Median 0.2 Sec Spectral Acceleration Hazard
Figure 16: Main Dam - Seismic Source Contributions to Median 1.0 Sec Spectral Acceleration Hazard
Figure 17: Kaitu Weir - Seismic Source Contributions to Median Peak Horizontal Acceleration Hazard

Figure 18: Kaitu Weir - Seismic Source Contributions to Median 0.2 Sec Spectral Acceleration Hazard
Figure 19: Kaitu Weir - Seismic Source Contributions to Median 1.0 Sec Spectral Acceleration Hazard
Figure 20: Weir II - Seismic Source Contributions to Median Peak Horizontal Acceleration Hazard
Figure 21: Weir II - Seismic Source Contributions to Median 0.2 Sec Spectral Acceleration Hazard
Figure 22: Weir II - Seismic Source Contributions to Median 1.0 Sec Spectral Acceleration Hazard
Figure 23: Weir III - Seismic Source Contributions to Median Peak Horizontal Acceleration Hazard
Figure 24: Weir III - Seismic Source Contributions to Median 0.2 Sec Spectral Acceleration Hazard
Figure 25: Weir III - Seismic Source Contributions to Median 1.0 Sec Spectral Acceleration Hazard
Figure 26: Main Dam – Uniform Hazard Spectra
Figure 27: Kaitu Weir – Uniform Hazard Spectra
Figure 28: Weir II – Uniform Hazard Spectra
Figure 29: Weir III – Uniform Hazard Spectra
Figure 30: Deaggregation 145-yr Return Period Peak Horizontal Acceleration
Figure 31: Deaggregation 145-yr Return Period 0.2 Sec Horizontal Acceleration
Figure 32: Deaggregation 145-yr Return Period 1.0 Sec Horizontal Acceleration
Figure 33: Deaggregation 475-yr Return Period Peak Horizontal Acceleration
Figure 34: Deaggregation 475-yr Return Period 0.2 Sec Horizontal Acceleration
Figure 35: Deaggregation 475-yr Return Period 1.0 Sec Horizontal Acceleration
Figure 36: Deaggregation 10,000-yr Return Period Peak Horizontal Acceleration
Figure 37: Deaggregation 10,000-yr Return Period 0.2 Sec Horizontal Acceleration
Figure 38: Deaggregation 10,000-yr Return Period 1.0 Sec Horizontal Acceleration
Figure 39: Deaggregation 145-yr Return Period Peak Horizontal Acceleration
Figure 40: Deaggregation 145-yr Return Period 0.2 Sec Horizontal Acceleration
Figure 41: Deaggregation 145-yr Return Period 1.0 Sec Horizontal Acceleration
Figure 42: Deaggregation 475-yr Return Period Peak Horizontal Acceleration
Figure 43: Deaggregation 475-yr Return Period 0.2 Sec Horizontal Acceleration
Figure 44: Deaggregation 475-yr Return Period 1.0 Sec Horizontal Acceleration
Figure 45: Deaggregation 10,000-yr Return Period Peak Horizontal Acceleration
Figure 46: Deaggregation 10,000-yr Return Period 0.2 Sec Horizontal Acceleration
Figure 47: Deaggregation 10,000-yr Return Period 1.0 Sec Horizontal Acceleration
Figure 48: Deaggregation 145-yr Return Period Peak Horizontal Acceleration
Figure 49: Deaggregation 145-yr Return Period 0.2 Sec Horizontal Acceleration
Figure 50: Deaggregation 145-yr Return Period 1.0 Sec Horizontal Acceleration
Figure 51: Deaggregation 475-yr Return Period Peak Horizontal Acceleration
Figure 52: Deaggregation 475-yr Return Period 0.2 Sec Horizontal Acceleration
Figure 53: Deaggregation 475-yr Return Period 1.0 Sec Horizontal Acceleration
Figure 54: Deaggregation 10,000-yr Return Period Peak Horizontal Acceleration
Figure 55: Deaggregation 10,000-yr Return Period 0.2 Sec Horizontal Acceleration
Figure 56: Deaggregation 10,000-yr Return Period 1.0 Sec Horizontal Acceleration
Figure 57: Deaggregation 145-yr Return Period Peak Horizontal Acceleration
Figure 58: Deaggregation 145-yr Return Period 0.2 Sec Horizontal Acceleration
Figure 59: Deaggregation 145-yr Return Period 1.0 Sec Horizontal Acceleration
Figure 60: Deaggregation 475-yr Return Period Peak Horizontal Acceleration
Figure 61: Deaggregation 475-yr Return Period 0.2 Sec Horizontal Acceleration
Figure 62: Deaggregation 475-yr Return Period 1.0 Sec Horizontal Acceleration
Figure 63: Deaggregation 10,000-yr Return Period Peak Horizontal Acceleration
Figure 64: Deaggregation 10,000-yr Return Period 0.2 Sec Horizontal Acceleration
Figure 65: Deaggregation 10,000-yr Return Period 1.0 Sec Horizontal Acceleration
Figure 66: Main Dam - Deterministic Hazard Results – Response Spectrum – 50th Percentile
Figure 67: Main Dam - Deterministic Hazard Results – Response Spectrum – 84th Percentile
Figure 68: Kaitu Weir - Deterministic Hazard Results – Response Spectrum – 50th Percentile
Figure 69: Kaitu Weir - Deterministic Hazard Results – Response Spectrum – 84th Percentile

Figure 70: Weir II - Deterministic Hazard Results – Response Spectrum – 50th Percentile
Figure 71: Weir II - Deterministic Hazard Results – Response Spectrum – 84th Percentile
Figure 72: Weir III - Deterministic Hazard Results – Response Spectrum – 50th Percentile
Figure 73: Weir III - Deterministic Hazard Results – Response Spectrum – 84th Percentile

List of Annexure

Annexure – A Chronological Catalogue of Non-Instrumental (Intensity) Data

This Page Left Blank Intentionally

EXECUTIVE SUMMARY

At the feasibility stage of the project, a seismic hazard evaluation was carried out using a deterministic approach for the selection of the seismic design parameters for the project. A Design Basis Earthquake (equivalent to Maximum Credible Earthquake, (MCE)) with a Peak Ground Acceleration (PGA) of 0.20g was then recommended for design of Kurram Tangi Dam.

A state of the practice seismic hazard assessment was performed using probabilistic and deterministic approaches to provide a comparison to the previously developed Design Basis Earthquake (PGA = 0.20g). The newly developed values follow the state of the practice in performing seismic hazard analyses, include updated relationships and follow International Commission on Large Dams (ICOLD) guidelines (ICOLD, 2010). The results are presented for each feature of the project, not only the dam site as calculated during the feasibility stage. The values are presented in Table ES-1.

Table ES-1: List of Project Features and Recommended Design Criteria

Feature	Recommended Design Criteria	Ground Motion (PGA, horizontal)[3] (g)			Critical Structure
		SEE	475	OBE	
Main Dam	SEE, 475 & OBE	0.80	0.18	0.09	Yes
Spillway –Gated Structure This includes the ability to access the gate controls and operate the spillway gates after an earthquake	SEE, 475 & OBE	0.80	0.18	0.09	Yes
Protective Dike for Spillway	OBE	-	-	0.09	No
Diversion Tunnels[1]	SEE, 475 & OBE	0.80	0.19	0.09	Yes
Kaitu Weir (18 feet high)	475 & OBE	-	0.19	0.09	No
Weir II (26 feet high)	475 & OBE	-	0.18	0.09	No
Weir III (75 feet high)[2]	SEE, 475 & OBE	0.70	0.17	0.09	Yes
Powerhouses	475 & OBE	-	0.19	0.09	No
Powerhouse Appurtenant Structures	475 & OBE	-	0.19	0.09	No
a. Tunnel (not including portals)	475 & OBE	-	0.19	0.09	No
b. Penstock	475 & OBE	-	0.19	0.09	No
Emergency power sources and control panels	SEE, 475 & OBE	0.80	0.19	0.09	Yes

Notes: 1. Potential failure of the valves, gates, and associated structural elements could result in uncontrolled release of the reservoir. 2. Failure may generate unacceptable downstream hazard. 3. If the feature listed has several locations the ground motion values are presented for the highest PGA, the structure (i.e. Main Dam or Weir) that is closest to the identified feature should be used.
SEE: Safety Evaluation Earthquake, 475: 475 Year Return Period Event, OBE: Operating Basis Earthquake (as defined by ICOLD)

The PGA developed for the feasibility level design (0.20g) is significantly lower than the PGA developed following current ICOLD guidelines (0.80g). One of the main differences in the current seismic hazard analysis compared to the previous analysis is that updated attenuation relationships were used in the calculations. In addition, the Kurram and Karak faults, located less than 10 km from the project site, were considered to be active in the current analysis.

The design values calculated in the current site specific hazard analysis were developed to provide a comparison to the feasibility level design values. It is assumed that the 0.60g increase in PGA will

require modifications that most-likely will have a major impact on the dam design. These modifications could negatively impact the cost and schedule.

1 INTRODUCTION

This document presents the results and findings of a Seismic Hazard Evaluation of the Kurram Tangi Multi-Purpose Project in Pakistan. The new analysis of seismic hazard in the region focuses on a review of earthquake occurrence, how this has been addressed in design development of the project, and any effects that the project may have on local seismicity.

This document is closely aligned with two other reports prepared as part of the project scope, the Geology and Site Investigations Report and Geotechnical Report. The Geology and Site Investigations Report is focused on the geological aspects of the project, with a concentration on the geological and geotechnical investigation programs conducted to characterize the site and project conditions, in support of the design of the project works and development of Tender Documents for construction. It incorporates review and commentary on geological and geotechnical hazards that may occur in the project area and the sites of individual project features, including issues such as reservoir slope stability. The Geotechnical Report concentrates more on the engineering geology and geotechnical engineering work conducted for the project, including interpretation of design parameters, development of geotechnical design criteria, and the geotechnical design of the civil works components of the project.

This Page Left Blank Intentionally

2 DATA SOURCES

The following is a list of data sources identified, made available and consulted regarding the geologic studies and investigation carried out to date for the project.

Table 2-1:Data Sources

No.	Document	Reference	Chapter No.	Remarks	Source
1	Feasibility Report	Annexure to the Main Report. Annexure - 1	CH – 1 : Introduction CH – 2: Geology and Geotechnical Studies, including brief description of seismic hazard (Text Only, some tables)	Feasibility report comprises of a Main Report, Annexures and Appendices. The findings of feasibility studies are given in the main report while details of the studies and analyses are provided in the Annexures and Appendices. Only text provided	Kurram Tangi Dam Consultants, 2004a
2	Detail Engineering Design Report	Volume - 1 (Text only)	CH – 1: Introduction CH – 3: Geology CH – 4: Construction Materials	The Detailed Engineering Design Report consists of Volume – 1 (text) and Volume - 2 (drawings) Only text provided	Kurram Tangi Dam Consultants, 2004b
3	PC – 1	All		Available	WAPDA, 2011
4	Rapid Assessment of Kurram Tangi Dam Construction – Final Report	All		Available	Elan Partners (Pvt.) Ltd., 2012

The following is a list of data sources identified, but not yet made available or consulted regarding geologic studies and investigations carried out to date.

Table 2-2: Data Sources Identified but not yet Available

No.	Document	Reference	Chapter No.	Remarks
1	Feasibility Report	Annexures to the Main Report. Annexure - 1	CH – 1 : Introduction CH – 2: Geology	No Drawings or Maps provided No detailed

			and Geotechnical Studies	information provided on seismicity such as fault maps, earthquake catalogs, or maps showing location of epicenters
2	Detail Engineering Design Report	Volume - 2		No Drawings or Maps provided or other supporting materials, such as aerial photographs, satellite imagery No detailed information provided on seismicity such as fault maps, earthquake catalogs, or maps showing location of epicenters
3	Bidding (Tender) Documents, including Drawings, Specifications, Terms of Contract	All		Not provided

Various Federal / Provincial Authorities, Consultants, and organizations contacted regarding gathering of project data are listed below.

Table 2-3:Contacts who aided in Gathering of Project Data

No.	Organization	Contact person	Remarks
1	Water and Power Development Authority (WAPDA), Head Office, WAPDA House, Lahore	Mr. Shahid Hamid: Director Small/Medium Dams	Focal point person in WAPDA House for KTDP. Meeting 22 Jan, 2013, at WAPDA House.
2	WAPDA, Head Office, WAPDA House, Lahore	M. Ashraf Abid; GM Planning and Development of WAPDA	Has overall responsibility of the KTDP. Meeting 22 Jan, 2013, at WAPDA House.
3	WAPDA, Head Office, WAPDA House, Lahore	Rashid Ali Bangash: GM North WAPDA	Based in Peshawar and directly In charge of KTDP in KPK. He was coincidently in Lahore and Mr. Shahid Hamid organized our meeting with him. Meeting 22 Jan, 2013, at WAPDA House.
4	WAPDA, Head Office, WAPDA House, Lahore	Dr. Raheal Ahmad Siddiqui: GM Land Acquisition & Resettlement	Responsible for environmental and resettlement components of Basha Dam Project and several other Hydropower projects

			being implemented by WAPDA. Meeting 22 Jan, 2013, at WAPDA House.
5	MM (Pakistan, Ltd). Lead consultant in Feasibility study and for Detailed Design of Kurram Tangi Dam Project (KTDP)	Tariq Mahmood; GM (Project) MM (Pakistan)	Meeting 24 Jan, 2013 at MMP offices. Formal requests made for project documentation.
6	CIRES Researcher and Professor at the Department of Geological Sciences, University of Colorado, Boulder,	Roger Bilham	Provided references and information on the general seismotechtonic setting
7	National Centre of Excellence in Geology, University of Peshawar	Asif Khan	Fault activity in project region
8	United State Geologic Survey	Oliver Boyd	Provided gridded Seismicity values as used in Boyd et al., 2007

This Page Left Blank Intentionally

3 EVALUATION OF QUALITY AND RECENCY OF DATA

The principal data sources available, i.e. the Feasibility and Detail Engineering Design Reports, were prepared in 2004 by the Kurram Tangi Dam Consultants JV (Design Consultants) and were approved by Water and Power Development Authority (WAPDA) (Design Consultants, 2004a & 2004b). It is believed that the data provided in these reports were true and credible but not necessarily complete or up-to-date. Moreover, critically important information was needed to properly complete the review and evaluation of data quality. The most critical information needed were text figures, illustrations, maps, and drawings intended to accompany the Feasibility and Detailed Design Reports but which were not provided.

As described in Section 4 below, during previous studies on the project, selection of the seismic design parameters for the project used methodologies and guidelines that are not in keeping with current practices for seismic hazard evaluations on dam projects, such as the industry standard guidelines published by the International Commission on Large Dams (ICOLD), Bulletin 72, 2010

.

This Page Left Blank Intentionally

4 BRIEF SUMMARY OF THE SUBJECT MATTER FINDINGS/SITUATION

For the evaluation of the seismic design parameters for the project, the tectonic and seismic environment of the project site was studied by the Design Consultants. Based on this, a seismic hazard evaluation was carried out using a deterministic approach for the selection of the seismic design parameters for the project. A Design Basis Earthquake (equivalent to MCE) of 0.20g was then recommended for design of the dam. Based on updated ICOLD guidelines, our review, and previous knowledge of the seismic conditions in this region of Pakistan, we consider the recommended seismic design parameters to be too low. In view of the seismotectonic setting of the project region, the seismic hazard evaluation should account for more realistic earthquake source modeling and include a Probabilistic Seismic Hazard Assessment (PSHA) in addition to a deterministic approach. The results of subsequent studies performed by the MWH Team are presented in the following sections.

This Page Left Blank Intentionally

5 BACKGROUND AND PURPOSE

In the previous evaluation of the seismic design parameters for the project, the Design Consultants had studied the tectonic and seismic environment of the project site and had carried out a basic seismic hazard evaluation using a deterministic approach in order to select seismic design parameters for the project. A Design Basis Earthquake (equivalent to MCE) of 0.20g was then recommended for the design of the dam but this recommended seismic design parameter is too low for a project located in this seismotectonic setting. We consider that a seismic hazard evaluation that is in keeping with current guidelines should account for updated earthquake source modeling and include a PSHA.

The proposed project includes a main dam and three weirs. The project features are shown in Plate 1.

This Page Left Blank Intentionally

6 SEISMOTECTONIC SETTING AND HISTORICAL EARTHQUAKES

6.1 Regional Tectonics and Stratigraphy

The collision tectonics in the Himalayas and geodynamic history of the region are represented by the Indus and Shyoke sutures which are distinct features resulting from the convergence of the Indian and Eurasian Plates. In northern Pakistan, another prominent tectonic feature is the Kohistan Island Arc, a zone sandwiched between the two plates (see Plate 2). In the west and northwest, near the Afghan border, collision involving the crystalline basement of the Indian Plate is substantially different from the collision between the Indian Plate and the Eurasian Plate. Unlike the Himalayas, thrusts related with collision have involved a transitional sub-oceanic crust rather than the crystalline basement (Asif et al., 2003).

In contrast to the Indian Plate-Kohistan collision zone in northern Pakistan, where the uplift has been so severe that the suture zone exposed the base of the Kohistan crust in contact with the basement gneisses of the Indian Plate, the Waziristan-Kurram suture zone between Indian Plate and Afghanistan preserves a more or less complete stratigraphic record of collision. Plate 3 shows the tectonic features of the Western Himalaya.

The Kohat Plateau is located towards the north and northeast of the project site. The northern boundary of the Kohat Plateau is marked by the Main Boundary Thrust (MBT), a long thrust running from Parachinar in the west to Murree in the east. Further east, it takes a sharp bend along the Hazara-Kashmir syntaxis and then extends all along the Himalayas up to Aasam. The southern boundary of the Kohat Plateau is marked by the Karak Thrust. Plate 4 illustrates the Kohat Plateau; faults are shown on Figure 1.

Immediately west of Bannu, the Pliocene-Pleistocene Ahmadzai conglomerates are deformed, involved in a monocline developed east of a major upright fault structure, the Kurram fault. This N-S fault runs parallel to the Chaman fault which represents the transform boundary between the Indian and Eurasian Plates on the western side of Pakistan.

East of the Bannu basin, the Salt Range and its Trans-Indus ranges are present; the boundary between these ranges is represented by the strike-slip Kalabagh fault. The trans-Indus ranges, the Bhittani range, Surghar range, and the Khisor range are bounded by thrust faults.

A detailed description of the stratigraphy of the project area is given in Annexure-1, Annex-Chapter-2 of the feasibility report and is therefore not repeated here.

It is clear that the project is located in a tectonically active region due to proximity of the collisional boundary of the Indian and the Eurasian plates. As the plate movement is still going on, stress develops in the shallow crust and is released in the form of earthquakes.

6.2 Significant Historic Earthquakes

The catalogue of historical earthquakes for this region is rather sparse and probably highly incomplete. The historical data are few and concentrated mainly on the centers of the colonial administration.

Before the establishment of seismological observatories, which began at the beginning of 20th century, intensity data collected from the historical records was the only source of earthquake information. Historical earthquake data includes a general account of damage/ loss to life and property. The historical pre-instrument earthquake data have been collected from the description of the earthquakes given in the memoirs or records of travelers, historians and writers. Such earthquake catalogues have been compiled by Ambraseys et al. 1975 and Quittmeyer and Jacob, 1979. A catalogue of historical record of earthquake in northern Pakistan is given in Annexure-A. From this catalogue, it reflects that northern Pakistan as a whole has remained an area of prominent earthquakes. The Taxila (25 A.D.) event is probably the most conspicuous one that changed the style of building construction.

The Kangra earthquake occurred on April 4, 1905 in the north-west Himalaya. The earthquake was located in northern India and was one of the first devastating earthquakes of the 20th century. The Punjab Government estimated that more than 20,000 of its ≈ 375,000 epicentral population were killed, and that 100,000 buildings were destroyed by the earthquake (Ambraseys & Bilham, 2000). The economic costs of recovering from the earthquake were estimated at 2.9 million (1905) rupees (Ambraseys & Bilham, 2000). Although this earthquake is not the only severe event known in the western Himalaya, it has the largest death toll and is the first to have occurred since the development of instrumental seismology. Gutenberg and Richter published a magnitude of Ms = 8 for the 1905 event. Subsequent estimates for the magnitude of the event range from M = 8.6 to Ms = 7.5 (this study used a M_w=8.5) (Ambraseys & Bilham, 2000).

The 1935 Quetta earthquake occurred on May 30, 1935, in Quetta, Pakistan. It is estimated that there were 30,000 fatalities (USGS, 2013). Ambrasey & Bilham (2009) calculated the magnitude of the event to be M_S=7.7. The towns of Quetta and Mastung were totally destroyed along with 100 villages (Ambrasey & Bilham, 2009). It is believed that this rupture was associated with the zone of faults that lie along the east edge of the Chiltan range with extends to the south passing the towns of Mastung and Kalat. The mechanism was most-likely a left lateral strike-slip event (Ambrasey & Bilham, 2009).

6.3 Catalog

An earthquake catalog was provided by NESPAK. This catalog included events from 1904 to June 30, 2012. The catalog was first updated using the International Seismological Centre (ISC) catalog to include events through the end of 2012. Then significant events not contained in the catalog but reported by Ambraseys and Bilham (2009) were also incorporated.

The updated composite seismic catalog contained magnitude values in the form of surface wave (M_S), body wave (m_b), local (M_L) or duration (M_D) magnitude types. For data to be used in seismic hazard analysis, all the magnitudes were converted to moment magnitude (M_W) by the following equations.

First, conversion from M_S and m_b to M_W was achieved through the latest equation suggested by Scordilis (2006):

$M_W = 0.67\ M_S + 2.07$ for $3.0 \leq M_S \leq 6.1$

$M_W = 0.99\ M_S + 0.08$ for $6.2 \leq M_S \leq 8.2$

$M_W = 0.85\ m_b + 1.03$ for $3.5 \leq m_b \leq 6.2$*

Where m_b is body–wave magnitude, M_S is surface-wave magnitude, and M_W is moment magnitude. *The conversion from m_b to M_W was used twice outside of this range (one was am$_b$ event of 6.5 another was 6.3).

Then, for those events that did not have M_S or m_b or fell outside the ranges suggested above the equations below were used. The value of M_L, up to 5.7, was taken equal to M_W as suggested by Idriss (1985) and supported by operators of local networks in Pakistan. Conversion of M_L to M_W beyond magnitude 5.7 was done by using the following equations suggested by Ambraseys and Bommer (1990) and Ambraseys and Bilham (2003):

$0.82\ (M_L) - 0.58\ (M_S) = 1.20$

$\text{Log Mo} = 19.09 + M_S$ for $M_S < 6.2$

$\text{Log Mo} = 15.94 + 1.5\ M_S$ for $M_S > 6.2$

$M_W = (2/3)\ \text{Log (Mo)} - 10.73$

Where, M_S is surface-wave magnitude, M_L is local magnitude, M_D is earthquake duration magnitude, M_W is moment magnitude and Mo is seismic moment.

If none of the other magnitude scales were available then the earthquake duration magnitude (M_D) was set equal to M_w. All events that used this final conversion were less than 4.5, except one having a M_D=5.8.

Table 6-1, shows events with a magnitude greater than 6 located within areal sources used for this study.

Table 6-1:Catalog of events greater than M_w 6.0

Event Year	Latitude	Longitude	Depth(km)	Magnitude
1505	69.10	34.50	0	7.20
1828	74.83	34.08	0	6.00
1832	71.00	36.50	0	7.30
1842	71.00	35.00	0	7.40
1842	71.00	35.00	0	7.40
1874	69.20	35.10	0	6.90
1885	74.38	34.60	0	6.90
1901	68.40	31.00	0	6.10
1902	67.00	38.50	40	6.20
1905[1]	76.00	33.00	25	8.50
1905	69.90	30.30	0	6.40
1906	68.00	36.50	32	7.00
1909	70.00	33.00	0	6.00
1911	72.80	38.00	26	7.60
1912	71.50	35.00	0	6.30
1914	75.30	32.80	33	6.20
1920	69.00	35.00	0	6.00
1920	69.00	35.00	0	6.00
1947	75.90	32.60	0	6.00
1948	67.70	36.40	33	6.50
1950	73.00	36.20	0	6.10
1950	75.90	32.60	0	6.10
1952	69.34	30.37	2	6.10
1956	67.48	35.13	33	7.30
1956	69.60	33.80	11	6.60
1956	71.00	36.50	0	6.10
1956	69.90	30.00	33	6.00
1958	67.00	35.00	0	6.20
1958	67.00	35.50	0	6.20
1958	71.00	36.50	0	6.10
1958	67.44	35.31	20	6.00
1962	69.20	36.50	50	6.80
1962	75.70	32.30	0	6.00
1965	73.00	37.42	15	6.10
1966	69.50	29.80	17	6.60
1966	69.80	30.20	17	6.40
1972	69.70	36.30	28	6.30
1972	73.33	35.94	45	6.30
1974	72.90	35.00	14	6.10
1981	73.60	35.68	30	6.00
1982	69.00	36.10	36	6.50
1984	70.50	34.60	9	6.00
1990	72.90	37.00	33	6.40

1991	70.80	36.40	0	6.80
1994	67.10	36.90	23	6.10
1998	70.10	37.10	29	6.60
1999	75.13	30.72	33	6.10
2000	71.20	36.50	0	6.20
2001	71.48	36.40	0	6.00
2002	74.59	35.35	13	6.30
2002	69.40	36.00	8	6.10
2002	69.20	35.90	10	6.00
2005	73.63	34.63	22	7.50
2008	71.30	37.30	10	6.10
2008	69.47	33.88	10	6.00
2010	70.91	36.61	0	6.30
2012	69.32	36.08	31	6.10

Notes: 1. 1905 Kangra event

6.4 Review of Prior Studies

A previous study in the project area performed by the Design Consultants and given in Annexure I, Appendix Chapter 2 of the Feasibility Report only included a deterministic approach to develop the seismic parameters for the dam and appurtenant structures. The resulting Design Basis Earthquake (equivalent to MCE) of 0.20g was recommended for the design of the dam. In light of the active tectonic environment and proximity to the transform boundary of the Indian and Eurasian tectonic plates, the previous seismic hazard evaluation is considered to have underestimated the seismic design parameters.

During previous studies, selection of the seismic design parameters used methodologies and guidelines that are not in keeping with current practices for seismic hazard evaluations on dam projects, such as the industry standard guideline published by the International Congress on Large Dams (ICOLD), Bulletin 72, 2010. The seismic hazard evaluation should account for more realistic earthquake source modeling and also use a probabilistic approach.

6.5 Purpose of Analyses

On the basis of review of the previous studies, it was decided that a re-evaluation of the seismic hazard analysis be carried out, to include:

- Effects of seismic potential of the Kurram and Karak Faults in the deterministic analysis.
- A probabilistic analysis based on recorded seismicity and maximum magnitude potential of the faults and/or areal seismic sources to evaluate the Operating Basis Earthquake (OBE) and Safety Evaluation Event (SEE) / Maximum Design Event (MDE) in accordance with ICOLD Guidelines.

The failure of the Kurram Tangi Dam, if an MCE were to occur, could pose a great environmental hazard. Therefore, a realistic evaluation of seismic hazard is imperative in mitigating the effects to the dam and appurtenant structures.

7 SEISMIC SOURCE CHARACTERIZATION

The seismic source model includes crustal fault sources, areal sources, and gridded seismicity. Earthquakes less than 50km deep were characterized as crustal seismicity and included in the crustal fault sources or the areal sources. For those events occurring at depths greater than 50km the gridded seismicity used to calculate an Earthquake Hazard Map of Afghanistan in 2007 were used (Boyd et al., 2007).

7.1 Crustal Fault Sources

Defined crustal faults within 50km of the project site were modeled as planar faults (see Figure 1). Additional faults were included that fell inside the defined source zones surrounding the project site (Zone 7 and Zone 5). The Chaman fault, which had several sources of reliable reference material on the slip rate and recurrence, was also modeled as a fault. Those areal sources which did not have any faults located within 50km, but were within 300km, were modeled as areal sources.

7.1.1 Kurram Thrust

The Kurram Thrust is a North northeast – West southwest (NNE – WSW) trending westward dipping (Kazmi, 1979) active tectonic feature separating the Kakar – Khorasan Flysch Basin in the north and west from the Bela Ophiolite thrust and fold belt in the east and south. The Kurram Thrust along with other sub-parallel thrust faults of the area such as the northern and southern Khorasan faults and the left-lateral, strike-slip Quetta fault, are considered seismically active. During the Quetta earthquake of 1935, ground rupturing occurred along the Quetta fault, which is more than 400 km away from the project. However, the same tectonic zone extends towards north and Kurram Fault marks the northern part of this tectonic zone. The surface trace of the Kurram Thrust is about 220 km. All project features are located on the footwall wall about 1 to 7 km from the surface trace of this fault. A slip rate of 1.32mm/yr was assigned to the Kurram Thrust, this is double the value reported by B. Kim (2012).

7.1.2 Karak Thrust

This north dipping fault is located on the boundary between the Bannu Basin and the Kohat Plateau. It is oriented from almost east to west. It has exhibits moderate dip angles and emplaces the rocks of the Jatta Gypsum and MamiKhel Formation over the Chinji Formation in the south. The Karak Fault represents the southernmost extension of the evaporatefacies exposed at the surface in the Kohat Plateau (Ahmad, 2003). All project features are located on the hanging wall of the Karak Thrust with R_{JB} values equal to zero. The mapped length of this fault is about 105 km. A slip rate of 0.72 mm/yr was assigned to the Karak Thrust, this is double the value reported by B. Kim (2012).

7.1.3 Murree Fault (MBT)

The most significant and active tectonic feature of regional extent in the northern Pakistan is the Main Boundary Thrust (MBT). It is the main frontal thrust of the Himalayan Range, extending along the Himalayan Arc for almost 2500 km from Assam in the east to Kashmir and Parachinar in the west. The MBT, along with other associated thrusts, forms the sharp conspicuous Hazara-Kashmir Syntaxis. This syntaxial bend is the most prominent tectonic feature of the area as all local major fault systems and geologic structures follow its trend. On the west side of the syntaxial knot, the MBT initially follows a rather southwest trend and then extends westward reaching Parachinar. The mapped length of this fault west of Hazara-Kashmir syntaxis is about 360 km, project features are located about 50 km from this fault.

Near its surface trace, the MBT dips northward at a steep angle, which becomes sub-horizontal with depth. The Islamabad-Rawalpindi area is located at a close distance south of the western limb of the MBT.

A number of large to major earthquakes have occurred along the Himalayan Arc east of the Hazara-Kashmir Syntaxis during the last two centuries, which places it amongst the most active regions of the world. A significant amount of seismicity recorded during the last century is associated with

surface and subsurface extensions of the MBT and other associated thrusts. Based on this data, Seeber et al. (1981) have shown that great earthquakes occurring along Himalayan Arc are probably related to slips taking place along this quasi-horizontal surface (detachment).

Based on the above, the MBT is considered active having seismic potential sufficient enough to generate major earthquakes. A slip rate of 8.0 mm/yr was assigned to the Murree Fault, this is double the value reported by B. Kim (2012).

7.1.4 Kalabagh Fault

The Kalabagh fault is a prominent right-lateral strike slip fault; located on the east of Kalabagh, and extending between Kalabagh and Mianwali. The overall trend of the fault is northwest-southeast. It truncates the western margin of Salt Range. The mapped length of this fault is about 48 km. Its northward extension splays into smaller northward trending Dinghot, Ainwan, and Surghar faults.

Neotectonic studies conducted along this fault during studies for the Kalabagh Dam Project have revealed (a) displacement/ uplifting of the Holocene terrace deposits and (b) fault traces under alluvial deposits. Seismic data also indicate a few earthquake epicenters located along this fault. Based on such evidence, this this fault is considered seismically active.

A description of the above described local tectonic features suggests that the entire northern part of Pakistan lies in the collisional zone of the northern part of the Indian Plate with associated faults that show evidence of fault movement during the Quaternary period and should therefore be considered seismically active. A slip rate of 0.48 mm/yr was assigned to the Kalabagh Fault, this is double the value reported by B. Kim (2012).

7.1.5 Bhittani Thrust

This is the major fault of the Pezu-Bhittani Ranges, passing through the crustal part of the Pezu Anticline all along its axial trace resulting in several compartments of the Pezu anticline. It is oriented in northwest to southeast direction and juxtaposes rocks of Chinji Formation in the hanging wall against the rocks of Nagri Formation in the footwall in the northwestern domain of the Pezu Anticline. In the central domain of the Pezu Anticline, Pezu Fault juxtaposes rocks of Chinji Formation in the hanging as well as footwall. In the southeastern domain of the Pezu Anticline, Pezu Fault brings rocks of Nagri Formation in the hanging wall against the rocks of Dhok Pathan Formation in the footwall. Its hanging wall is dipping towards the Bannu Basin in the northeast at moderate to steep angle (45°~68°) whereas its footwall is dipping towards the Tank Basin in the southwest with moderate angle (28°~56°). Its map extension along the trend is more than 21 km based on its location with respect to the Pezu Anticline, it is believed to be of transpressional nature with dextral movement. A slip rate of 0.34 mm/yr was assigned to the Bhittani Thrust, this is double the value reported by B. Kim (2012).

7.1.6 Khisor Thrust

The Khisor range forms a thin layer of sedimentary cover overlying basement rocks. It probably represents the southernmost expression of the deformations associated with the continental collision. The southern frontal face of the Khisor range forms a thrust fault called Khisor fault which the result of the northward drift of the Indian plate. It has a total length of about 60 km. Seismicity data suggest that the Khisor range shows a low level of seismic activity. A slip rate of 0.86 mm/yr was assigned to the Khisor Thrust, this is double the value reported by B. Kim (2012).

7.1.7 Surghar Range Thrust

Surghar Fault is a regional fault along which Mesozoic rocks of the Surghar Range are thrust southwards over the Punjab foreland, marking the range front. It displays contrasting geometric variations within the rocks along the strike (Ahmad, 2003). The Surghar Fault is believed to be a strongly emergent thrust to the west having shallowly folded thrust sheet. Towards the east, Surghar Fault translates into a tip-stick thrust front with its thrust sheet tightly folded and disrupted by several out of sequence thrust faults with about 5.6 km shortening calculated to have taken place along this fault (Ahmad et al., 1999).The mapped length of this fault is about 69 km. A slip rate of

0.60 mm/yr was assigned to the Surghar Range Thrust, this is double the value reported by B. Kim (2012).

7.1.8 Panjal Thrust

Panjal Thrust is an important active tectonic feature of regional significance. It runs northwards and parallel to the Main Boundary Thrust on the western side of Hazara- Kashmir Syntaxis. Both the faults; while coming gradually closer to each other join together about 5 km north of Balakot (Wadia 1931, Calkin et al. 1975, Bossart et al. 1984 and Greco 1991).

A left lateral strike slip fault cuts across both the Panjal Thrust and MBT approximately 6 km south of Balakot, from where onwards the Panjal Thrust continues its independent journey southwards. It is traceable up to Garhi Habibullah from where onward it gets concealed under the Quaternary deposits. The thrust comprises several segments having accumulated length of about 130 km.

Towards the west this fault passes through Gandghar Range near Haripur and joins Khairabad Fault located on the northern side of Attock-Cherat Range, hence it is sometimes referred as Panjal-Khairabad fault.

The geologic positioning and seismicity associated with Panjal fault renders it as an active regional tectonic feature capable of generating large earthquakes. A slip rate of 4.92 mm/yr was assigned to the Panjal Fault, this is double the value reported by Kim (2012).

7.1.9 Chaman Fault

The Chaman fault system is a left lateral strike slip fault more than 1,000 km long. The fault trace extends from the Hindu Kush region in northeastern Afghanistan south-southwestern through eastern Afghanistan into western Pakistan. In 1505, an earthquake having an estimated magnitude of Ms 7.3 occurred near Kabul, Afghanistan producing about 40–60 km of surface rupture and several meters of vertical offset (Quittmeyer and Jacob, 1979; Ambraseys and Bilham, 2003).

Based on studies of aerial photographs and Quaternary geomorphology, Tapponier and others (1981) and Wellman (1965) estimated slip rates on the Chaman fault system to be between 2 and 20 mm/yr. Lawrence and others (1992) suggested that the slip rate on the southern end of the fault may be higher where it enters western Pakistan; they estimate the slip ranges from about 19 to 24 mm/yr. Bernard et al. (2000) estimate that the slip on the Chaman Fault could range between 17 to 24 mm/yr. The United States Geological Survey (USGS) (2007) selected a slip rate of 10 mm/yr in their development of a PSHA in Afghanistan. Despite the large uncertainty in the estimated slip rate, part of the Chaman fault system is located within 200km of the site and poses some seismic hazard, albeit small. A slip rate of 2, 10, and 24 mm/yr with equal weighting are assigned to the Chaman Fault.

7.2 Areal Sources

To model the distribution of earthquakes within an area, several areal source zones are used. NESPAK identified 17 areal sources in and around Pakistan which had similar tectonic and seismic characteristics. Of those 17 source zones 8 are used in this study, as shown in Figure 2. The selection and use of areal sources was based on the distance from the project site. All faults within 50km of the project site were modeled as faults, except for the Chaman fault, which had several sources of reliable reference material on the slip rate and recurrence. Those areal sources which did not have any faults located within 50km but were within 300km were modeled as areal sources. Areal source zones 5 and 7 are represented by crustal faults and are not included in the analysis. The creation of Zone 12 New was necessary to include the seismicity within Zone 12 not associated with the Chaman Fault. A description of each of the source zones used in this study is listed below.

7.2.1 Zone 1

This zone covers the Hindukush seismic zone which is characterized by intermediate to deep seismicity associated with sharp subduction of the Indian Plate. This is the most active seismic zone in this region.

7.2.2 Zone 2

This zone covers the Pamir-Karakoram area north of the Main Karakoram Thrust (MKT) which falls in the Eurasian Plate. This zone is moderately active and characterized by shallow tectonic activity.

7.2.3 Zone 3

This zone covers the Kohistan Island Arc which is bounded between the MKT and the MMT. This zone is seismically active and several damaging earthquakes of shallow origin have been recorded in this area. This zone is also characterized by shallow tectonics.

7.2.4 Zone 4

This zone represents the Himalayan area east of the Hazara-Kashmir Syntaxial bend and cover Kashmir and Indian Territory east of Kashmir. This zone is seismically very active and a number of large damaging earthquakes have been recorded during the last 500 years. Shallow seismicity with thrust environment is predominant in this zone.

7.2.5 Zone 6

This zone covers the Potwar area between the MBT and the Salt Range Thrust (SRT) where thrust faulting is predominant. This area shows a low to moderate level of seismic activity.

7.2.6 Zone 8

This zone represents the Punjab plain area south of the SRT. This area is covered by thick alluvial deposits which are mostly underlain by Basement rocks. This area shows a low level of seismic activity, associated predominantly with strike slip faults.

7.2.7 Zone 11

This zone covers the Suleiman ranges which run north to south, parallel to the Waziristan-Kurram suture zone. A number of active faults showing moderate level of seismicity are present in this zone.

7.2.8 Zone 12 NEW

This zone covers the Kurram Waziristan ophiolite belt which is governed predominantly by thrust tectonics. This zone is characterized by the moderate level of shallow seismicity. This zone is a subset of Zone 12, as defined by NESPAK. The areal source zone was abbreviated in the west so that the Chaman fault could be included as a fault source.

7.3 Gridded Seismicity

A gridded seismicity file was developed by the USGS for a preliminary earthquake hazard map of Afghanistan. Because this work included all of Northwestern Pakistan, the grid ranged from longitude of 56 degrees to 79 degrees and ranged from latitude of 26 degrees to 41 degrees, it was used for this analysis. The USGS subdivided the catalog into five depth ranges, 0–50 km, 50–100 km, 100–150 km, 150–200 km, and 200–250 km, the first depth range (0-50 km) was not included in this study. Contributions from crustal faults and areal source zones were used instead.

Earthquake rates for each of the other four depth subsets (50-250 km) were based on a grid with nodes spaced at in increments of 0.1° in latitude and longitude following the methodology of Frankel and others (1996). Earthquakes were assumed to occur at a rate that follows a Gutenberg-Richter distribution with a b-value of 1.0 and the rate for each grid cell was computed by counting earthquakes (Weichert, 1980) with Mw equal to or greater than 4.5 between 1964 and 2004. This time period was selected based on a consistent summary catalog complied by Bergman (2006) that spanned 1964 to 2004 and in 1964 the Worldwide Standardized Seismographic Network was deployed and data for about M4.5 events were readily available. The uncertainty was accounted for spatially smoothing these rates over a distance greater than the grid node spacing. Grid nodes for the four deeper subsets between 50 and 250-km depth are smoothed with a 2-dimensional Gaussian kernel that has a correlation distance of 50 km.

8 PROBABILISTIC SEISMIC HAZARD ANALYSIS (PSHA)

The following sections describe the PSHA methodology, inputs for analysis, and results. The PSHA was performed to better understand the likelihood of the potential earthquake sources, to correlate the DSHA with period of returns, and to evaluate the contribution of the seismic sources for a given period of return (e.g. deaggregation).

8.1 PSHA Code and Methodology

The methodology for PSHA was developed by Cornell (1968), and is used to provide a framework in which uncertainties in size, location and rate of recurrence of earthquakes can be considered to provide a probabilistic understanding of seismic hazard.

A PSHA can be described as a procedure of four steps (Kramer, 1996):

1.) Identification and characterization of earthquake sources, along with the assignment of a probability distribution to each source zone.

2.) Characterization of earthquake recurrence.

3.) Determination of ground motion produced at the site by earthquakes of any possible size occurring at any possible point in each source zone.

4.) Calculation of the probability that the ground motion parameter will be exceeded during a particular time period given uncertainties in earthquake location, earthquake size and ground motion parameters.

The calculations for this report were performed using the computer code HAZ43, which was developed by Dr. Norman Abrahamson. Earlier versions of this code were verified under the Pacific Earthquake Engineering Research Center (PEER) PSHA Code Verification Workshop (Wong et al., 2004).

8.2 PSHA Source Characterization

8.2.1 Fault Sources

Potentially active and active crustal faults located within 50km of the site were included in the analysis. Additional faults were included that fell inside the defined source zones surrounding the project site (Zone 7 and Zone 5). The Chaman fault, which has several sources of reliable reference material on the slip rate and recurrence, was also modeled as a fault. Those areal sources which did not have any faults located within 50km but were within 300km were modeled as areal sources.

Due to the incompleteness of fault parameters, it was assumed that the dip for thrust faults ranged between 30-60 degrees and strike slip faults were assumed to have a dip of 90 degrees. It was also conservatively assumed that the slip rates were double those computed by Kim (2012). Wells and Coppersmith (1994) equation for all faults using the surface rupture length assumed for full fault rupture was used to develop the maximum magnitude.

The faults were modeled as both characteristic and truncated exponential. Characteristic events were assigned a probability of 0.7 and the exponential model was weighted 0.3. The weighting was to set as such to balance out the two different models. The truncated distribution predicts a higher ratio of lower magnitudes to higher magnitudes than is observed on a single fault. In contrast, the characteristic model, in its most simple application, predicts fewer earthquakes on a fault than are generally observed. Additional information on the fault parameters can be found in Table 8-1.

Table 8-1: Fault Parameters

Name	Type [1]	Distance [2](km)	Fault Length(km)	Maximum Magnitude (Mw)[3]	Dip (degrees)	Slip Rate (mm/yr) [5]	NESPAK Source Zone[6]
Kurram Thrust	R	6	220	7.8	30-60	1.32	7
Karak Thrust	R	7	105	7.4	30-60	0.72	7
Khisor Fault	R	94	60	7.1	30-60	0.86	7
Kalabagh Fault	SS	92	48	7.0	90	0.48	7
Bhittani Thrust	R	85	21	6.6	30-60	0.34	7
Surghar Range Thrust	R	71	69	7.0	30-60	0.60	7
Murree Fault (MBT)	R	47	360	8.0	30-60	8.0	5
Panjal Thrust	R	112	212	7.8	30-60	4.92	5
Chaman Fault	SS	193	~1000	7.9[4]	90	2,10,24	12

Notes:
1. R=Reverse, SS=Strike Slip 2. Distance from main dam to fault trace. 3. Maximum Magnitude developed using Wells & Coppersmith magnitude-fault length relations. 4. Maximum magnitude of Chaman Fault as reported in Boyd et al., 2007.5.Slip rate doubled from that reported by B. Kim,2012(except Chaman Fault).6. Source zones listed are not included in the study except for Zone 12, which was revised to Zone 12 NEW and does not include the Chaman Fault.

8.2.2 Areal Sources

Areal sources assume earthquakes can occur at any possible site in the source zone and are uniformly distributed inside the areal source. To estimate probabilistic ground motions for the site, recurrence parameters are required for the seismic zones.

The first step in developing recurrence parameters is to calculate the catalog completeness. This was performed by creating Stepp (1972) completeness plots. The plots were developed starting at a minimum magnitude of 4.0 and carried out for each 0.5 magnitude units. The larger magnitude events were lumped into a single bin, given the sparseness and incomplete record keeping of such events. **Figure 3** illustrates the Stepp completeness plots. The catalog completeness is presented in Table 8-2

Table 8-2:Catalog Completeness Values

Magnitude Range	Catalog Complete (in years before 2012)
4.0-4.5	10
4.5-5.0	10
5.0-5.5	10
5.5-6.0	60
6.0-6.5	60
6.5-7.0	85

7.0-7.5	85
7.5+	100

After developing the catalog completeness the dependent events such as, foreshocks, aftershocks, or smaller events within an earthquake swarm were removed. The USGS program ClusterY2K was implemented to remove these dependent events. After the completeness intervals for each magnitude range was developed and dependent events were removed the characterization of the frequency of events was computed. Recurrence relationships were estimated following the maximum likelihood procedure developed by Weichert (1980).

A common way to characterize this frequency is by using the Gutenberg-Richter relationship. This recurrence law is based on a linear relationship when the magnitude is plotted against the logarithm of frequency of events. The magnitude-frequency relation expressed in its cumulative form is:

$$\log N(M) = a - bM$$

where M is the magnitude and N is the cumulative frequency of earthquakes greater than or equal to magnitude M. The maximum likelihood line is characterized by the line slope, or b-value, and the activity rate of zero magnitude (a). For this study, a minimum magnitude of 5.0 was used for both the recurrence estimates and also for the PSHA.

Areal source zones numbered 1-4, 6, 8, 11, were selected based on previous research performed by NESPAK. Zone 12 New was created based on Zone 12; however this source zone was reduced so that the Chaman fault could be included as a fault source and not lead to double counting of the seismic source. Because the number of earthquakes within each of these source zones was limited, a regional b-value was developed using the Weichert method (1980). The regional b-value was calculated to be 1.15. This regional b-value was then fixed and for each source zone a visual estimate of the recurrence was performed to estimate an a-value for each of the source zones. The maximum magnitude for each source zone was estimated by adding 0.5 magnitude units to the maximum magnitude reported in the areal source. For those source zones which had a maximum reported magnitude less than 6.0 the maximum magnitude was assigned to be 6.5. Figures 4 through 12, present the recurrence plots corresponding to each areal source. These areal source zones were also limited to events occurring within 50 km depth and were run with the crustal attenuation relationships selected for this study. Additional information regarding the selection of the areal source zones are provided in Section 7.2. Table 8-3 summarizes the areal sources and parameters used as input into the PSHA.

Table 8-3:Areal Sources used in the PSHA

Seismic Zone1	Source Type	Depth (km)	Maximum Magnitude (Mw)	a	b
Zone 1	Crustal	< 50	8.1	6.05	1.15
Zone 2	Crustal	< 50	6.5	5.2	1.15
Zone 3	Crustal	< 50	7.9	5.5	1.15
Zone 4	Crustal	< 50	8.5	5.9	1.15
Zone 6	Crustal	< 50	6.5	5.0	1.15
Zone 8	Crustal	< 50	6.6	5.1	1.15
Zone 11	Crustal	< 50	7.1	5.7	1.15
Zone 12NEW	Crustal	< 50	6.6	4.7	1.15
AFDEEP	DEEP Continental	50-100	8.5[4]	gridded	1.0
AFDEEPER	DEEP Continental	100-150	8.5[4]	gridded	1.0
AF4	DEEP Continental	150-200	8.5[4]	gridded	1.0
AF5	DEEP Continental	200-250	8.5[4]	gridded	1.0

Notes:

1. Seismic Zones 1-4, 6, 8, 11 & 12NEW provided by NESPAK with minor modifications, see **Figure 2**

for plot. AFDEEP, AFDEEPER, AFD4, & AFD5 from Preliminary Earthquake Hazard Map of Afghanistan, Open-File Report 2007–1137, Boyd et al., 2007.

2. Minimum earthquake magnitude M5.0 adopted for all source zones.
3. Parameters a and b are derived from the magnitude recurrence relationship.
4. 1905 Kangra Event

8.2.3 Deep Continental Source Zones

Deep continental earthquakes (up to 250km deep) occur within 150km of the project site. The USGS published a preliminary Earthquake Hazard Map of Afghanistan in 2007, where the deep continental zones were modeled based on smoothed gridded seismicity (Boyd et al., 2007). This grid extended from longitude of 56 degrees to 79 degrees and ranged from latitude of 26 degrees to 41 degrees. These gridded results for a longitude 28.2 degrees to 38.2 degrees and latitude 65.5 degrees to 75.5 degrees were used as input into the hazard analysis.

8.3 PSHA Ground Motion Prediction Equations

8.3.1 Crustal Seismicity

Based on work completed by M.A. Shah et al., 2012, there is currently one region specific ground motion prediction equation for Northern Pakistan. This Ground Motion Prediction Equation (GMPE) is available for the calculation of the PGA for the magnitude range M5.8 to M7.6, and at distances greater than 20km. Comparison of the model proposed by M.A. Shah et al. 2012 with other Next Generation of Ground-Motion Attenuation Models (NGA) relationships shows that the PGA predicted by Shah's model is in good agreement with Abrahamson and Silva, 2008, and Campbell and Bozorgnia, 2008 (see Figure 13).

Since no region-specific ground motion prediction model is available to estimate all of the required spectral periods and magnitude ranges needed for both the PSHA and DSHA, those developed in the NGA project, which have been shown to be applicable worldwide, were considered. These GMPEs are the Abrahamson-Silva (2008), Boore-Atkinson (2008), Campbell-Bozorgnia (2008), Chiou-Youngs (2008) all of which provide horizontal PGA, and 5% damped elastic pseudo-response spectral accelerations in the period range of 0 to 10 seconds for shallow crustal earthquakes. The Idriss (2008) model was not selected to be used in this study due to the limitations in estimating events at distances larger than 150km. Several faults and areal sources were located at distances greater than 150km, such as the Chaman fault. Table 8-4 lists the relationships and the associated weights.

Table 8-4: Ground Motion Prediction Equations used in the PSHA for Crustal Faults

GMPE	Weight
Abrahamson & Silva (2008)	0.25
Boore & Atkinson (2008)	0.25
Campbell & Borzongia (2008)	0.25
Chiu and Young (2008)	0.25

8.3.2 Deep Events

There are no empirical relationships developed to calculate the ground motion from continental earthquakes 50-250km and deeper. Therefore, we rely on subduction zone ground motion prediction equations, specifically those for the deeper intraslab earthquakes. The GMPE used in this study along with the weights are presented in Table 8-5 In this analysis, deep continental earthquakes (> 50km) were modeled using relationships developed by BCHydro (2010), Zhao et al. (2006), and Youngs et al. (1997). These GMPEs were selected based on their applicability to the site and have been assigned different weights based on their suitability for the seismotectonic setting in

northwestern Pakistan. The Youngs et al (1997) equation as well as the Zhao et al. (2006) were run for rock site conditions which are assumed to be equal to the selected Vs30 of 760 m/s. The GMPE developed by Atkinson and Boore (2003) was not used in this study due to the strong scaling with depth. It should be noted that none of the models considered were developed specifically for deep continental earthquakes.

Table 8-5: Ground Motion Prediction Equations used in the PSHA for Deep Continental Earthquakes

GMPE	Weight
Youngs and others (1997), Rock	0.25
Zhao et al. (2006)	0.25
BCHydro (2010) Subduction - Variable Central DeltaC1	0.25
BCHydro (2010) Subduction - Variable Lower DeltaC1	0.13
BCHydro (2010) Subduction - Variable Upper DeltaC1	0.12

8.4 Other PSHA Parameters

The depth to top of coseismic rupture (Z_{TOR}) was assumed to be 0km for all planar faults, fault width (W) was assumed to be 15 km, the average shear-wave velocity in top 30 m of site profile (V_{s30}) was assigned to be 760 m/s, and 0.034 was used for the depth to 1.0 km/sec velocity horizon ($Z_{1.0}$) and 0.64 was used for the depth of 2.5 km/s shear-wave velocity horizon ($Z_{2.5}$).

8.5 PSHA Results

The PSHA calculates the annual frequency of exceeding a specified ground motion level. Ground motions at the project site are calculated for the average horizontal component of motion in terms of PGA and response spectral acceleration (SA) at 5% damping for oscillator periods between 0.01 and 10 seconds. The hazard curves are shown for four different sites: Kurram Tangi Main Dam, Kaitu Weir, Weir II and Weir III. The hazard curves are shown in Figure 14 through Figure 25, along with contributing sources. Figures 26 through 29, show the uniform hazard spectra for the six selected return periods of 145 years, 475 years, 975 years, 2500 year, 5000 year and 10,000 years (corresponding to 50,10, 5, 2, 1, 0.5 percent annual exceedence in 50 years). Tables 8-6, 8-8, 8-9 and 8-10 summarize the results for the six different return periods for the Main Dam, Kaitu Weir, Weir II, and Weir III. Discussion for each of the sites is presented in the following sections.

8.5.1 Kurram Tangi Main Dam

The results of the PSHA show that the Kurram Fault is a significant contributor to the PGA hazard after about 400 years to 850 years, afterwards the Karak Fault leads the hazard. For return periods less than 400 years, the Deep Background events have the greatest contribution to the PGA hazard curve. At a spectral acceleration of 0.2 seconds the Kurram Fault is again the single most contributors to the hazard at return periods greater than 200 years with the Karak Fault leading the hazard around 20,000 years. The Deep Background events controlling for the lower return periods (10 to about 200 years). Finally, at spectral acceleration of 1.0 second the hazard is controlled by the other crustal faults until a return period of about 1,000 years where the Murree Fault is the lead contributor to the hazard until about 3,000 years. For the remainder of the return periods the Kurram Fault contributes until about 15,000 years and then the Karak fault leads the hazard.

Table 8-6: Mean Probabilistic Ground Motion (g, freefield) for Kurram Tangi Dam Site

Period (sec)	Return Period (years)					
	145	475	975	2,475	5,000	10,000
0	0.09	0.18	0.26	0.43	0.59	0.80
0.08	0.09	0.18	0.26	0.43	0.59	0.80
0.1	0.11	0.23	0.33	0.54	0.75	1.02
0.15	0.16	0.32	0.46	0.77	1.06	1.45
0.2	0.18	0.36	0.53	0.87	1.21	1.65
0.25	0.21	0.42	0.61	1.01	1.44	1.96
0.3	0.21	0.42	0.61	1.03	1.48	2.03
0.4	0.20	0.39	0.57	0.96	1.39	1.91
0.5	0.18	0.36	0.53	0.89	1.27	1.76
0.6	0.15	0.31	0.45	0.76	1.08	1.51
0.75	0.13	0.27	0.39	0.65	0.93	1.27
1	0.12	0.23	0.34	0.56	0.82	1.10
1.5	0.097	0.196	0.285	0.475	0.677	0.923
1.75	0.072	0.149	0.218	0.367	0.513	0.708
2	0.046	0.096	0.141	0.235	0.333	0.453
3	0.038	0.081	0.120	0.201	0.278	0.384
4	0.032	0.069	0.102	0.170	0.237	0.320
5	0.018	0.043	0.064	0.108	0.148	0.203
7.5	0.012	0.028	0.044	0.074	0.105	0.138
10	0.010	0.022	0.033	0.058	0.083	0.113

8.5.1.1 Kurram Tangi Dam Site - Deaggregation

The hazard at the Kurram Tangi Dam site was deaggregated to evaluate which sources (faults), magnitudes and distance combinations are the strongest contributors to the hazard at a particular oscillator period and a particular return period (Figure 30 through Figure 38).

The deaggregation of hazard shows the probability density for selected distance and magnitude bins. A deaggregation was performed at the PGA and at periods of 0.2 and 1.0 seconds for the following return periods: 145, 475, and 10,000years (Figure 30 through Figure 38). These return periods were selected because they correspond to the recommended design guidelines (ICOLD, 2010), see Section 11. The deaggregation results are included in Table 8-7. The mean magnitude, distance and epsilon correspond to the average magnitude, distance and epsilon (number of standard deviations).

Table 8-7: Deaggregation Results for Dam Site

Return Period	Spectral Acceleration	Mean Magnitude	Mean Distance	Mean Epsilon
145	PGA	6.7	80	0.20
145	0.2s	6.6	74	0.28
145	1.0s	7.4	142	0.18
475	PGA	7.0	51	0.24
475	0.2s	6.9	46	0.31
475	1.0s	7.7	94	0.27
10,000	PGA	7.6	12	0.81
10,000	0.2s	7.6	11	0.82
10,000	1.0s	7.8	15	0.90

8.5.2 Kaitu Weir

Table 8-8: Mean Probabilistic Ground Motion (g, free field) for Kaitu Weir

Period (sec)	Return Period (years)					
	145	475	975	2,475	5,000	10,000
0	0.09	0.19	0.29	0.47	0.65	0.86
0.08	0.09	0.19	0.29	0.47	0.65	0.86
0.1	0.12	0.24	0.36	0.60	0.82	1.09
0.15	0.16	0.34	0.51	0.86	1.17	1.57
0.2	0.18	0.39	0.58	0.96	1.34	1.78
0.25	0.21	0.45	0.67	1.12	1.59	2.10
0.3	0.21	0.44	0.66	1.13	1.62	2.16
0.4	0.20	0.41	0.61	1.04	1.52	2.05
0.5	0.18	0.38	0.56	0.95	1.38	1.89
0.6	0.16	0.32	0.47	0.81	1.15	1.61
0.75	0.13	0.27	0.40	0.69	0.98	1.37
1	0.12	0.23	0.34	0.59	0.86	1.17
1.5	0.098	0.197	0.288	0.489	0.721	0.987
1.75	0.073	0.149	0.218	0.374	0.539	0.770
2	0.046	0.095	0.140	0.238	0.351	0.487
3	0.038	0.080	0.118	0.202	0.292	0.416
4	0.031	0.068	0.100	0.172	0.248	0.351
5	0.018	0.042	0.063	0.109	0.158	0.222
7.5	0.012	0.028	0.043	0.076	0.111	0.155
10	0.010	0.021	0.033	0.059	0.088	0.125

8.5.2.1 Kaitu Weir - Deaggregation

The hazard at the Kaitu Weir site was deaggregated to evaluate which sources (faults), magnitudes and distance combinations are the strongest contributors to the hazard at a particular oscillator period and a particular return period (Figure 39 through Figure 47).

The deaggregation of hazard shows the probability density for selected distance and magnitude bins. A deaggregation was performed at the PGA and at periods of 0.2 and 1.0 seconds for the following return periods: 145, 475, and 10,000 years (Figure 39 through Figure 47). These return periods were selected because they correspond to the recommended design guidelines (ICOLD, 2010), see Section 11.

8.5.3 Weir II

Table 8-9: Mean Probabilistic Ground Motion (g, freefield) for Weir II

Period (sec)	Return Period (years)					
	145	475	975	2,475	5,000	10,000
0	0.09	0.18	0.25	0.41	0.57	0.78
0.08	0.09	0.18	0.25	0.41	0.57	0.78
0.1	0.11	0.22	0.32	0.52	0.72	0.99
0.15	0.15	0.31	0.45	0.73	1.02	1.40
0.2	0.18	0.35	0.51	0.84	1.16	1.60
0.25	0.20	0.41	0.59	0.97	1.38	1.90
0.3	0.21	0.41	0.59	0.99	1.42	1.97

0.4	0.19	0.38	0.56	0.93	1.33	1.85
0.5	0.18	0.36	0.51	0.86	1.23	1.71
0.6	0.15	0.30	0.44	0.74	1.04	1.46
0.75	0.13	0.26	0.38	0.63	0.90	1.24
1	0.114	0.228	0.330	0.547	0.791	1.069
1.5	0.097	0.194	0.280	0.463	0.657	0.901
1.75	0.072	0.147	0.215	0.357	0.500	0.688
2	0.045	0.096	0.139	0.230	0.324	0.442
3	0.038	0.081	0.118	0.197	0.271	0.372
4	0.031	0.069	0.101	0.166	0.231	0.311
5	0.018	0.043	0.064	0.106	0.144	0.197
7.5	0.012	0.028	0.044	0.073	0.102	0.134
10	0.010	0.021	0.033	0.057	0.080	0.110

8.5.3.1 Weir II - Deaggregation

The hazard at the Weir site was deaggregated to evaluate which sources (faults), magnitudes and distance combinations are the strongest contributors to the hazard at a particular oscillator period and a particular return period (Figure 48 through Figure 56).

The deaggregation of hazard shows the probability density for selected distance and magnitude bins. A deaggregation was performed at the PGA and at periods of 0.2 and 1.0 seconds for the following return periods: 145, 475, and 10,000 years (Figure 48 through Figure 56). These return periods were selected because they correspond to the recommended design guidelines (ICOLD, 2010), see Section 11.

8.5.4 Weir III

Table 8-10: Mean Probabilistic Ground Motion (g, freefield) for Weir III

Period (sec)	Return Period (years)					
	145	475	975	2,475	5,000	10,000
0	0.09	0.17	0.23	0.37	0.51	0.70
0.08	0.09	0.17	0.23	0.37	0.51	0.70
0.1	0.11	0.21	0.29	0.46	0.64	0.88
0.15	0.15	0.29	0.41	0.65	0.90	1.23
0.2	0.17	0.32	0.46	0.74	1.03	1.42
0.25	0.19	0.37	0.53	0.86	1.21	1.67
0.3	0.20	0.38	0.54	0.87	1.24	1.73
0.4	0.18	0.36	0.51	0.83	1.17	1.64
0.5	0.17	0.33	0.47	0.77	1.09	1.53
0.6	0.15	0.29	0.41	0.66	0.94	1.30
0.75	0.13	0.25	0.35	0.57	0.81	1.12
1	0.11	0.22	0.31	0.50	0.71	0.97
1.5	0.094	0.186	0.264	0.427	0.598	0.829
1.75	0.070	0.142	0.205	0.329	0.460	0.630
2	0.044	0.092	0.132	0.215	0.298	0.410
3	0.037	0.078	0.113	0.182	0.251	0.342
4	0.031	0.066	0.097	0.154	0.215	0.289
5	0.018	0.041	0.061	0.100	0.135	0.183
7.5	0.012	0.027	0.042	0.068	0.096	0.126
10	0.010	0.021	0.031	0.054	0.075	0.103

8.5.4.1 Weir III - Deaggregation

The hazard at the Weir III site was deaggregated to evaluate which sources (faults), magnitudes and distance combinations are the strongest contributors to the hazard at a particular oscillator period and a particular return period (Figure 57through Figure 65).

The deaggregation of hazard allows the probability density to be evaluated for selected distance and magnitude bins. A deaggregation was performed at the PGA and at periods of 0.2 and 1.0 seconds for the following return periods: 145, 475, and 10,000 years (Figure 57 through Figure 65). These return periods were selected because they correspond to the recommended design guidelines (ICOLD, 2010), see Section 11. The deaggregation results are included in Table 8-11. The mean magnitude, distance and epsilon correspond to the average magnitude, distance and epsilon (number of standard deviations).

Table 8-11: Deaggregation Results for Weir III

Return Period	Spectral Acceleration	Mean Magnitude	Mean Distance	Mean Epsilon
145	PGA	6.7	89	0.28
145	0.2s	6.7	81	0.36
145	1.0s	7.4	149	0.21
475	PGA	7.0	61	0.37
475	0.2s	7.0	55	0.43
475	1.0s	7.7	103	0.35
10,000	PGA	7.5	15	0.66
10,000	0.2s	7.5	13	0.70
10,000	1.0s	7.7	21	0.79

8.6 Comparison to other Studies

Previous PSHA have been completed for Northwestern Pakistan at each of the major cities. This project is the closest to the city of Bannu (approximately 30 km north, northwest – longitude 70.6056 and latitude 32.9889). Therefore, the hazard was also calculated using the models implemented in this study for the city of Bannu.

Monalisa et al. (2007) using the Ambraseys et al. (1996) and Boore et al. (1997) attenuation relations calculated a PGA of 0.07g for a return period of 475 years. The Pakistan Meteorological Department and NORSAR (2006) using the attenuation model proposed by Ambraseys et al. (1996) present a slightly higher value of 0.08g for a return period of 500 years. Finally, B. Kim (2012) in his dissertation calculated a PGA of 0.16g using all five of the NGA relations (Abrahamson-Silva (2008), Boore-Atkinson (2008), Campbell-Bozorgnia (2008), Chiou-Youngs (2008), and Idriss (2008)). This study calculated a PGA of 0.15g using all of the NGA relations except for Idriss (2008), see Section8.3.1. The Monalisa et al. (2007) and the Pakistan Meteorological Department and NORSAR (2006) hazard studies only included diffuse areal source zones and did not include fault sources. The increase in PGA shown in Kim's work and in this study can be explained by the inclusion of the active Karak fault which is located less than 10 km from the city of Bannu and the difference in selection of ground motion prediction equations. As discussed previously the Idriss (2008) equation was not used in this study due to the limitations in estimating events at distances larger than 150km.

This Page Left Blank Intentionally

9 DETERMINISTIC SEISMIC HAZARD ANALYSIS (DSHA)

A deterministic analysis considers only one scenario for each earthquake source. The methodology, inputs and results are included below.

9.1 DSHA Methodology

The approach used for the DSHA generally follows the procedures developed by Kramer (1996), as summarized below:

1. Identify and characterize sources capable of producing significant ground motions at the site.
2. Select source to site distance parameters for each source zone, consistent with the selected GMPE.
3. Select the controlling earthquake.
4. Define the hazard at the site in terms of ground motions produced by the controlling earthquake.

9.2 DSHA Inputs

The main dam and all of the weirs are located on the footwall of the Kurram Thrust and the hanging wall of the Karak Thrust. The Kurram and Karak thrust faults were considered as primary sources in the deterministic analysis along with the Murree Fault or western portion of the Main Boundary Thrust. Several other faults located at distances greater than 50km were not considered in the deterministic analysis. **Table 9-1** contains the three faults considered in the deterministic analysis and the input parameters. The Wells and Coppersmith (1994) equation, for all faults using the surface rupture length assumed for full fault rupture, was used to develop the maximum magnitude. The depth to top of coseismic rupture (Z_{TOR}) was assumed to be 0km, fault width (W) was assumed to be 15km, the average shear-wave velocity in top 30m of site profile (V_{s30}) was assigned to be 760 m/s, and 0.034 was used for the depth to 1.0 km/sec velocity horizon ($Z_{1.0}$) and 0.64 was used for the depth of 2.5 km/s shear-wave velocity horizon ($Z_{2.5}$). A dip of 30 degrees was assumed for all faults. The same GMPE that were used in the PSHA were again used for the deterministic analysis. The region specific GMPE developed by M.A. Shah et al., 2012, was not used to calculate the PGA because the distances and/or maximum magnitudes were outside the range for which the equation was developed.

Table 9-1: Faults considered in Deterministic Seismic Hazard Analysis

Fault	Maximum Magnitude	Distance (km)[1]	Dip (degrees)	Rupture Distances(km) R_{RUP}, R_{JB}, R_X
		MAIN DAM		
Kurram Thrust	7.8	6	30	6,6,6
Karak Thrust	7.4	7	45	5,0,7
Murree Fault (MBT)	8.0	47	30	47,47,47
		KAITU WEIR		
Kurram Thrust	7.8	1	30	1,1,1
Karak Thrust	7.4	11	45	7.8,0,11
Murree Fault	8.0	53	30	53,53,53

(MBT)				
			WEIR II	
Kurram Thrust	7.8	8	30	8,8,8
Karak Thrust	7.4	5	45	3.5,0,5
Murree Fault (MBT)	8.0	48	30	48,48,48
			WEIR III	
Kurram Thrust	7.8	14	30	14,14,14
Karak Thrust	7.4	1	45	0.7,0,1
Murree Fault (MBT)	8.0	53	30	53,53,53

Notes: 1. Distance from project site to surface trace.

9.3 DSHA Results

The results of the deterministic analysis are summarized in Table 9-2 and Figures 66 and 73. These results show that the controlling fault for all of the sites is the Karak Thrust Fault located at a distance range of 1km to 6km from the project features. This fault is shown to have a maximum magnitude of 7.4 and a maximum median PGA of 0.74g, and an 84th percentile PGA of 1.27g. All of the weirs and the main dam are located on the hanging wall of the Karak thrust which causes the extreme hazard, as shown in the high PGAs.

Table 9-2: PGA for Deterministic Assessment

Fault	Maximum Magnitude (Mw)	Distance (km)[1]	NGA Peak Ground Acceleration (PGA)g	
			50th percentile	84th percentile
			MAIN DAM	
Kurram Thrust	7.8	6	0.39	0.67
Karak Thrust	7.4	7	0.70	1.20
Murree Fault (MBT)	8.0	47	0.12	0.21
			KAITU WEIR	
Kurram Thrust	7.8	1	0.56	0.96
Karak Thrust	7.4	11	0.62	1.07
Murree Fault (MBT)	8.0	53	0.11	0.19
			WEIR II	
Kurram Thrust	7.8	8	0.34	0.59
Karak Thrust	7.4	5	0.74	1.27
Murree Fault	8.0	48	0.12	0.21

(MBT)				
WEIR III				
Kurram Thrust	7.8	14	0.26	0.44
Karak Thrust	7.4	1	0.72	1.24
Murree Fault (MBT)	8.0	53	0.11	0.19
Notes: [1]Distance from project site to surface trace.				

This Page Left Blank Intentionally

10 RESERVOIR TRIGGERED SEISMICITY (RTS)

Reservoir-triggered seismicity (RTS) is a phenomenon, which although accepted by the scientific community is not well understood, and is difficult to predict. At this time, RTS is described as earthquake events that are triggered by the filling of a reservoir, or by water-level changes or fluctuations during operation of the reservoir. It is believed that RTS primarily represents the release of pre-existing tectonic strain, with the reservoir being only a perturbing influence (Yeats et al, 1997; USCOLD, 1997; ICOLD, 2011). Thus, the reservoir does not actually cause or induce the seismicity, it merely triggers the release of the accumulated, naturally occurring tectonic strain that already existed. In this regard, the term "triggered seismicity" is currently preferred over "induced seismicity" (the former terminology used until about the late 1980's). RTS events occur only as a result of the incremental effects of reservoir load and the build-up of pore water pressure to make them happen.

Throughout the world, several thousand dams have been constructed and are impounding reservoirs which are operating without any observed RTS. Compared to the large number of operating reservoirs, there are only a very few instances of possible RTS cases. Out of some 11,000 worldwide "large" dams, only a small number have triggered known seismic activity (USCOLD, 1997). A large dam according to the ICOLD definition is one more than 33 feet (15 m) high or one between 33 and 49 feet (10 and 15 m) high satisfies one of the following criteria:

- more than 1640 feet (500 m) long;
- reservoir capacity exceeding 811 acre-feet (1 Mm3, or 1 x 106 m3); or
- spillway capacity exceeding 70,629 ft3/s (2,000 m3/s)

Gupta (2002) reports, more than 90 sites have been identified globally where earthquakes have been triggered by filling of water reservoirs. It is uncommon for a reservoir to experience RTS, 0.08%, based on 11,000 reservoirs of which 90 experienced RTS. At those reservoirs where RTS has been suspected, the maximum reported earthquake magnitudes for RTS events are primarily much less than M 6.0 (M is assumed equivalent to Mw), and typically in the micro earthquake, or small macro earthquake range (i.e., < M 4.0). These are nearly all below the range felt by humans and are only detectable by local seismographs.

Kurram Tangi Dam is proposed to be a concrete face rock fill dam with a height of 322 feet (98 meters) and a length of 1035 feet (316 meters). Based on ICOLD's Bulletin, *Reservoirs and Seismicity: State of Knowledge* (2011), it is suggested that dams correctly designed are fully covered against the possible triggered event. For example, in this study the safety evaluation earthquake (SEE) for the dam site is above the 50th percentile deterministically-evaluated with a magnitude 7.4 located on the Karak Fault at a R_{RUP} distance of 5km; this would also be the largest RTS event that could occur based on the seismotectonic framework (see **Section 9.2**). Structures and facilities in the vicinity of the dam may or may not be correctly designed to withstand this RTS event. However, it is unlikely that a RTS event could occur.

10.1 Characteristics of Reservoir-Triggered Seismicity

Research into the causes of RTS, based on its nature, pattern and geophysical and geo-mechanical characteristics as well as statistical and empirical evaluations of the occurrence of RTS have resulted in the identification of several physical, tectonic, and geologic characteristics that appear to be common to RTS cases, and contribute to the incidence of RTS (USCOLD, 1997). The attributes that are considered in evaluating the probability of RTS include;

a) reservoir depth;
b) reservoir volume;
c) the tectonic stress state; and
d) the rock type underlying the reservoir.

The probabilities are considered conditional and represent the total chance for RTS to occur as a result of reservoir filling and operation. Conditional probabilities are developed for each single attribute, as well as for all the attributes combined.

Reservoir Parameters: The filling history and the rate of filling appear to be important regarding the potential for and triggering of RTS. RTS is more likely where a reservoir is filled rapidly. The maximum water depth and the maximum reservoir volume appear to be the most significant factors in the generation of RTS. RTS is more likely at deep reservoirs (i.e. greater than about 90 m), than at shallower reservoirs, and it is more likely where the reservoir volume is greater than about 1.0E10 cubic meters. The Kurram Tangi reservoir will have a maximum depth 268 feet (82 meters), and a maximum volume of about 0.914 million acre-feet (1,127 million m^3). The depth was estimated from dam height and type as done by Packer et al. (1979). The formula is as follows: earth or rock dams less than 100 meters in height, the dam height was multiplied by 0.90.

Geologic and Hydrogeologic Parameters: RTS appears to be more common where reservoirs are underlain by sedimentary rock sequences compared to metamorphic and igneous terrains. In addition, more permeable lithologies appear to be more susceptible to RTS because they may allow more effective pore-water pressure increases at depth. The Kurram Tangi reservoir is underlain by sedimentary and metamorphic bedrock units.

Tectonic Parameters: The presence of pre-existing active tectonics is important. Most, if not all reported cases of RTS with earthquakes greater than magnitude M=5.0 had pre-existing active faults in the Area of Influence (AOI) of the reservoir. In addition, areas with active extensional (e.g., normal-slip faults) or shear (e.g., strike-slip faults) stress/tectonics are more likely to have RTS than areas with active compressional (e.g., reverse-slip faults) stress / tectonics. RTS is not likely to occur in areas lacking active tectonics, and it is not likely to re-activate, faults that are inactive in their current tectonic regimes. The Kurram Tangi reservoir is located in a regional reverse-slip or thrust-type tectonic regime. One or more potentially active faults within 6km of the reservoir area could be activated due to RTS.

10.2 RTS Empirical Calculations

For the Kurram Tangi Dam Project, the conditional probability of RTS was calculated using the methodology of Baecher and Keeney (1982) using the deep, very deep dataset. The definitions for reservoir attribute states from Baecher and Keeney (1982) are presented in Table 10-1 below.

Table 10-1: Definitions for Reservoir Attribute States

Attribute	State			
	1	2	3	4
Depth	d_1 very deep(over 150m)	d_2 deep(92 to 150m)	$d_3$shallow(less than 92m)	$d_4$not known
Volume	v_1 very large(over 100 x $10^8 m^3$)	v_2 large(12 to 100 x $10^8 m^3$)	$v_3$small(less than 12 x $10^8 m^3$)	$v_4$not known
Stress State	s_1 extensional	$s_2$compressional	$s_3$shear	$s_4$not known
Fault Activity	f_1 active fault	$f_2$no active faults present	$f_3$not known	
Geology	g_1 sedimentary	$g_2$metamorphic	$g_3$igneous	$g_4$not known

Source: Baecher and Keeney, 1982
Notes: The abbreviations used in the table are: d, depth; v, volume; s, stress state; f, fault activity; g, geology.

Kurram Tangi reservoir has the following attributes:

Reservoir depth:	Shallow (86 m) - *State 3*;
Reservoir volume:	Small (11.3 million m^3) - *State 3*;
Tectonic stress state:	Thrust (reverse-slip faulting environment) - *State 2*
Fault Activity:	Active- *State 1*; and
Geology:	Sedimentary- *State 1*.

Table 10-2 shows the results of the single attribute analysis for the dataset compiled by Baecher and Keeney (1982); corresponding probabilities for the project are in bold.

Table 10-2: Single Attribute Analysis – Conditional Probability of RTS Given Only One Attribute

Attributes	State		
	1	2	3
Depth	0.27 [0.24]	0.11 [0.10]	
Volume	0.25 [0.22]	0.23 [0.21]	**0.09** [0.07]
Stress State	0.11	**0.14**	0.17
Fault Activity	**0.20**	-	-
Geology	**0.20**	0.10	0.12-

Source: Baecher and Keeney, 1982. Round off errors were identified, but not revised, see brackets for reported values. See Table 16 for assigned states (1-3).

10.2.1 Single Attribute Analysis

The single attribute analysis looks at the conditional probability of RTS given only one reservoir attribute (depth, volume, stress state, fault activity or geology). This analysis assumes that the attributes are independent of each other. The results are presented based on the deep or very deep reservoir criteria. With these reservoir attributes, the single attribute conditional probabilities for RTS at the Kurram Tangi Project range from 0.09 to 0.20 (i.e. there would be 9 percent to 20 percent chance of RTS occurring as a result of reservoir filling and operation, see Table 10-2 for corresponding values in bold).

10.2.2 Multi-Attribute Analysis

Independent discrete, dependent discrete and dependent mixed (discrete / continuous) cases were calculated using a multi-attribute analysis. The first analysis, independent discrete, calculates the probability of RTS assuming independence between the attributes. The second analysis, dependent discrete, calculates the probability of RTS based on correlations between discrete volume and depth. The third analysis, dependent mixed case, is based on the correlation between continuous depth and volume and the other states (stress state, faulting and geology) are independent discrete. A probability of 1 was assumed if data was not available for any of the attributes.

The results for the independent discrete analysis are 18 percent, dependent discrete is 28 percent and the dependent continuous is 25 percent. Again, this only means that there is an 18 -28 percent chance that a RTS event of any magnitude could occur.

10.2.3 Conclusions on Reservoir-Triggered Seismicity

The Kurram Tangi Dam Project will have a shallow and small reservoir, which puts the likelihood of RTS occurring as very low. A probability of 1 was assumed for any of the components that were not available due to data constraints- this is shown in Table 10-2, where there is no data for shallow reservoirs or a depth State 3. This occurred for both the depth and volume in the multi-attribute analysis for the dependent discrete and dependent mixed. This is because there are no data available for small and shallow reservoirs that have had RTS. This is not to say RTS did not occur at the site only that it was not large enough to be detected. The resulting magnitude from RTS is estimated to be less than M 5.0. In the context of the design event (M>7.4) used in the DSHA, this is thought to pose little additional hazard to the project.

Available geologic data and geological studies carried out on satellite imagery suggest that there is no likelihood of rock slides around the dam and on the reservoir rims. Therefore, the hazard of rockslides during a strong earthquake is insignificant.

This Page Left Blank Intentionally

11 CONCLUSIONS AND RECOMMENDATIONS FOR DESIGN BASIS EARTHQUAKE

ICOLD guidelines for Large Dams were followed to provide guidance on the Safety Evaluation Earthquake (SEE), Operating Basis Event (OBE) and the Design Earthquake for the dam and appurtenant structures. A list of project features was provided by the Design Consultant (MMP, 2013).

11.1 Discussion on Recommended Design Criteria

11.1.1 Safety Evaluation Earthquake

Because the dam is a high hazard structure, with large potential consequences in terms of life and property should it fail catastrophically, it is recommended that the Safety Evaluation Earthquake (SEE) be defined as the 10,000 year return period event. This guidance is based on (ICOLD) Bulletin 72 (2010):

> "The Safety Evaluation Earthquake (SEE) is the maximum level of ground motion for which the dam should be designed or analyzed. For dams whose failure would present a great social hazard the SEE will normally be characterized by a level of motion equal to that expected at the dam site from the occurrence of a deterministically-evaluated maximum credible earthquake or of the probabilistically-evaluated earthquake ground motion with a very long return period, for example 10,000 years. Deterministically-evaluated earthquakes may be more appropriate in locations with relatively frequent earthquakes that occur on well-identified sources, for example near plate boundaries. The SEE ground motion shall be taken as the maximum of the probabilistically and deterministically-evaluated ground motions."

It is common practice in California to use the 50th percentile DSHA results for those events occurring on faults with a slip rate less than 1 mm/yr. The Karak fault, the controlling event for all sites, has a slip rate of 0.72 mm/yr; therefore the 50th percentile was compared to the 10,000 year return period. Previous studies conducted for this project only performed a deterministic assessment at the dam site and used the median or 50th percentile event, which led to a PGA of 0.2g. This is not in keeping with current ICOLD guidelines which define the SEE as deterministically evaluated earthquake or 10,000 year return period event, whichever is greater. As shown in **Figure 10-2,** the MCE is defined as the 50th percentile event occurring on the Karak Thrust Fault with a maximum magnitude of 7.4 at a R_{RUP} distance of 6km. Therefore the 10,000 year return period event, as calculated from the PSHA, is recommended as the SEE. The PGA from the 10,000 year event at the dam site has a PGA of 0.80g.

It is further recommended by ICOLD that the SEE should be used as the design event for all components of the dam necessary for retaining or controlling water and for those critical for dam safety.

11.1.2 Operating Basis Earthquake

Again following ICOLD guidelines the Operating Basis Earthquake represents the level of ground motion at the dam site for which only minor damage is acceptable. ICOLD recommends the following:

> "The dam, appurtenant structures and equipment should remain functional and damage should be easily repairable, from the occurrence of earthquake shaking not exceeding the OBE. In theory the OBE can be determined from an economic risk analysis but this is not always practical or feasible. In many cases, it will be appropriate to choose a minimum return period of 145 years (i.e. a 50 % probability of not being exceeded in 100 years). Since the consequences of exceeding the OBE are normally economic, it may be justified to use a more severe or less value."

Therefore it is recommended that the OBE be defined as the 145 year event as calculated from the PSHA.

11.1.3 475 Year Return Event or Local Building Code

Finally, it is recommended that the design basis for appurtenant structures, excluding those that are critical for dam safety, be the 475 year return period event. It is further recommended that the local seismic building code be followed if it is greater than the 475 year event, as presented in this report.

11.2 Evaluation of Design Criteria

By separating all components into critical or non-critical structures the design criteria can be evaluated. The definition of a critical structure and non-critical structure are as defined in ICOLD, 2002.

> – ***Critical structures:*** A critical structure is one whose seismic failure is the loss of function or damage which could lead to failure of the main dam and/or other important appurtenant structures. Failure may result in uncontrolled releases of water from the reservoir, and/or generate unacceptable downstream hazard. The design should provide a structure able to safely withstand the MDE, it means a structure able to operate and make releases to protect the dam against failure.
>
> – ***Non-critical structures****:* a non-critical structure or "non-safety related" structure is one in which failure or damage would not lead to failure of and /or damage to the main dam, nor would it inhibit the making of required releases to protect the dam. The design should provide a structure able to operate after the OBE.

ICOLD guidelines recommend that if the safety of a dam is critically dependent on operability of an associated structure, then the structure should be designed to resist the SEE. Table 11-1 attempts to evaluate each of the components and establish design criteria; however the final evaluation of seismic safety should be based on engineering judgment and experience with similar structures. A site specific seismic hazard evaluation was included for the main dam, Kaitu Weir, Weir II and Weir III; the recommended design criteria shown in Table 11-1 should use the hazard evaluation that is the closest to the identified feature.

Table 11-1: List of Project Features and Recommended Design Criteria

Feature	Recommended Design Criteria	Ground Motion (PGA, horizontal)[3](g)			Critical Structure
		SEE	475	OBE	
Main Dam	SEE, 475& OBE	0.80	0.18	0.09	Yes
Spillway –Gated Structure This includes the ability to access the gate controls and operate the spillway gates after an earthquake	SEE, 475 & OBE	0.80	0.18	0.09	Yes
Protective Dike for Spillway	OBE	-	-	0.09	No
Diversion Tunnels[1]	SEE, 475 & OBE	0.80	0.19	0.09	Yes
Kaitu Weir (18 feet high)	475 & OBE	-	0.19	0.09	No
Weir II (26 feet high)	475 & OBE	-	0.18	0.09	No
Weir III (75 feet high)[2]	SEE, 475& OBE	0.70	0.17	0.09	Yes
Powerhouses	475 & OBE	-	0.19	0.09	No
Powerhouse Appurtenant Structures	475 & OBE	-	0.19	0.09	No
a. Tunnel (not including portals)	475 & OBE	-	0.19	0.09	No

b. Penstock	475 & OBE	-	0.19	0.09	No
Emergency power sources and control panels	SEE, & 475	0.80	0.19	0.09	Yes

Notes: 1. Potential failure of the valves, gates, and associated structural elements could result in uncontrolled release of the reservoir. 2. Failure may generate unacceptable downstream hazard. 3. If the feature listed has several locations the ground motion values are presented for the highest PGA, the structure (i.e. Main Dam or Weir) that is closest to the identified feature should be used.
SEE: Safety Evaluation Earthquake, 475: 475 Year Return Period Event, OBE: Operating Basis Earthquake

This Page Left Blank Intentionally

12 LIMITATIONS AND RECOMMENDATIONS FOR ADDITIONAL STUDIES

This study was based on an assigned shear wave velocity in the top 30 m (V_{S30}) of 760 m/s, which generally corresponds to soft rock. Surface geology can significantly influence the amplitude, frequency content and duration of seismic motions felt at the ground surface. Therefore, if it is found that during further investigations the selected shear wave velocity is no longer valid then the results of the PSHA and DHSA should be recomputed or run through a computer program (such as SHAKE)for conducting equivalent linear seismic response analyses of horizontally layered soil deposits. It is further recommended that all major structures be founded on bedrock due the potential for liquefaction.

Two active faults, as identified by NESPAK, are located within1km to 6km of the main dam and weirs. It was assumed that the main dam and weirs are located on the footwall of the Kurram Fault and the hanging wall of the Karak Fault. It is recommended that these faults be clearly mapped and if the location or distances to any of these faults differ then the PSHA and DSHA the results be revised. Ground motions on sites located on the hanging wall are significantly higher than those located on the footwall.

The hazard curves and deaggregations are presented in terms of the PGA, 0.2 second, and 1.0 second spectral acceleration. If time histories are to be developed, then the period of interest should be calculated for that structure and then a deaggregation can be performed for the specified period or period range.

This Page Left Blank Intentionally

13 REFERENCES

Abrahamson, N. (2005, Spring). Course Notes. *State of the Practice of Seismic Hazard Evaluation.* Berkeley, CA.

Abrahamson, N. A., & Silva, W. J. (1997). Empirical Response Spectral Attenuation Relations for Shallow Crustal Earthquakes. *Seismological Research Letters, vol. 68, no. 1*, 94-127.

Abrahamson, N., & Silva, W. (2008, February). Summary of the Abrahamson & Silva NGA Ground-Motion Relations. *Earthquake Spectra Vol. 24, No.1*, 67-97.

Ahmad, S., Ali, F., Sayab, M., Ahmad, I., & Hamidullah, S. (1999). Structural geometry of the Himalayan Frontal Thrust Zones: Surghar Range, Pakistan. *Geological Bulletin, University of Peshawar, Pakistan.*

Ahmed, S. (2003). *A comparative study of structural style in the Kohat plateau, Northwest Himalayas.* National Center of Excellence in Geology, University of Peshwar, Pakistan: Unpublished Ph D. Thesis.

Ambraseys et al. (1975). The Patan Earthquake of 24 December1974. *UNESCO Publication.*

Ambraseys, N. N., & Bommer, J. J. (1990). Uniform magnitude re-evaluation for the strong motion database of Europe and adjacent areas. *European Earthquake Engineering, Vol.4 No.2.*

Ambraseys, N., & Bilham, R. (2000). *A note on the Kangra Ms = 7.8 earthquake of 4 April 1905.* Current Science 79.

Ambraseys, N., & Bilham, R. (2003). *Earthquakes in Afghanistan.* Seismological Research Letters, v. 42.

Ambraseys, N., & Bilham, R. (2009). The tectonic setting of Bamiyan and seismicity in and near Afghanistan for the past 12 centuries. In C. Margottini (Ed.), *UNESCO Special Publication: The Destruction of the Giant Buddha Statues in Bamiyan, Central Afghanistan, UNESCO's emergency activities for the recovering and rehabilitation of cliff and niches.* (pp. 67-94).

Ambraseys, N., & Bilham, R. (n.d.). *The tectonic setting of Bamiyan and seismicity in and near Afghanistan for the past 12 centuries.*

Ambraseys, N., & Simpson. (2001, January). 1996, Relationship for Attenuation of Ground Motions, Summary of Published Attenuation Relations for Peak Ground Acceleration. *ESEE report No. 01-1.*

Anglin, F. M., & Buchbinder, G. G. (1985). Induced seismicity at the LG3 Reservoir, James Bay, Quebec, Canada. *Bulletin of the Seismological Society of America, 75*(4), 1067-1076.

Atkinson, G. M., & Boore, D. M. (2003). Empirical ground-motion relations for subduction-zone earthquakes and their application to Cascadia and other regions. *Bulletin of Seismological Society of America, v. 93*, 1703-1729.

Avouac et al. (2006). The 2005, Mw 7.6 Kashmir earthquake: Sub-pixel correlation of ASTER images and seismic waveforms analysis. *Earth and Planetary Science Letters 249*, 514-528.

Baecher, G. B., & Keeney, R. L. (1982, April). Statistical Examination of Reservoir-Induced Seismicity. *Bulletin of the Seismological Society of America, 72 No.2*, 553-569.

BC Hydro. (2010). *PSHA for Western Canada: Volume 3-Ground Motion Models, BC Hydro Report E658.* Vancouver, Canada: BC Hydro.

Bergman, E. A. (2006). *A comprehensive earthquake catalogue for the Afghanistan region, in Dewey, J.W.,ed., Seismicity of Afghanistan and Vicinity.* U.S. Geological Survey Open-File Report 2006–1185.

Bergman, E. A., & Engdahl, E. R. (n.d.). *The seismicity pattern of the 2008 Wenchuan, China, Mw 7.9 mainshock and aftershocks from a calibrted multiple event relocation technique.* University of Colorado at Boulder.

Bergman, E. A., Engdahl, E. R., Ruomei, S., & Zhongliang, W. (n.d.). The Seismicity Pattern of the 2008 Wenchuan, China, Mw 7.9 Mainshock and Aftershocks from a Calibrated Multiple Event Relocation Techique.

Bernard, M., Shen-Tu, B., Holt, W. E., & Davis, D. M. (2000). *Kinematics of active deformation in the Sulaiman Lobe and Range, Pakistan.* Journal of Geophysical Research.

Bilham, R., & Ambraseys, N. (2004). Apparent Himalayan slip deficit from summation of seismic moments for Himalayan earthquakes, 1500-2000. *Current Science.*

Bilham, R., & Wallace, K. (2005). Future Mw>8 earthquakes in the Himalaya: implications from the 26 Dec 2004 Mw=9.0 earthquake on India's eastern plate margin. *Geological Survey India, Special Publication 85*, 1-14.

Boore et al. (1997). Equations for Estimating Horizontal Response Spectra and Peak Acceleration from Western North American Earthquakes: A Summary of Recent Work. *Seismological Research Letters, vol. 68, no. 1*, 128-153.

Boore, D. M., & Atkinson, G. M. (2008, February). Ground-Motion Prediction Equations for the Average Horizontal Component of PGA, PGV, and 5%-Damped PSA at Spectral Periods between 0.01 s and 10.0 s. *Earthquake Spectra, Volume 24, No. 1*, 99-138.

Bossart et al. (1984). A new structural interpretation of the Hazara-Kashmir Syntaxis (southern Himalaya) Pakistan . *Kashmir Journal Geology Vol.2.*

Boyd, O. S., Mueller, C. S., & Rukstales, K. S. (2007). *Preliminary probablistic seismic hazard maps for Afghanistan.* U.S. Geological Survey Open-File Report 2007-1137.

Burchfiel, B. C., Royden, L. H., van der Hilst, R. D., Chen, Z., King, R. W., Li, C., et al. (2008). A geological and geophysical context for the Wenchuan earthquake of 12 May 2008, Sichuan, People's Republic of China. *GSA Today*, 4-11.

Calkin et al. (1975). Geology of the southern Himalaya in Hazara, Pakistan and adjacent areas. *U.S. Geological Survey, Professional Paper 716-C*, C 1-29.

Campbell, K. W., & Bozorgnia, Y. (2008). NGA ground motion model for the geometric mean horizontal component of PGA, PGV, PGD and 5% damped linear elastic response spectra for periods ranging from 0.01 to 10 s. . *Earthquake Spectra 24*, 139-171.

Chiou, B. S., & Youngs, R. R. (2008). An NGA Model for the Average Horizontal Component of Peak Ground Motion and Response Spectra. *Earthquake Spectra 27*, 173-215.

Cornell, C. A. (1968). Engineering seismic riks analysis. *Bulletin of Seismological Society of America, Vol.58, No. 5*, 1583-1606.

Coward et al. (1986). Tectonics in the NW Himalayas. (M. P. Coward, & A. C. Rie, Eds.) *Geological Society London Special Publication 19*, 203-219.

Dahm, T. e. (2012). Recommendation for the discrimination of human-related earthquakes. *Journal of Seismology*.

Delinger, R. P., & Bufe, C. G. (1982). Reservoir conditions related to induced seismicity at The Geysers steam reservoir, Northern California. *Bulletin of the Seismological Society of America, 72*(4), 1317-1327.

Dinske, C., & Shapiro, S. A. (2012). Seismotectonic state of reservoirs inferred from magnitude. *Journal of Seismology*.

Division of Safety of Dams (DSOD). (2002). *Guidelines for Use of the Consequence-Hazard Matrix for Selection of Ground Motion Parameters.* Department of Water Resources.

Elan Partners (Pvt.) Ldt. (2012). *Rapid Assesment Kurram Tangi Dam Construction.* Islamabad: Elan Partners (Pvt.) Ldt.

Fineti et al. (1979). The Pakistani segment of the DSS-profile Nanga Parbat - Karakul (1974-1975). *Bollettino Geofisico Teorica ed Applicata 21*, 159-169.

Frankel, A., Mueller, C., Barnhard, T., Perkins, D., Leyendecker, E., Dickman, N., et al. (1996). *National seismic-hazard maps - Documentation June 1996.* U.S. Geological Survey Professional Paper 1515.

Gansser, A. (1964). *Geology of the Himalaya.* London: Wiley Inter-Science.

Greco, A. (1991). Stratigraphy, metamorphism and tectonics of the Hazara-Kashmir syntaxis area. *Kashmir Journal Geology Vol. 8 & 9*.

Gupta, H. K. (2002). *A review of recent studies of triggered earthquakes by artificial water reservoirs with special emphasis on earthquakes in Koyna, India.* Earth-Science Reviews.

Gupta, H. K., & Rajendran, K. (1986). Larg artificial water reservoirs in the vicinity of the Himalayan foothills and reservoir-induced seismicity. *Bulletin of the Seismological Society of America, 76*(1), 205-215.

Heukroth, & Karim. (1970). Earthquake history, seismicity and tectonics of the regions of Afghanistan. *Seismic Centre, Kabul University*.

Hilderbrand et al. (2001). An old origin for an active mountain range: geology and geochronology of the eastern Hindu Kush, northwest Pakistan. *Geolgical Society of America Bulletin No. 113*, 625-639.

Hussain, A., & Yeats, R. S. (2006). The Balakot-Bagh Fault that triggered the October 8,2005 earthquake and other Active Faults in the Himalayan Foreland Region. *Internationtal Conference on Earthquake in Pakistan, January 18-19.* Islamambad: Geological Survey of Pakistan.

ICOLD (International Commission on Large Dams). (1989). Guidelines for selecting seismic

parameters for large dams. Paris.

ICOLD. (2002). Seismic Design and Evaluation of Structures Appurtenant to Dams. *Bulletin 123*.

ICOLD Committee on Seismic Aspects of Dam Design. (2010). *Selecting Seismic Parameters for Large Dams - Guidelines.* Bulletin 72.

ICOLD Committee on Seismic Aspects of Dam Design. (2011). *Reservoirs and Seismicity - State of Knowledge.* Bulletin 137.

Idriss, I. M. (1985). Evaluating seismic risk in engineering practice. *Proceedings of the 11th International Conference on Soil Mechanics and Foundation Engineering.* San Francisco.

Jackson, J., & Yielding, G. (n.d.). Source studies of the Hamran, Darel, and Patan earthquake in Kohistan, Pakistan. In K. Miller (Ed.). Proceedings of the Int. Conference, International Karakoram Project, Vol. 2.

Jacob, K. H., Pennington, W. D., Ambruster, J., Seeber, L., & Farhatulla, S. (1979). Tarbela Reservoir, Pakistan: a region of compressional tectonics with reduced seismicity upon inital reservoir filling. *Bulletin of the Seismological Society of America, 69*(4), 1175-1192.

Jain et al. (2000). Empirical attenuation relationships for the Himalayan earthquakes based on Indian stong motion data. *Proceedings of the Sixth International Conference on Seismic Zonation.* Palm Springs.

Jan, M. Q., & Howie, R. A. (1981). The mineralogy and geochemistry of the metamorphosed basics and ultrabasic rocks of the Jijal Complex, Kohistan, NW Pakistan. *Journal of Petroleum Vol. 22*.

Jouanne, F., Latif, M., Majid, A., Kausar, A., Pecher, A., & Mugnier, J. L. (2006). *Current shortening across the Himalayas: quantification of interseismic deformation in Nepal and first results of postseismic deformation in Pakistan after the 8th October earthquake.* Unpublished.

Kaneda et al. (2008). Surface rupture of the 2005 Kashmir, Pakistan Earthquake and Its Active Tectonic Implication. *Bulletin of the Seismological Society of America*, 521-557.

Kazmi, & Qasim. (1997). Geology and Tectonics of Pakistan. *Graphic Publishers*.

Kazmi, A. H., & Jan, M. Q. (1997). *Geology and Tectonics of Pakistan.* Karachi, Pakistan: Graphic Publishers.

Kazmi, A. Z. (1979). Active Fault Systems of Pakistan. *Geodynamics of Pakistan*.

Khushid, M., Yielding, G., Ahmad, S., Davidson, I., Jackson, J. A., King, G., et al. (1984). The seismicity of northern Pakistan. *Tectonophysics, 109*, 209-226.

Kim, B. (2012). *Seismic Hazard Analysis and Seismic Slope Stability evaluation using discrete faults in Northwestern Pakistain.* Urbana-Champaign: University of Illinois at Urbana-Champaign.

Kramer, S. L. (1996). *Geotechnical Earthquake Engineering.* Prentice-Hall.

Kumar et al. (2006). Paleoseismic evidence of great surface rupture earthquakes along the Indian Himalaya. *Journal of Geophysical Research Vol. 111 B03304*, 1-19.

Kurram Tangi Dam Consultants (Design Consultants). (2004a). *Kurram Tangi Dam Feasibility Study.*

Kurram Tangi Dam Consultants (Design Consultants).

Kurram Tangi Dam Consultants (Design Consultants). (2004b). *Design Report Kurram Tangi Dam.* Kurram Tangi Dam Consultants (Design Consultants).

Lawrence, R. D., Hasan Khan, S., & Nakata, T. (1992). Chaman Fault, Pakistan-Afghanistan. (R. a. Bucknam, Ed.) *Major active faults of the world—Results of IGCP Project 206*, pp. 196-223.

Macfarlane, Allison ; Sorkhabi, Rasoul B; Quade, Jay;. (1999). *Himalaya and Tibet: Mountain Roots to Mountain Tops, Special Paper 328.* The Geologic Society of America.

MMP, MM Pakistan (Pvt) Ltd. (2013, January 29). Kurram Tangi Dam Project - Presentation to MWH and USAID. Lahore, Pakistan.

MonaLisa, & Khwaja, A. H. (2005). Seismic Activity along the Main Boundary Thrust (MBT), Pakistan. *Geologic Bulletin University of Peshawar, Vol.38*, 23-30.

Monalisa, Khwaja, A. A., & Qasim, J. (2007). *Seismic hazard assessment of the NW Himalayan fold-and-thrust belt, Pakistan, using probabilistic approach.* Journal of Earthquake Engineering.

Munir-Ul-Hassan, M., & Mirza, K. (2007). Stratigraphic Aspect of Recent Earthquake Occured Along the Balakot-Bagh Fault, North-West Himalayas, Pakistan. *Journal of Himalayan Earth Sciences 39*, 39-48.

Nakata et al. (1991). *Special publication 21, Active faults of Pakistan: map sheets and inventories.* Hiroshima University, Hiroshima.

National Engineering Services Pakistan. (2009). *General Fault Map.* Retrieved March 24, 2009, from Earthquake Reconstruction and Rehabilitation Authority: http://www.erra.gov.pk/Map%20Pages/General%20Fault%20Map/General_Fault_Map.htm

Neelum-Jhelum Consultants. (2008). *Seismic Risk Review/Re-evaluation Neelum-Jhelum Hydroelectric Project.* Neelum-Jhelum Consultants.

NESPAK and MWH. (2013). *Seismic Hazard for Kurram Tangi Dam Project.*

Packer, D. R., Cluff, L. S., Knuepfer, P. L., & Withers, R. J. (1979). *Study of Reservoir Induced Seismicity.* San Francisco: Woodward-Clyde Consultants.

Pakistan Meterological Department. (2007). *Seismic Hazard Analysis and Zonation for Pakistan, Azad Jammu and Kashmir.*

Pakistan Water & Power Development Authority. (2011). *Goverment of Pakistan Planning Commisson PC-I Form.* Lahore: Pakistan Water & Power Development Authority.

Pivnik, D. A., & Wells, N. A. (1996). The transition form Tethys to the Himalaya as recorded in northwest Pakistan. *Bulletin of Geological Society of America, Vol. 108*.

Quittmeyer, & Jacob. (1979). Historical and modern seismicity of Pakistan, Afghanistan, northwestern India and southeastern Iran. *Bulletin of Seismological Society of America, Vol.63, No.3*.

Quittmeyer, R. C., & Jacob, K. H. (1979). *Historical and modern seismicity of Pakistan, Afghanistan, northwestern India and southwestern Iran.* Bulletin of Seismological Society of America, v.69.

Roeloffs, E. A. (1988). Fault stability changes beneath a reservoir with cyclic variations in water level. *Journal of Geophysical Research, 93*(B3), 2107-2124.

Scordilis, E. M. (2006). Empirical global relations converting Ms and mb to moment magnitude. *Journal of Seismicity*, 225-236.

Searle et al. (1999). The tectonic evolution of the Kohistan-Karakoram collision belt along Karakoram Highway transect, north Pakistan. *Techtonics No. 18*, 929-949.

Seeber et al. (1981). Seismicity and continental subduction in the Himalayan arc, in Zagros-Hindukush-Himalayas Geodynamic Evolution. *AGU Geodynamic Series, Vol. 3.*

Seeber L. et al. (1996). *A short walk up the naked mountain.* USA: Lamont Doherty Geological Observatory.

Seeber, & Armbuster. (1979). Seismicity of the Hazara arc in Northern Pakistan: decollement vs. basement faulting. (A. Farah, & K. A. DeJong, Eds.) *Geol. Surv. North Pakistan J. Metam. Geol. 7*, 111-125.

Seeber, L., & Jacob, K. H. (1976). Micro-earthquakes survey northern Pakistan, Preliminary Results and tectonic implications. *Proccedings of Symposium on Himalayan Geology.* Paris: CNRS.

Shah, M. A., Iqbal, T., Qaisar, M., Ahmed, N., & Tufail, M. (2012). Development of Attenuation Relationship for Northern Pakistan. *World Conference of Earthquake Engineering* . Lisboa.

Stepp, J. C. (1972). Analysis of completeness of earthquake sample in Puget Sound area and its effect on statistical estimates of earthquake hazard. *Pro. Inern. Conf Microzonation v.2*, (pp. 897-910).

Tapponnier, P., King, G., & Bollinger, L. (2006). Active Faulting and Seismic Hazard in the Western Himalayan Syntaxis,. *International Conference on 8 October 2005 Earthquake in Pakistan: Its Implications & Hazard Mitigation* (pp. 6-7). Islamabad: Director General, Geological Survey of Pakistan.

Tapponnier, P., Mattaurer, M., Proust, F., & Cassaigneau, C. (1981). *Mesozoic ophiolites, sutures and large-scale tectonic movements in Afghanistan.* Earth and Planetary Sciences Letters.

(n.d.). *Tectonic Map of Pakistan.* Geological Survey of Pakistan.

Trelor et al. (1990). Cooling and uplift histories of the crystalline stack of Indian plate internal zones west of Nanga Parbat, Pakistan Himalaya. *Tectonophysics 180*, 323-349.

US Committee on Large Dams. (1997). *Reservoir Triggered Seismicity.*

US Geological Survey. (2013, March 6). *Historic World Earthquakes*. Retrieved July 9, 2013, from US Geological Survey: http://earthquake.usgs.gov/earthquakes/world/historical_country.php

Wadia, D. N. (1944). *Geology of India.* London: Macmillan and Co.

Weichert, D. H. (1980). *Estimation of earthquake recurrence parameters for unequal observation periods for different magnitudes.* Bulletin of Seismological Society of America, v. 70.

Wellman, H. W. (1965). *Active wrench faults of Iran, Afghanistan, and Pakistan.* Geologische Rundschau, v 55, no.3.

Wells, & Coppersmith. (1994). New empirical relationships among magnitude, rupture length, rupture width, rupture area and surface displacement. *Bulletin of the Seismological Society of America Vol. 84 No.4*.

Wong, I. G., Thomas, P. A., & Abrahamson, N. (2001). The PEER-Lifelines validation of software used in probabilistic seismic hazard analysis. (M. Y. Kavazanjian, Ed.) *Geotechnical Engineering for Transportation Projects, 1*, 807-815.

Yeats, R. S., Sieh, K. E., & Allen, C. A. (1997). *Geology of Earthquakes.* New York, NY: Oxford University Press.

Youngs, R. C.-J. (1997). Strong ground motion attenuation relationships for subduction zones earthquakes. *Seismological Research Letters, v. 68*, 58-73.

Zanchi et al. (2000). Mantle exhumation along Tirch Mir fault zone, NW Pakistan: pre-mid-Cretaceous accretion of the Karakoram terrane to the Asian margin. *Geological Society of London, Special Publication, 170*, 277-293.

Zhao. J., Z. J. (2006). Attenuation Relations of Strong Ground Motion in Japan Using Site Classification Based on Predominant Period. *Seismological Society of America, Vol. 96, No. 3*, 898-913.

Zoback, M. D., & Hickman, S. (1982). In situ study of the physical mechanisms controlling induced seismicity at Monticello Reservoir, South Carolina. *Journal of Geophysical Research, 87*(B8), 6959-6974.

This Page Left Blank Intentionally

LIST OF PLATES

Plate 1: Project Features

Plate 2: Plate Tectonic Setting of the Project Region

Plate 3: Tectonic Map of the Western Himalaya

Plate 4: Structural Map of Bannu Basin, Kohat and Potwar Plateaus

This Page Left Blank Intentionally

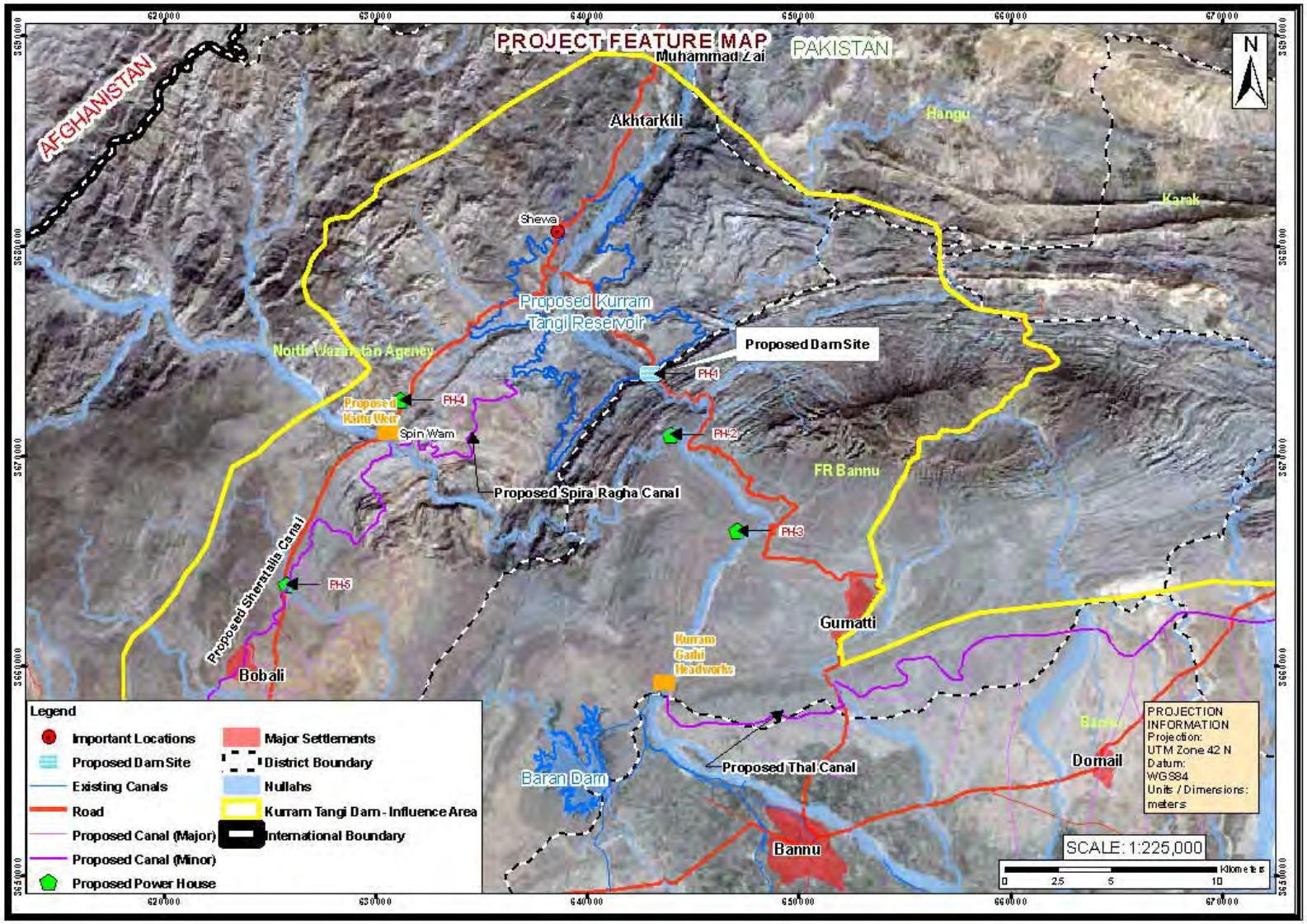

Source: NESPAK, 2013

MWH®	Project Features	Plate 1

This Page Left Blank Intentionally

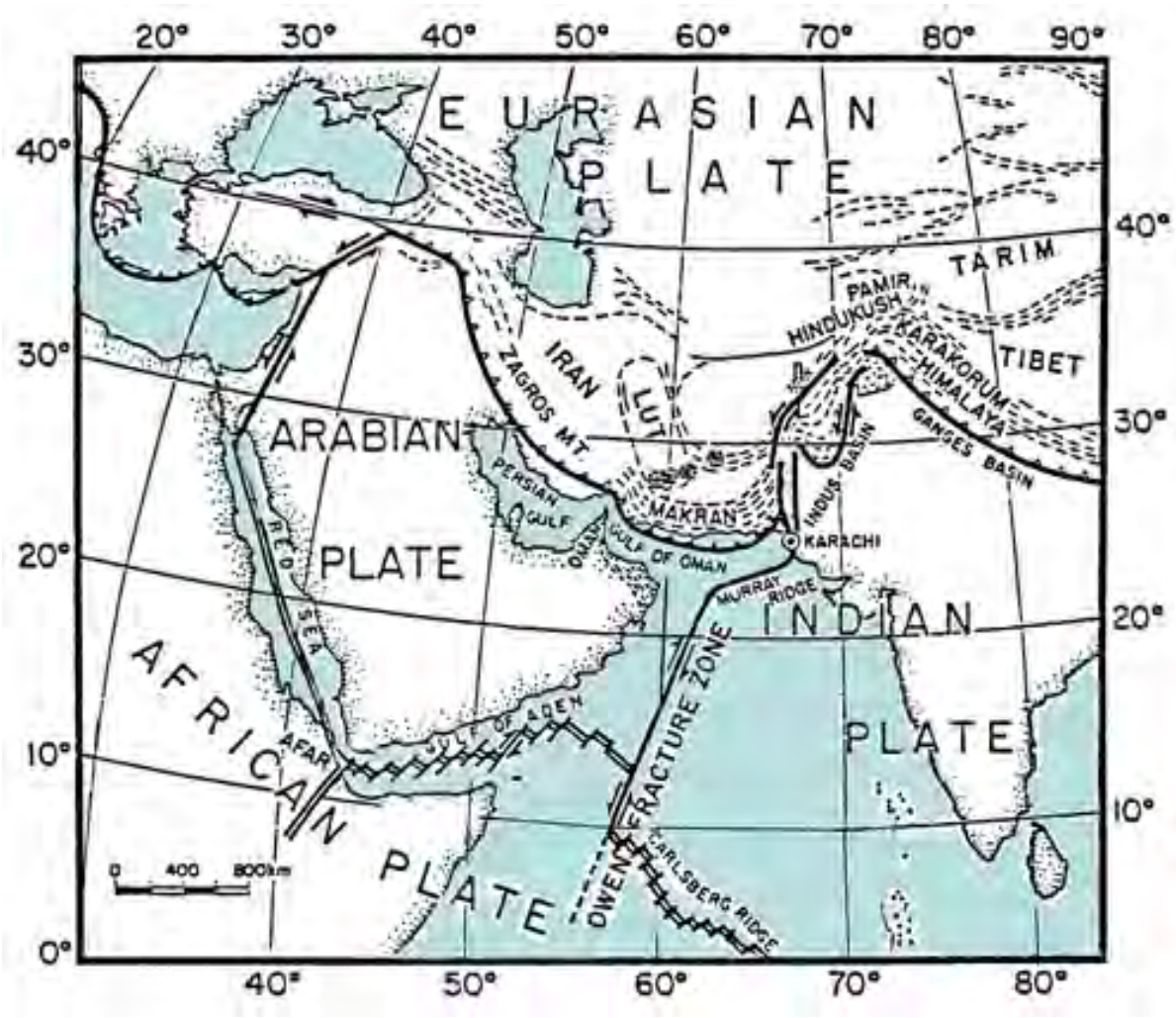

Source: NESPAK, 2013

MWH®	Plate Tectonic Setting of the Project Region	Plate 2

This Page Left Blank Intentionally

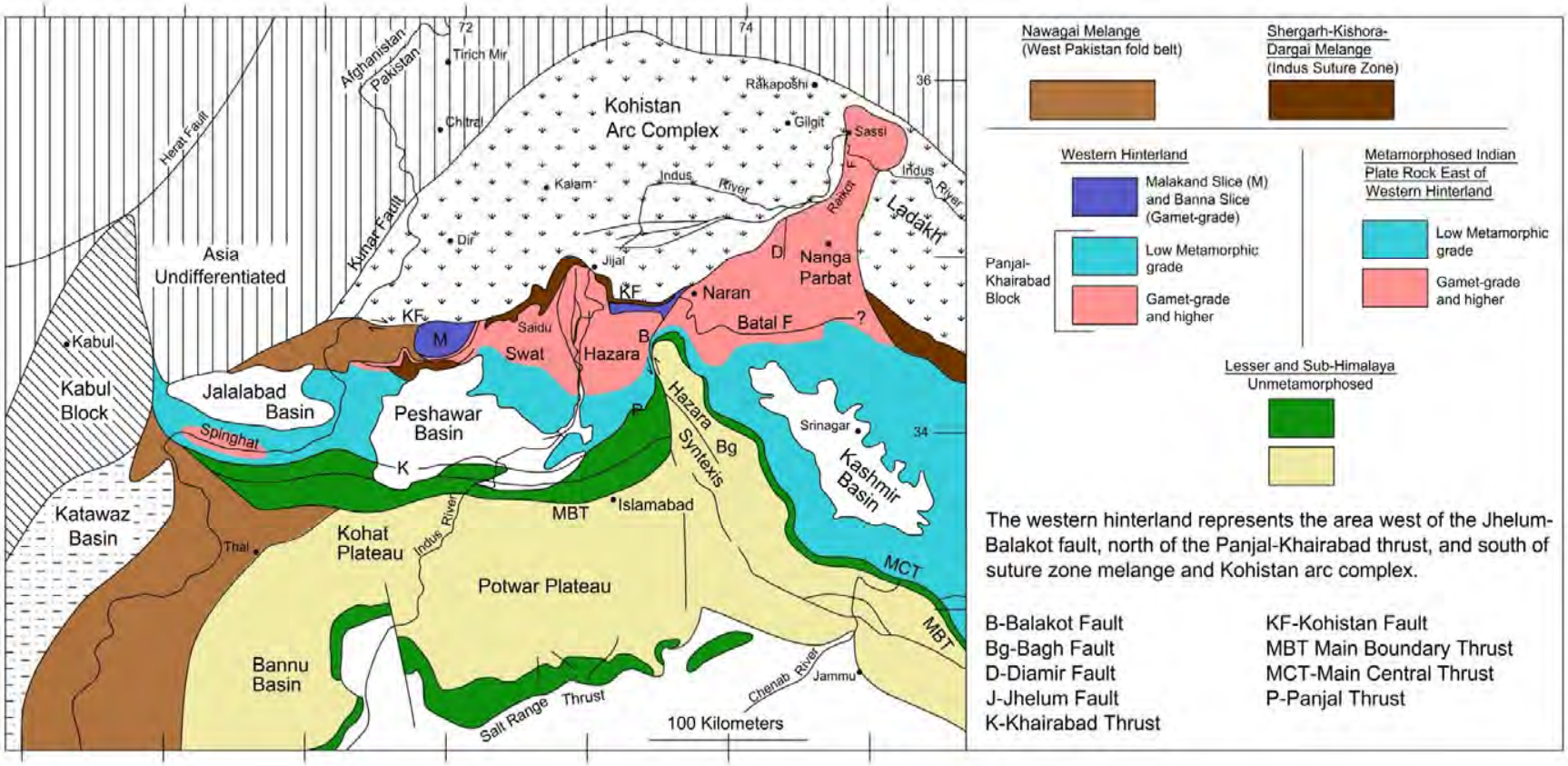

Source: NESPAK, 2013

MWH®	Tectonic Map of the Western Himalaya	Plate 3

This Page Left Blank Intentionally

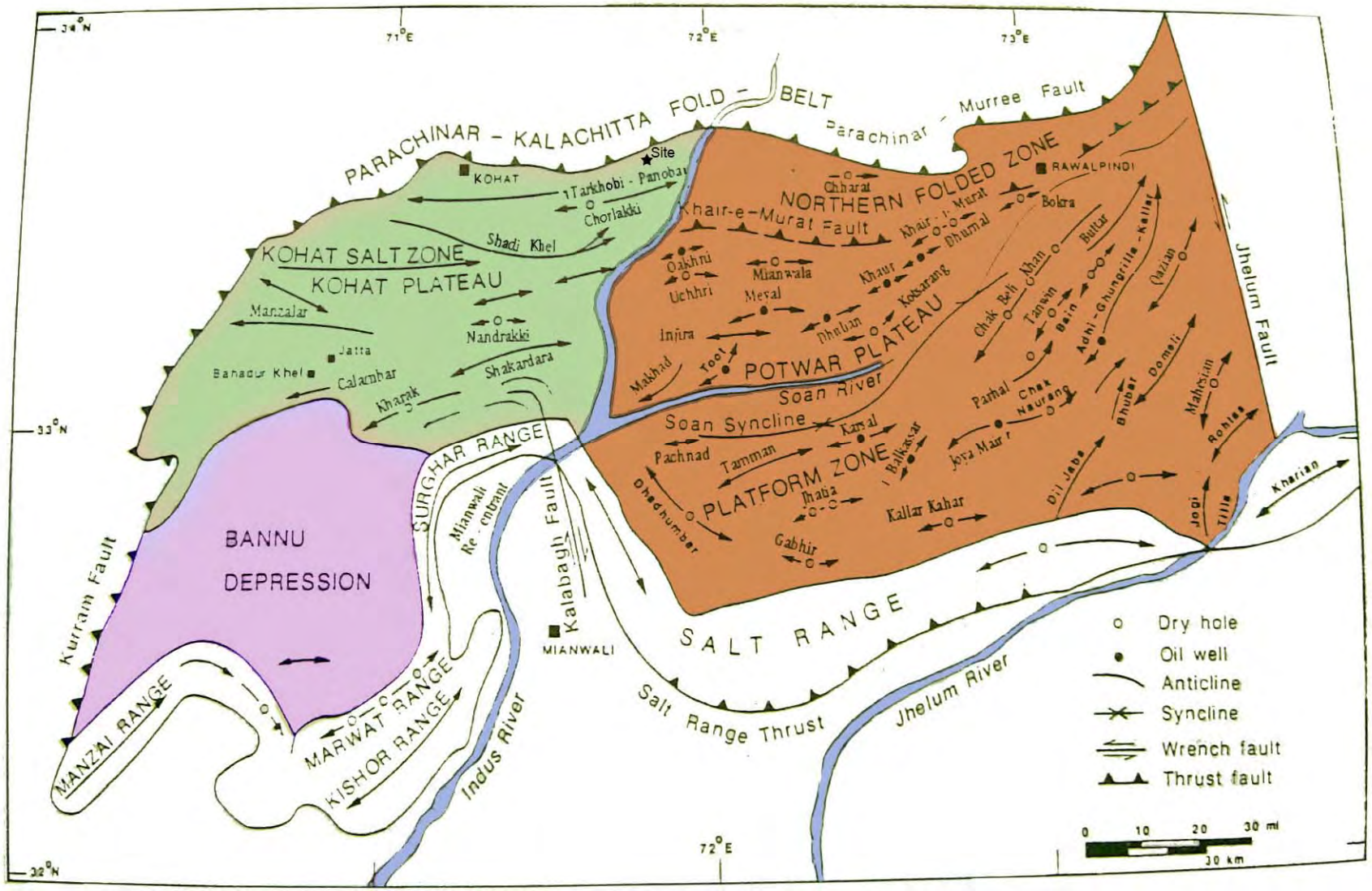

Source: NESPAK, 2013

MWH®

Structural Map of Bannu Basin, Kohat and Potwar Plateaus

Plate 4

This Page Left Blank Intentionally

LIST OF FIGURES

Figure 1: Active Faults within 50 km of the Project Site

Figure 2: Areal Source Zones

Figure 3: Catalog Completeness - Stepp Plot

Figure 4: Gutenberg-Richter Relationship – Zones 1-4, 6, 8, 11 and 12NEW

Figure 5: Gutenberg-Richter Relationship – Zones 1

Figure 6: Gutenberg-Richter Relationship – Zones 2

Figure 7: Gutenberg-Richter Relationship – Zones 3

Figure 8: Gutenberg-Richter Relationship – Zones 4

Figure 9: Gutenberg-Richter Relationship – Zones 6

Figure 10: Gutenberg-Richter Relationship – Zones 8

Figure 11: Gutenberg-Richter Relationship – Zones 11

Figure 12: Gutenberg-Richter Relationship – Zones 12NEW

Figure 13: Comparison of Different Ground Motion Prediction Equations with the Pakistan Model (Magnitude 6.4)

Figure 14: Main Dam - Seismic Source Contributions to Median Peak Horizontal Acceleration Hazard

Figure 15: Main Dam - Seismic Source Contributions to Median 0.2 Sec Spectral Acceleration Hazard

Figure 16: Main Dam - Seismic Source Contributions to Median 1.0 Sec Spectral Acceleration Hazard

Figure 17: Kaitu Weir - Seismic Source Contributions to Median Peak Horizontal Acceleration Hazard

Figure 18: Kaitu Weir - Seismic Source Contributions to Median 0.2 Sec Spectral Acceleration Hazard

Figure 19: Kaitu Weir - Seismic Source Contributions to Median 1.0 Sec Spectral Acceleration Hazard

Figure 20: Weir II - Seismic Source Contributions to Median Peak Horizontal Acceleration Hazard

Figure 21: Weir II - Seismic Source Contributions to Median 0.2 Sec Spectral Acceleration Hazard

Figure 22: Weir II - Seismic Source Contributions to Median 1.0 Sec Spectral Acceleration Hazard

Figure 23: Weir III - Seismic Source Contributions to Median Peak Horizontal Acceleration Hazard

Figure 24: Weir III - Seismic Source Contributions to Median 0.2 Sec Spectral Acceleration Hazard

Figure 25: Weir III - Seismic Source Contributions to Median 1.0 Sec Spectral Acceleration Hazard

Figure 26: Main Dam – Uniform Hazard Spectra

Figure 27: Kaitu Weir – Uniform Hazard Spectra

Figure 28: Weir II – Uniform Hazard Spectra

Figure 29: Weir III – Uniform Hazard Spectra

Figure 30: Deaggregation 145-yr Return Period Peak Horizontal Acceleration

Figure 31: Deaggregation 145-yr Return Period 0.2 Sec Horizontal Acceleration

Figure 32: Deaggregation 145-yr Return Period 1.0 Sec Horizontal Acceleration

Figure 33: Deaggregation 475-yr Return Period Peak Horizontal Acceleration

Figure 34: Deaggregation 475-yr Return Period 0.2 Sec Horizontal Acceleration
Figure 35: Deaggregation 475-yr Return Period 1.0 Sec Horizontal Acceleration
Figure 36: Deaggregation 10,000-yr Return Period Peak Horizontal Acceleration
Figure 37: Deaggregation 10,000-yr Return Period 0.2 Sec Horizontal Acceleration
Figure 38: Deaggregation 10,000-yr Return Period 1.0 Sec Horizontal Acceleration
Figure 39: Deaggregation 145-yr Return Period Peak Horizontal Acceleration
Figure 40: Deaggregation 145-yr Return Period 0.2 Sec Horizontal Acceleration
Figure 41: Deaggregation 145-yr Return Period 1.0 Sec Horizontal Acceleration
Figure 42: Deaggregation 475-yr Return Period Peak Horizontal Acceleration
Figure 43: Deaggregation 475-yr Return Period 0.2 Sec Horizontal Acceleration
Figure 44: Deaggregation 475-yr Return Period 1.0 Sec Horizontal Acceleration
Figure 45: Deaggregation 10,000-yr Return Period Peak Horizontal Acceleration
Figure 46: Deaggregation 10,000-yr Return Period 0.2 Sec Horizontal Acceleration
Figure 47: Deaggregation 10,000-yr Return Period 1.0 Sec Horizontal Acceleration
Figure 48: Deaggregation 145-yr Return Period Peak Horizontal Acceleration
Figure 49: Deaggregation 145-yr Return Period 0.2 Sec Horizontal Acceleration
Figure 50: Deaggregation 145-yr Return Period 1.0 Sec Horizontal Acceleration
Figure 51: Deaggregation 475-yr Return Period Peak Horizontal Acceleration
Figure 52: Deaggregation 475-yr Return Period 0.2 Sec Horizontal Acceleration
Figure 53: Deaggregation 475-yr Return Period 1.0 Sec Horizontal Acceleration
Figure 54: Deaggregation 10,000-yr Return Period Peak Horizontal Acceleration
Figure 55: Deaggregation 10,000-yr Return Period 0.2 Sec Horizontal Acceleration
Figure 56: Deaggregation 10,000-yr Return Period 1.0 Sec Horizontal Acceleration
Figure 57: Deaggregation 145-yr Return Period Peak Horizontal Acceleration
Figure 58: Deaggregation 145-yr Return Period 0.2 Sec Horizontal Acceleration
Figure 59: Deaggregation 145-yr Return Period 1.0 Sec Horizontal Acceleration
Figure 60: Deaggregation 475-yr Return Period Peak Horizontal Acceleration
Figure 61: Deaggregation 475-yr Return Period 0.2 Sec Horizontal Acceleration
Figure 62: Deaggregation 475-yr Return Period 1.0 Sec Horizontal Acceleration
Figure 63: Deaggregation 10,000-yr Return Period Peak Horizontal Acceleration
Figure 64: Deaggregation 10,000-yr Return Period 0.2 Sec Horizontal Acceleration
Figure 65: Deaggregation 10,000-yr Return Period 1.0 Sec Horizontal Acceleration
Figure 66: Main Dam - Deterministic Hazard Results – Response Spectrum – 50th Percentile
Figure 67: Main Dam - Deterministic Hazard Results – Response Spectrum – 84th Percentile
Figure 68: Kaitu Weir - Deterministic Hazard Results – Response Spectrum – 50th Percentile
Figure 69: Kaitu Weir - Deterministic Hazard Results – Response Spectrum – 84th Percentile
Figure 70: Weir II - Deterministic Hazard Results – Response Spectrum – 50th Percentile

Figure 71: Weir II - Deterministic Hazard Results – Response Spectrum – 84th Percentile

Figure 72: Weir III - Deterministic Hazard Results – Response Spectrum – 50th Percentile

Figure 73: Weir III - Deterministic Hazard Results – Response Spectrum – 84th Percentile

This Page Left Blank Intentionally

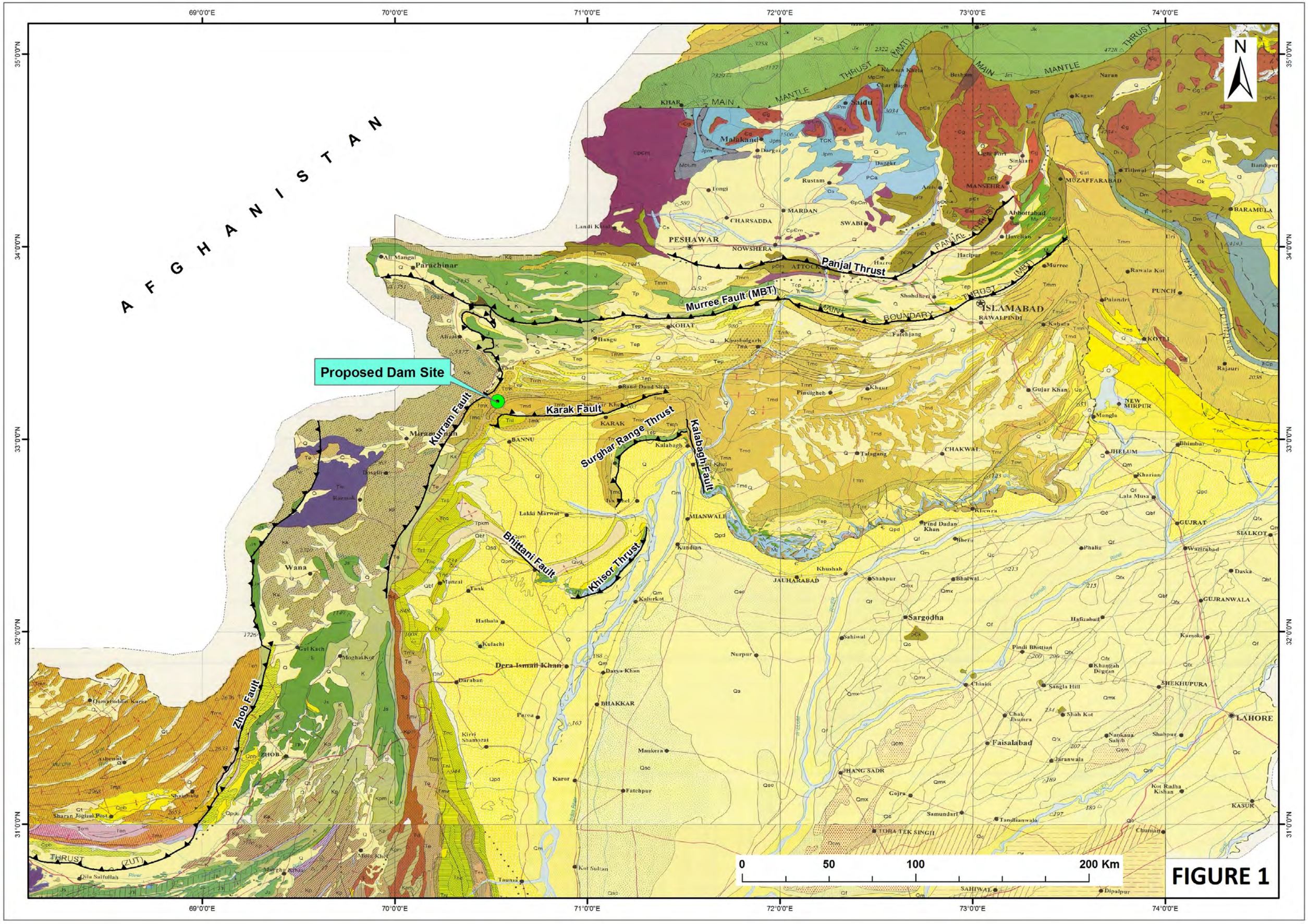
AFGHANISTAN
Proposed Dam Site
Panjal Thrust
Murree Fault (MBT)
Karak Fault
Kurram Fault
Surghar Range Thrust
Kalabagh Fault
Bhittani Fault
Khisor Thrust
Zhob Fault
MAIN MANTLE THRUST (MMT)
MAIN BOUNDARY THRUST (MBT)
THRUST (ZUT)
PESHAWAR
ISLAMABAD
RAWALPINDI
MARDAN
CHARSADDA
NOWSHERA
ATTOCK
KOHAT
BANNU
KARAK
MIANWALI
JAUHARABAD
Sargodha
Faisalabad
JHANG SADR
TOBA TEK SINGH
LAHORE
GUJRANWALA
GUJRAT
JHELUM
CHAKWAL
MUZAFFARABAD
MANSEHRA
Abbottabad
Murree
Dera Ismail Khan
BHAKKAR
Karor
Wana
ZHOB
Naran
Kagan
Besham
Saidu
Malakand
Rustam
Swabi
Haripur
Rawala Kot
PUNCH
KOTLI
Rajauri
Gujar Khan
NEW MIRPUR
Mangla
Bhimbar
Kharian
Lala Musa
Khewra
Pind Dadan Khan
Phalia
Wazirabad
SIALKOT
Daska
Kamoke
Hafizabad
SHEKHUPURA
Shahpur
Kot Radha Kishan
KASUR
Chunian
Dipalpur
SAHIWAL
Samundari
Tandlianwala
Gojra
Jaranwala
Chak Jhumra
Shah Kot
Nankana Sahib
Sangla Hill
Chiniot
Pindi Bhattian
Khangah Dogran
Kundian
Khushab
Bhalwal
Shahpur
Sahiwal
Nurpur
Kalurkot
Lakki Marwat
Tank
Hathala
Kulachi
Daraban
Paroa
Mankera
Fatehpur
Kot Sultan
Tauma
Gul Kach
Moghal Kot
Qamaruddin Karez
Ashewan
Shajnwala
Sharan Jogizai Post
Qila Saifullah
Musa Khel
Mirgha Khan
Ali Mangal
Parachinar
Afzal
Hangu
Khushalgarh
Rand Daud Shah
Pindigheb
Talagang
Kalabagh
Dargai
Landi Kotal
Shahdheri
Fatehjang
Hazro
Havelian
Amb
Dhir
Tirhwal
Bandipur
Kohala
Dhir
Tiri
Tarbela
Mirpur
Bhimber
Chenab
Jhelum
Indus
Kabul
Swat
Kurram
Tochi
Gomal
Zhob
Pakistan
Afghanistan
0 50 100 200 Km
N

FIGURE 1

This Page Left Blank Intentionally

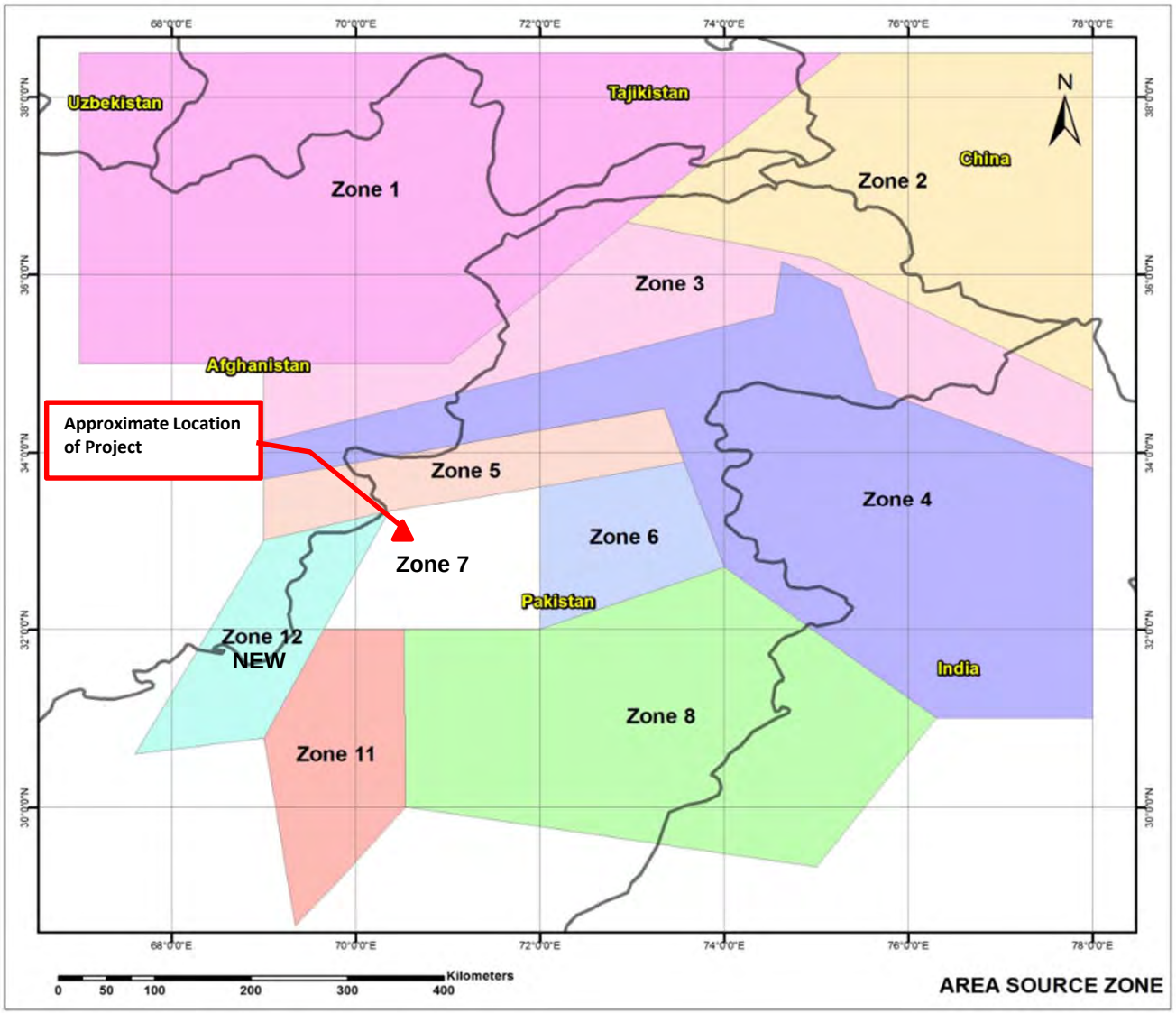

Figure Prepared by NESPAK

MWH®	Areal Source Zones	Figure 2

This Page Left Blank Intentionally

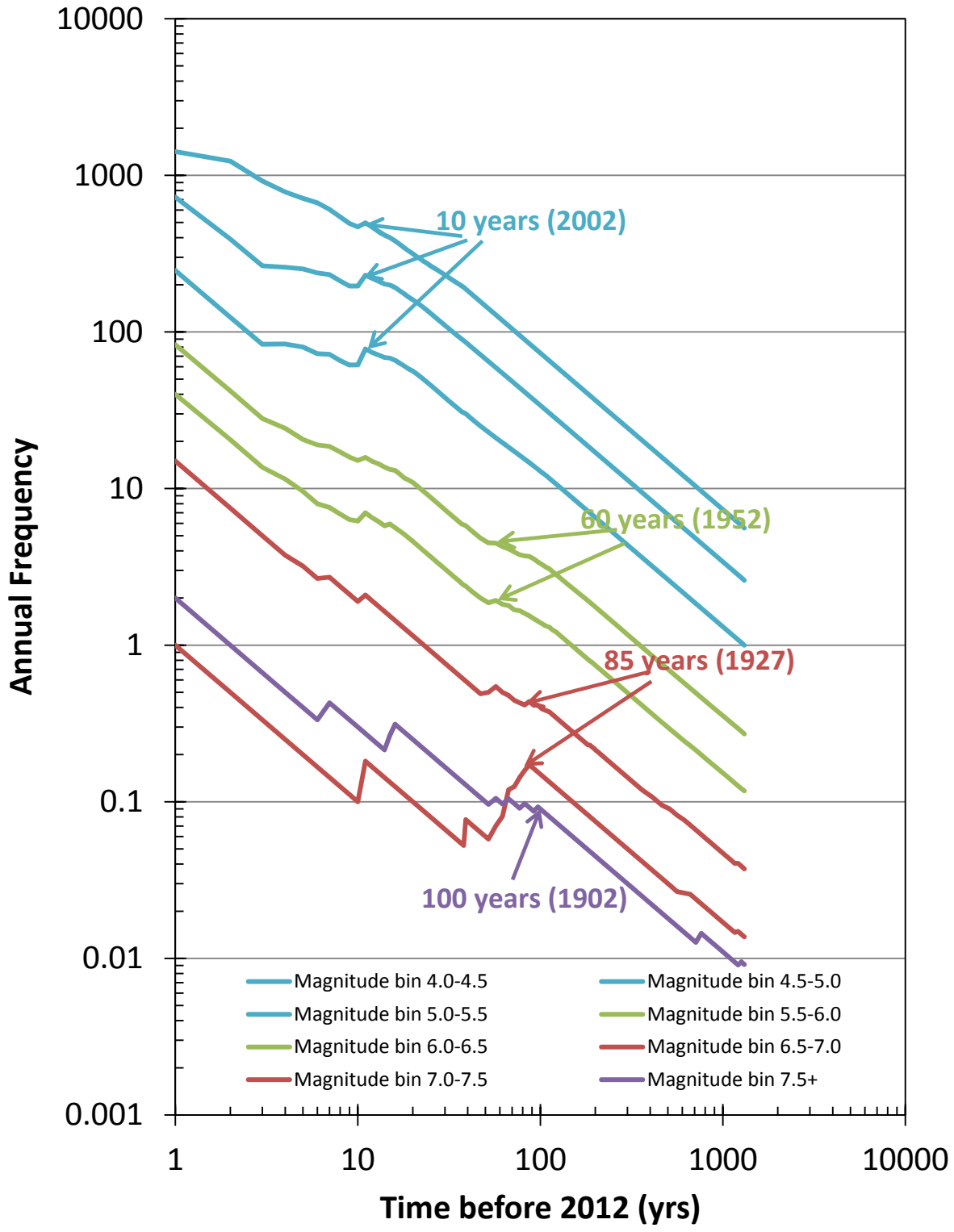

MWH®	Catalog Completeness -Stepp Plot	Figure 3

This Page Left Blank Intentionally

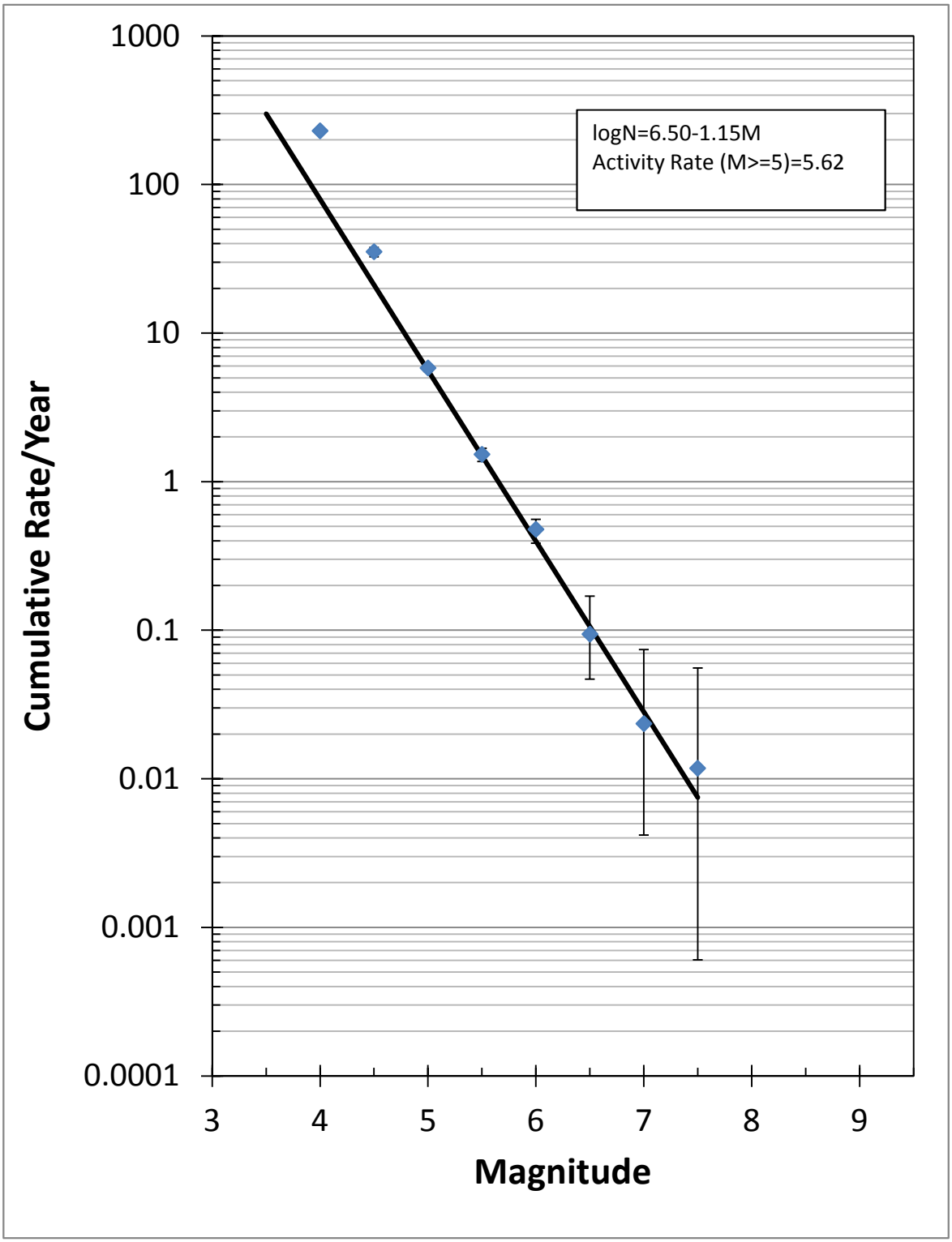

MWH®

Gutenberg-Richter Relationship
Zones 1-4, 6, 8, 11 and 12NEW

Figure 4

This Page Left Blank Intentionally

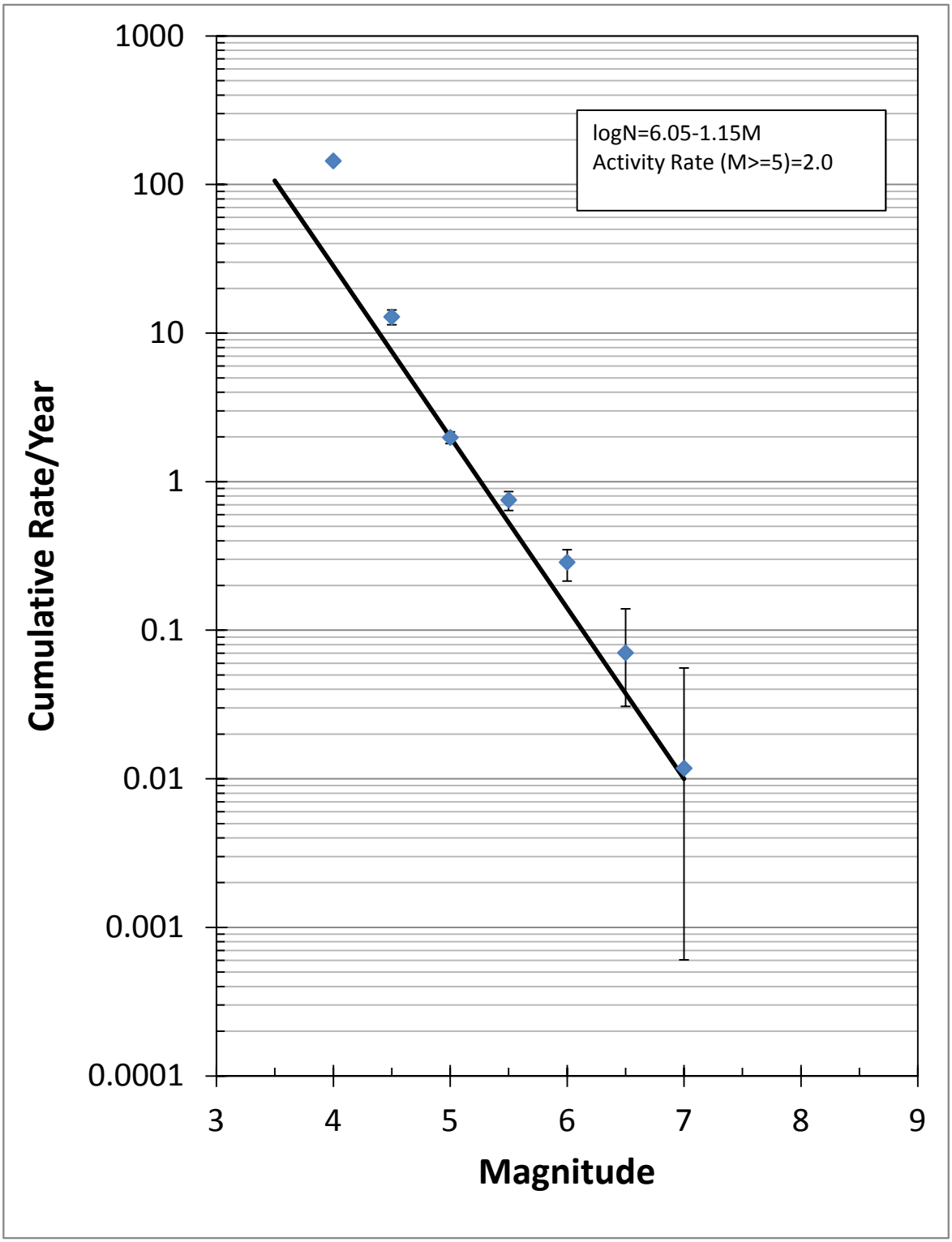

MWH®

Gutenberg-Richter Relationship
Zone 1

Figure 5

This Page Left Blank Intentionally

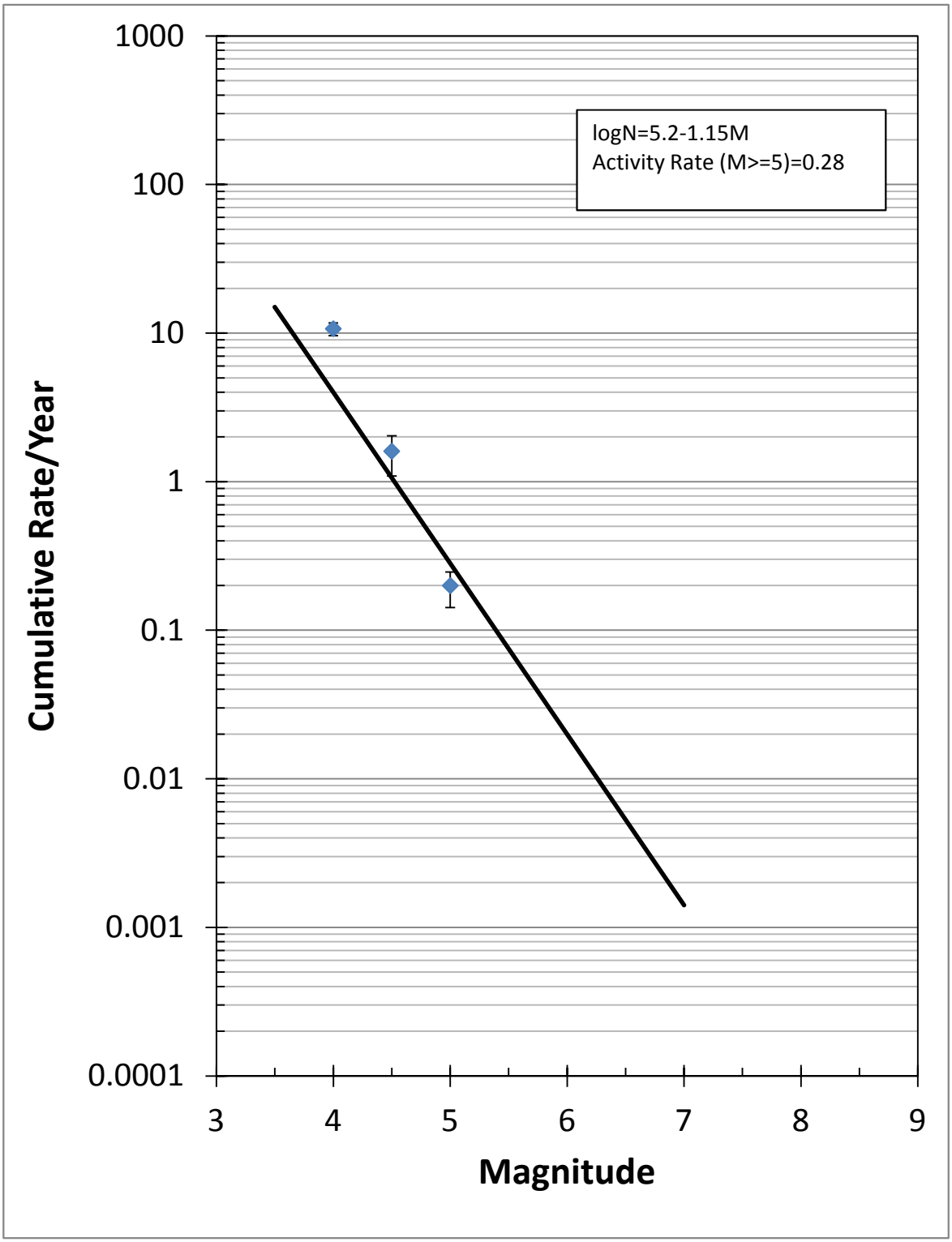

MWH®

Gutenberg-Richter Relationship
Zone 2

Figure 6

This Page Left Blank Intentionally

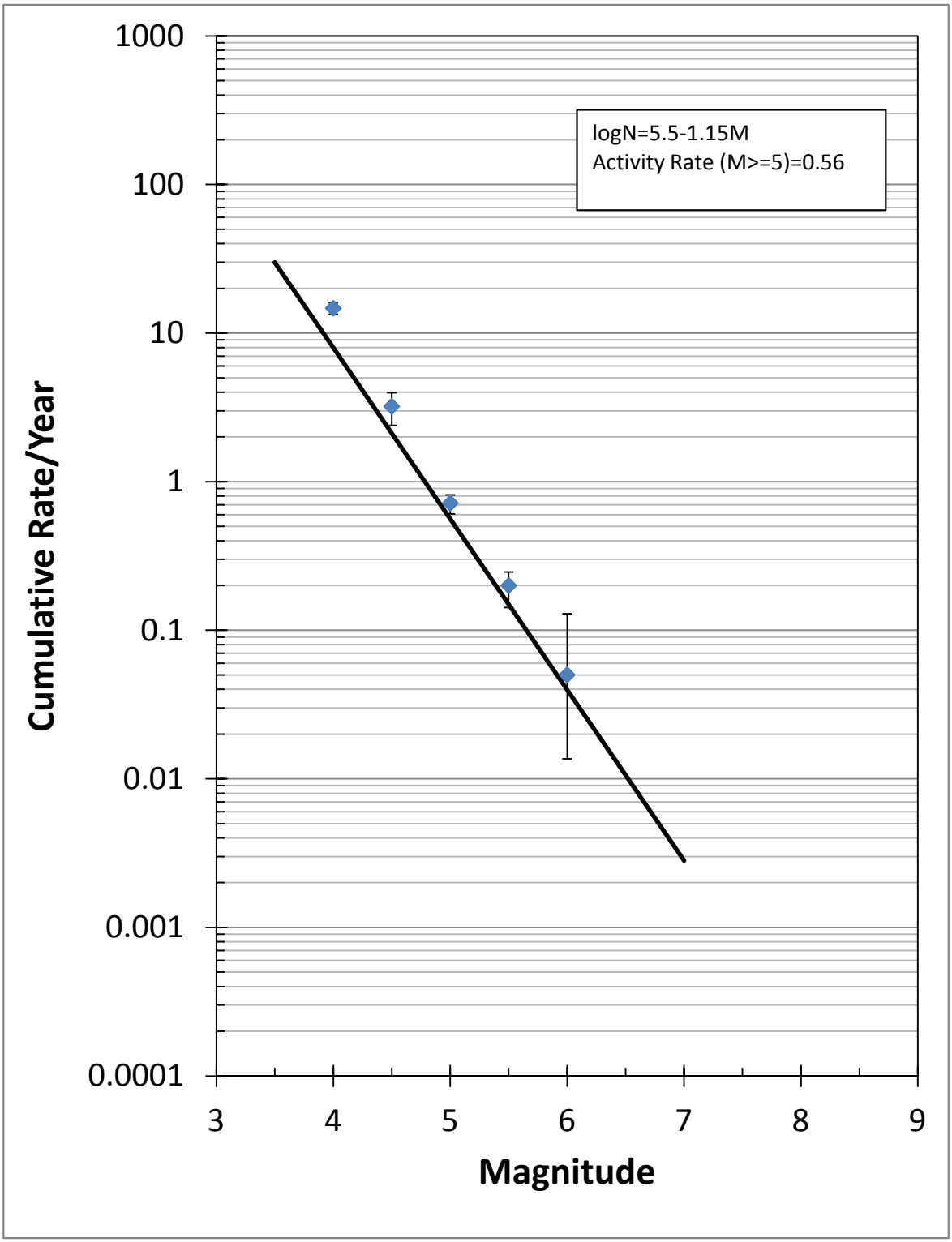

MWH®

Gutenberg-Richter Relationship
Zone 3

Figure 7

This Page Left Blank Intentionally

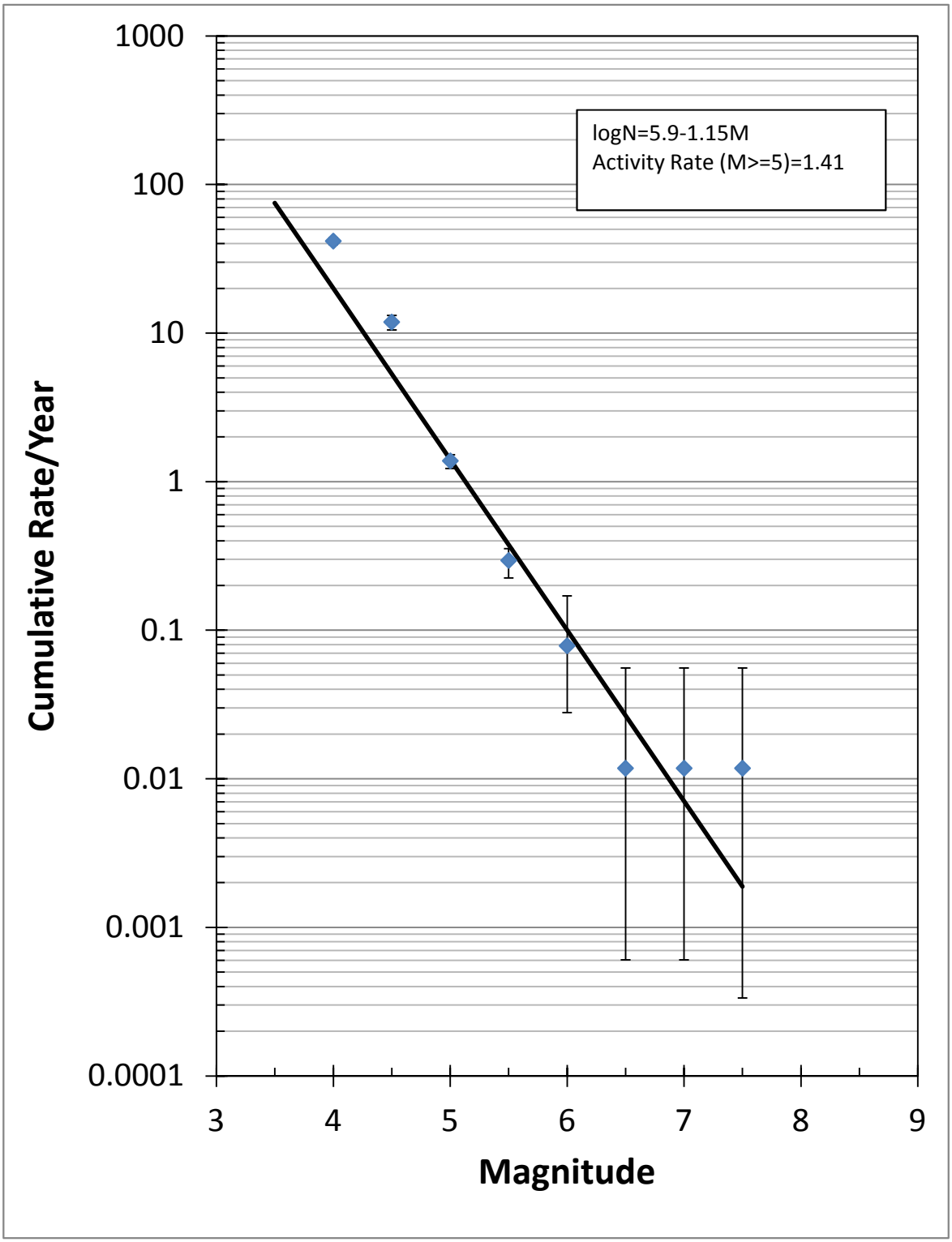

MWH®

Gutenberg-Richter Relationship
Zone 4

Figure 8

This Page Left Blank Intentionally

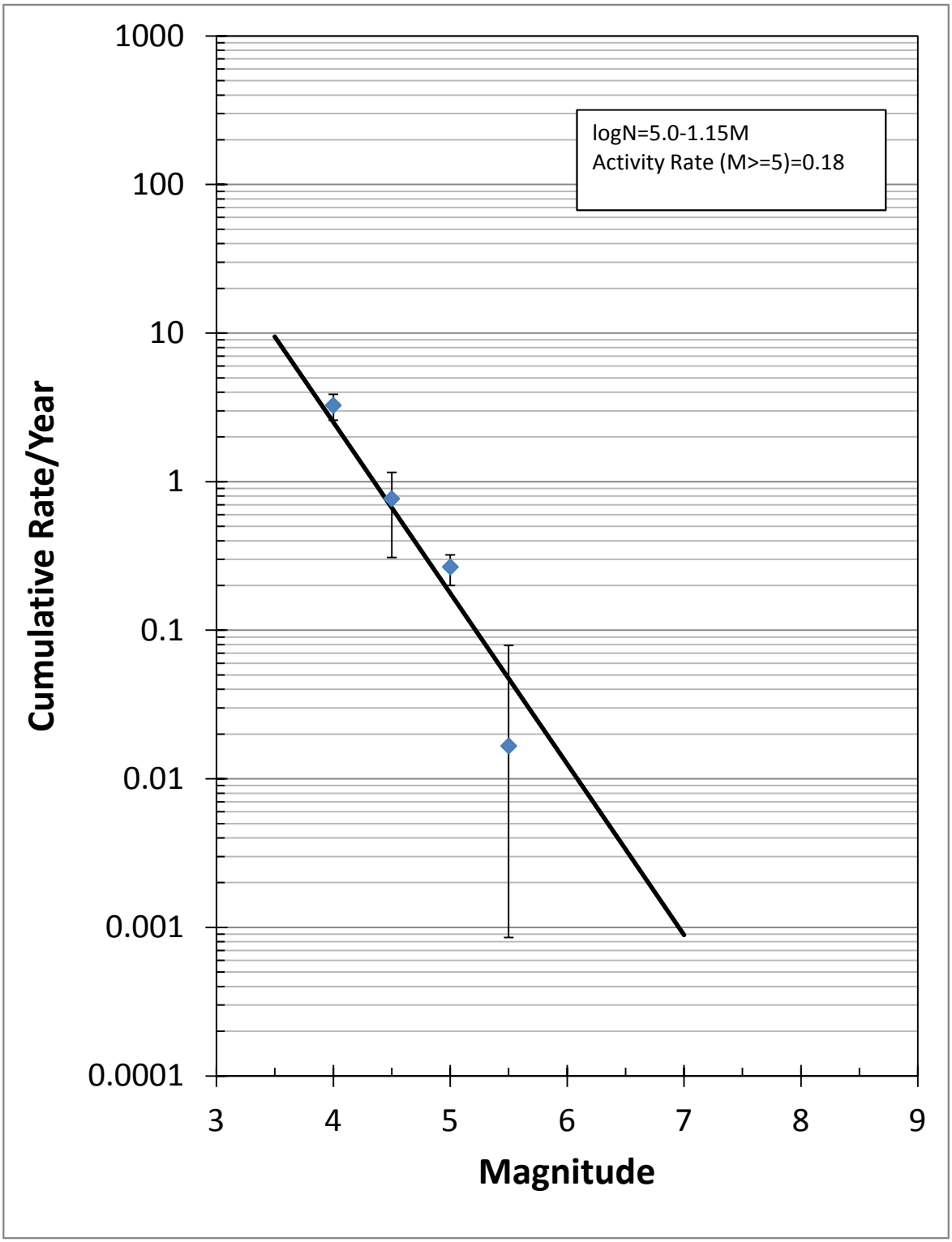

MWH®

Gutenberg-Richter Relationship
Zone 6

Figure 9

This Page Left Blank Intentionally

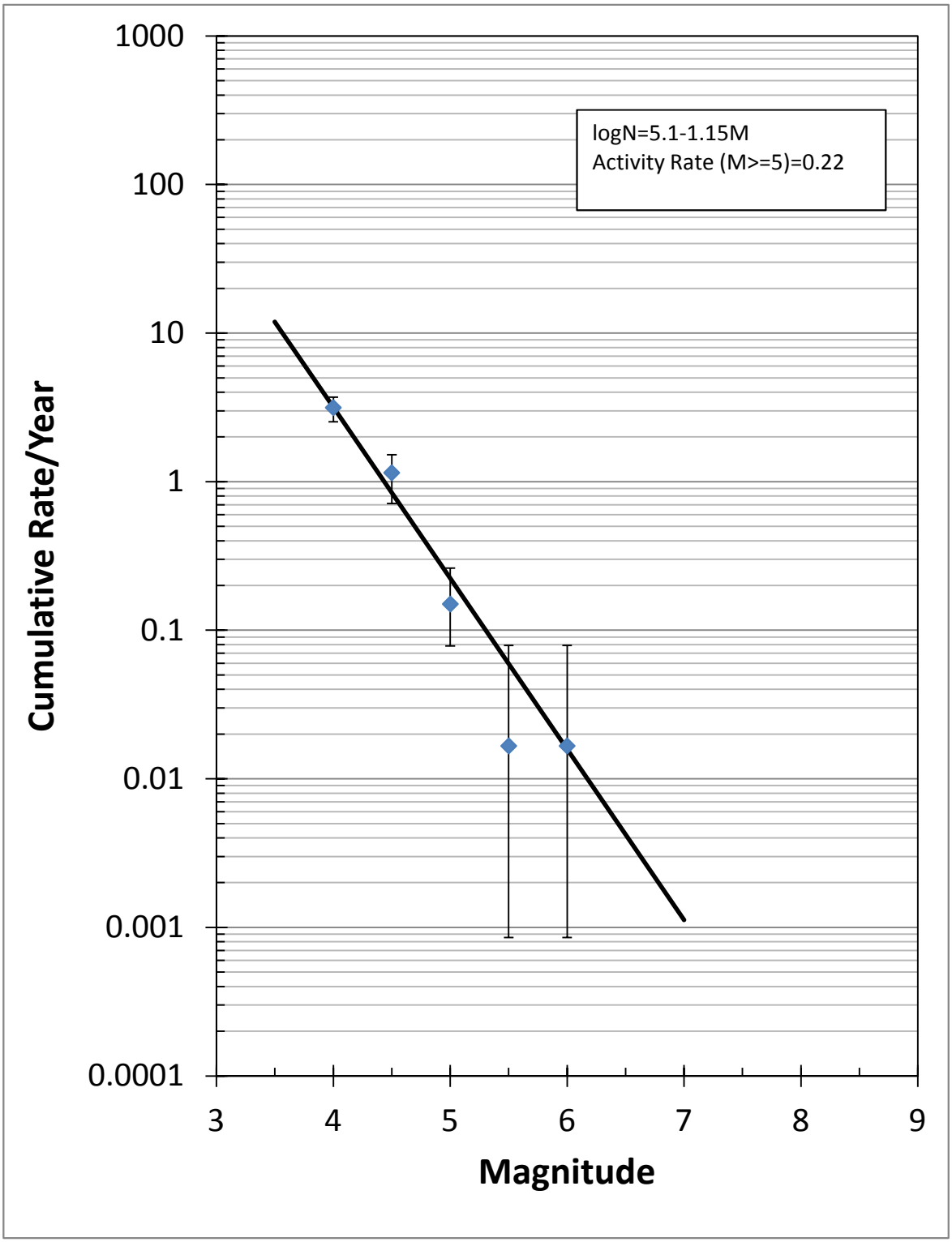

MWH®

Gutenberg-Richter Relationship
Zone 8

Figure 10

This Page Left Blank Intentionally

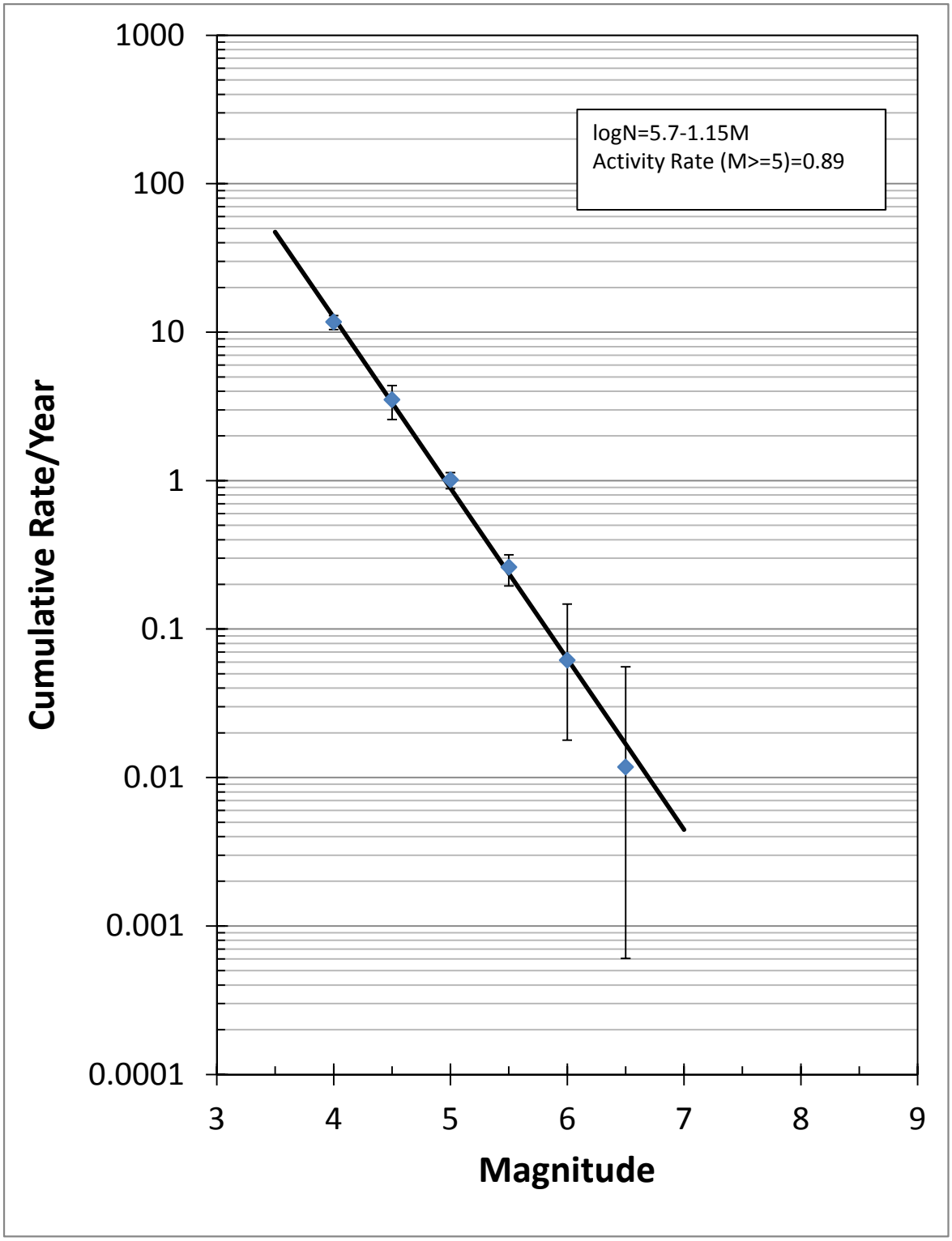

MWH®

Gutenberg-Richter Relationship
Zone 11

Figure 11

This Page Left Blank Intentionally

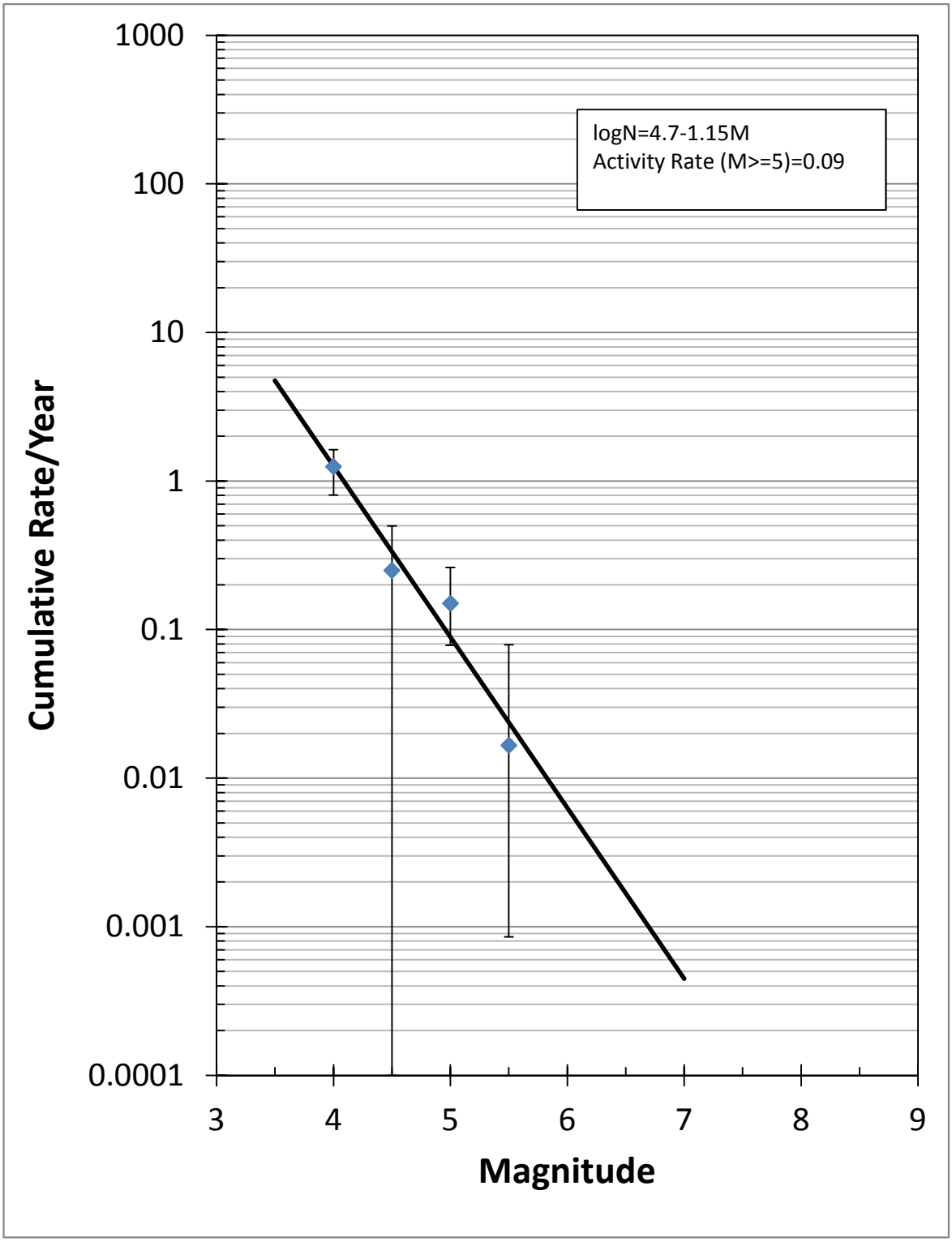

MWH®

Gutenberg-Richter Relationship
Zone12NEW

Figure 12

This Page Left Blank Intentionally

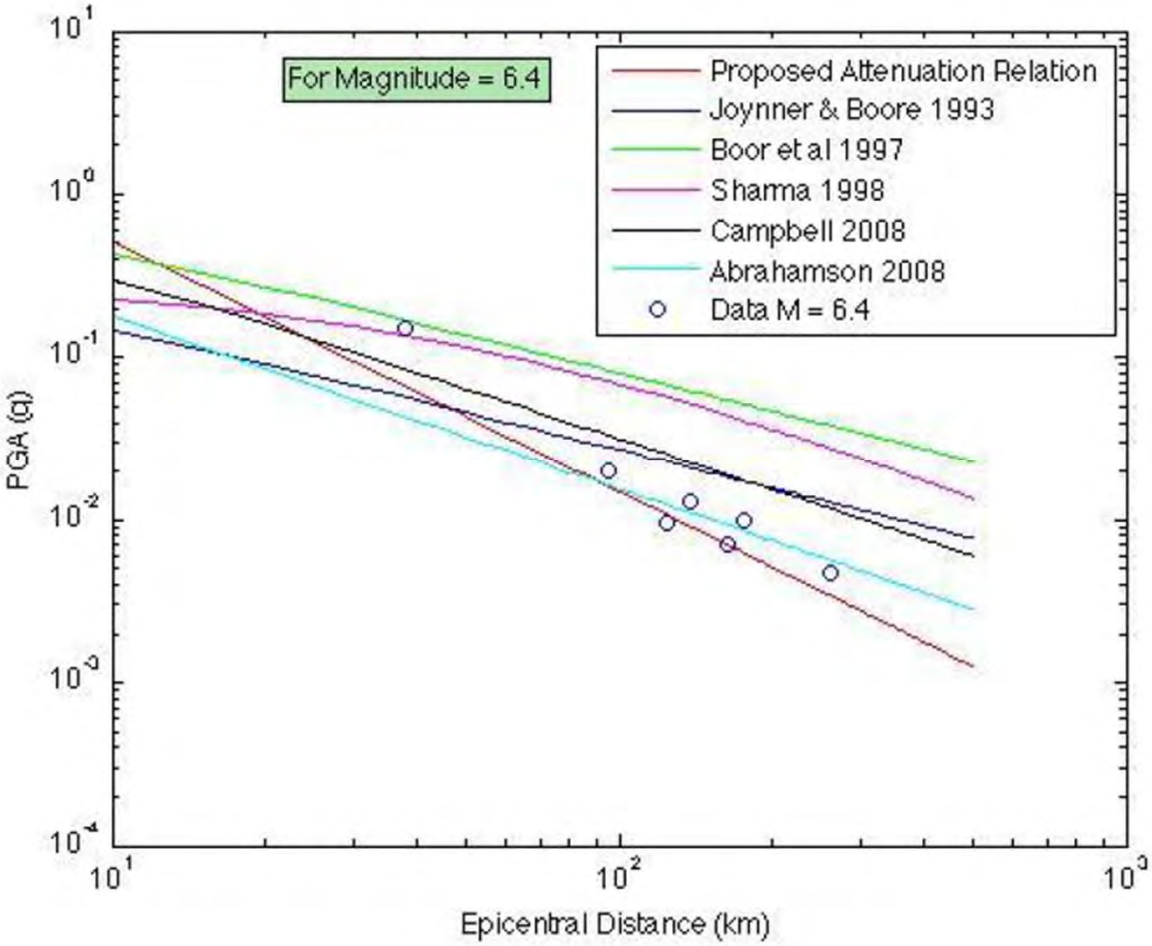

Source: Development of Attenuation Relationship for Northern Pakistan, Shah et al., 2012

MWH®	Comparison of Different Ground Motion Prediction Equations with the Pakistan Model (Magnitude 6.4)	Figure 13

This Page Left Blank Intentionally

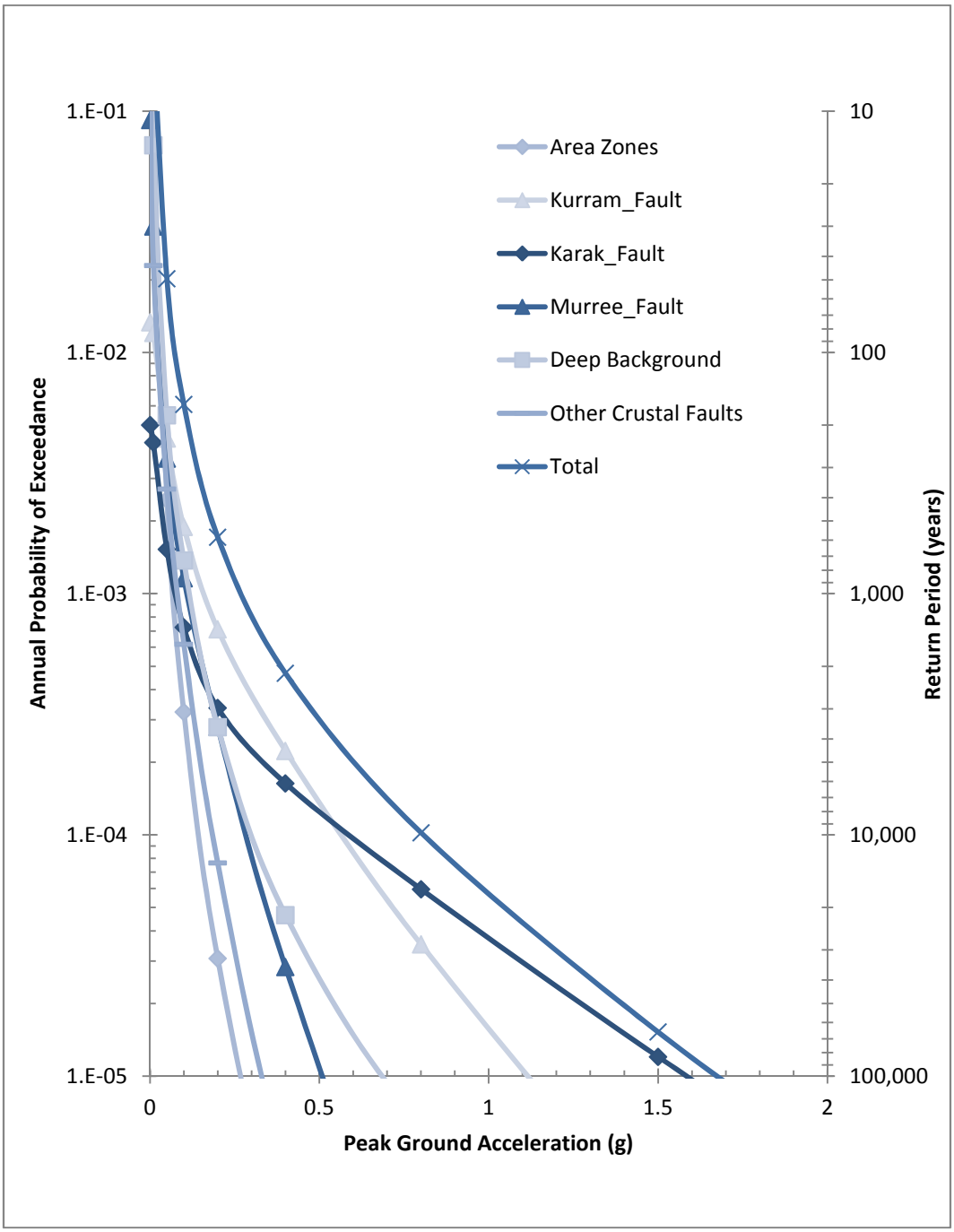

MWH®	Main Dam - Seismic Source Contributions to Median Peak Horizontal Acceleration Hazard	Figure 14

This Page Left Blank Intentionally

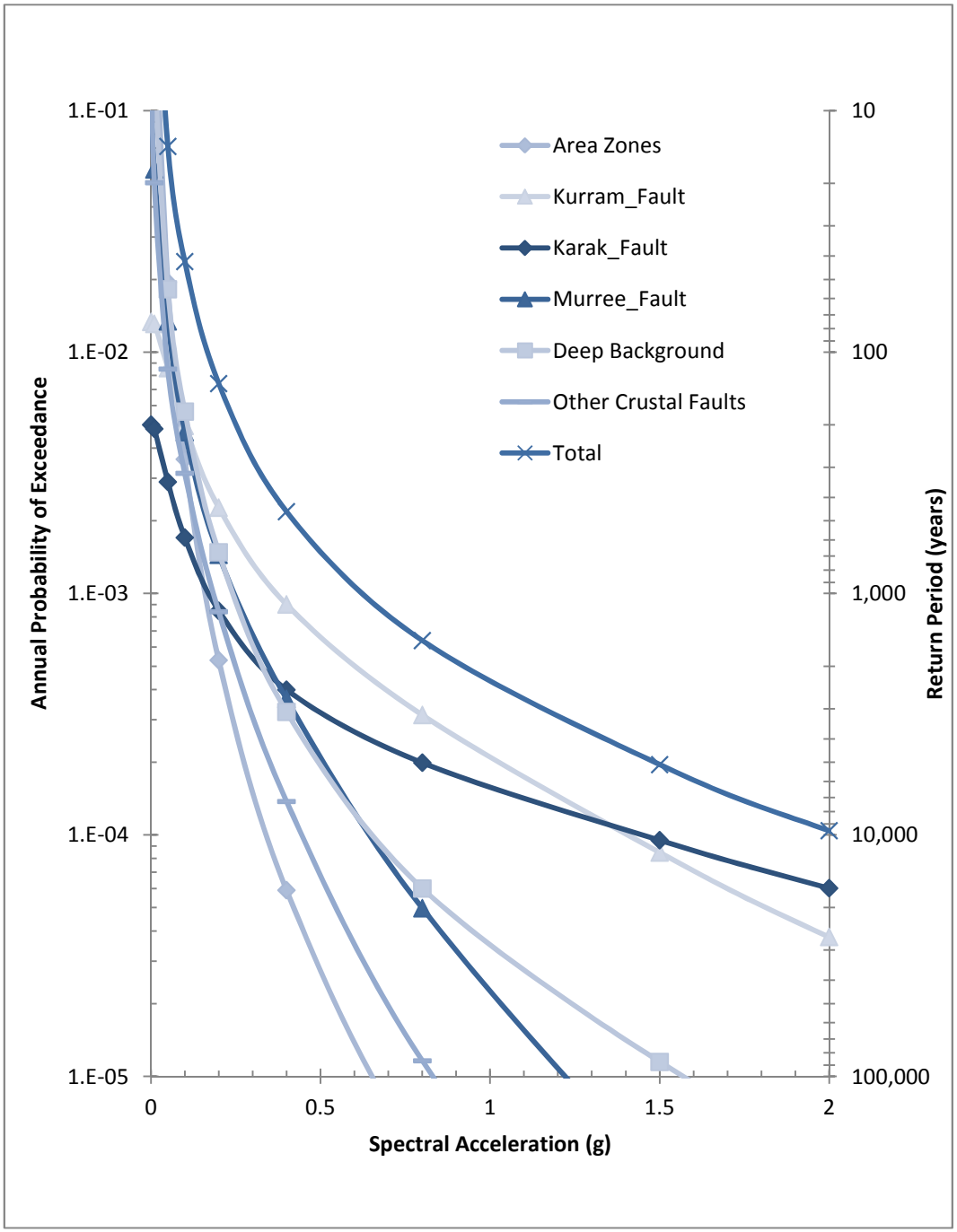

MWH®

Main Dam - Seismic Source Contributions to Median 0.2 Sec Spectral Acceleration Hazard

Figure 15

This Page Left Blank Intentionally

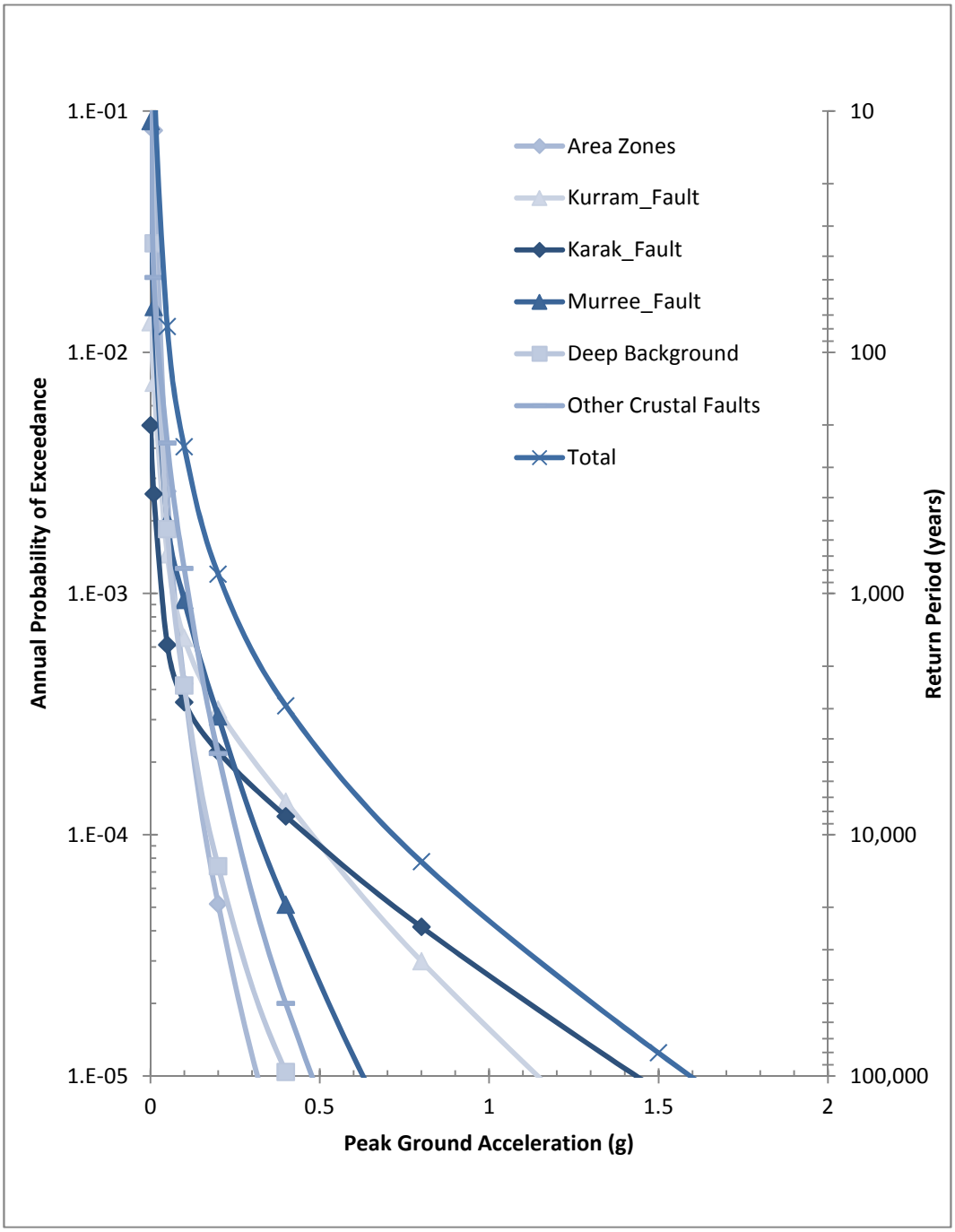

MWH®

Main Dam - Seismic Source Contributions to Median
1.0 Sec Spectral Acceleration Hazard

Figure 16

This Page Left Blank Intentionally

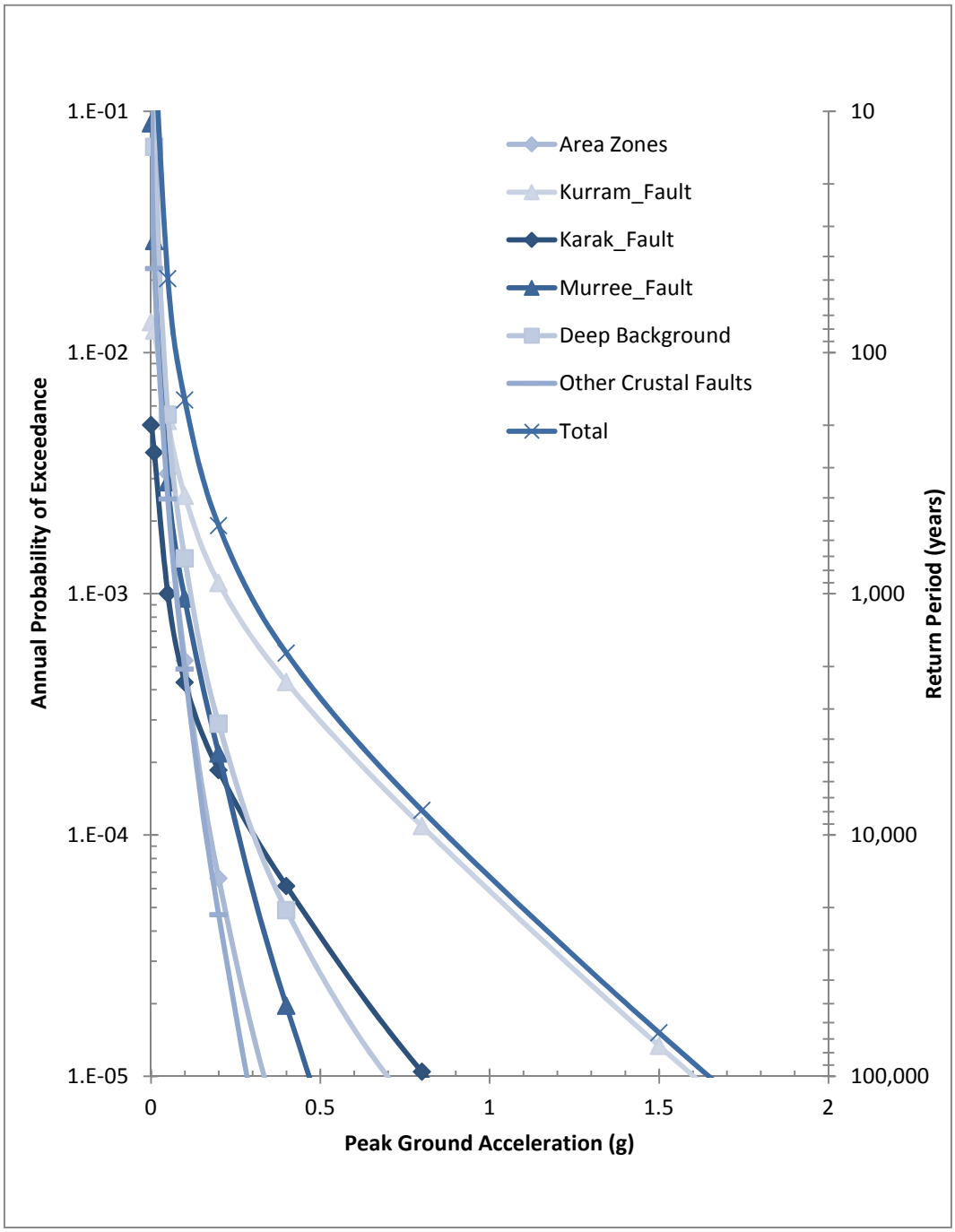

MWH®

Kaitu Weir - Seismic Source Contributions to Median Peak Horizontal Acceleration Hazard

Figure 17

This Page Left Blank Intentionally

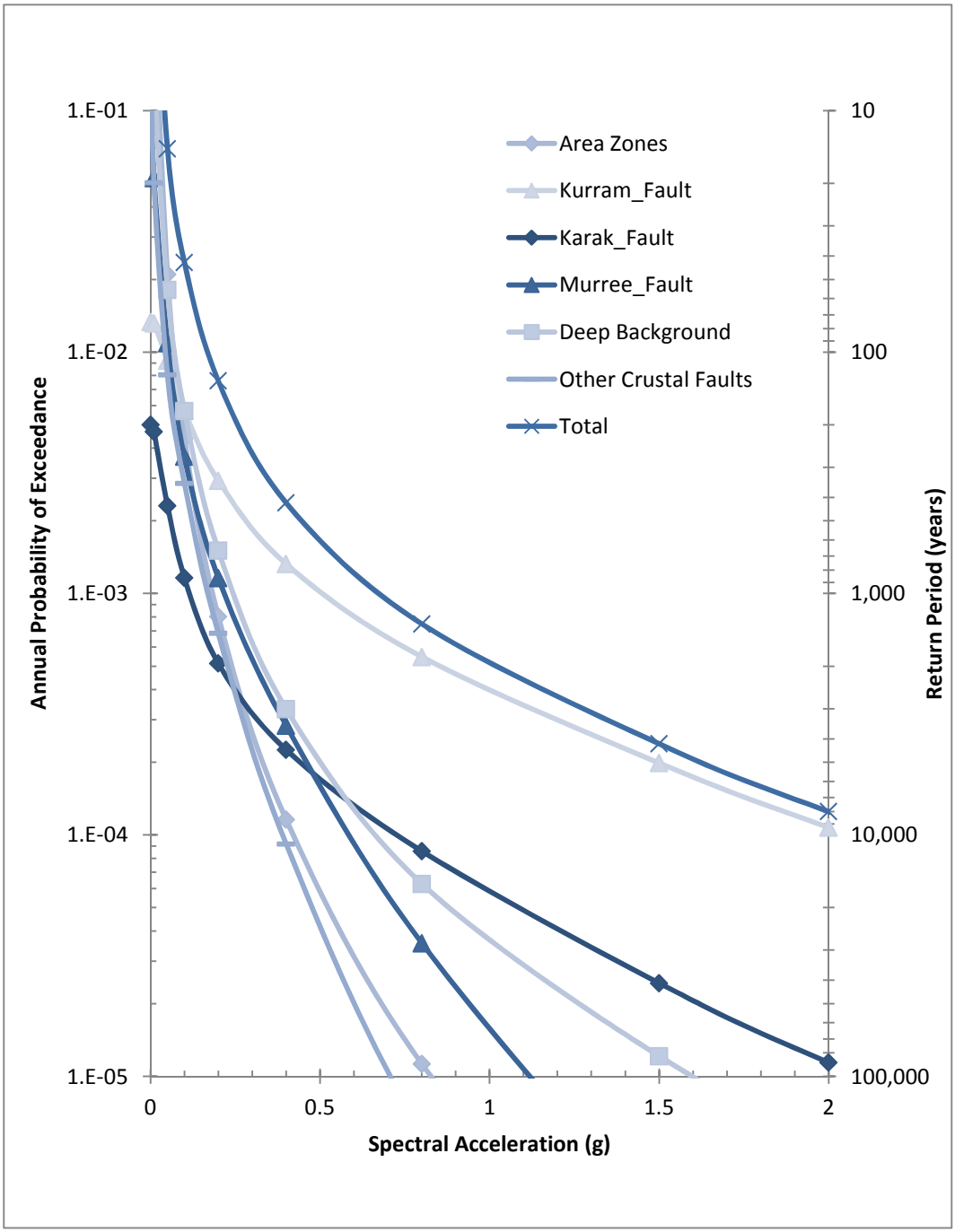

MWH®

Kaitu Weir - Seismic Source Contributions to Median 0.2 Sec Spectral Acceleration Hazard

Figure 18

This Page Left Blank Intentionally

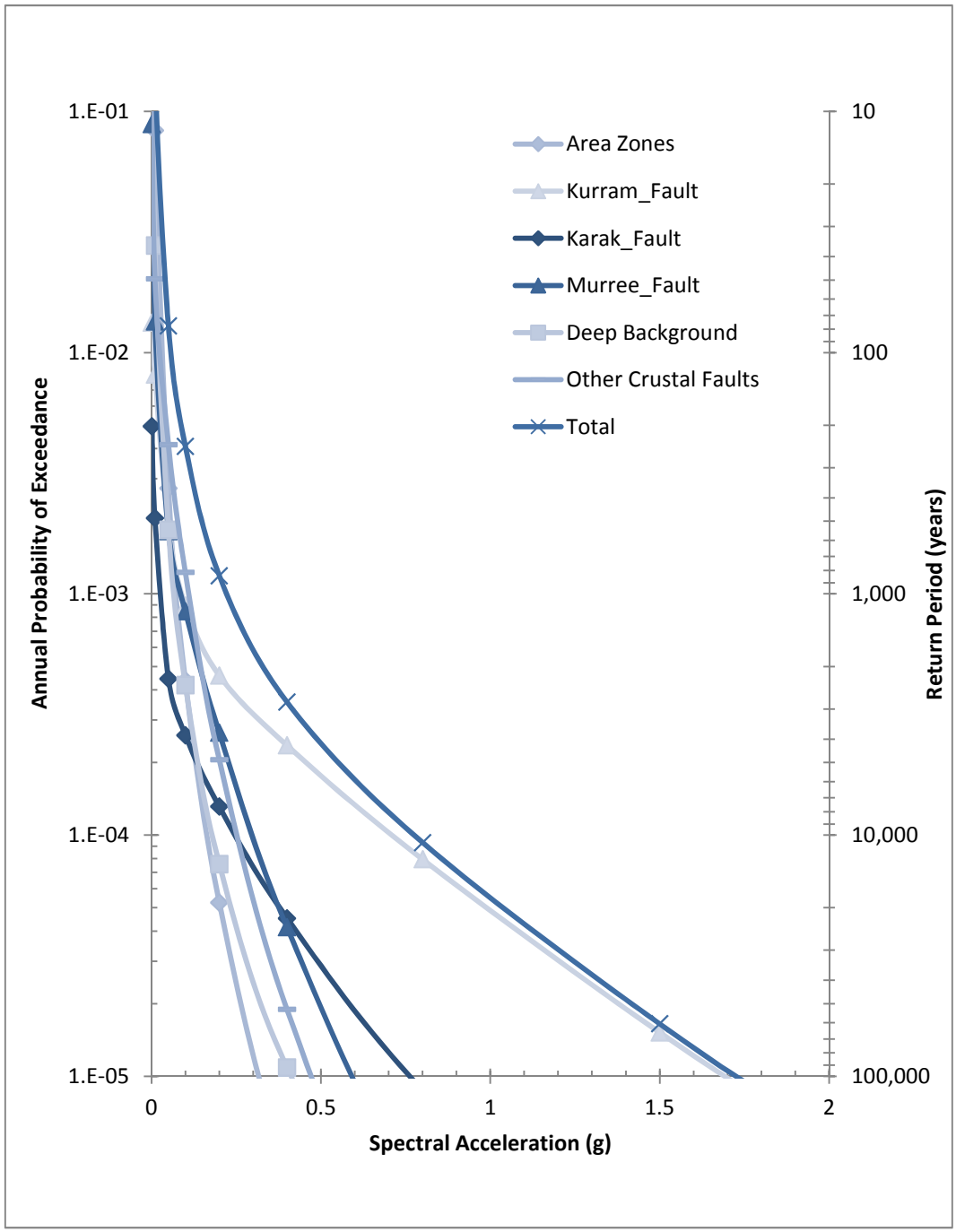

MWH®	Kaitu Weir - Seismic Source Contributions to Median 1.0 Sec Spectral Acceleration Hazard	Figure 19

This Page Left Blank Intentionally

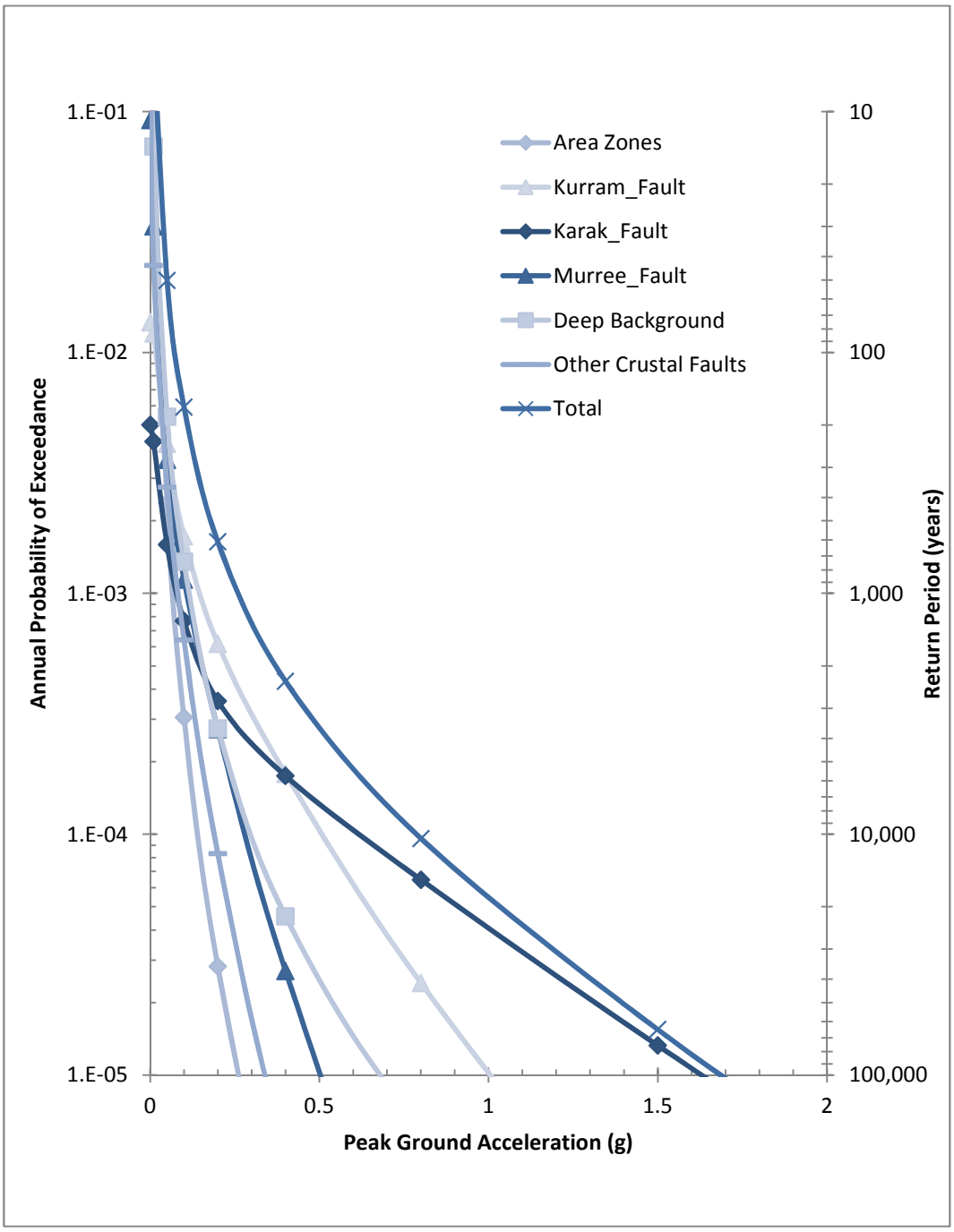

MWH®

Weir II - Seismic Source Contributions to Median Peak Horizontal Acceleration Hazard

Figure 20

This Page Left Blank Intentionally

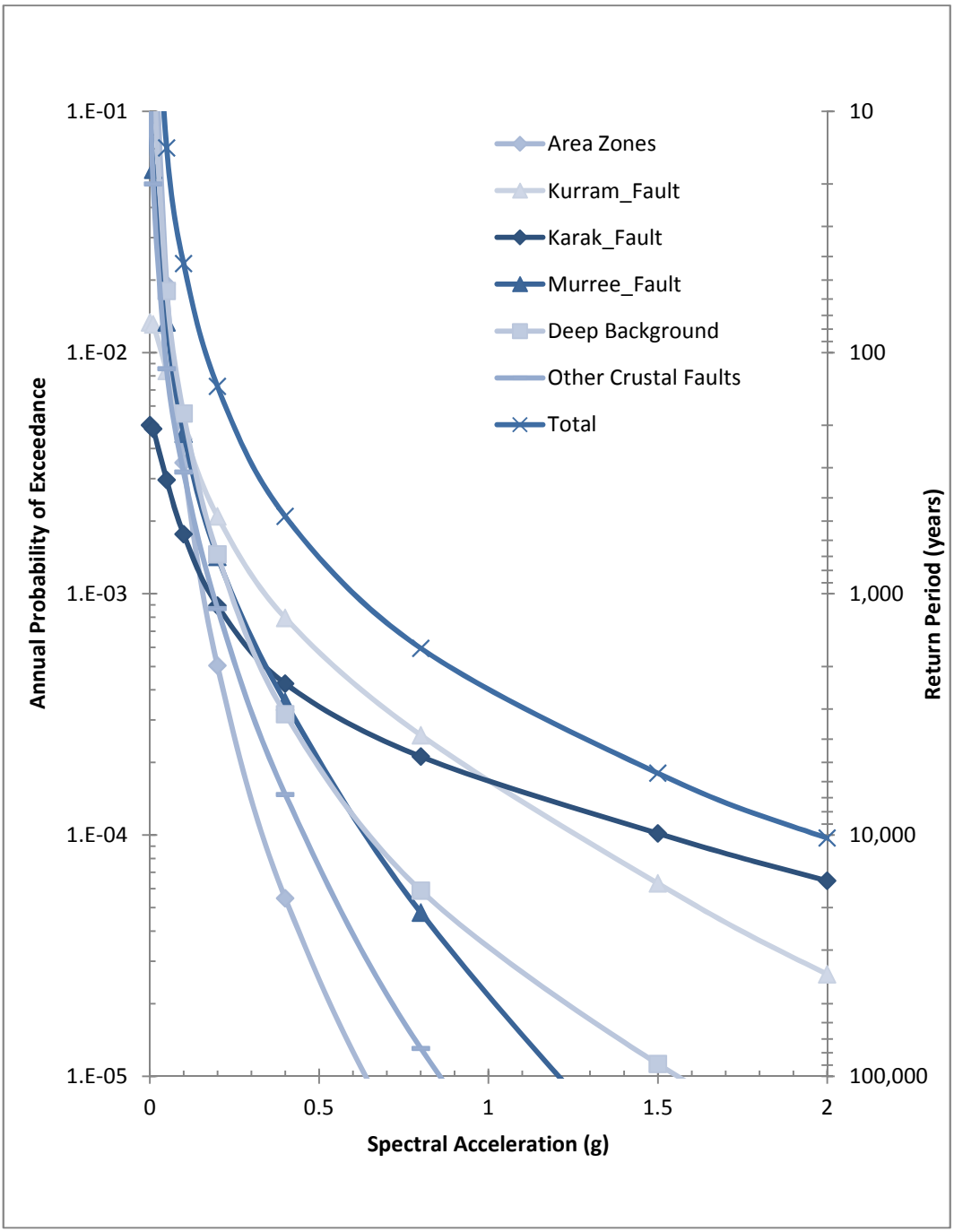

MWH®

Weir II - Seismic Source Contributions to Median 0.2 Sec Spectral Acceleration Hazard

Figure 21

This Page Left Blank Intentionally

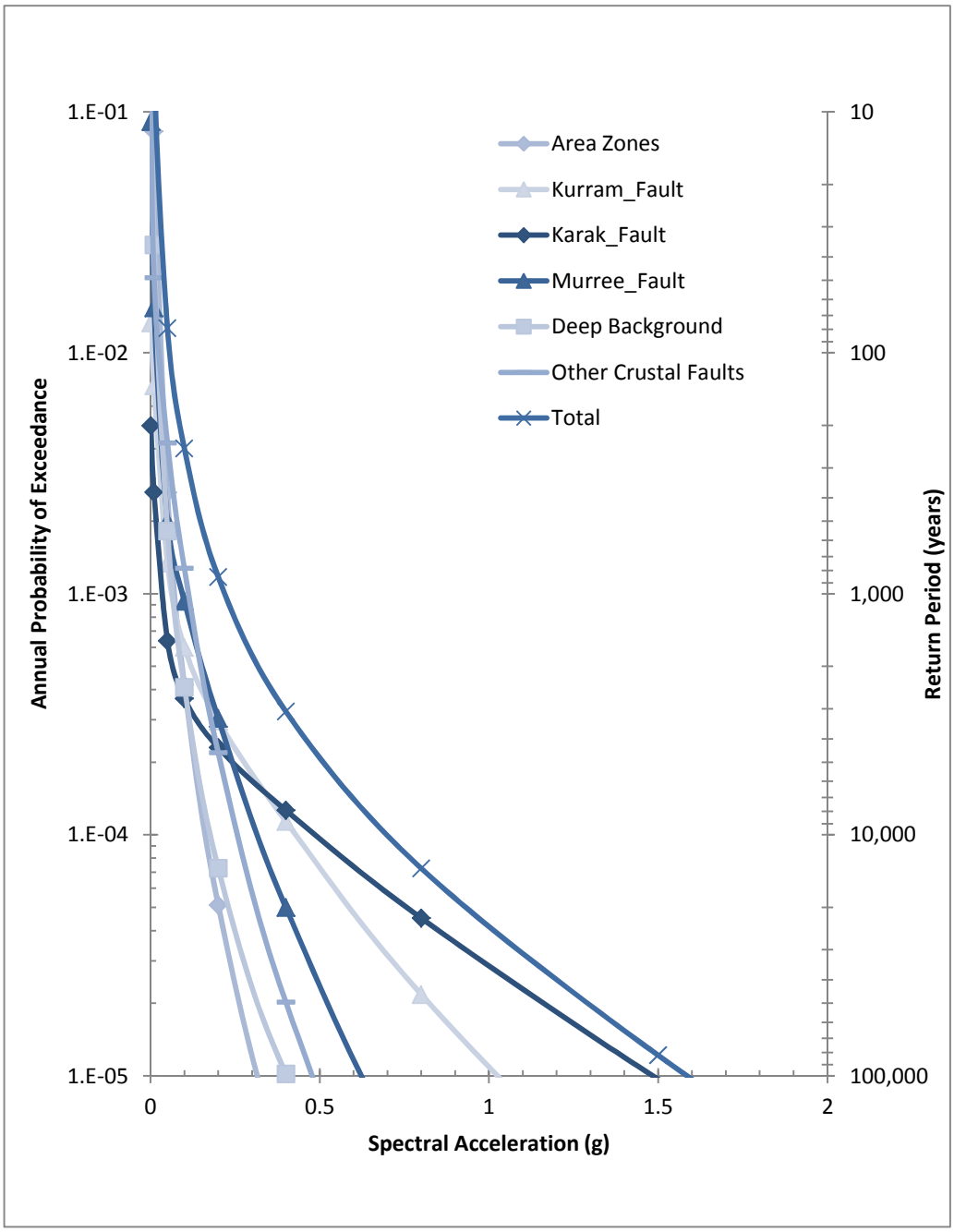

MWH®

Weir II - Seismic Source Contributions to Median 1.0 Sec Spectral Acceleration Hazard

Figure 22

This Page Left Blank Intentionally

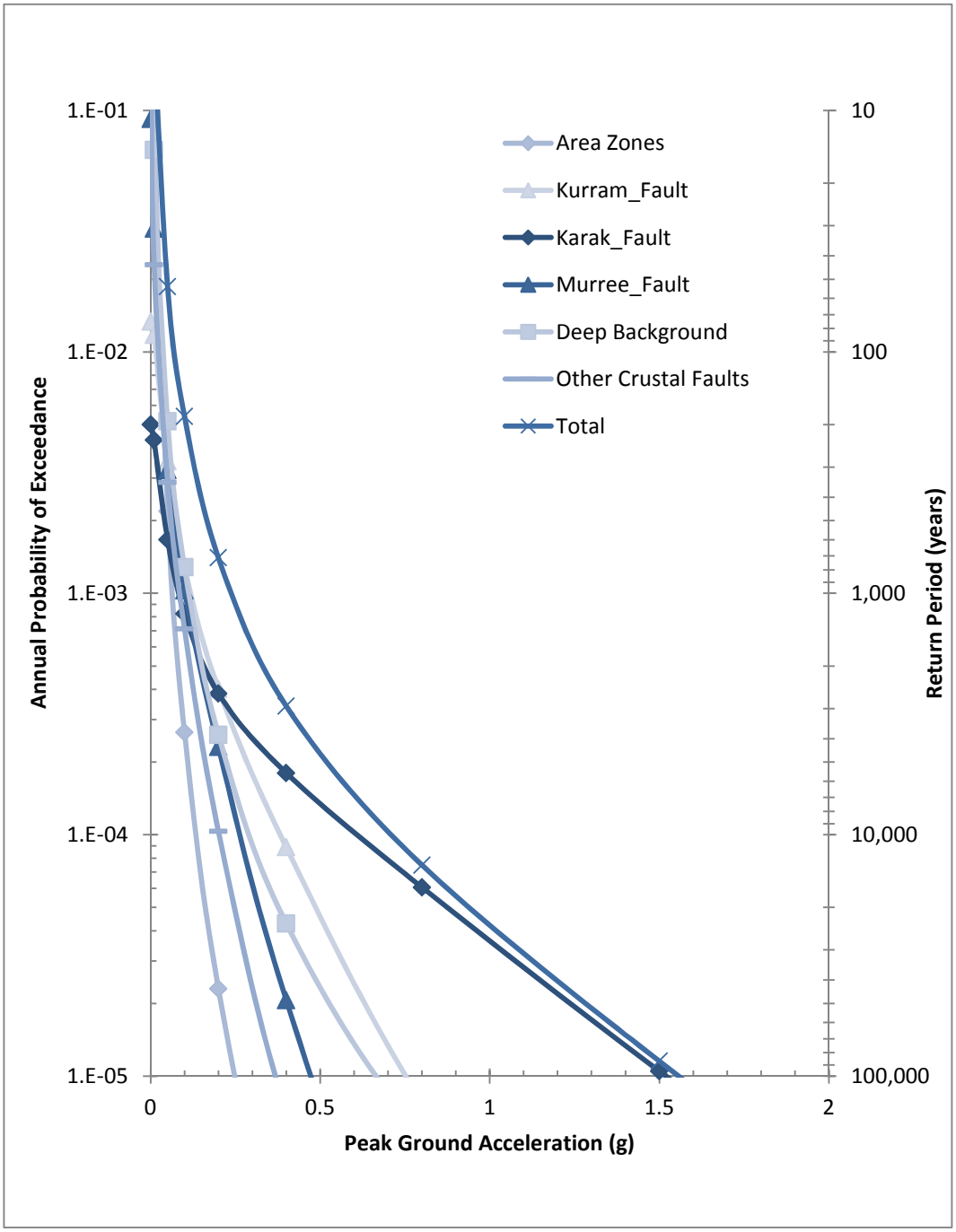

MWH®

Weir III - Seismic Source Contributions to Median Peak Horizontal Acceleration Hazard

Figure 23

This Page Left Blank Intentionally

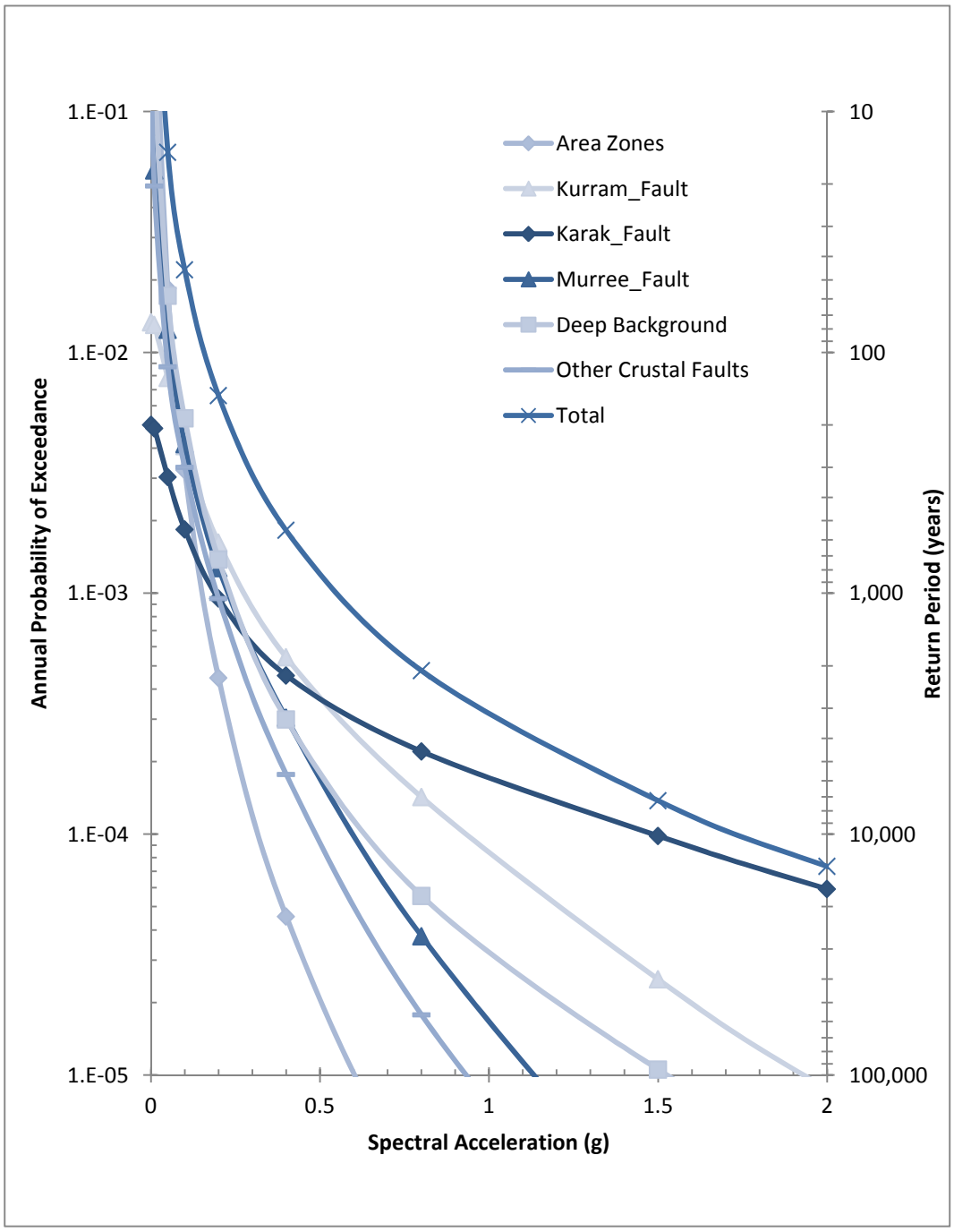

MWH®

Weir III - Seismic Source Contributions to Median 0.2 Sec Spectral Acceleration Hazard

Figure 24

This Page Left Blank Intentionally

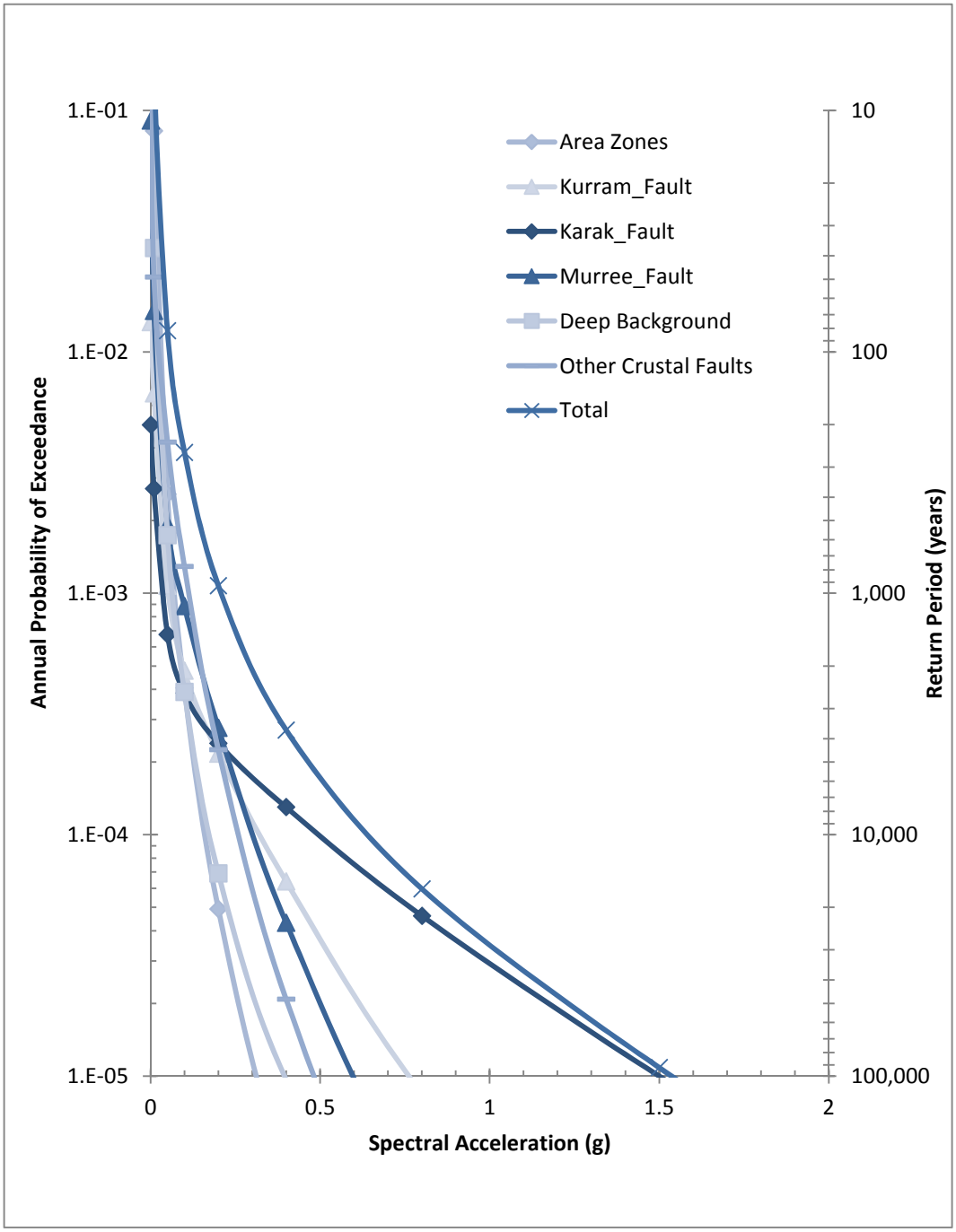

MWH®

Weir III - Seismic Source Contributions to Median 1.0 Sec Spectral Acceleration Hazard

Figure 25

This Page Left Blank Intentionally

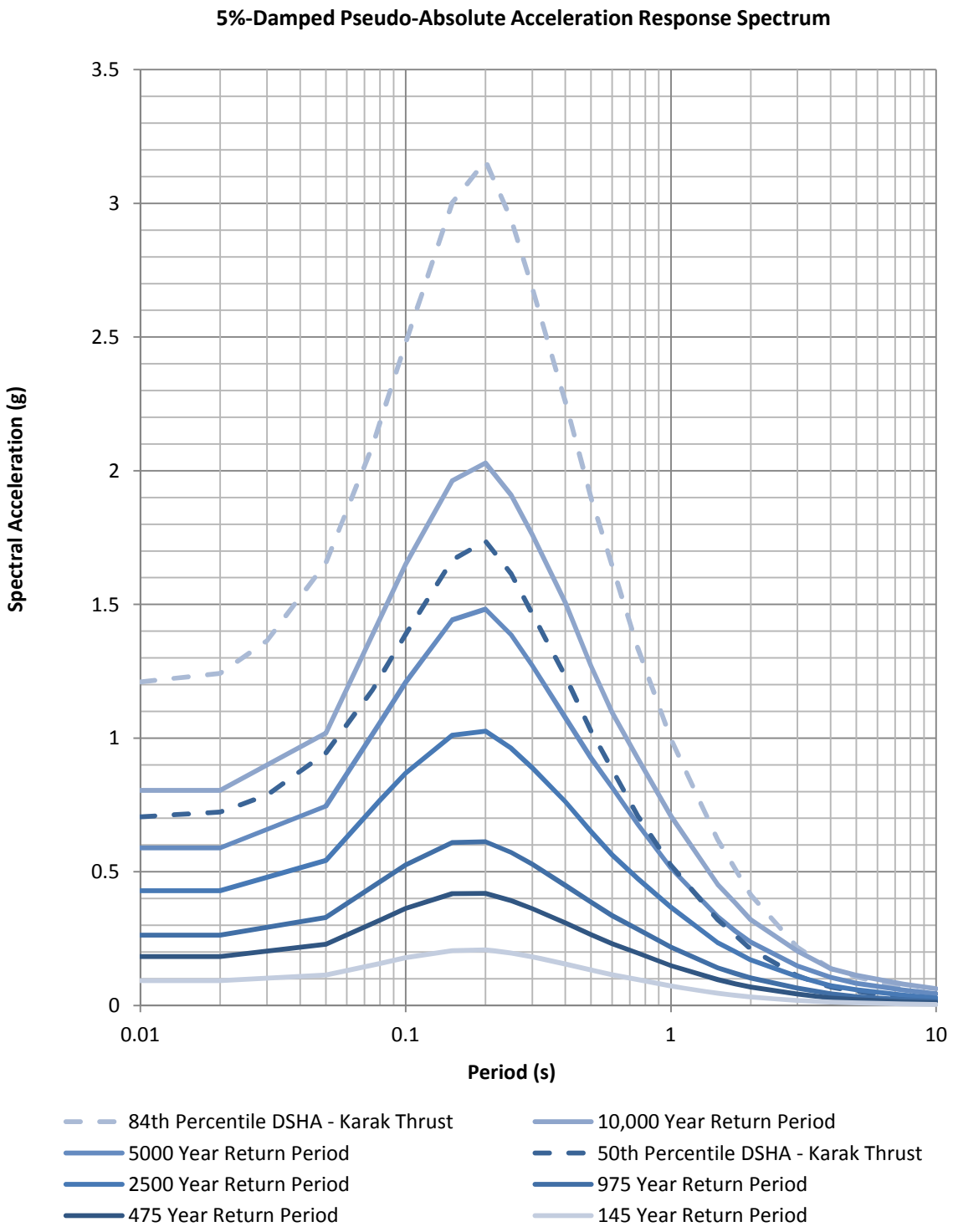

MWH®	Main Dam - Uniform Hazard Spectra	Figure 26

This Page Left Blank Intentionally

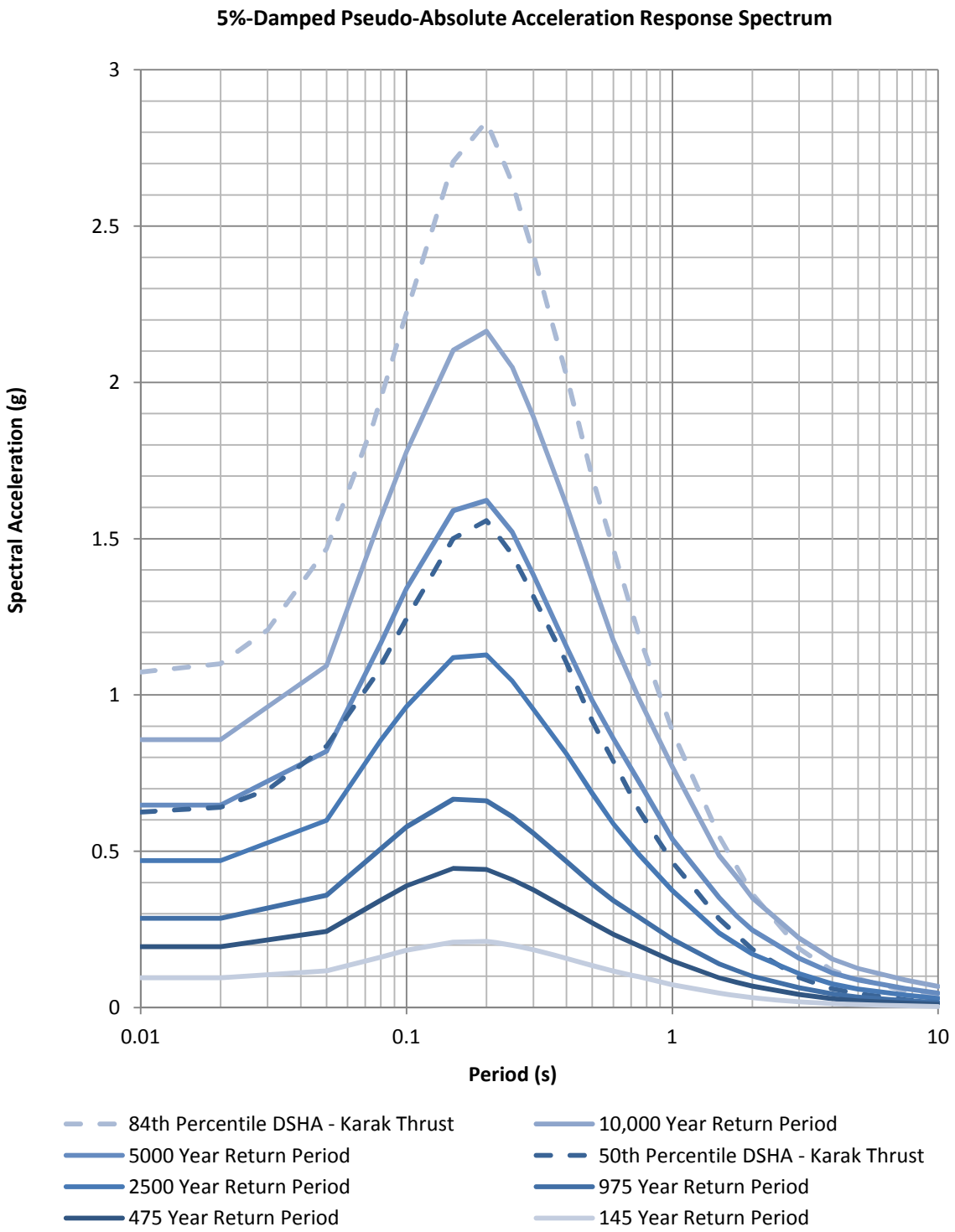

MWH®	Kaitu Weir - Uniform Hazard Spectra	Figure 27

This Page Left Blank Intentionally

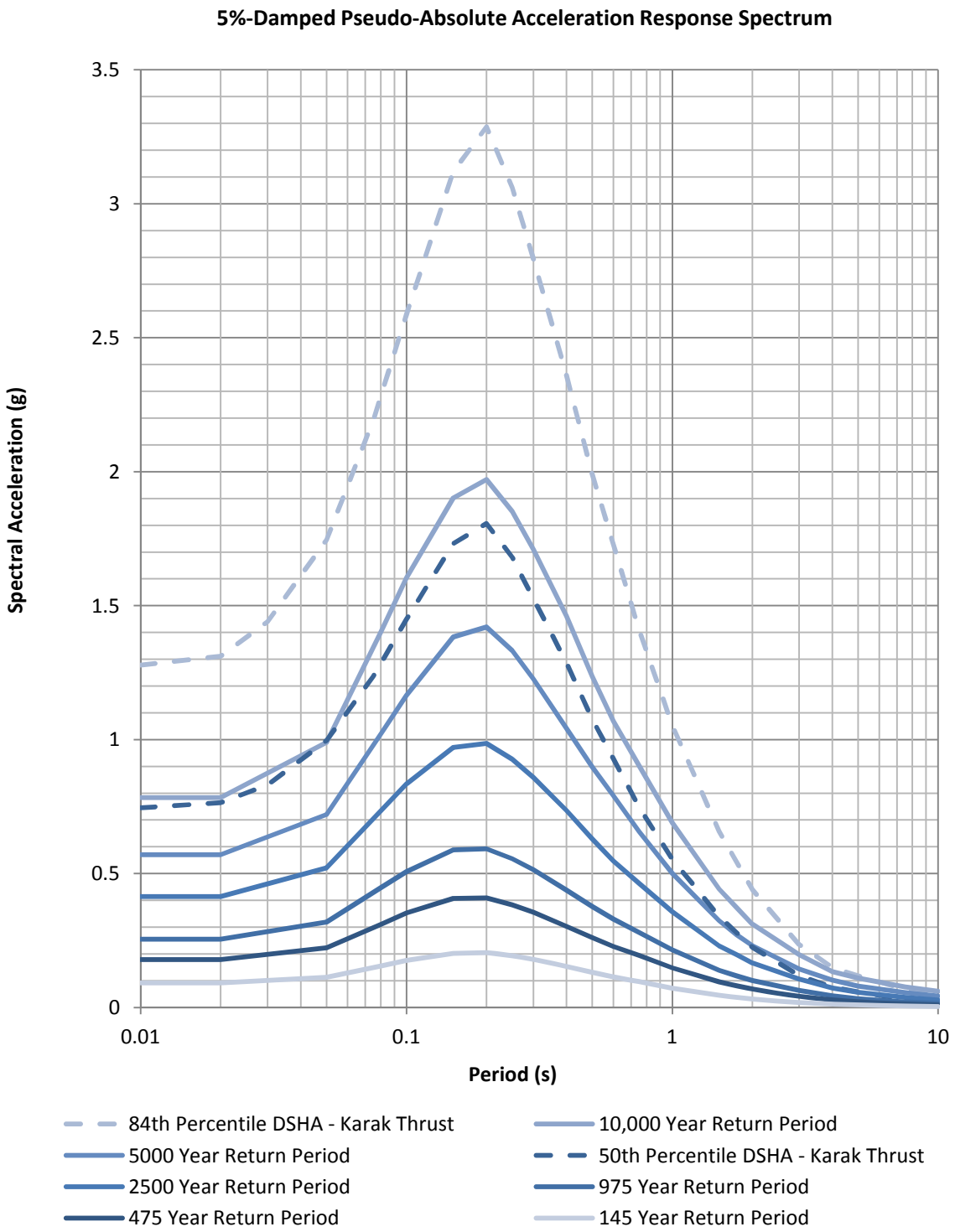

MWH®	Weir II - Uniform Hazard Spectra	Figure 28

This Page Left Blank Intentionally

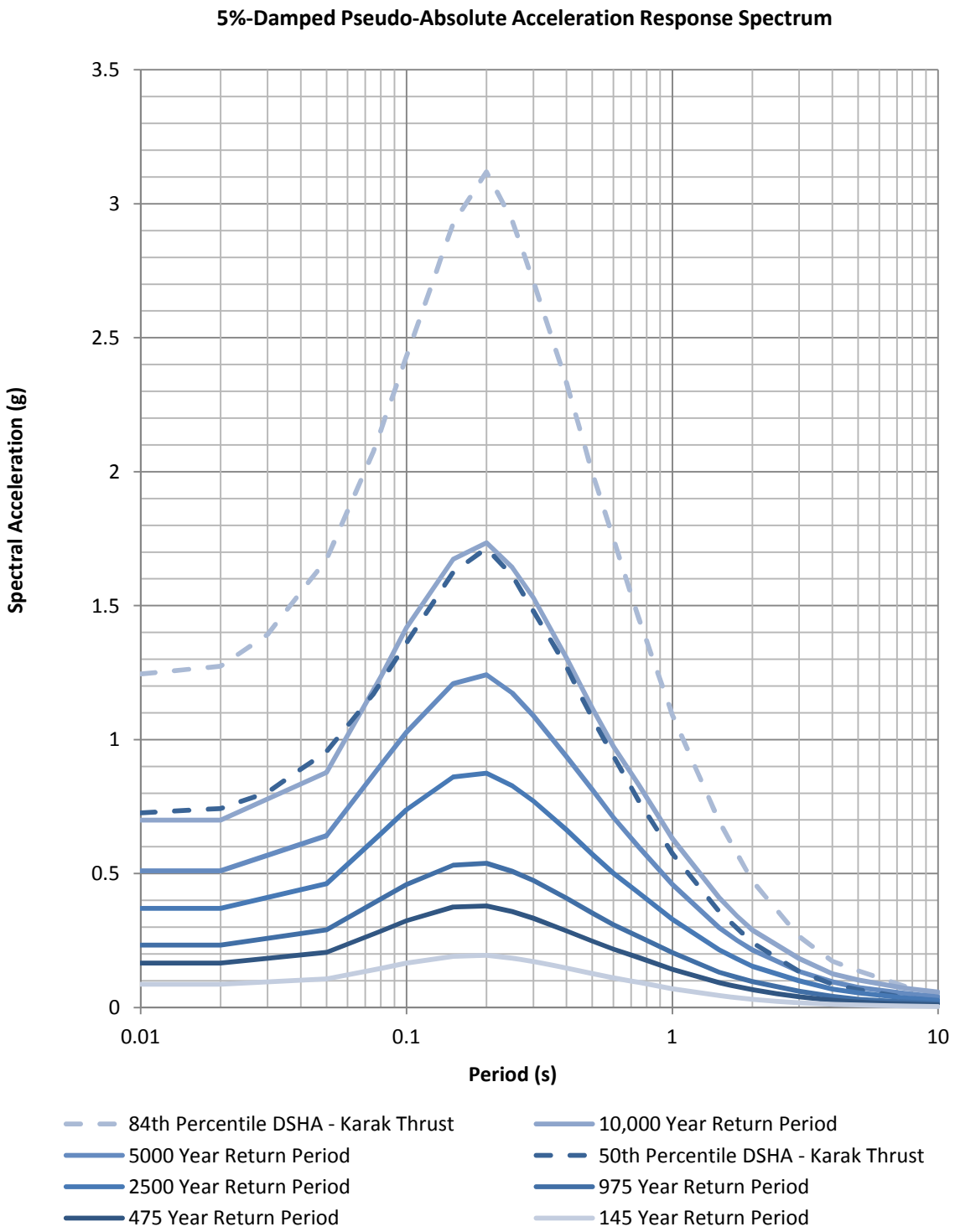

MWH®	Weir III - Uniform Hazard Spectra	Figure 29

This Page Left Blank Intentionally

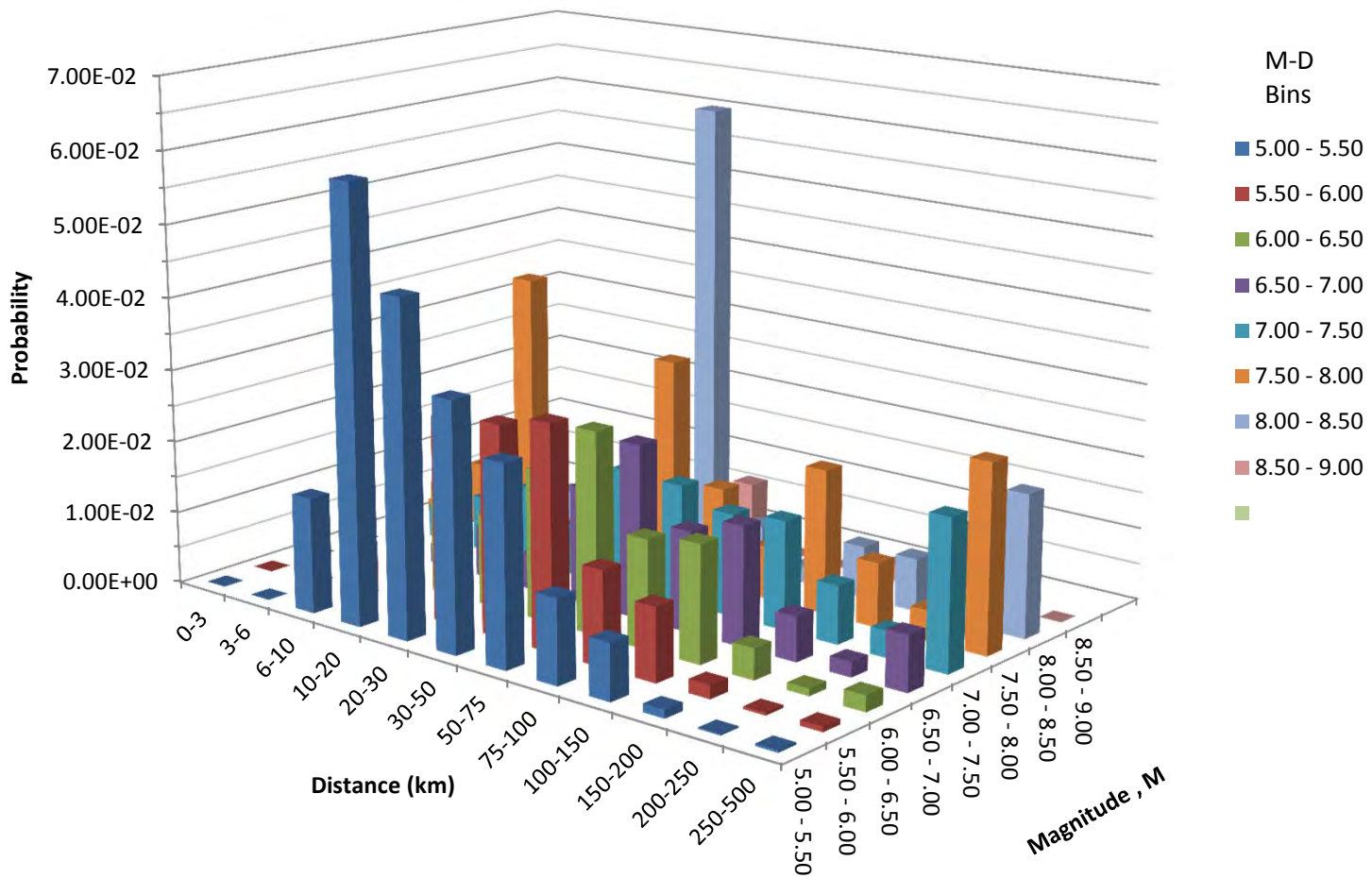

MWH®

Deaggregation 145-yr Return Period Peak Horizontal Acceleration

Figure 30

This Page Left Blank Intentionally

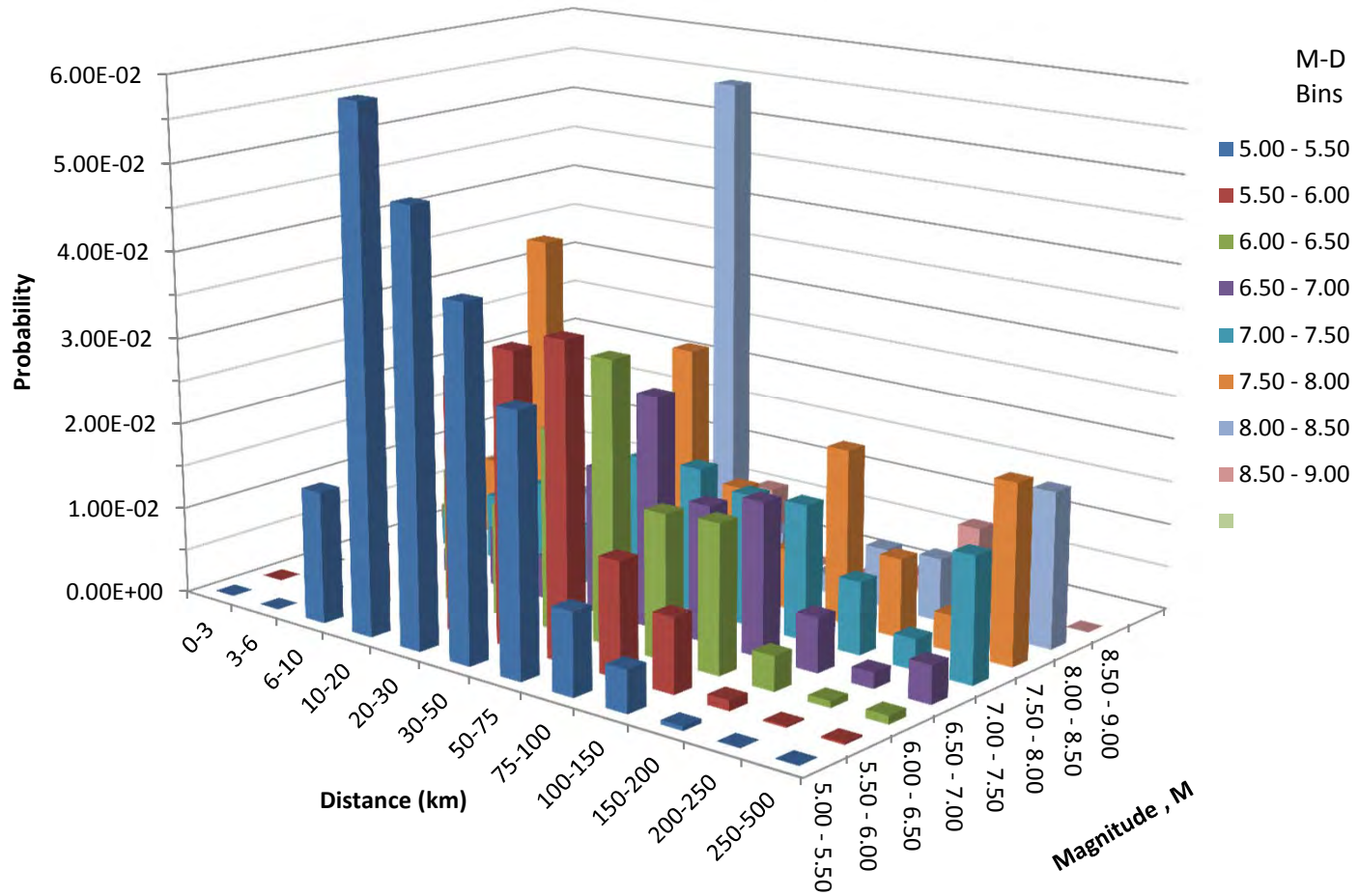

MWH®

Deaggregation 145-yr Return Period 0.2 Sec Horizontal Acceleration

Figure 31

This Page Left Blank Intentionally

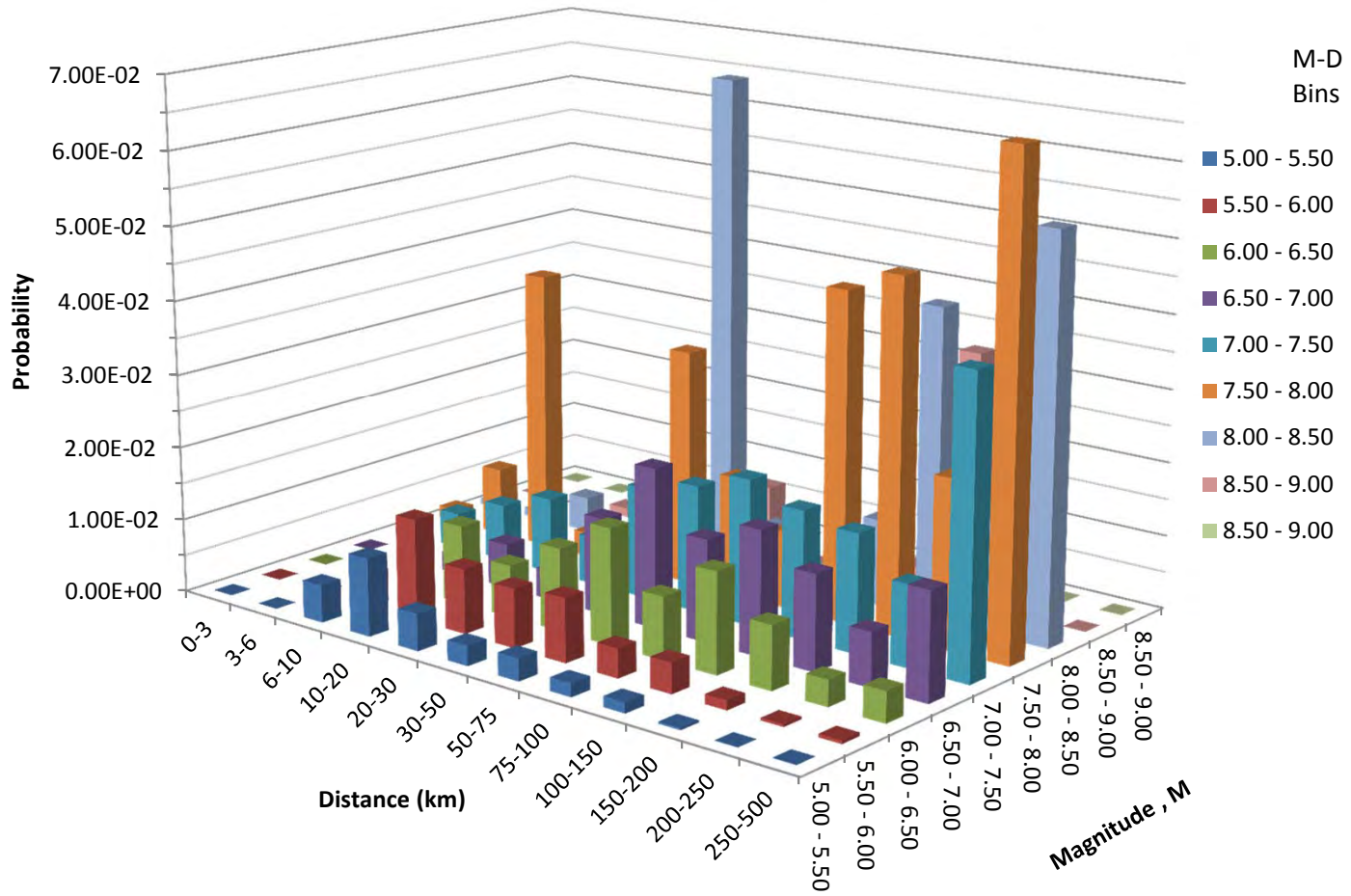

MWH®

Deaggregation 145-yr Return Period 1.0 Sec Horizontal Acceleration

Figure 32

This Page Left Blank Intentionally

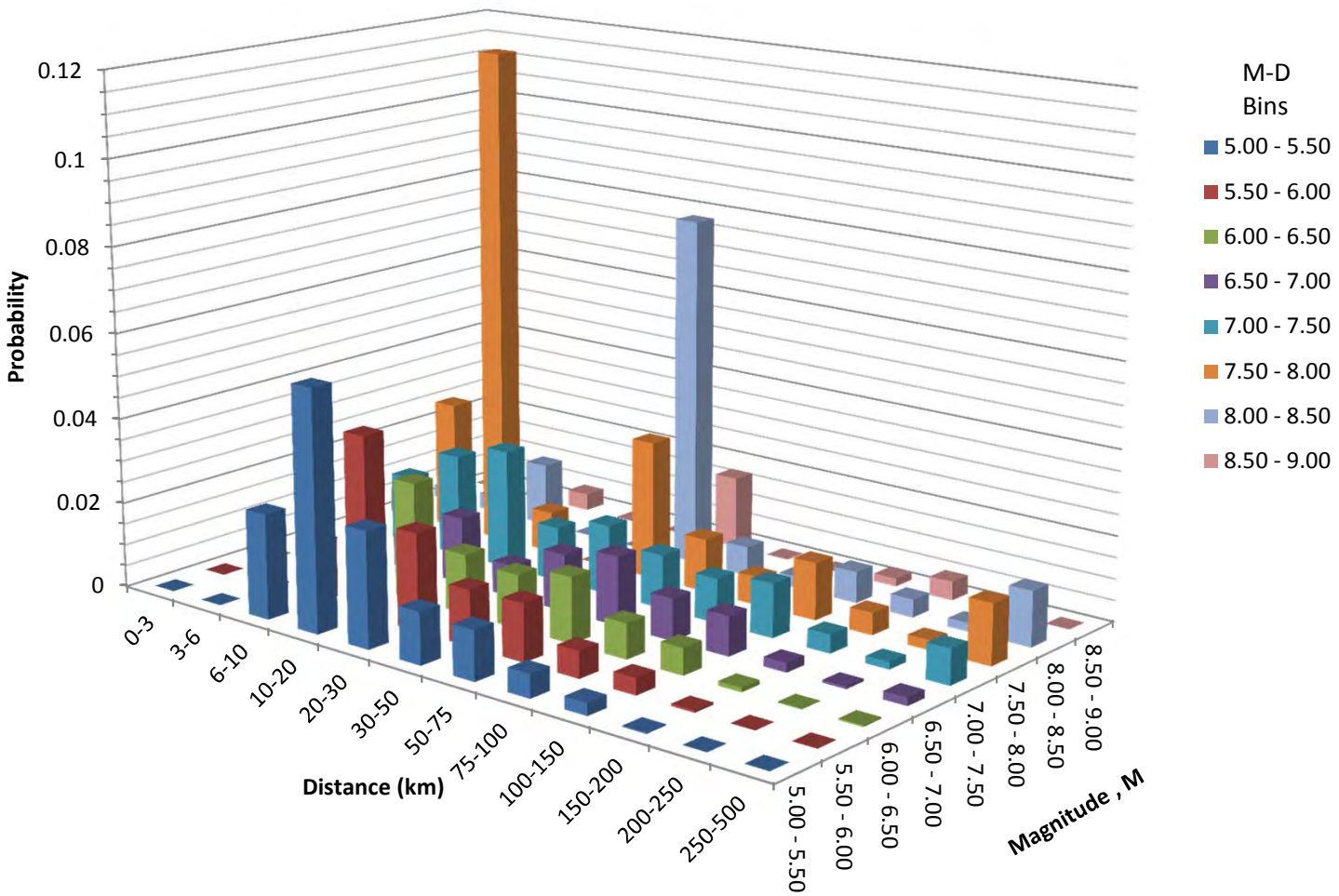

MWH®

Deaggregation 475-yr Return Period Peak Horizontal Acceleration

Figure 33

This Page Left Blank Intentionally

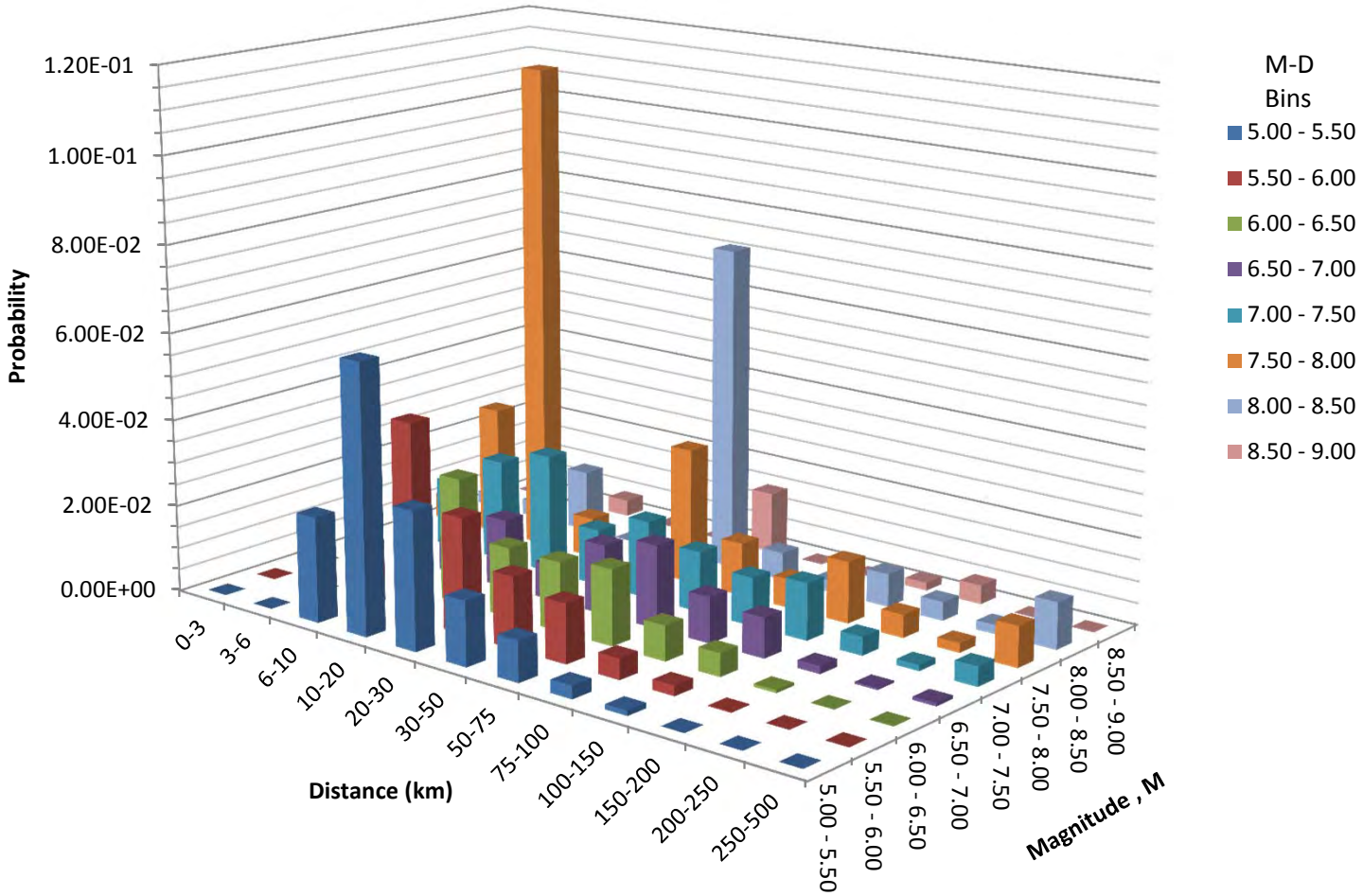

MWH®

Deaggregation 475-yr Return Period 0.2 Sec Horizontal Acceleration

Figure 34

This Page Left Blank Intentionally

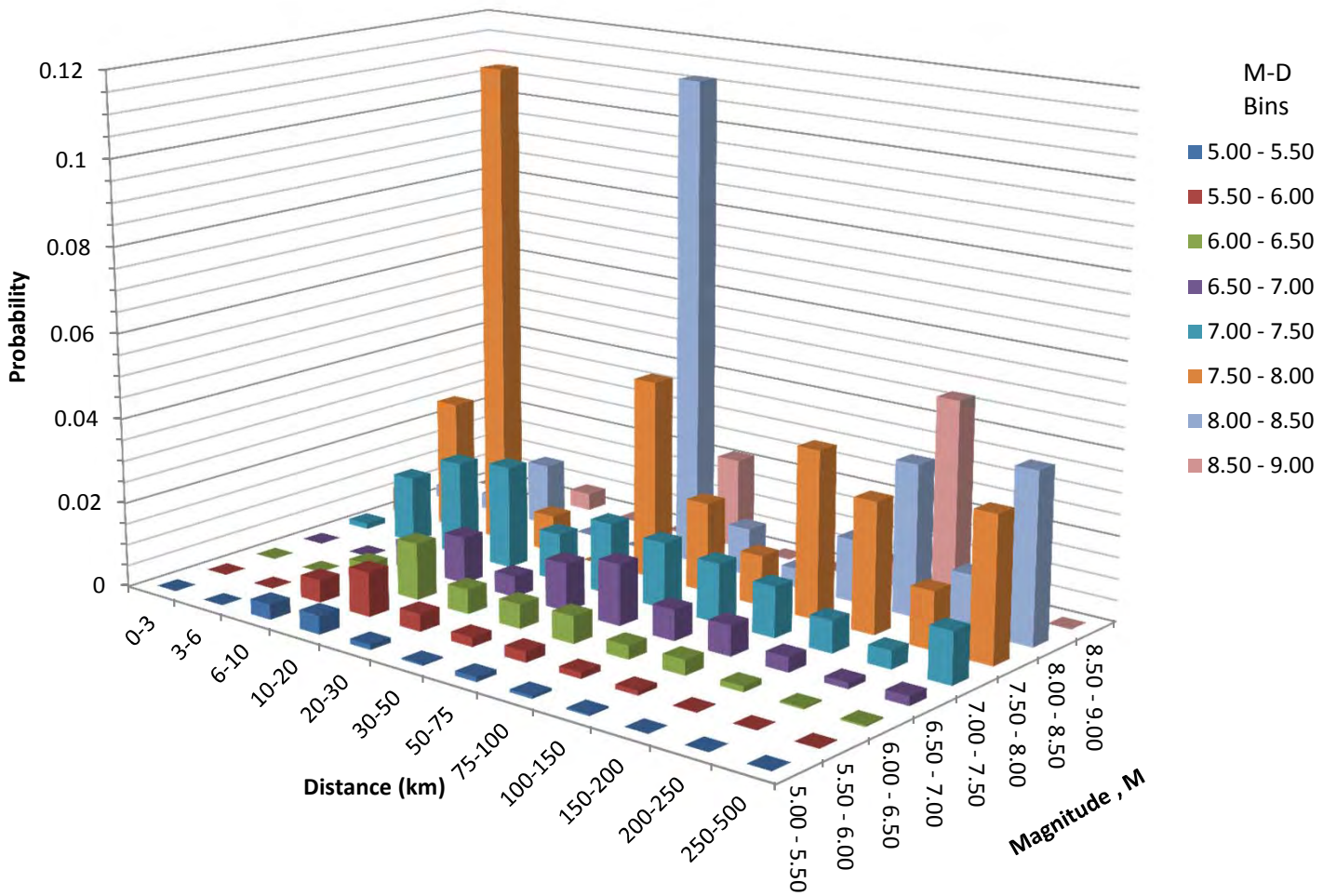

MWH®

Deaggregation 475-yr Return Period 1.0 Sec Horizontal Acceleration

Figure 35

This Page Left Blank Intentionally

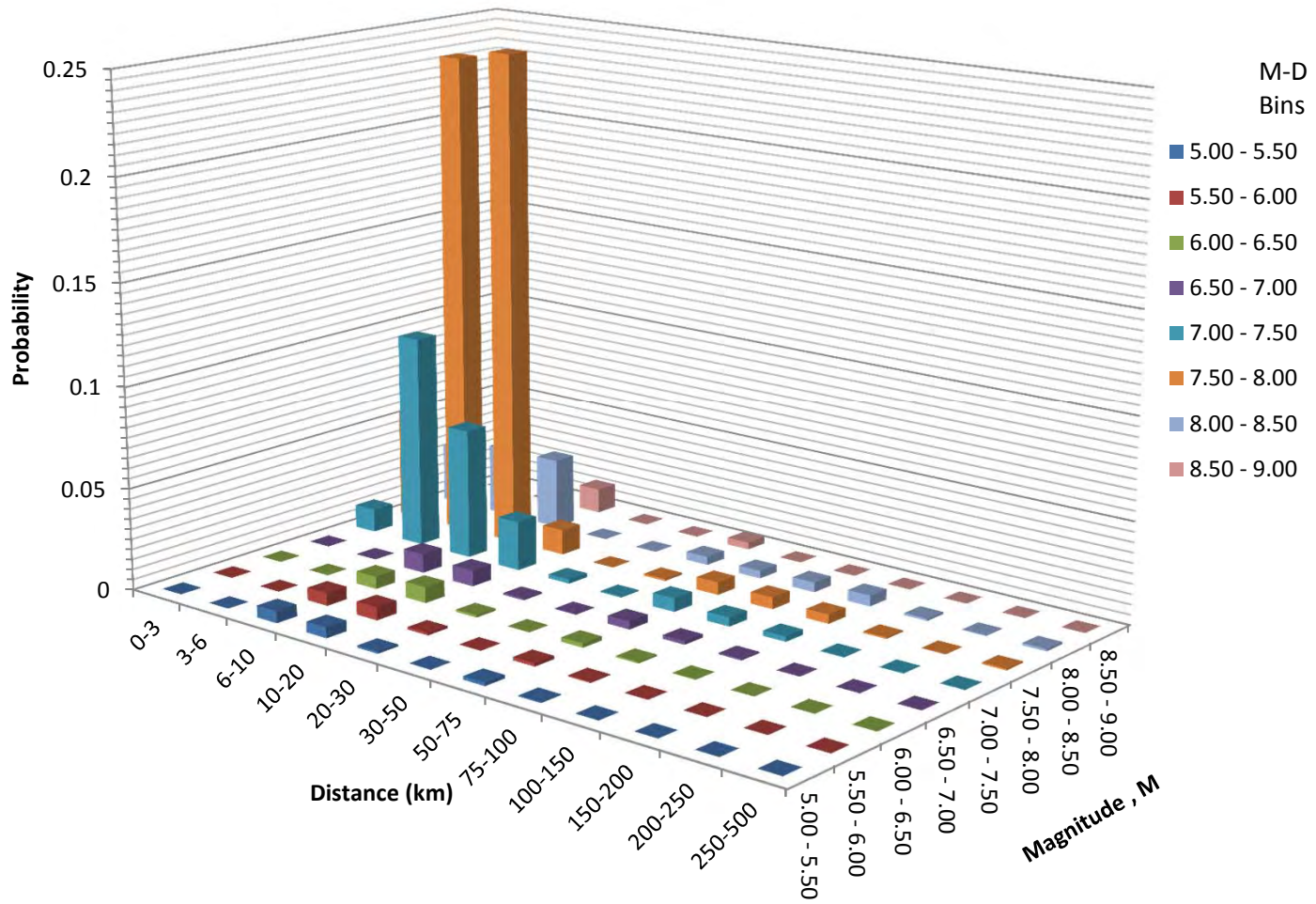

MWH®

Deaggregation 10,000-yr Return Period Peak Horizontal Acceleration

Figure 36

This Page Left Blank Intentionally

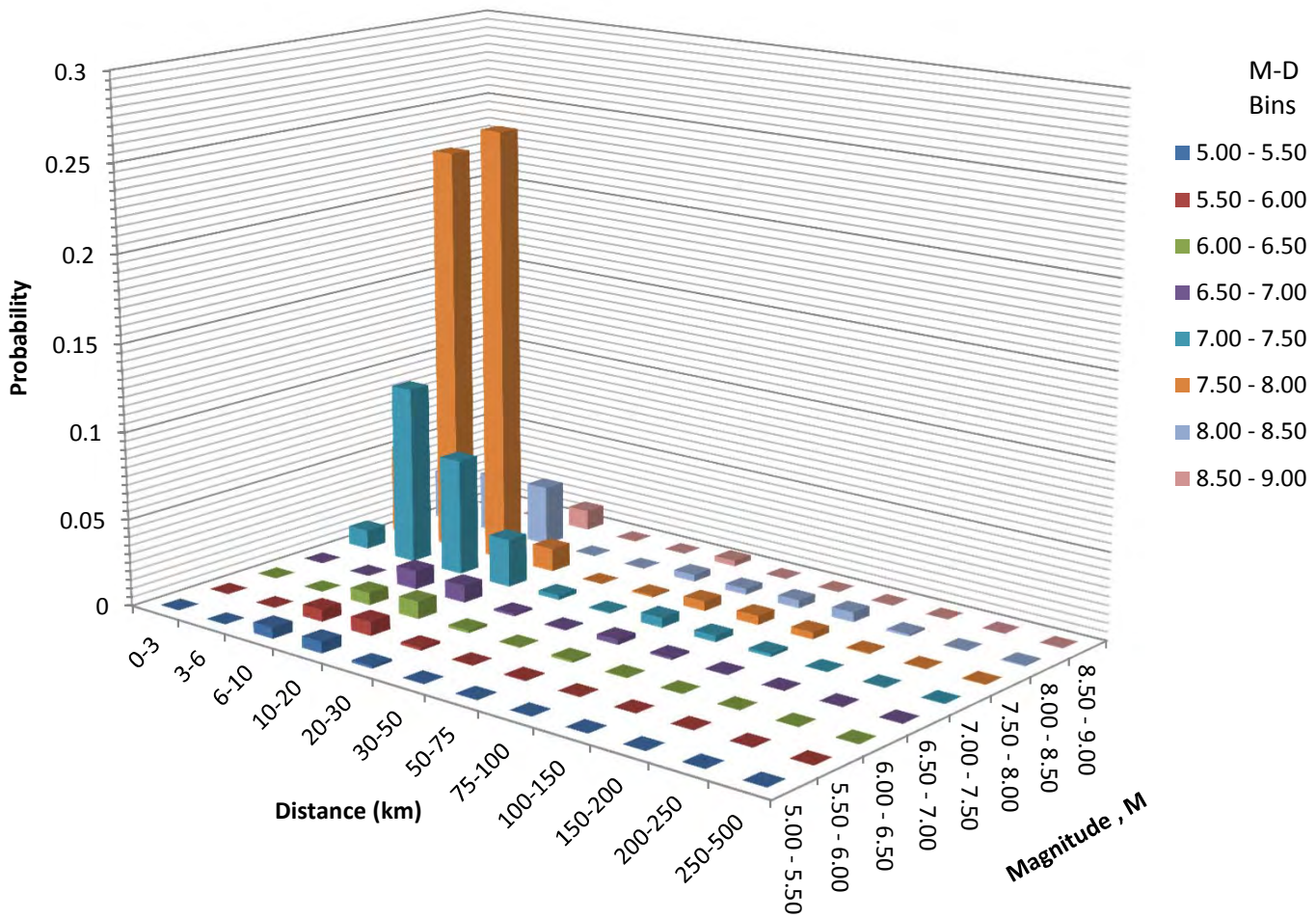

MWH®

Deaggregation 10,000-yr Return Period 0.2 Sec Horizontal Acceleration

Figure 37

This Page Left Blank Intentionally

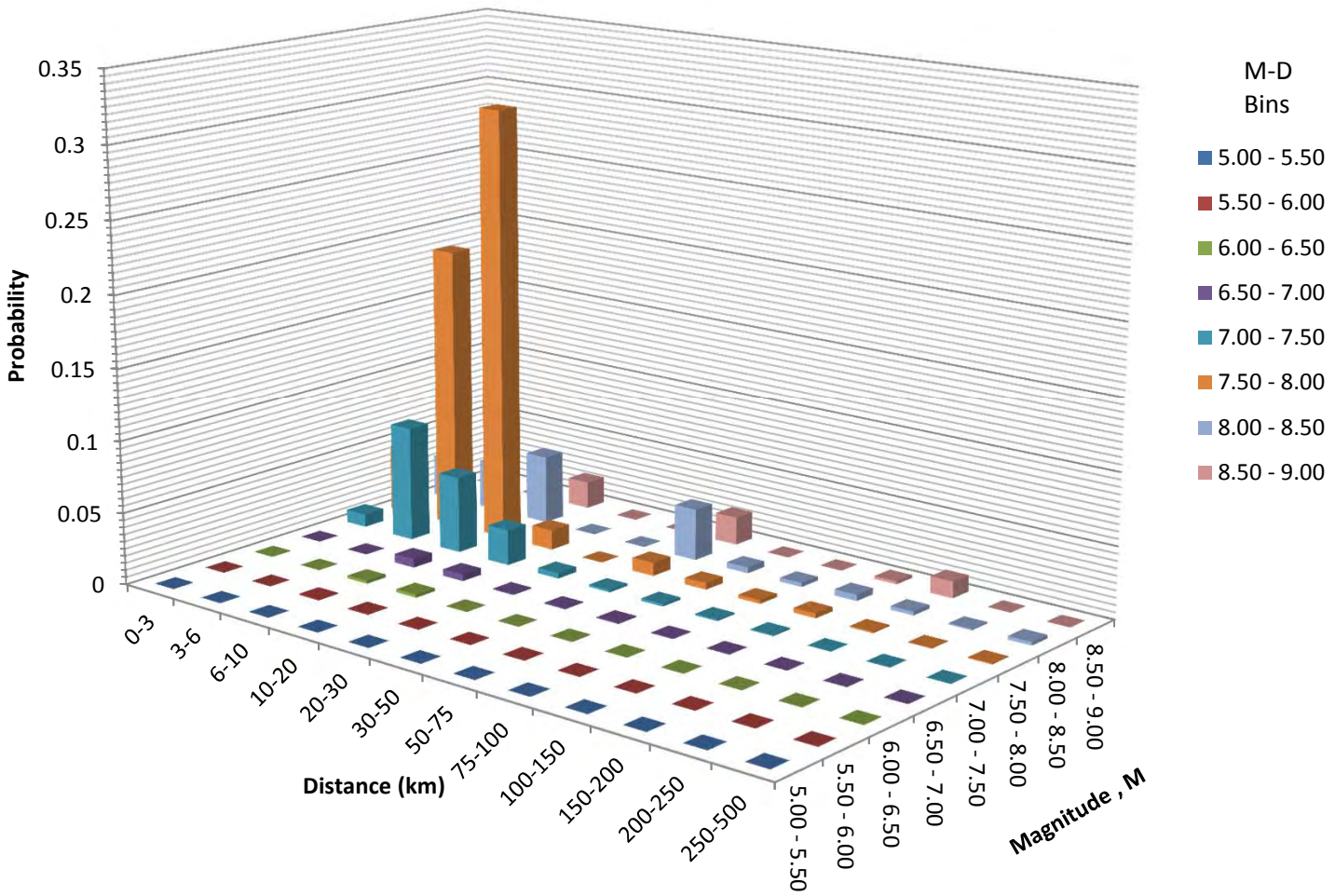

MWH®

Deaggregation 10,000-yr Return Period 1.0 Sec Horizontal Acceleration

Figure 38

This Page Left Blank Intentionally

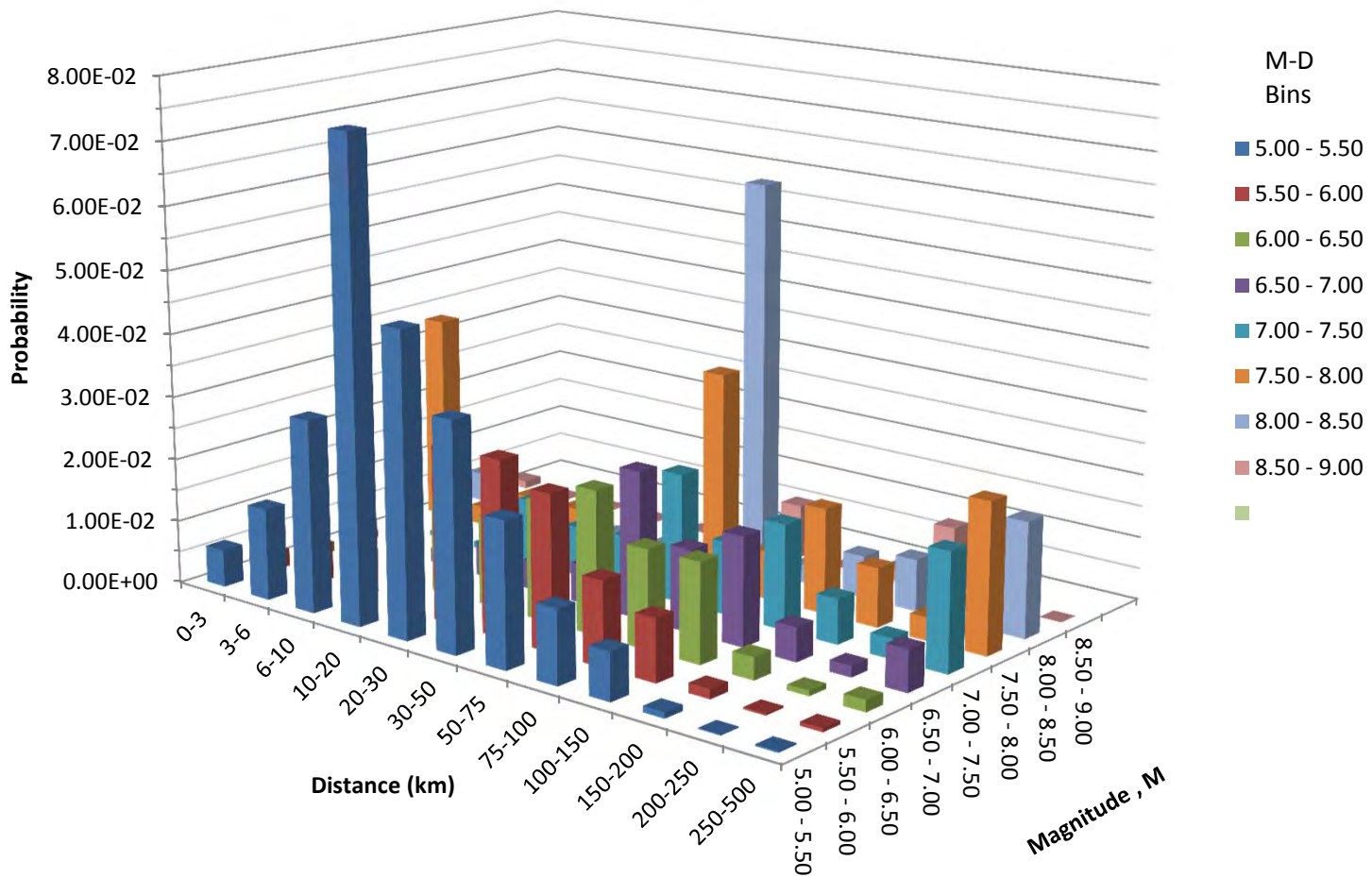

MWH®

Deaggregation 145-yr Return Period Peak Horizontal Acceleration

Figure 39

This Page Left Blank Intentionally

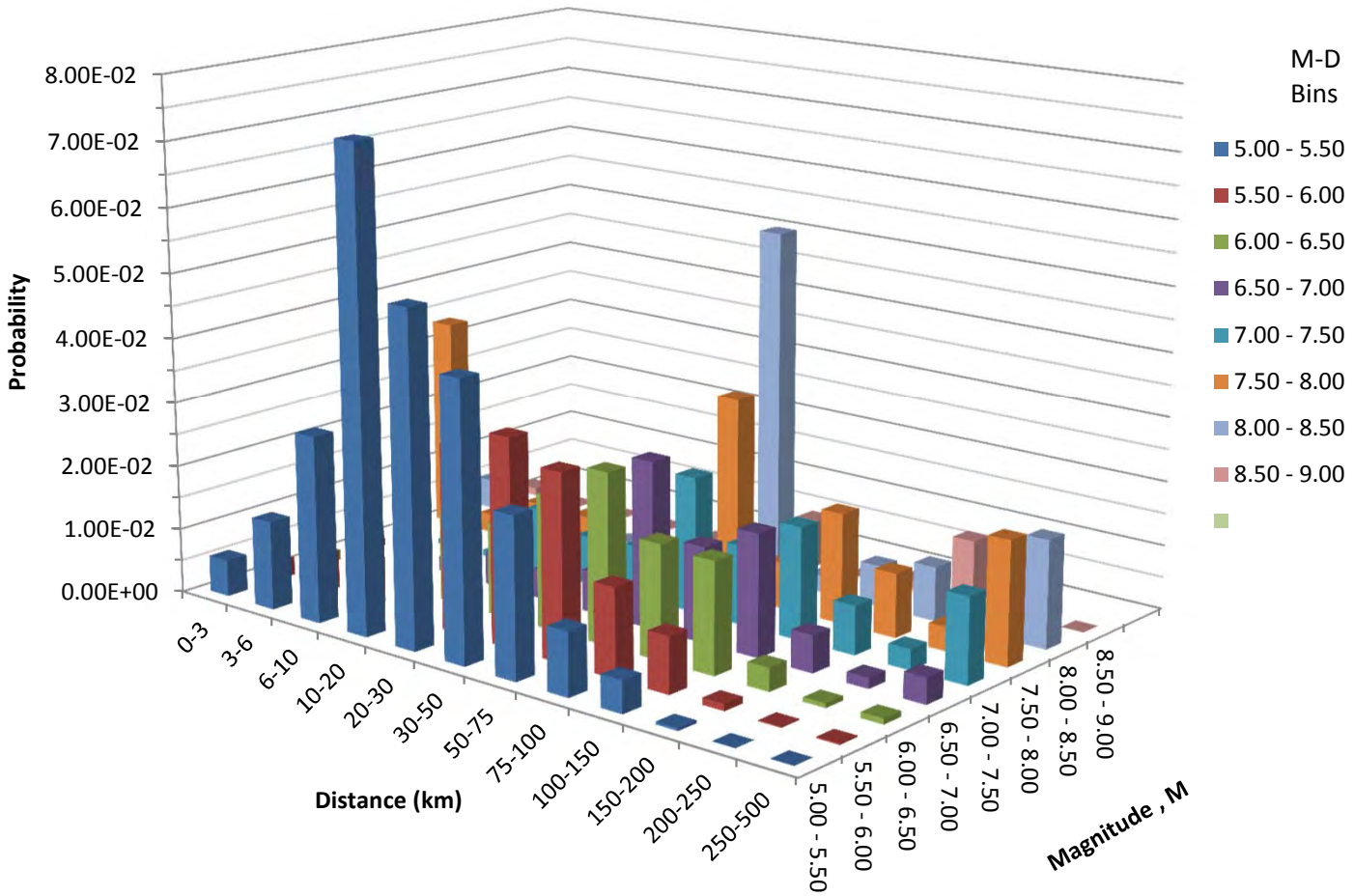

MWH®

Deaggregation 145-yr Return Period 0.2 Sec Horizontal Acceleration

Figure 40

This Page Left Blank Intentionally

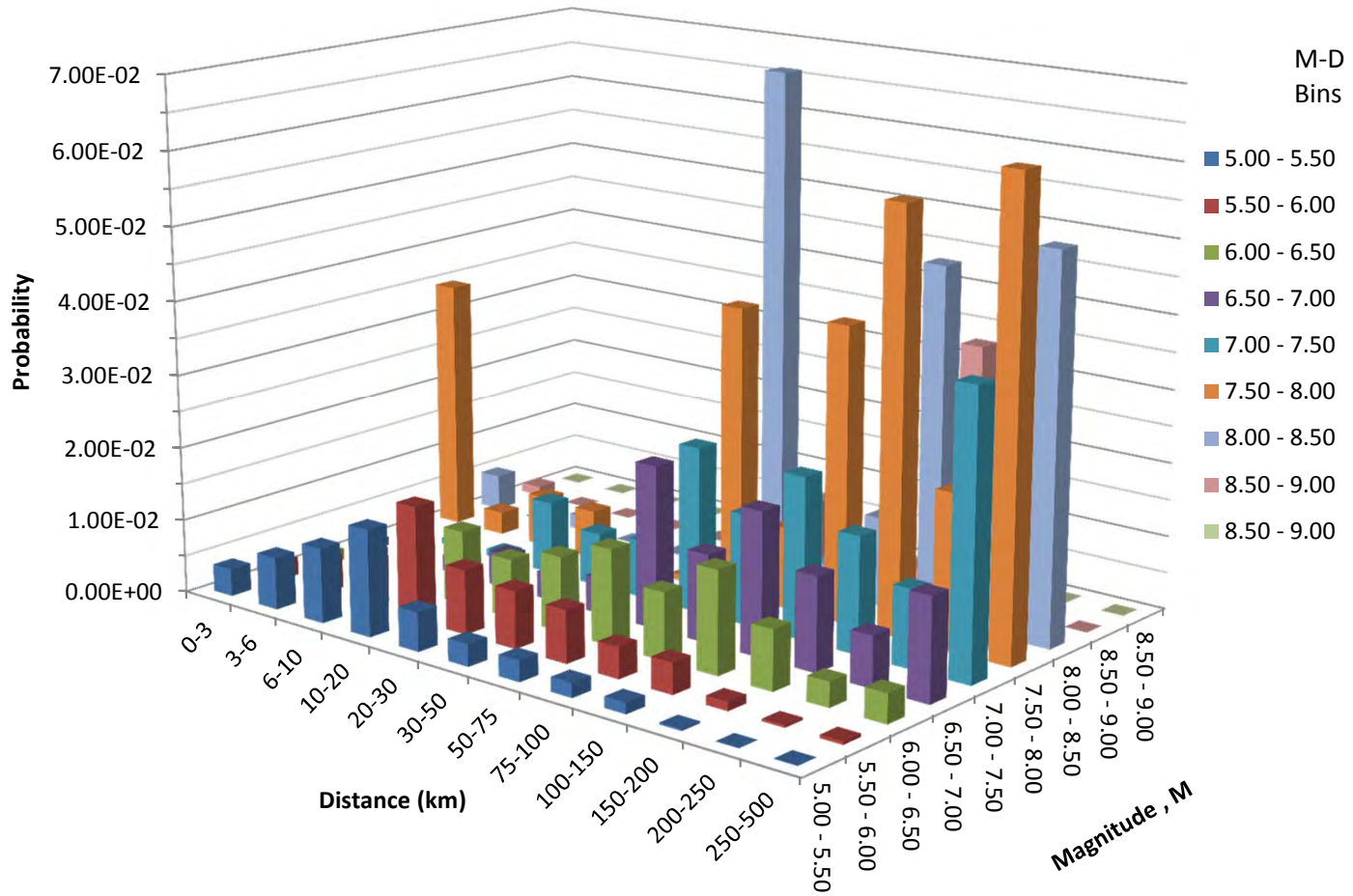

MWH®

Deaggregation 145-yr Return Period 1.0 Sec Horizontal Acceleration

Figure 41

This Page Left Blank Intentionally

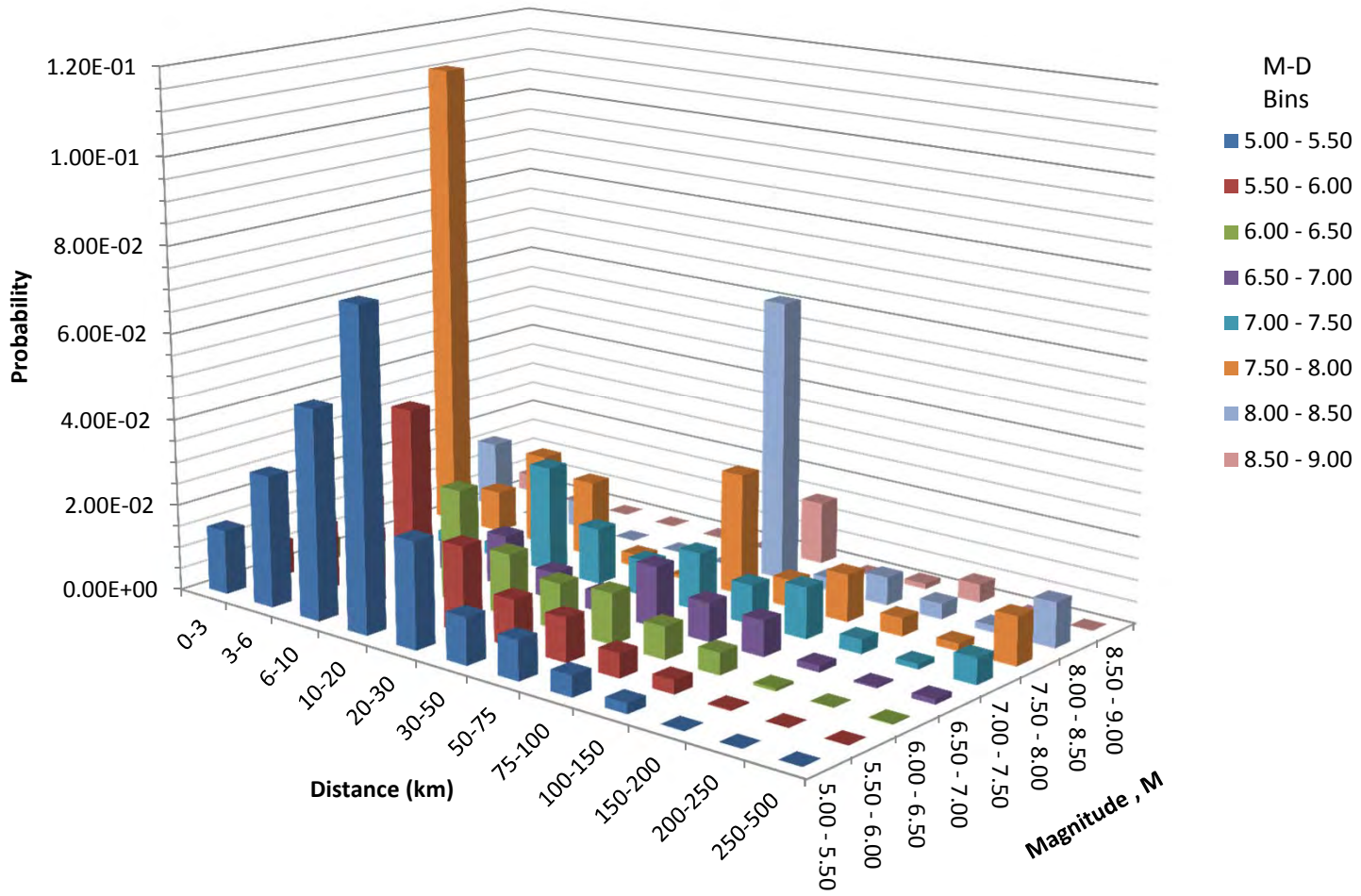

MWH®

Deaggregation 475-yr Return Period Peak Horizontal Acceleration

Figure 42

This Page Left Blank Intentionally

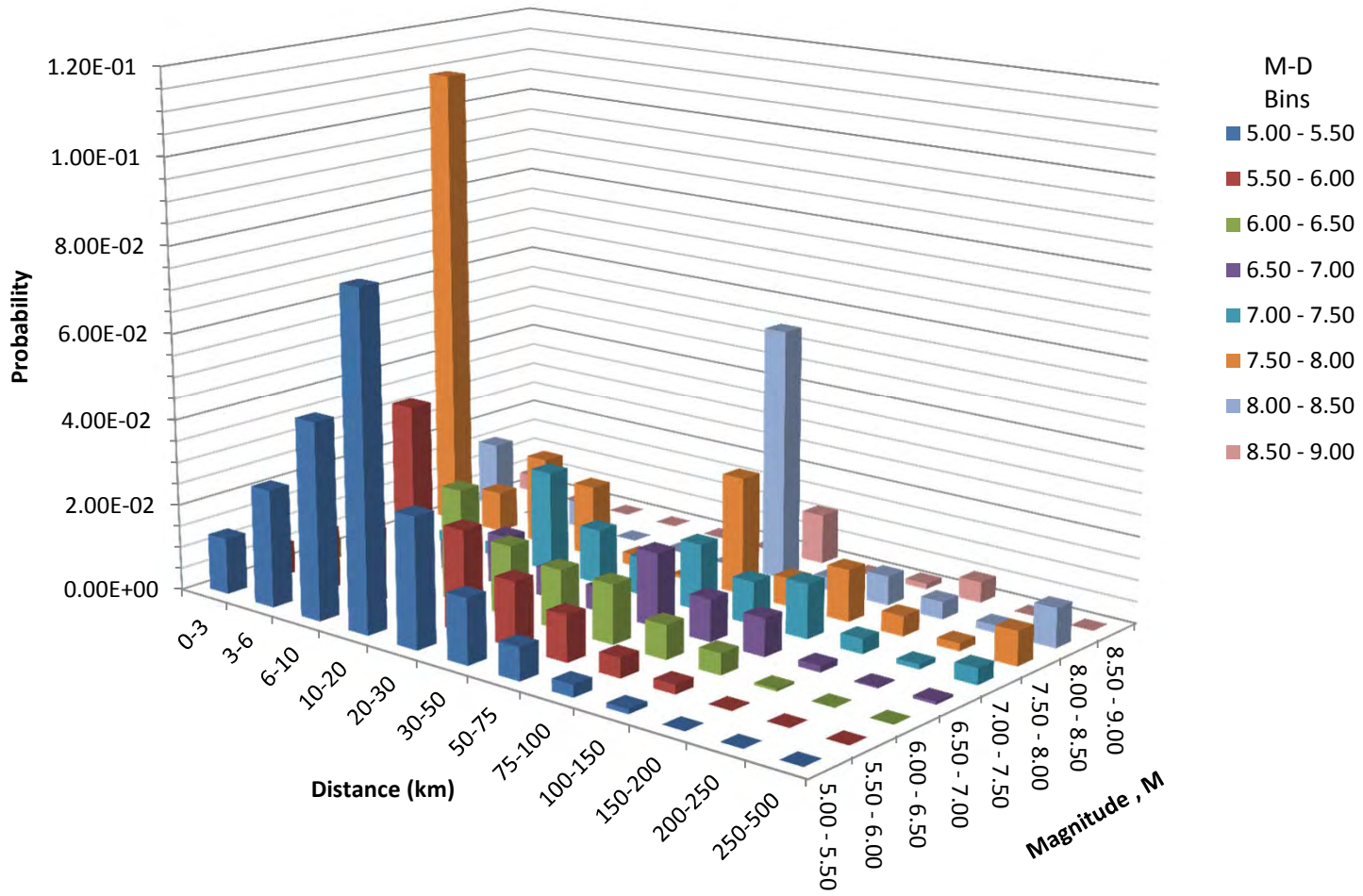

MWH®

Deaggregation 475-yr Return Period 0.2 Sec Horizontal Acceleration

Figure 43

This Page Left Blank Intentionally

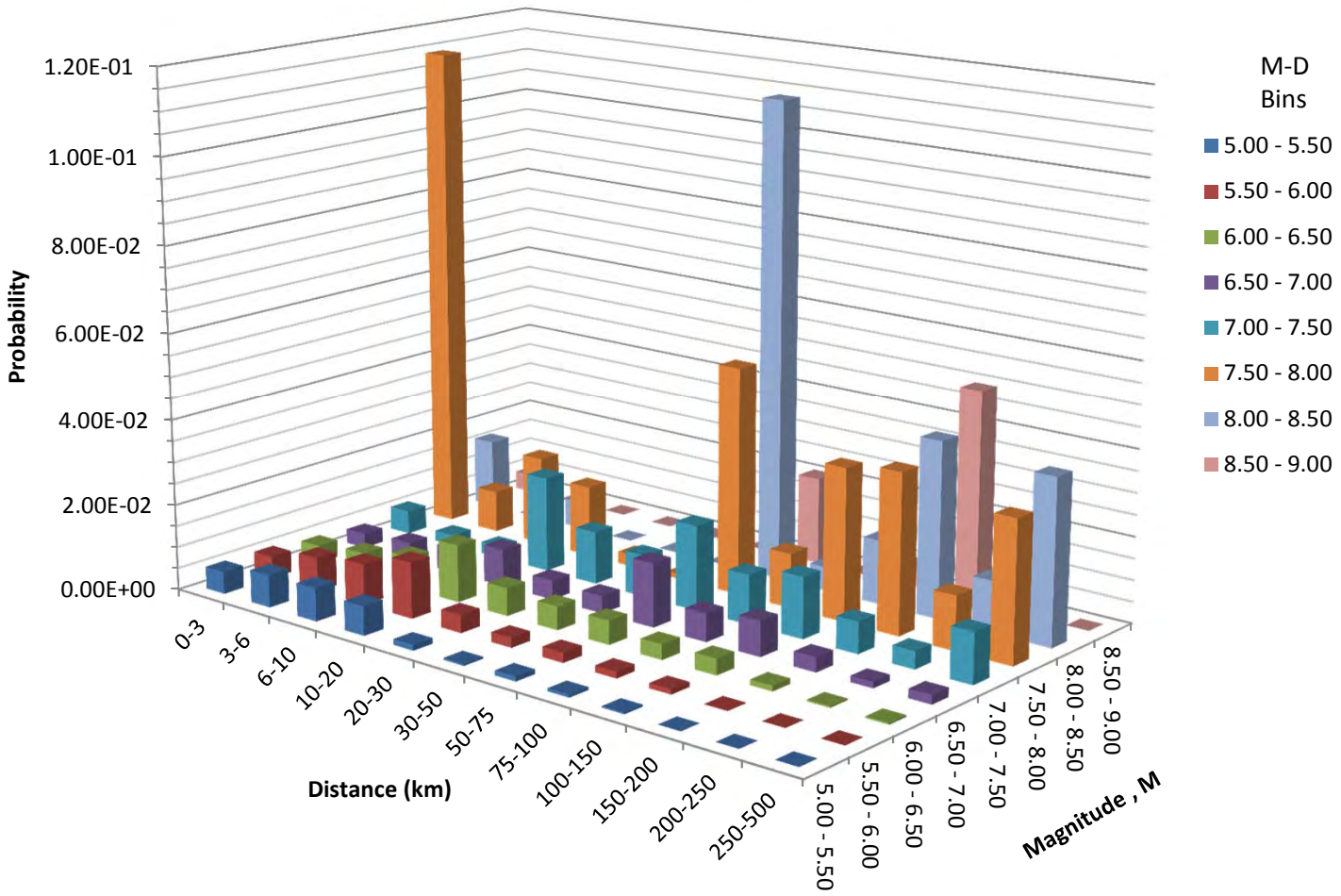

MWH®

Deaggregation 475-yr Return Period 1.0 Sec Horizontal Acceleration

Figure 44

This Page Left Blank Intentionally

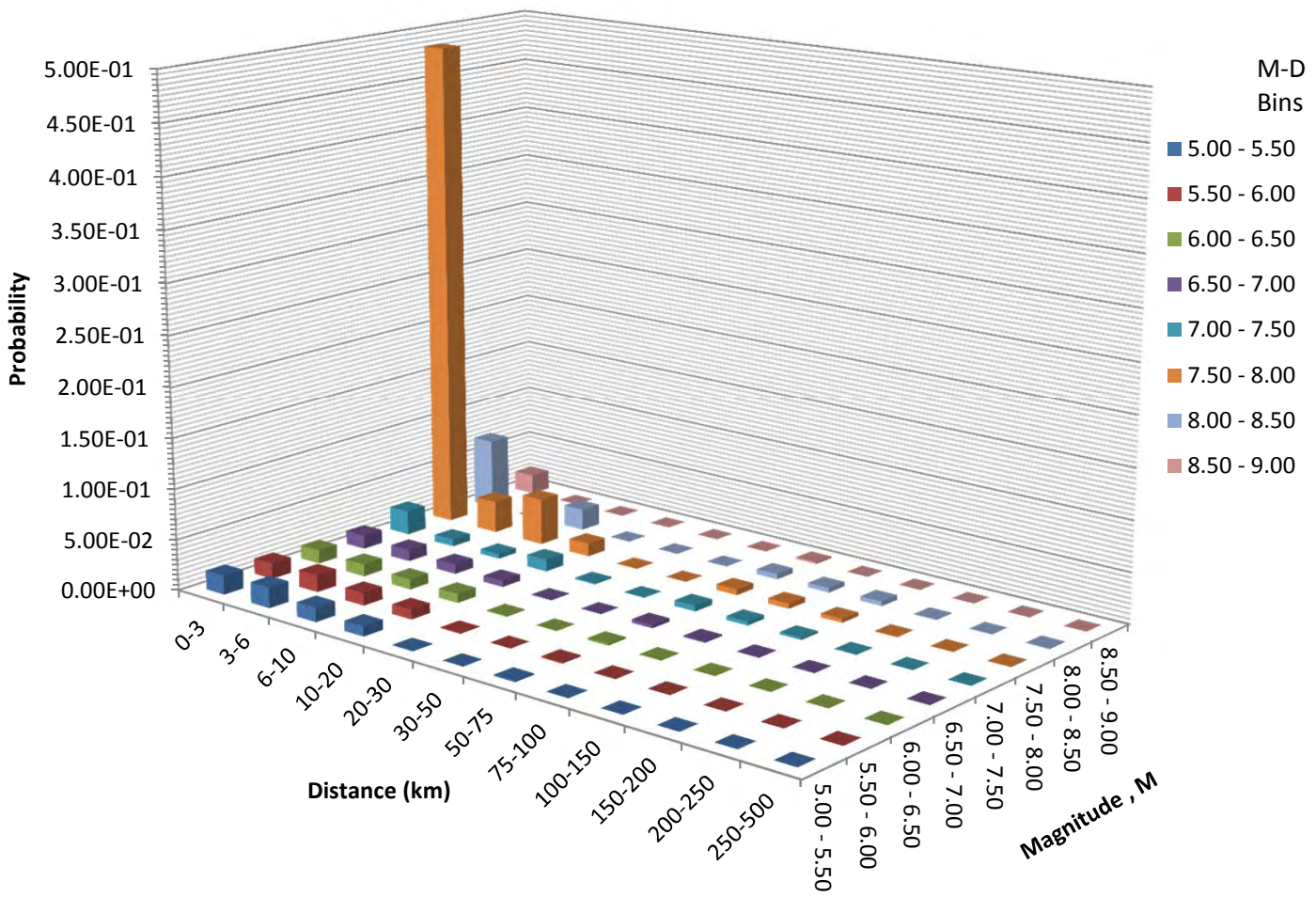

MWH®

Deaggregation 10,000-yr Return Period Peak Horizontal Acceleration

Figure 45

This Page Left Blank Intentionally

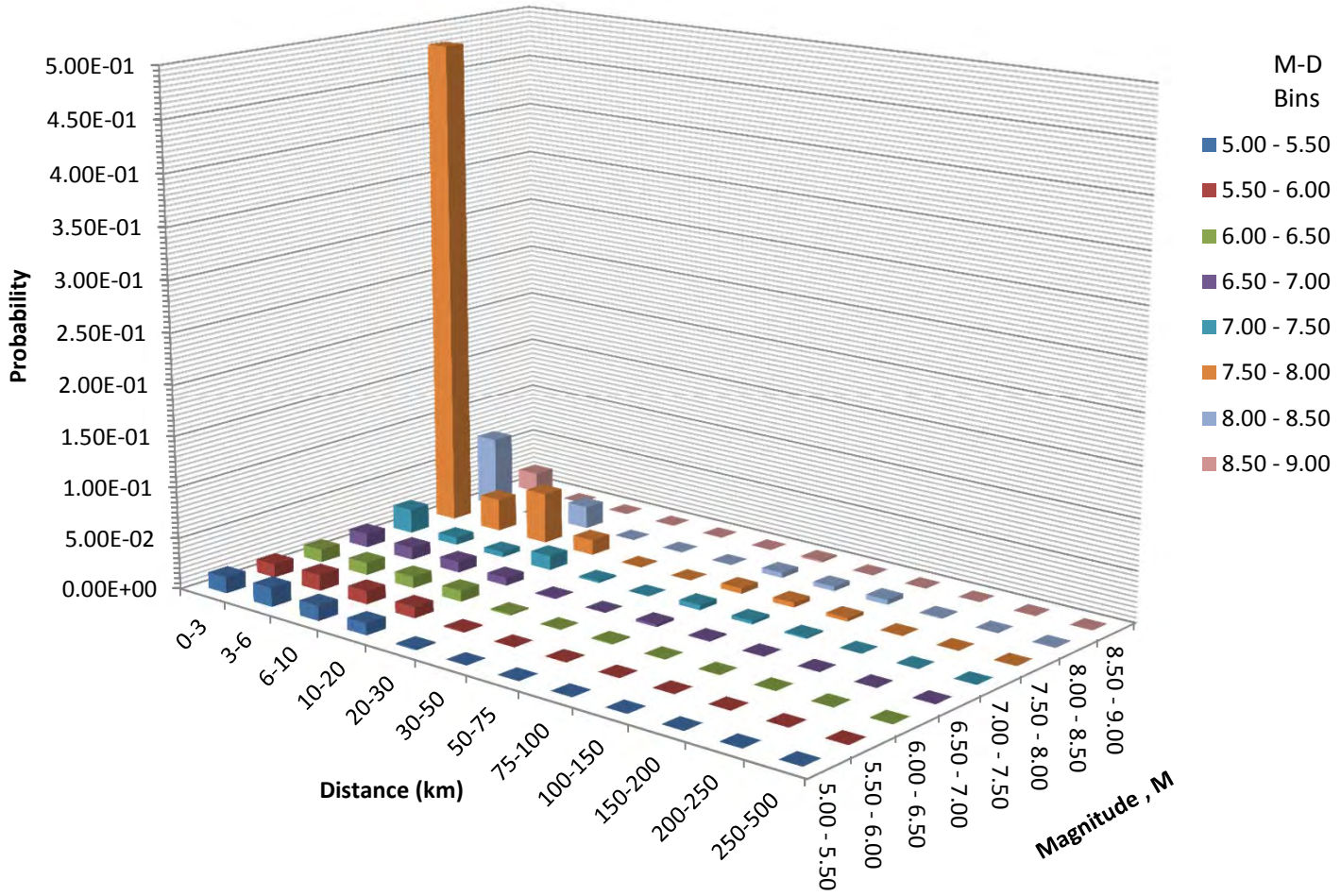

MWH®

Deaggregation 10,000-yr Return Period 0.2 Sec Horizontal Acceleration

Figure 46

This Page Left Blank Intentionally

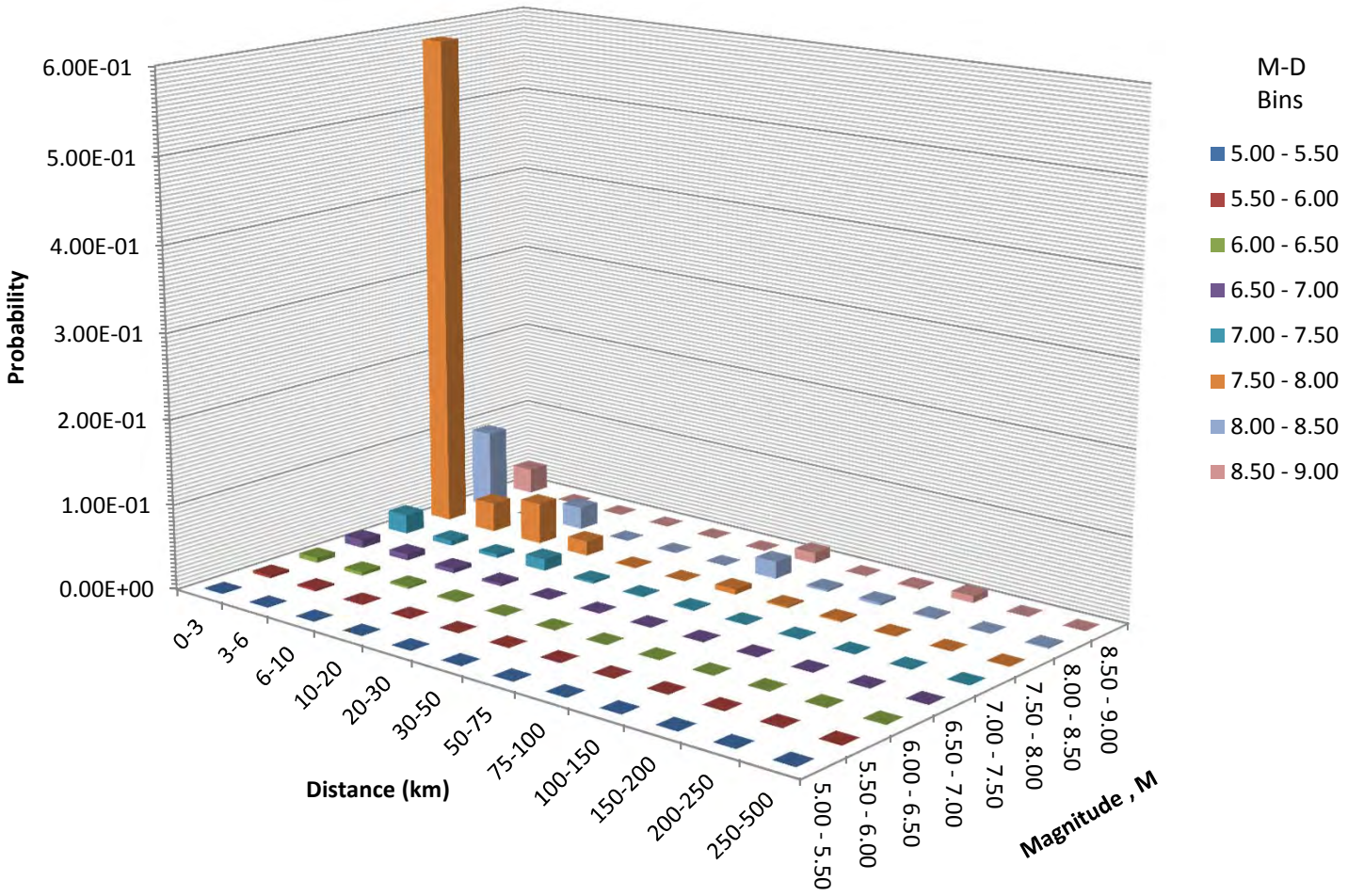

MWH®

Deaggregation 10,000-yr Return Period 1.0 Sec Horizontal Acceleration

Figure 47

This Page Left Blank Intentionally

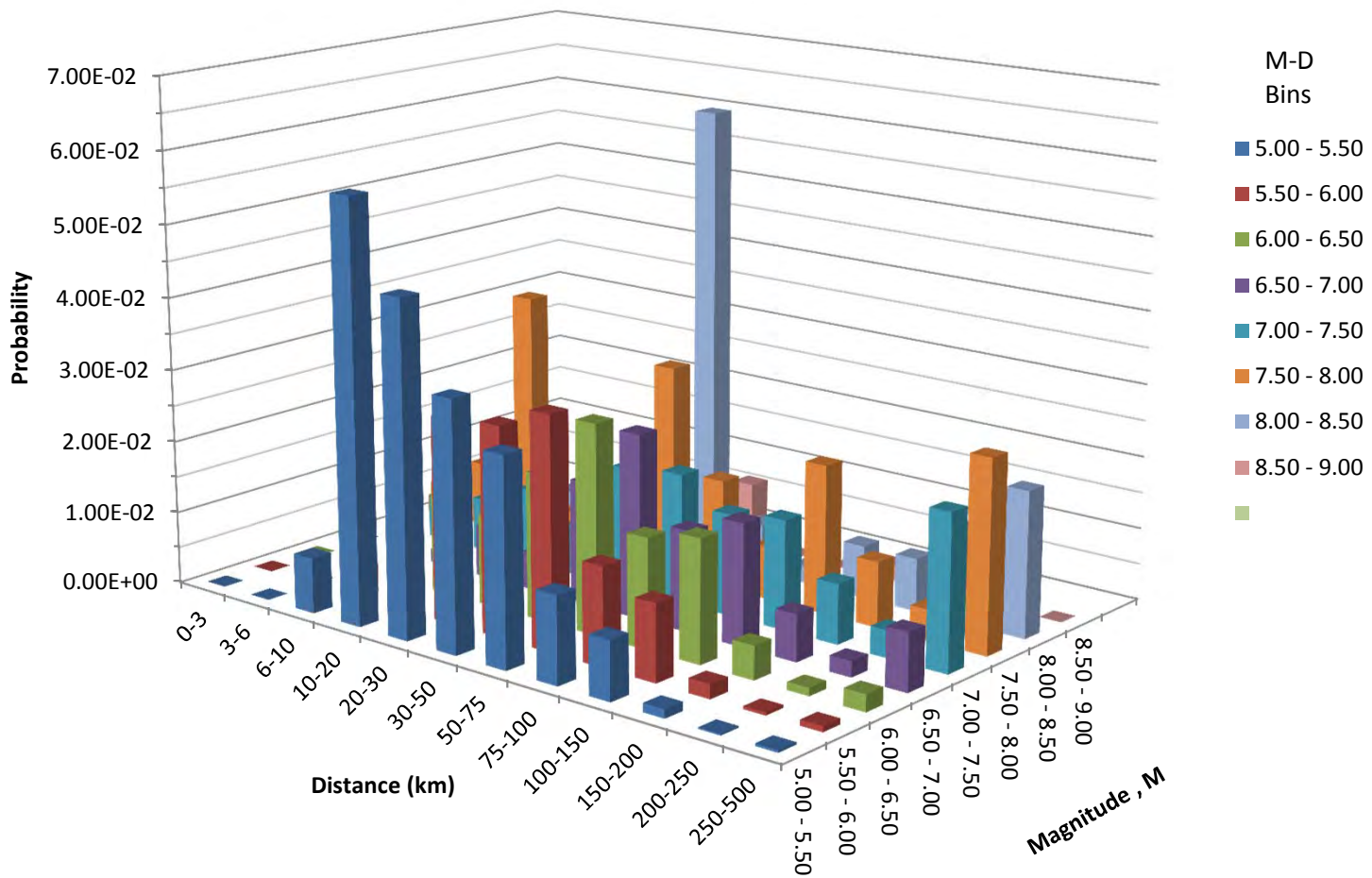

MWH®

Deaggregation 145-yr Return Period Peak Horizontal Acceleration

Figure 48

This Page Left Blank Intentionally

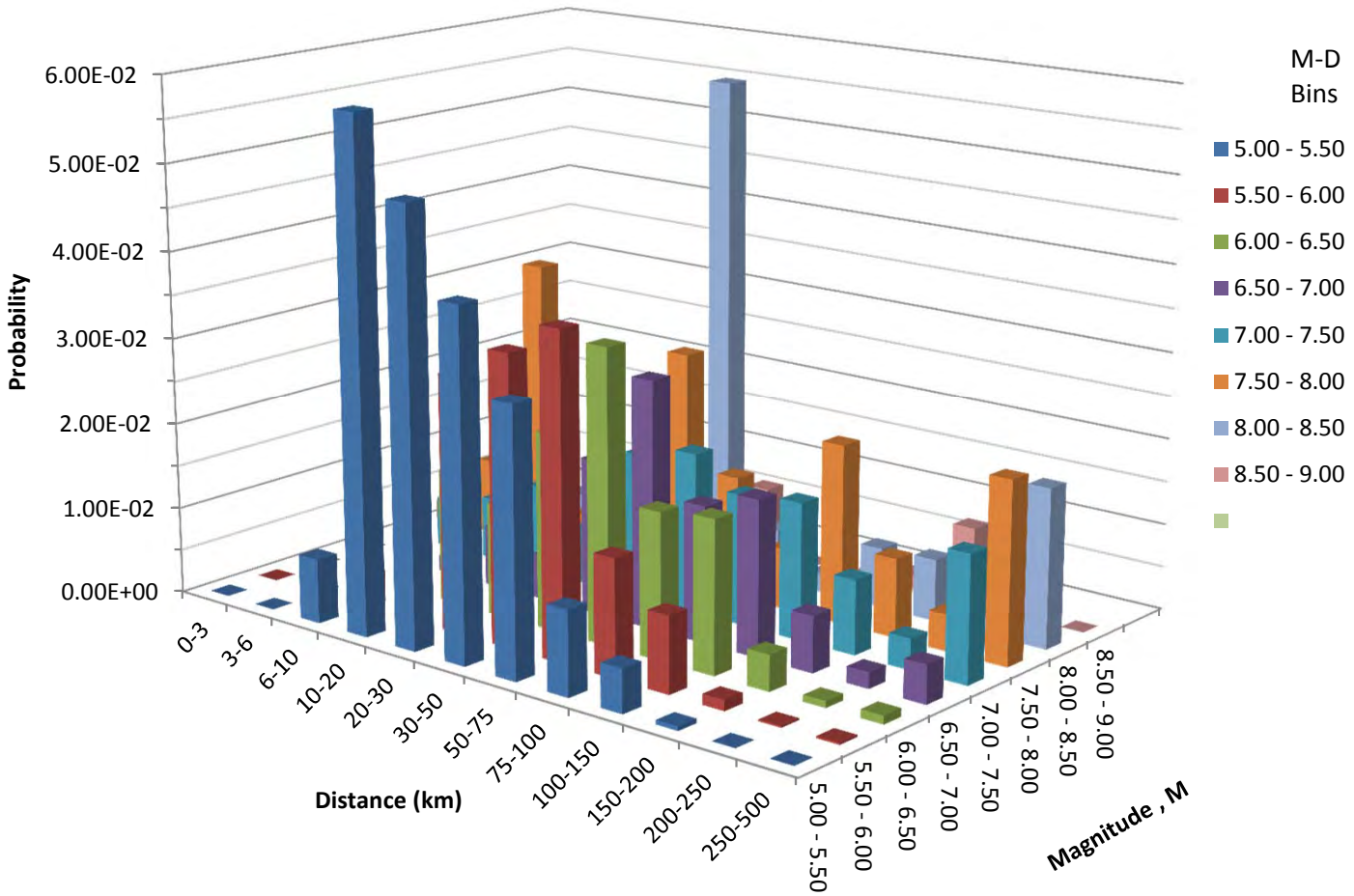

MWH®

Deaggregation 145-yr Return Period 0.2 Sec Horizontal Acceleration

Figure 49

This Page Left Blank Intentionally

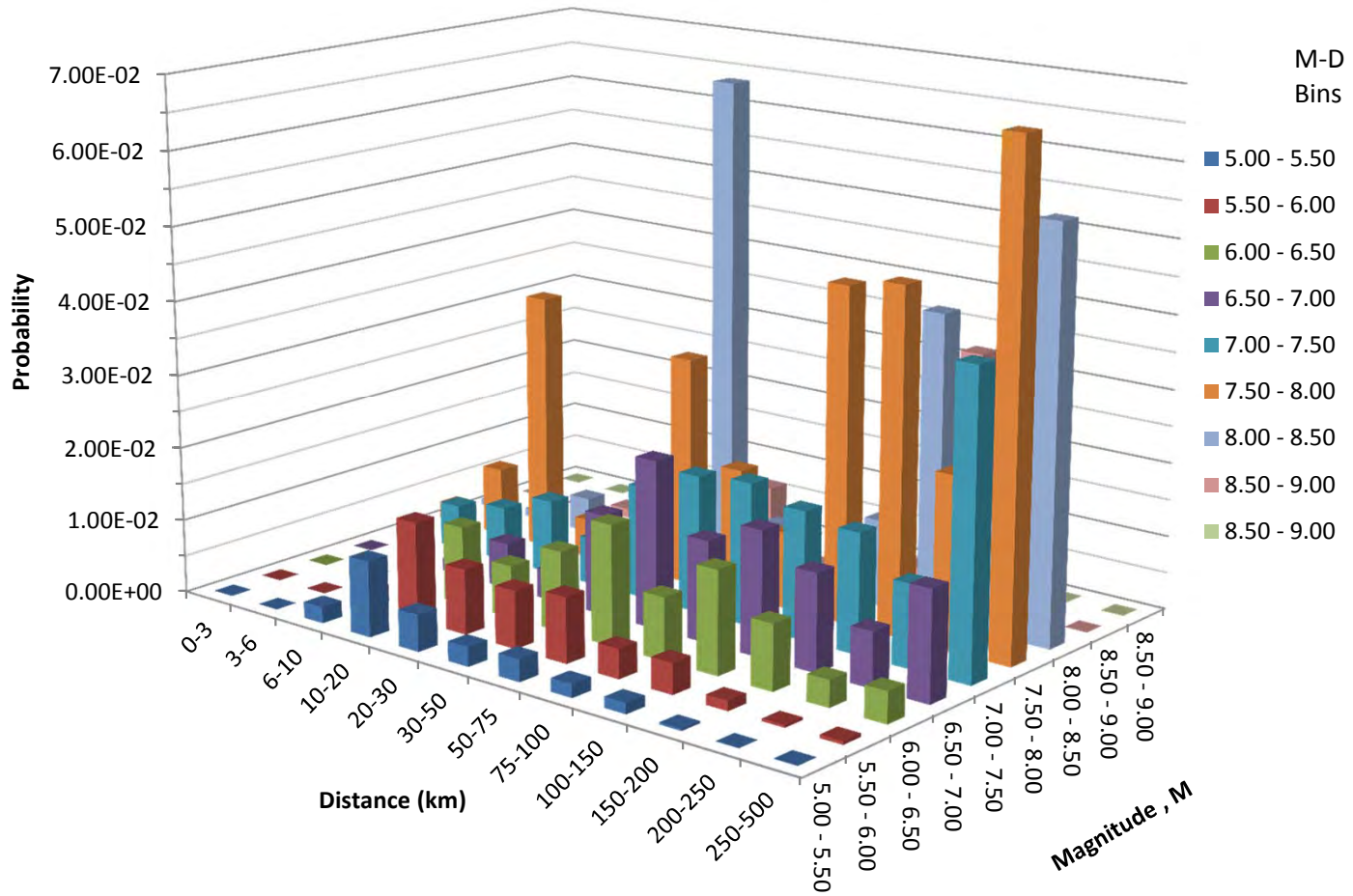

MWH®

Deaggregation 145-yr Return Period 1.0 Sec Horizontal Acceleration

Figure 50

This Page Left Blank Intentionally

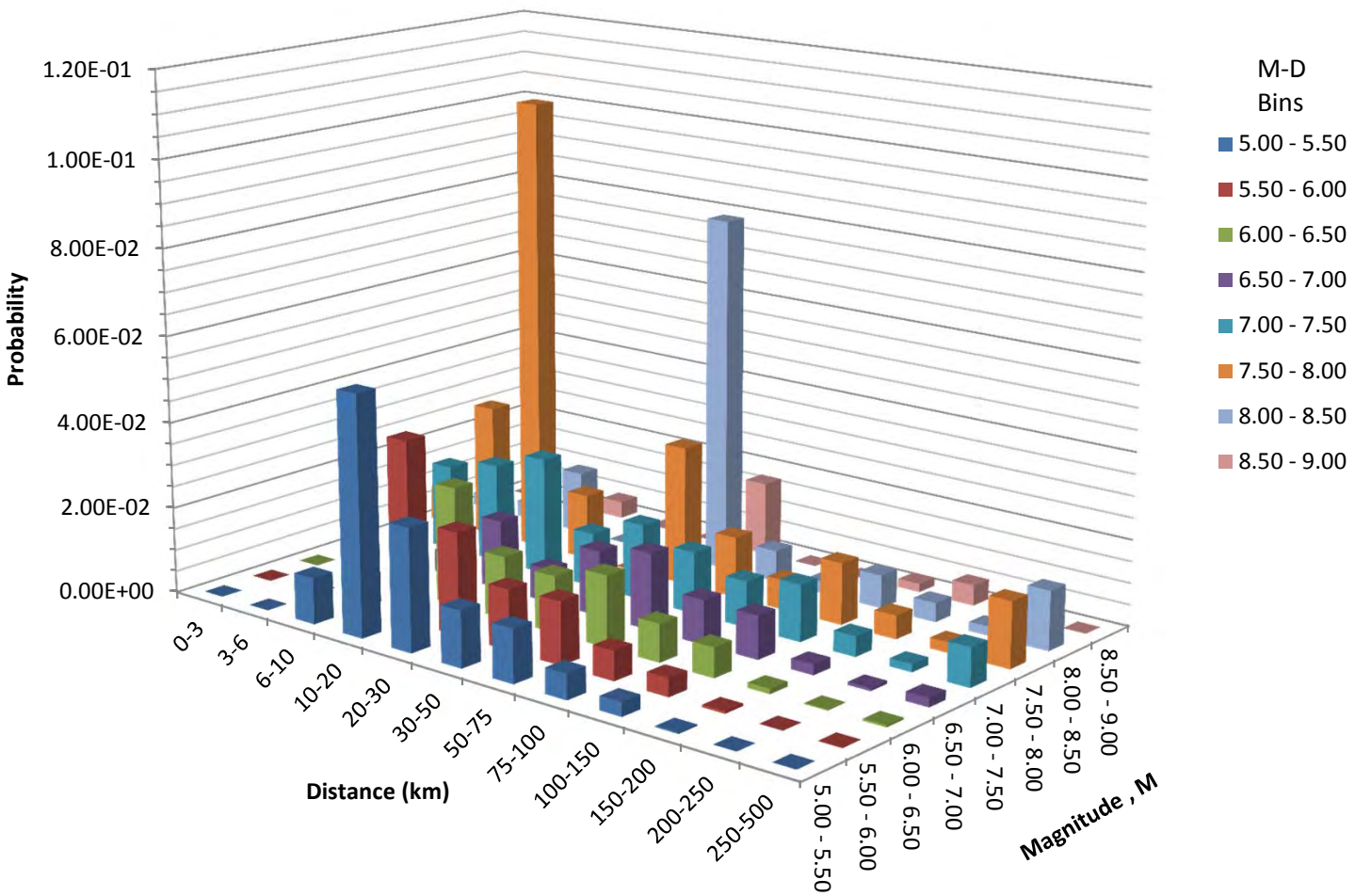

MWH®

Deaggregation 475-yr Return Period Peak Horizontal Acceleration

Figure 51

This Page Left Blank Intentionally

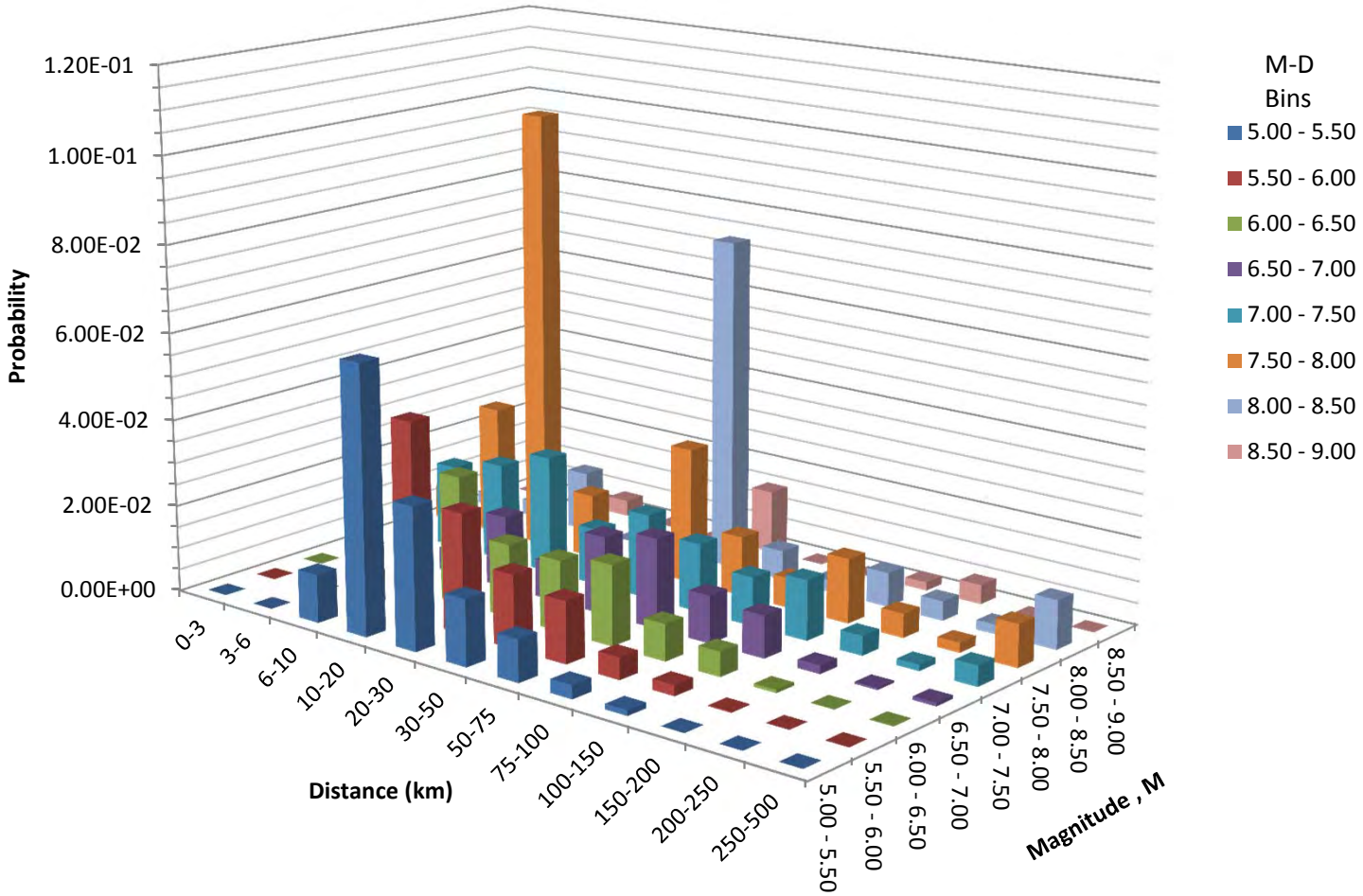

MWH®

Deaggregation 475-yr Return Period 0.2 Sec Horizontal Acceleration

Figure 52

This Page Left Blank Intentionally

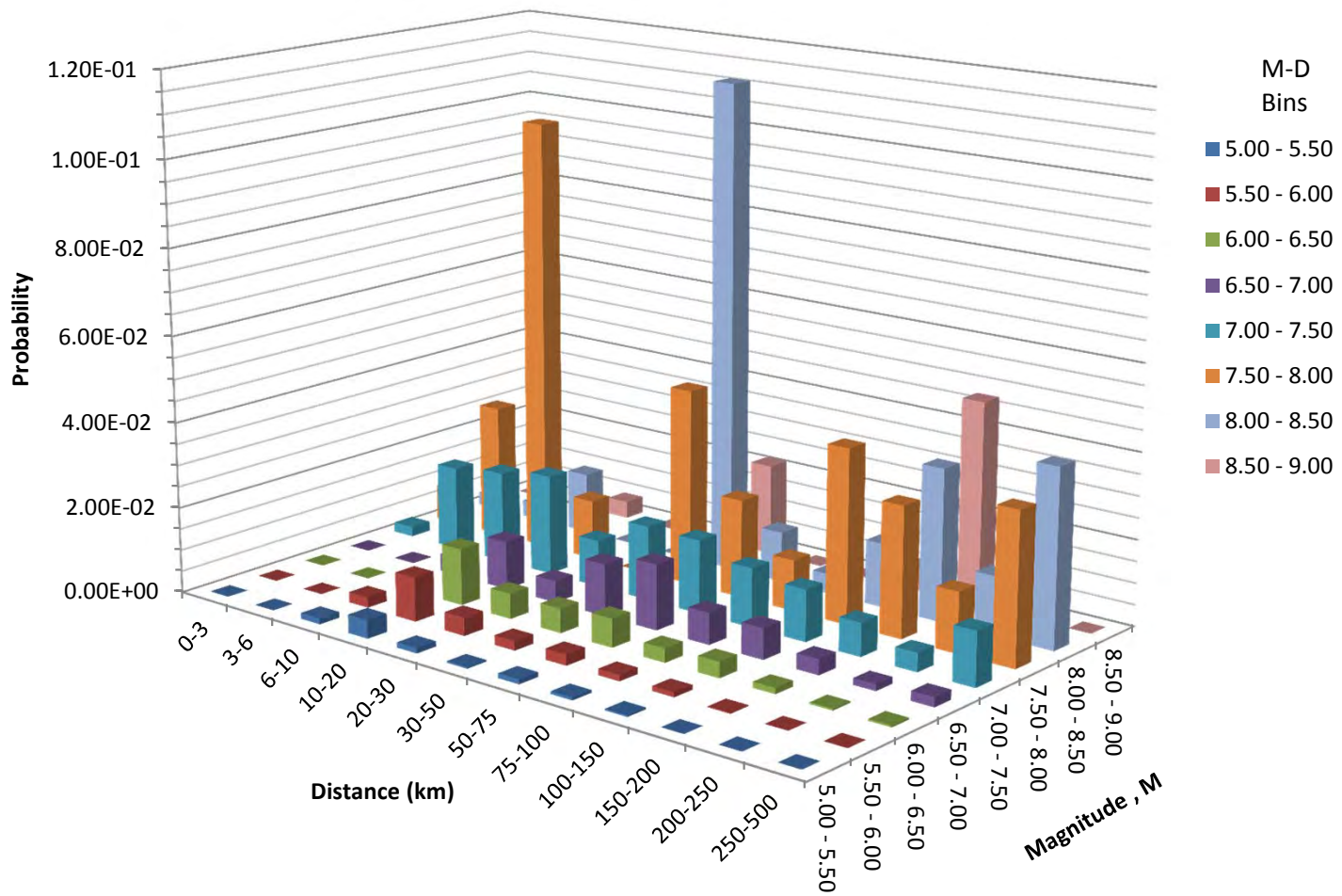

MWH®

Deaggregation 475-yr Return Period 1.0 Sec Horizontal Acceleration

Figure 53

This Page Left Blank Intentionally

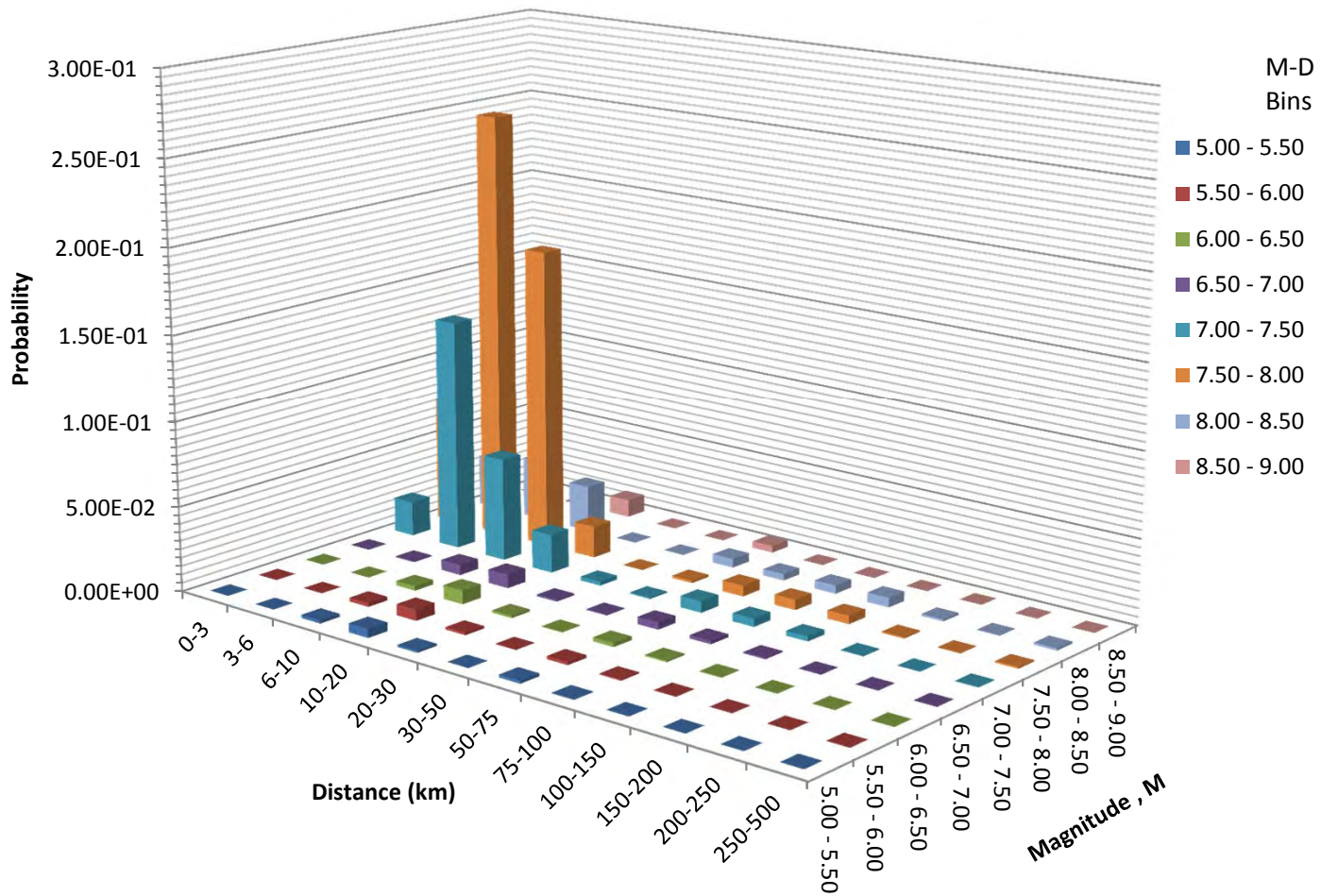

MWH®

Deaggregation 10,000-yr Return Period Peak Horizontal Acceleration

Figure 54

This Page Left Blank Intentionally

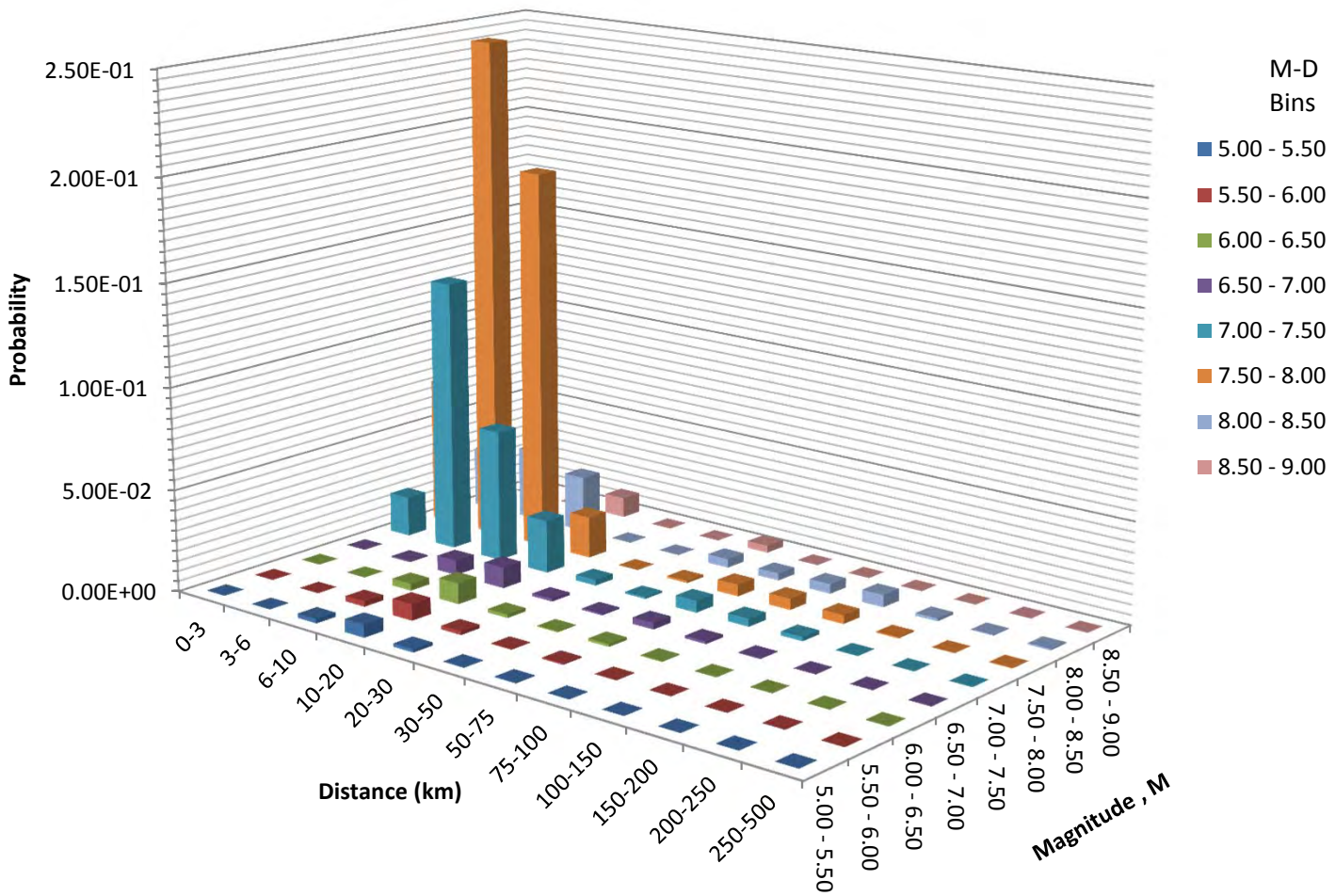

MWH®

Deaggregation 10,000-yr Return Period 0.2 Sec Horizontal Acceleration

Figure 55

This Page Left Blank Intentionally

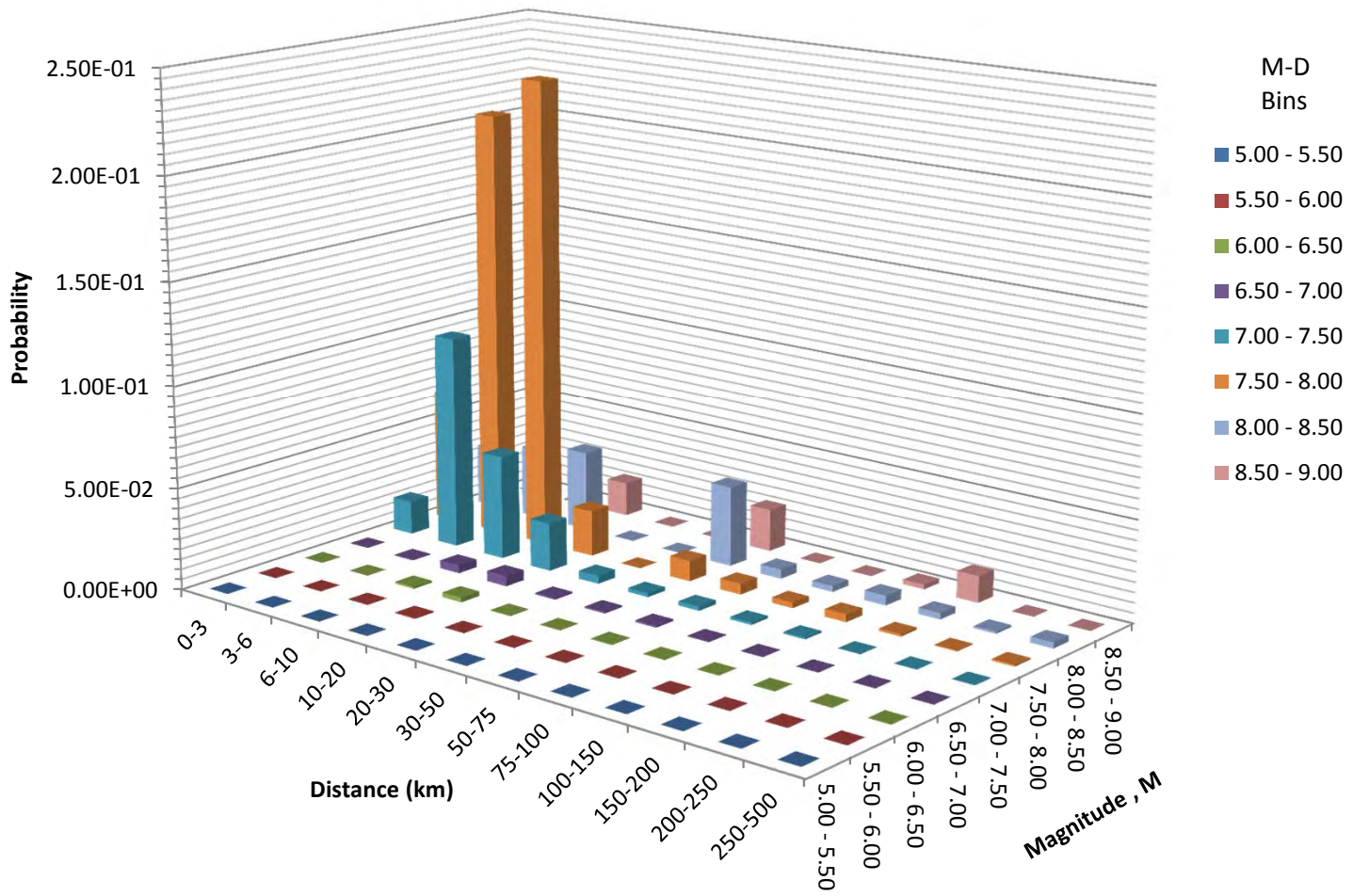

MWH®

Deaggregation 10,000-yr Return Period 1.0 Sec Horizontal Acceleration

Figure 56

This Page Left Blank Intentionally

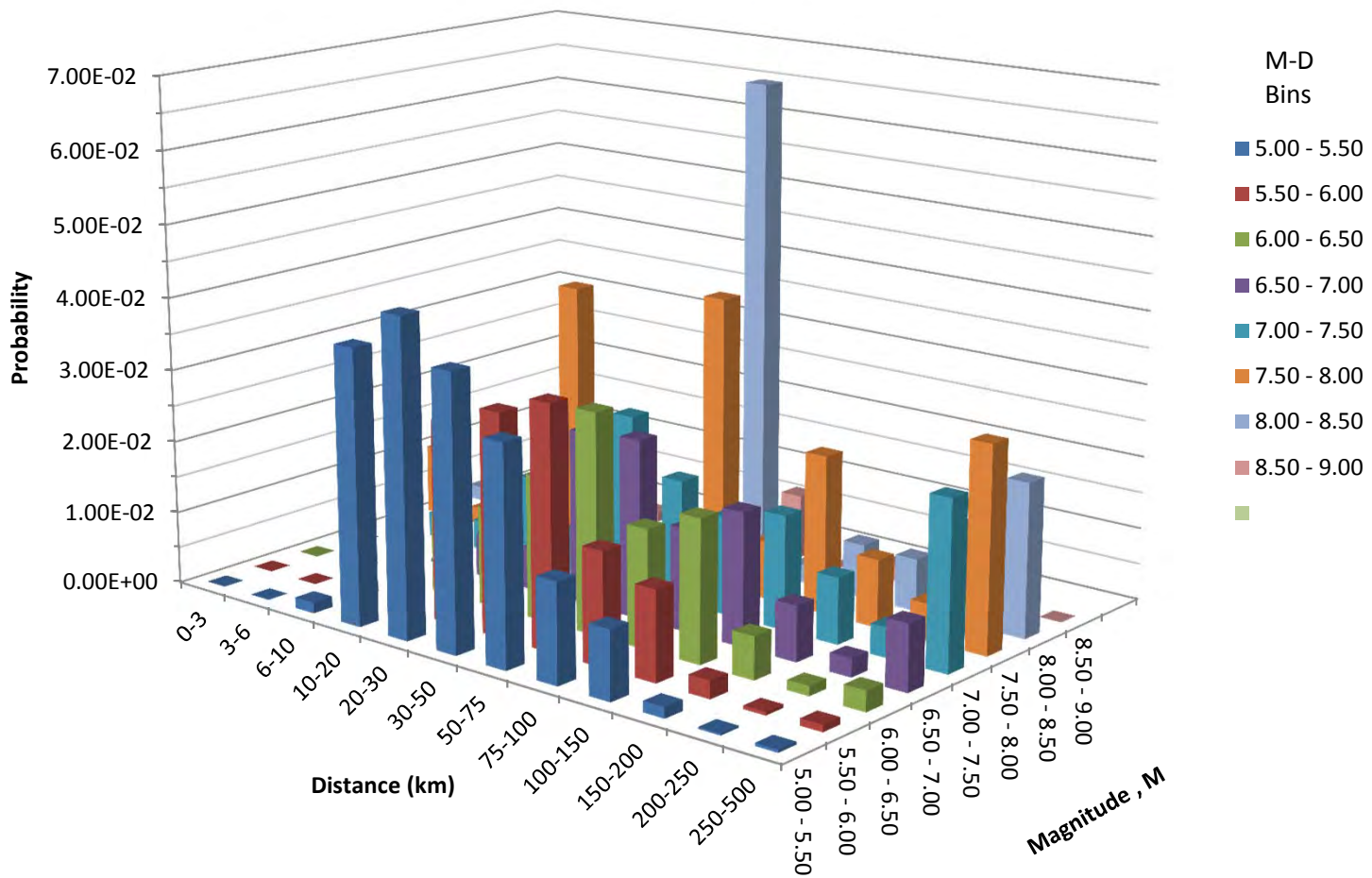

MWH®

Deaggregation 145-yr Return Period Peak Horizontal Acceleration

Figure 57

This Page Left Blank Intentionally

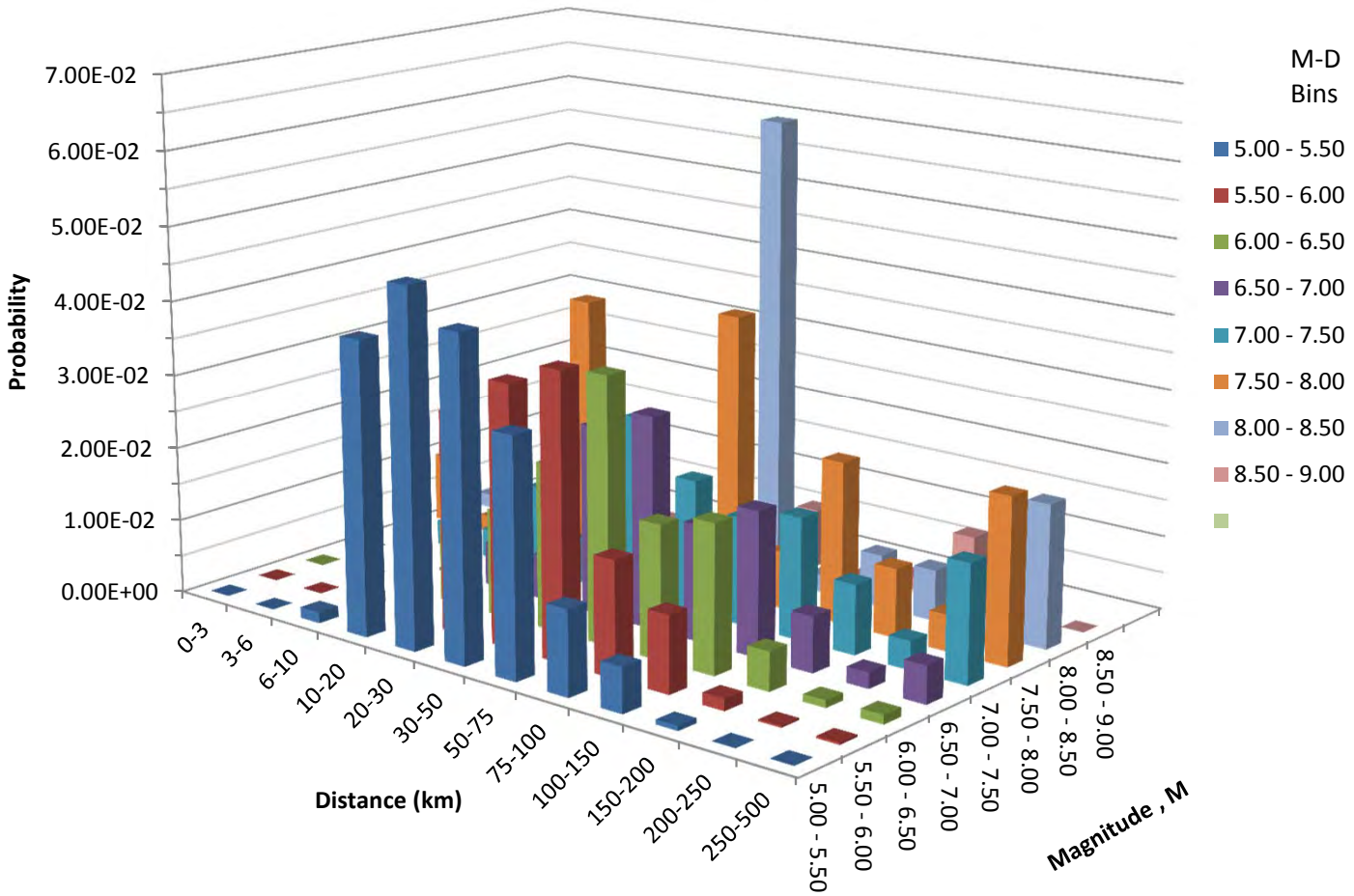

MWH®

Deaggregation 145-yr Return Period 0.2 Sec Horizontal Acceleration

Figure 58

This Page Left Blank Intentionally

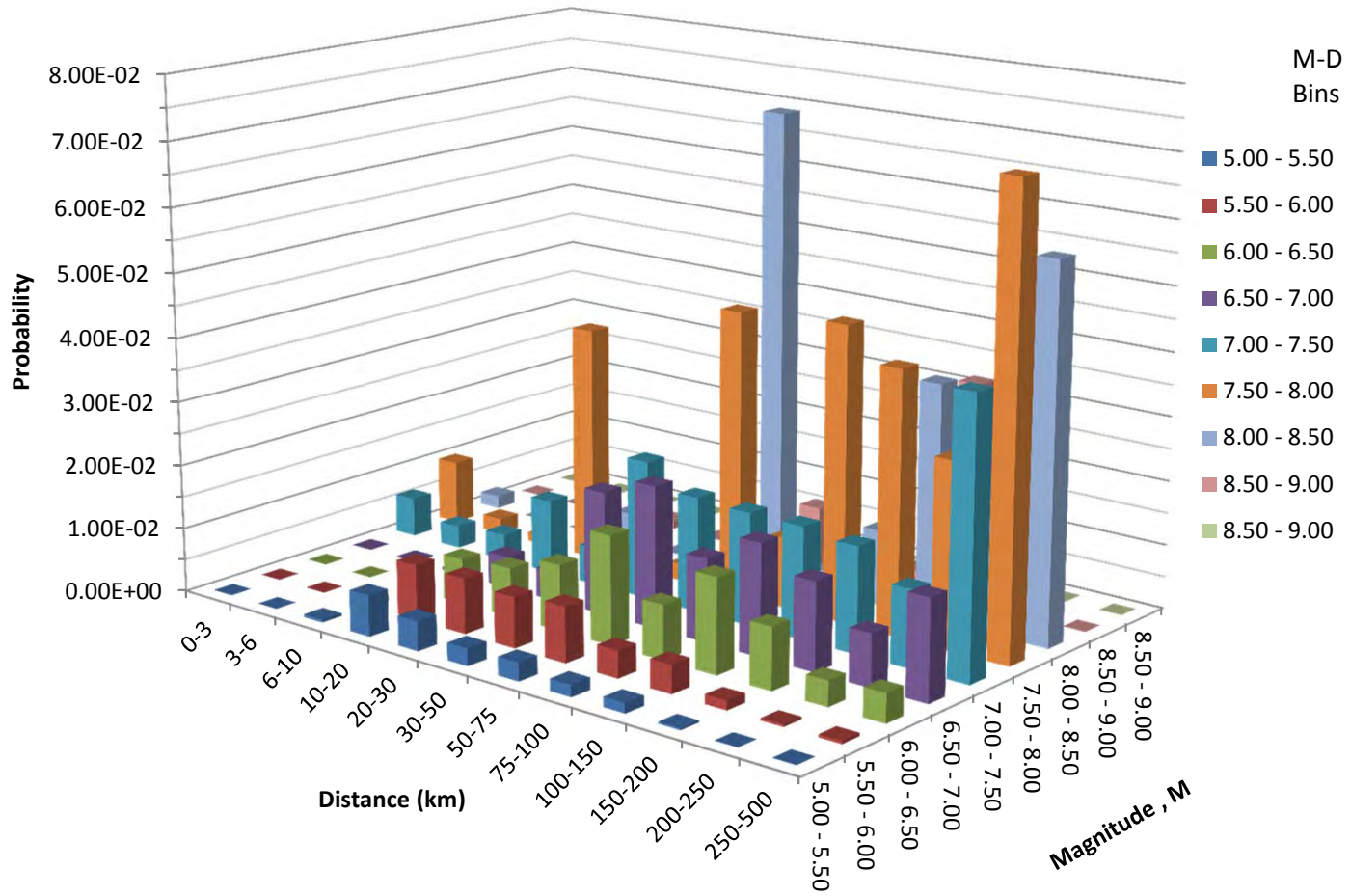

MWH®

Deaggregation 145-yr Return Period 1.0 Sec Horizontal Acceleration

Figure 59

This Page Left Blank Intentionally

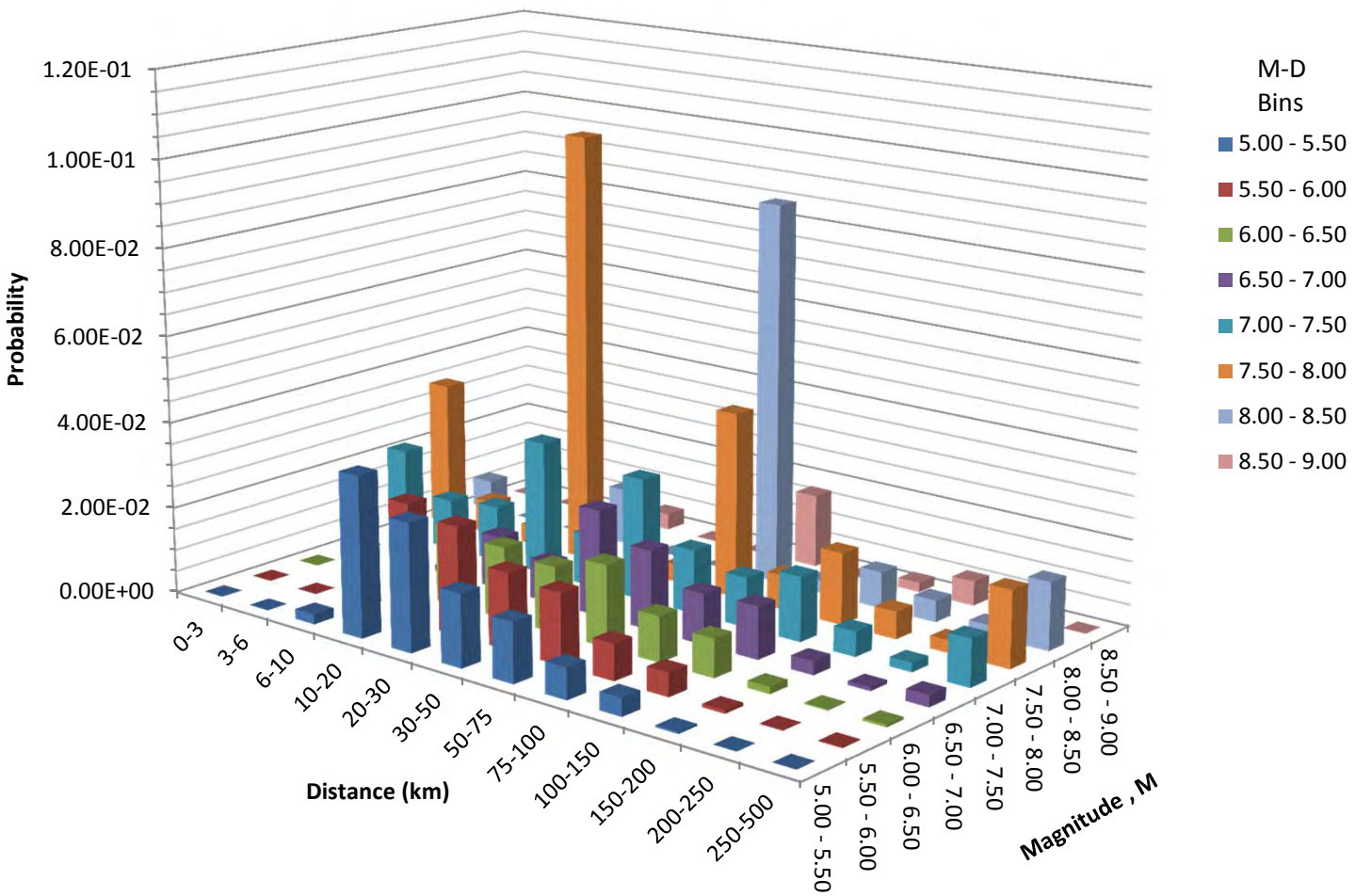

MWH®

Deaggregation 475-yr Return Period Peak Horizontal Acceleration

Figure 60

This Page Left Blank Intentionally

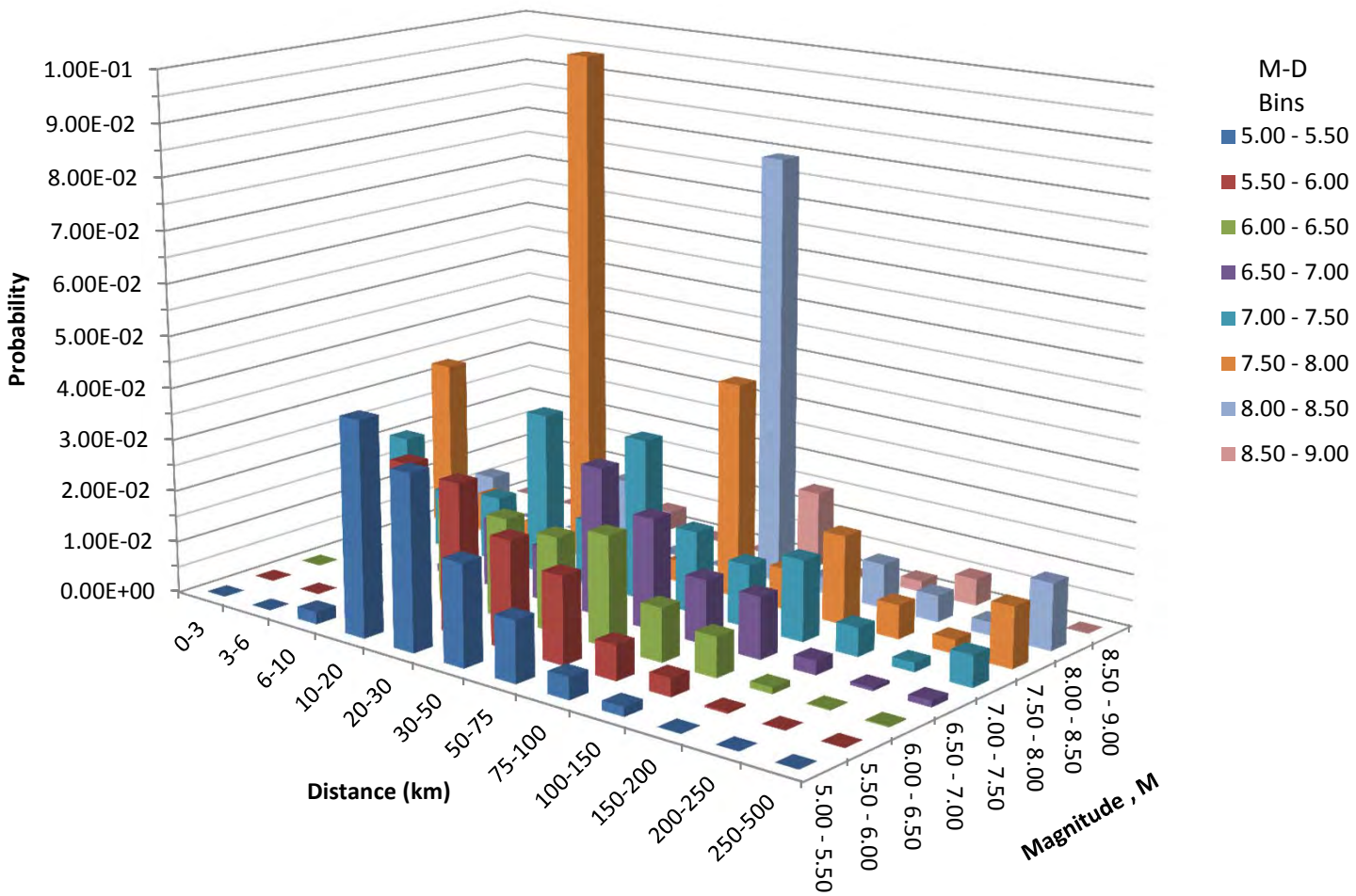

MWH®

Deaggregation 475-yr Return Period 0.2 Sec Horizontal Acceleration

Figure 61

This Page Left Blank Intentionally

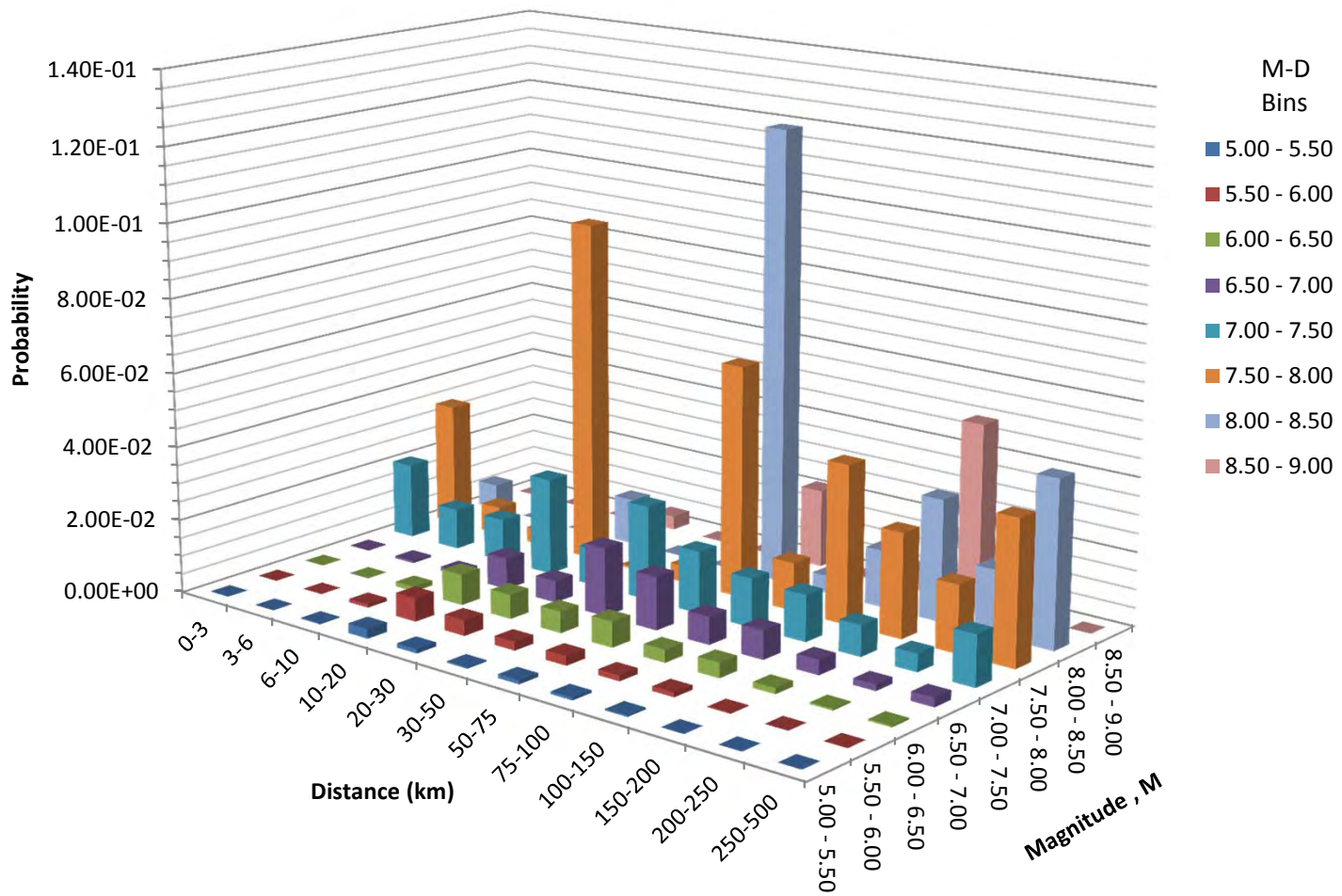

MWH®

Deaggregation 475-yr Return Period 1.0 Sec Horizontal Acceleration

Figure 62

This Page Left Blank Intentionally

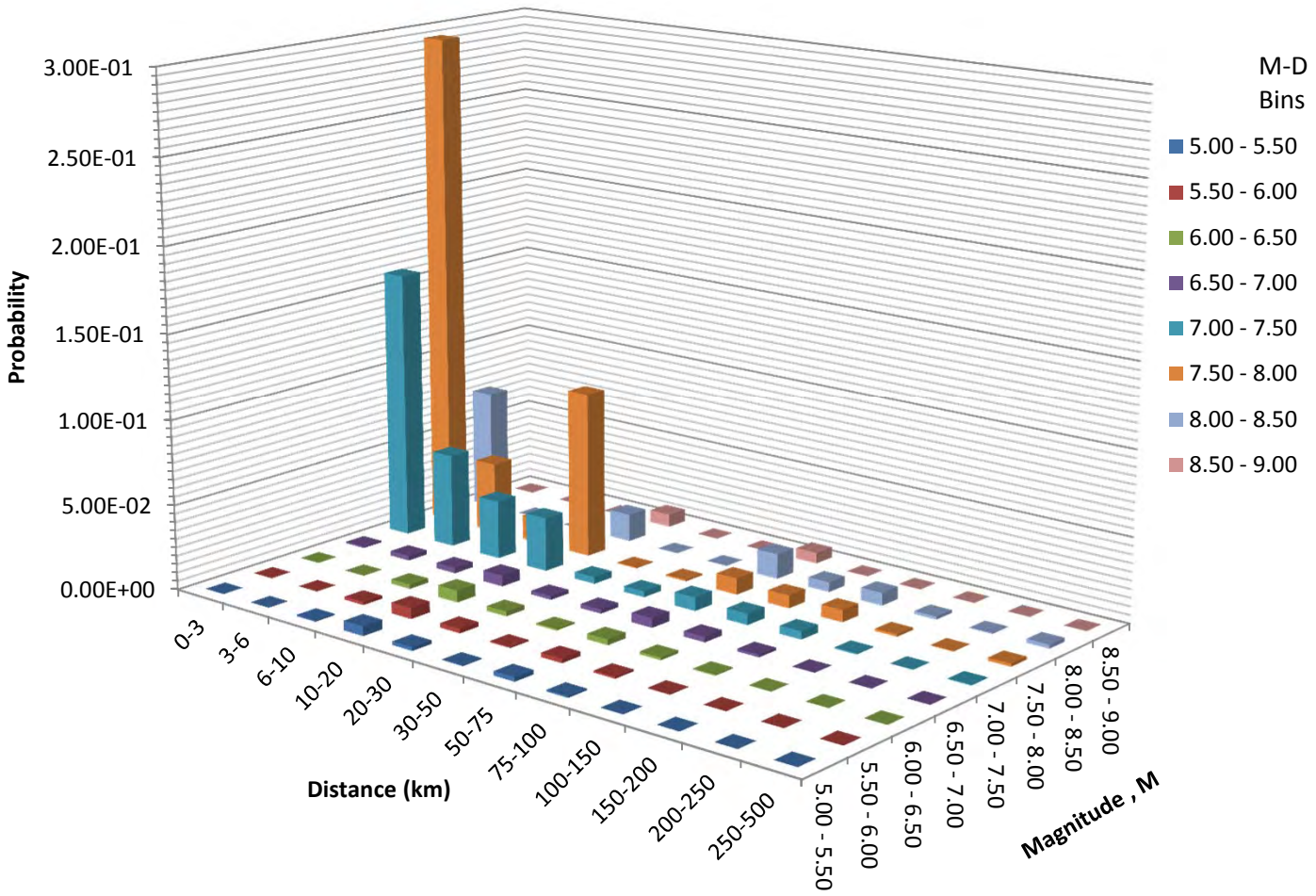

MWH®

Deaggregation 10,000-yr Return Period Peak Horizontal Acceleration

Figure 63

This Page Left Blank Intentionally

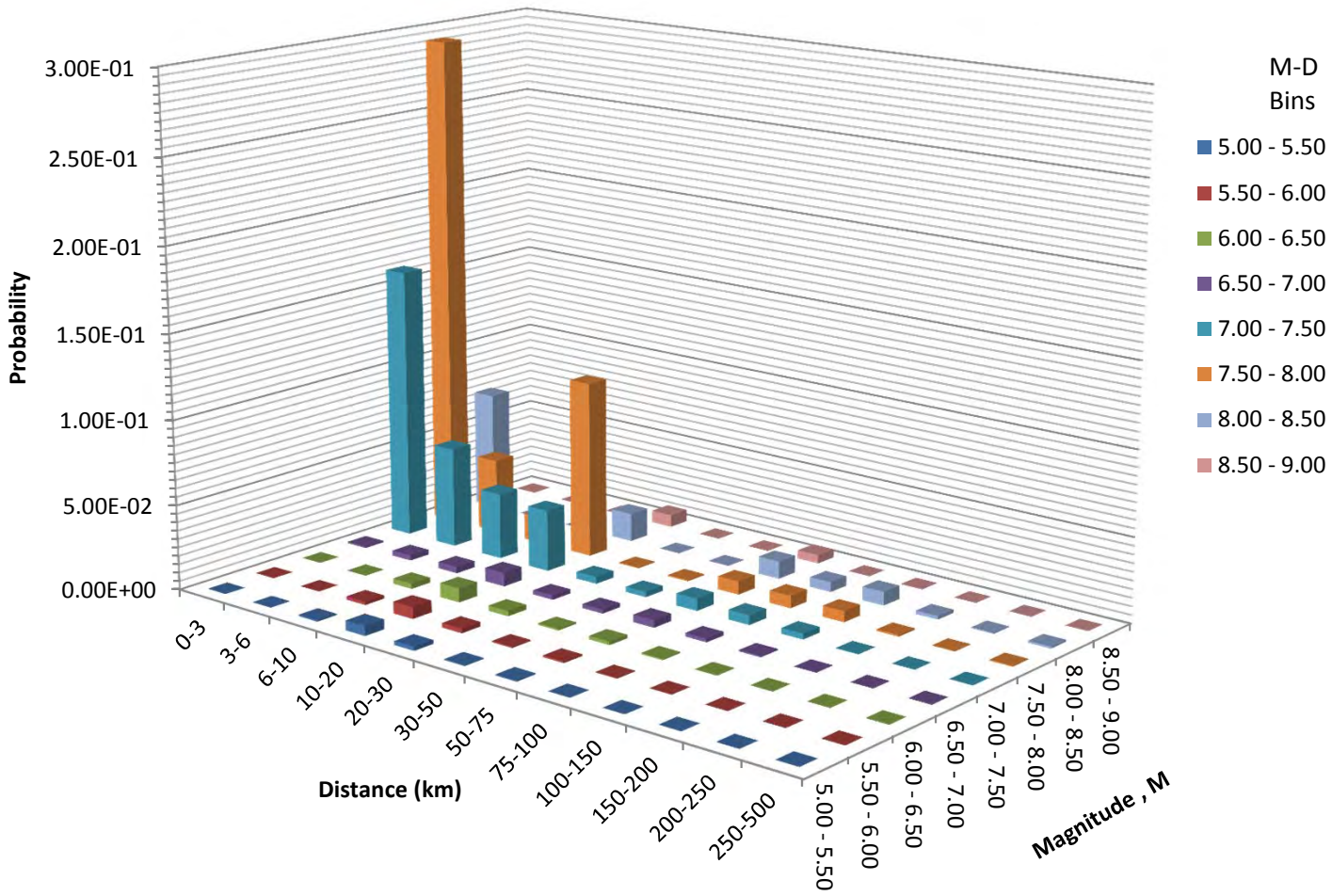

MWH®

Deaggregation 10,000-yr Return Period 0.2 Sec Horizontal Acceleration

Figure 64

This Page Left Blank Intentionally

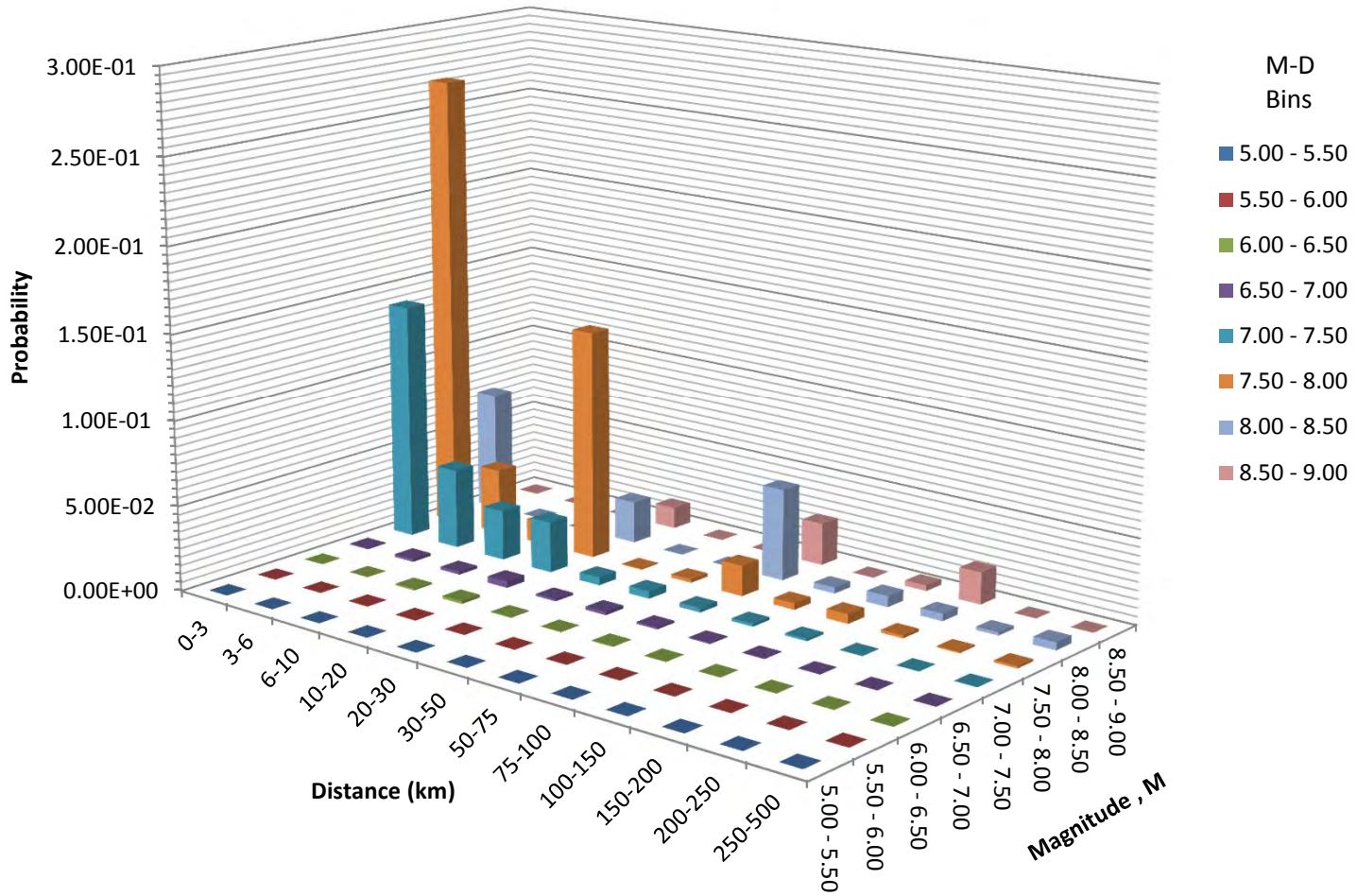

MWH®

Deaggregation 10,000-yr Return Period 1.0 Sec Horizontal Acceleration

Figure 65

This Page Left Blank Intentionally

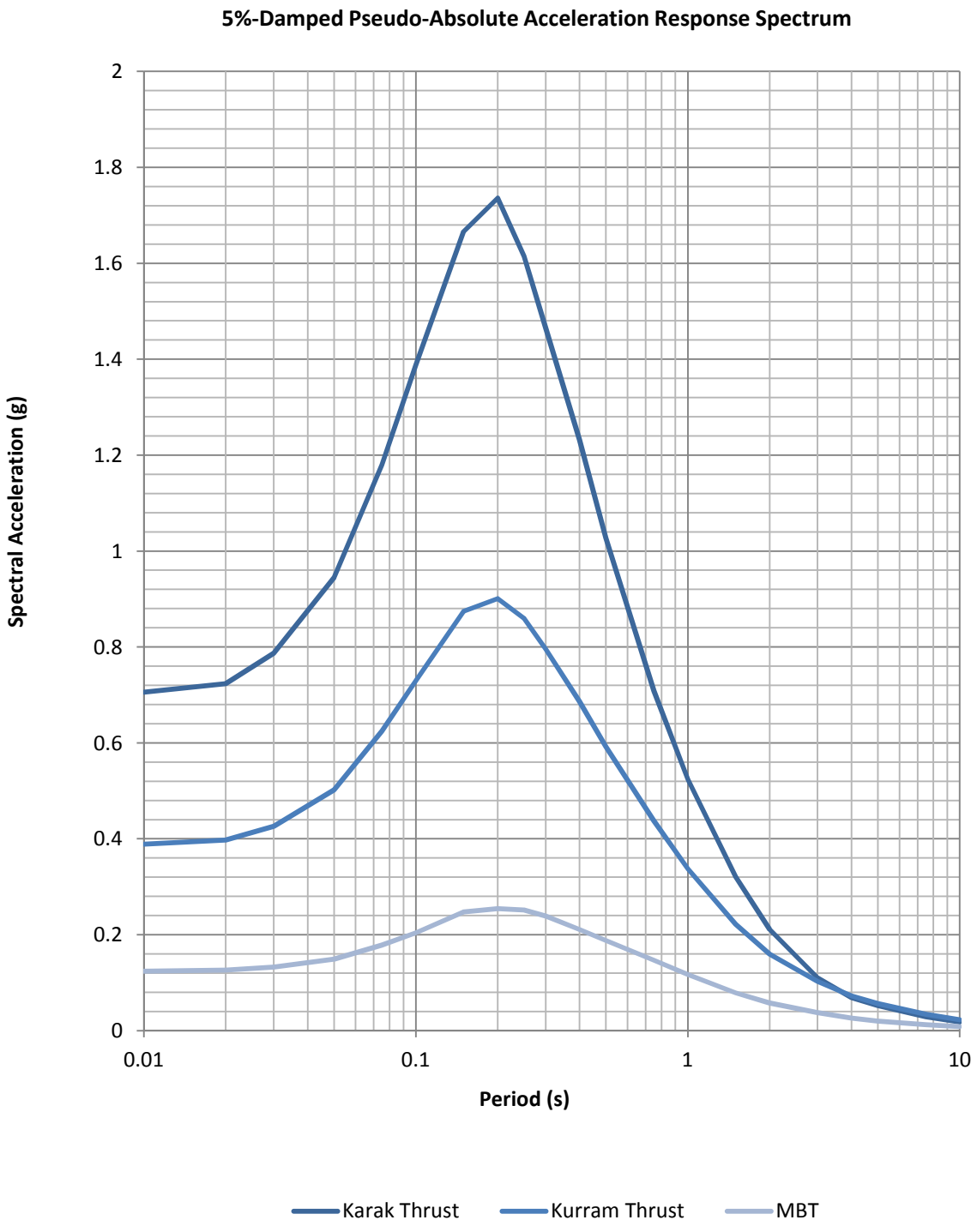

MWH®	Main Dam - Deterministic Hazard Results Response Spectrum - 50th Percentile	Figure 66

This Page Left Blank Intentionally

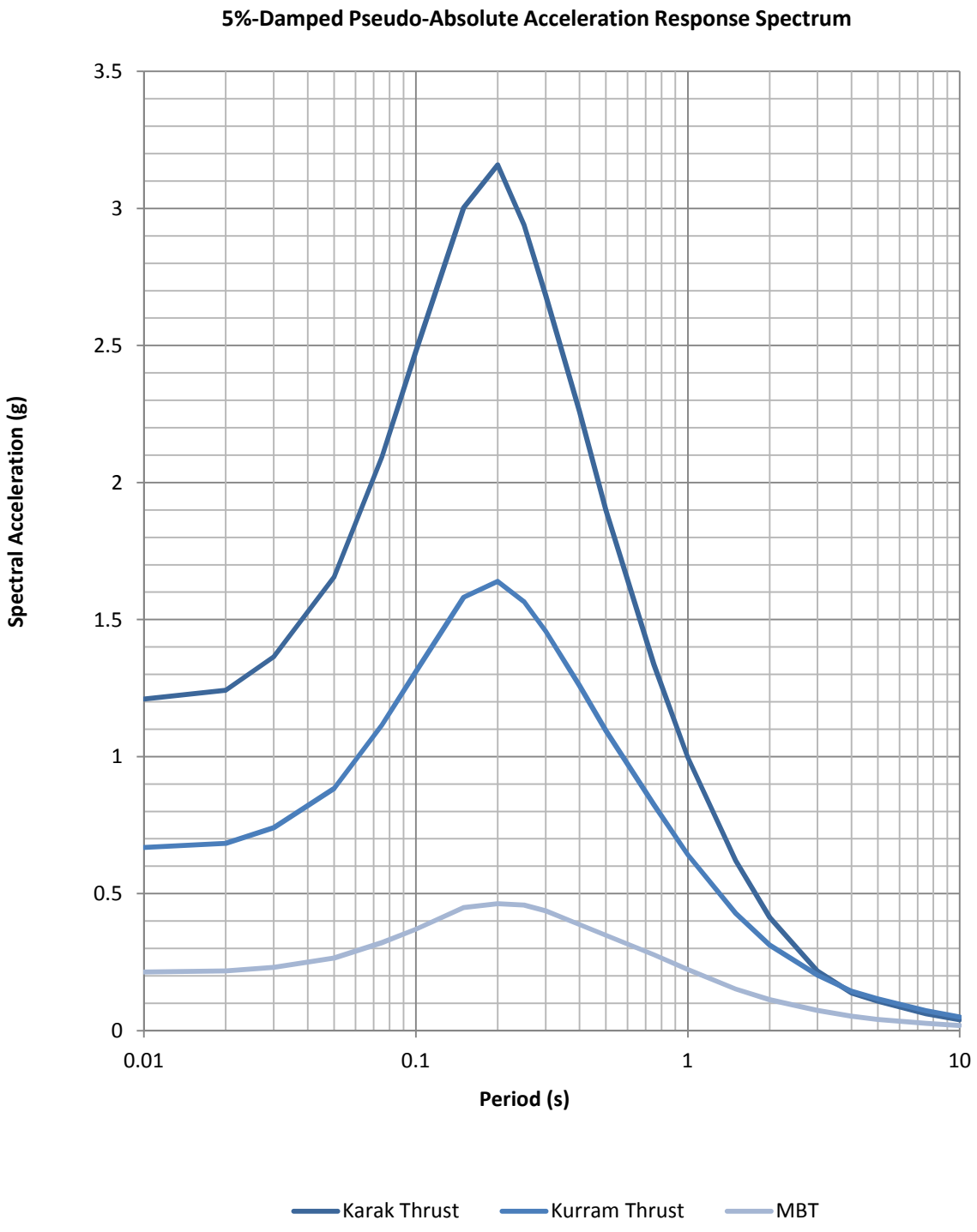

MWH®	Main Dam - Deterministic Hazard Results Response Spectrum - 84th Percentile	Figure 67

This Page Left Blank Intentionally

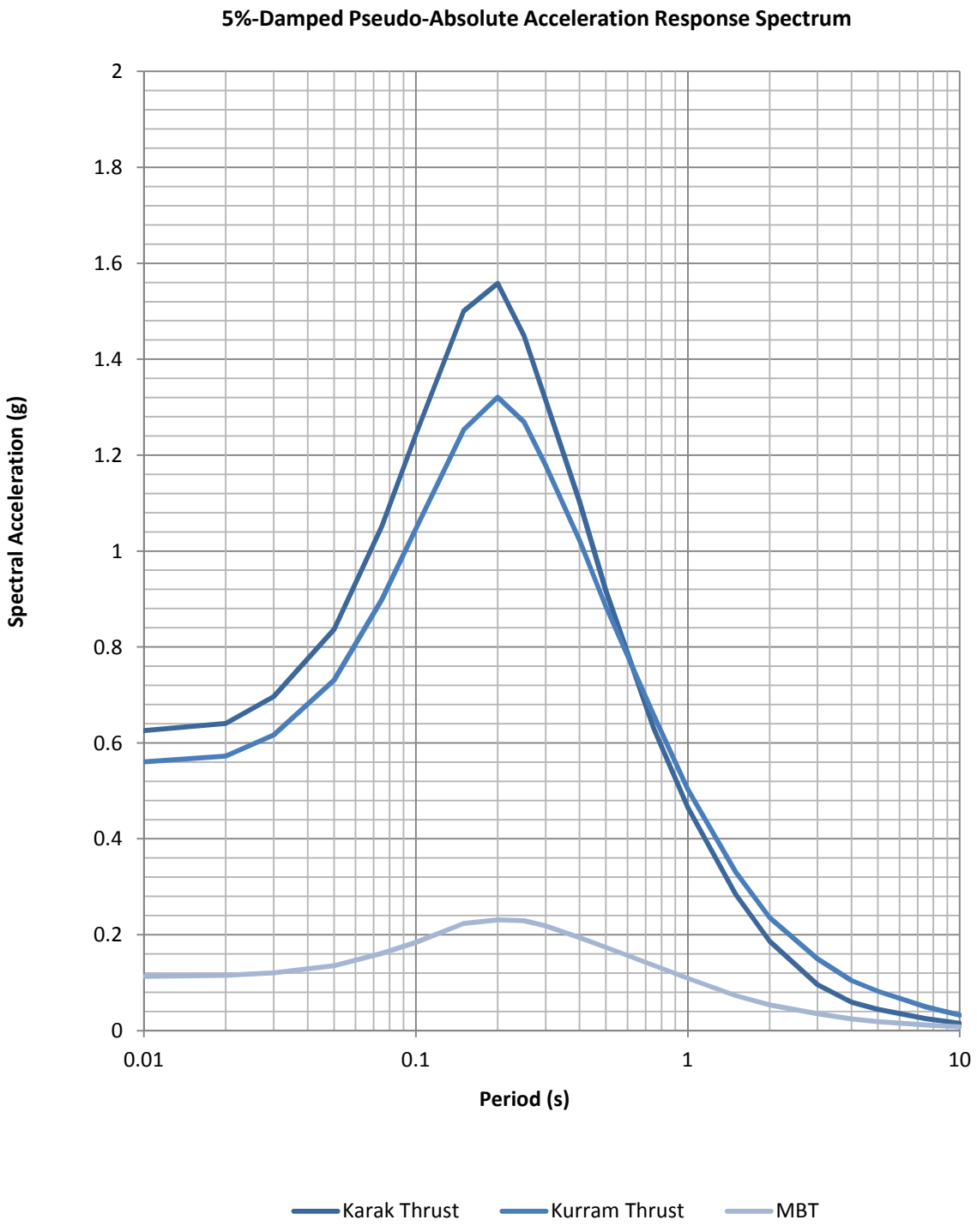

MWH®	Kaitu Weir - Deterministic Hazard Results Response Spectrum - 50th Percentile	Figure 68

This Page Left Blank Intentionally

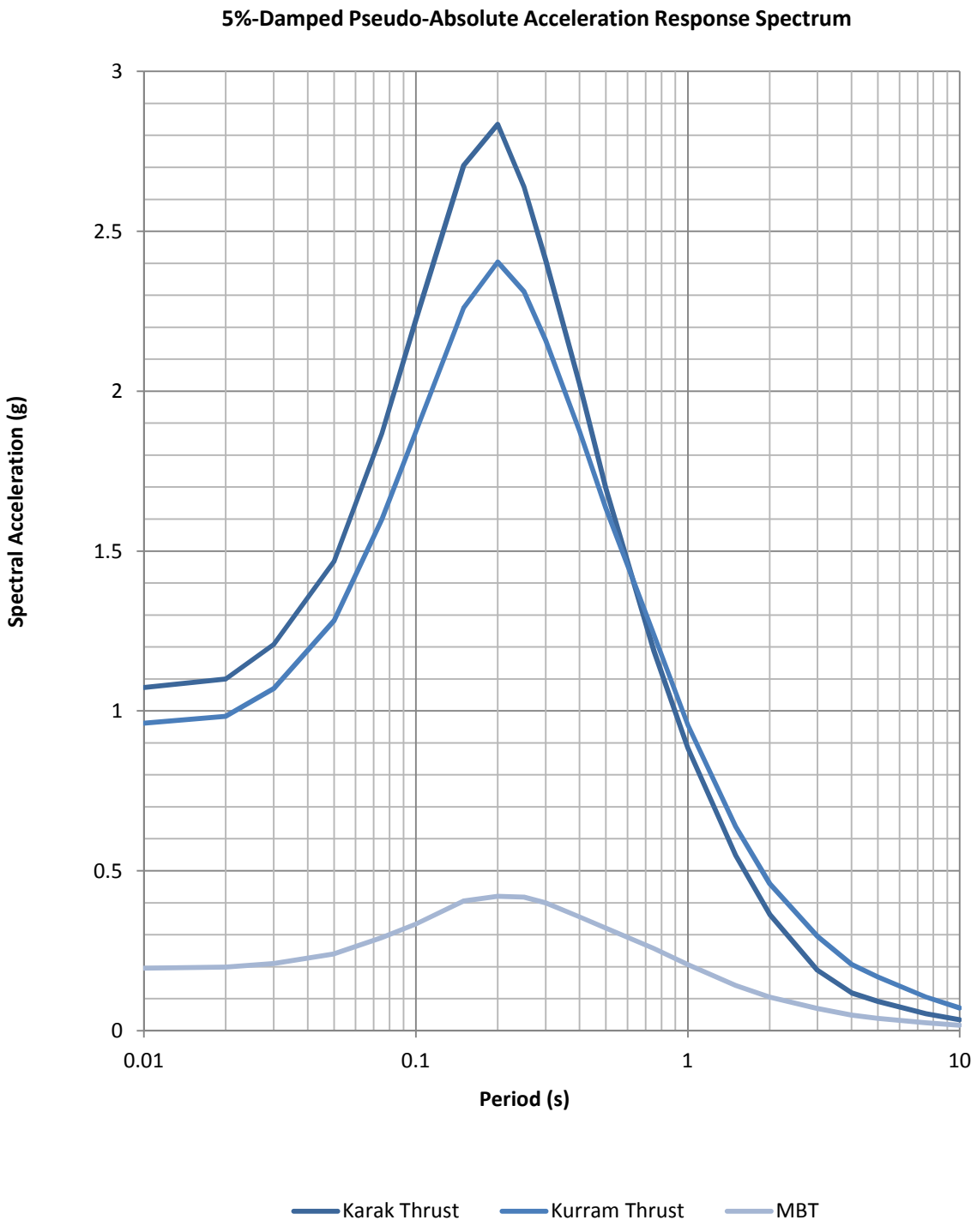

MWH®	Kaitu Weir - Deterministic Hazard Results Response Spectrum - 84th Percentile	Figure 69

This Page Left Blank Intentionally

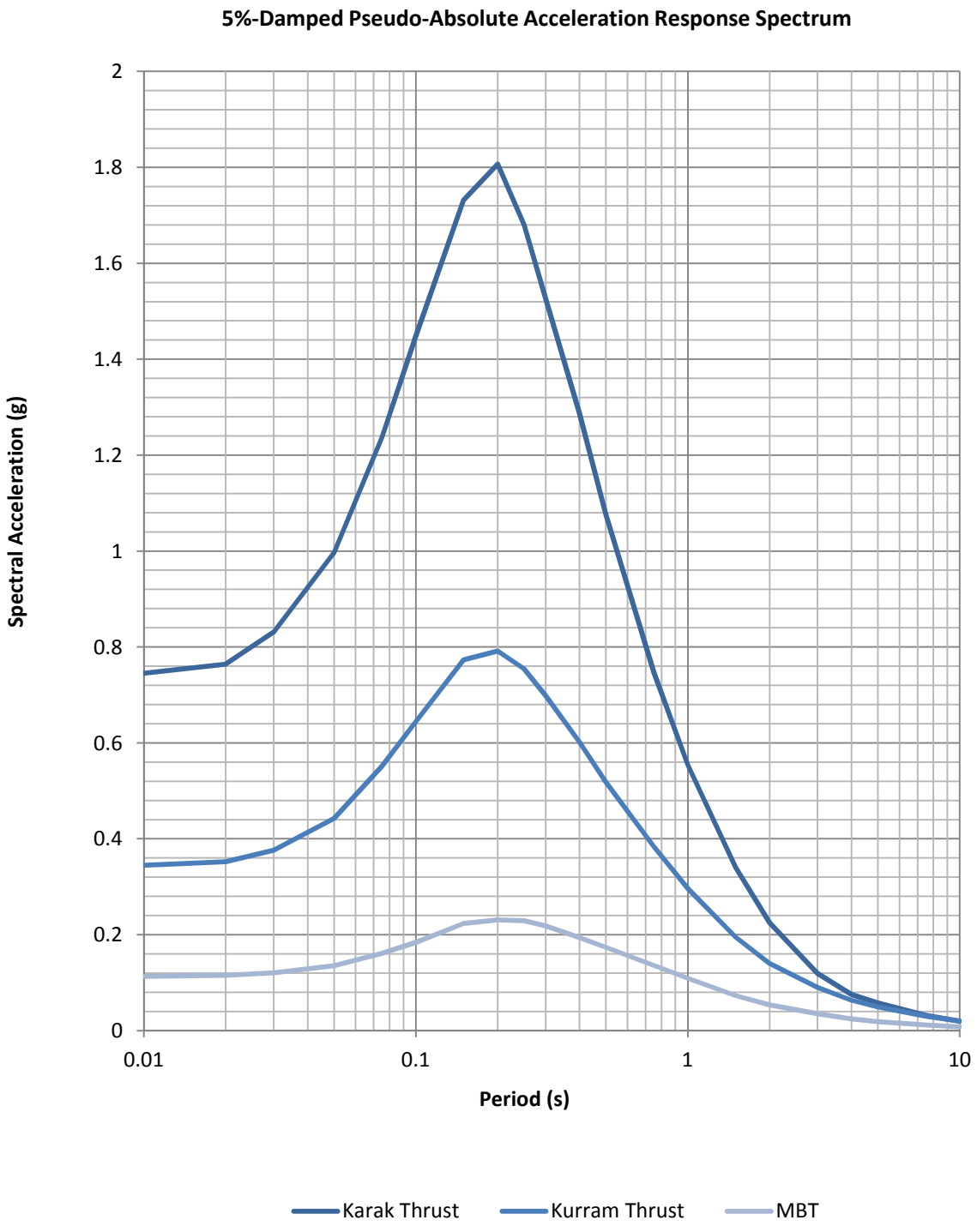

MWH®

Weir II - Deterministic Hazard Results
Response Spectrum - 50th Percentile

Figure 70

This Page Left Blank Intentionally

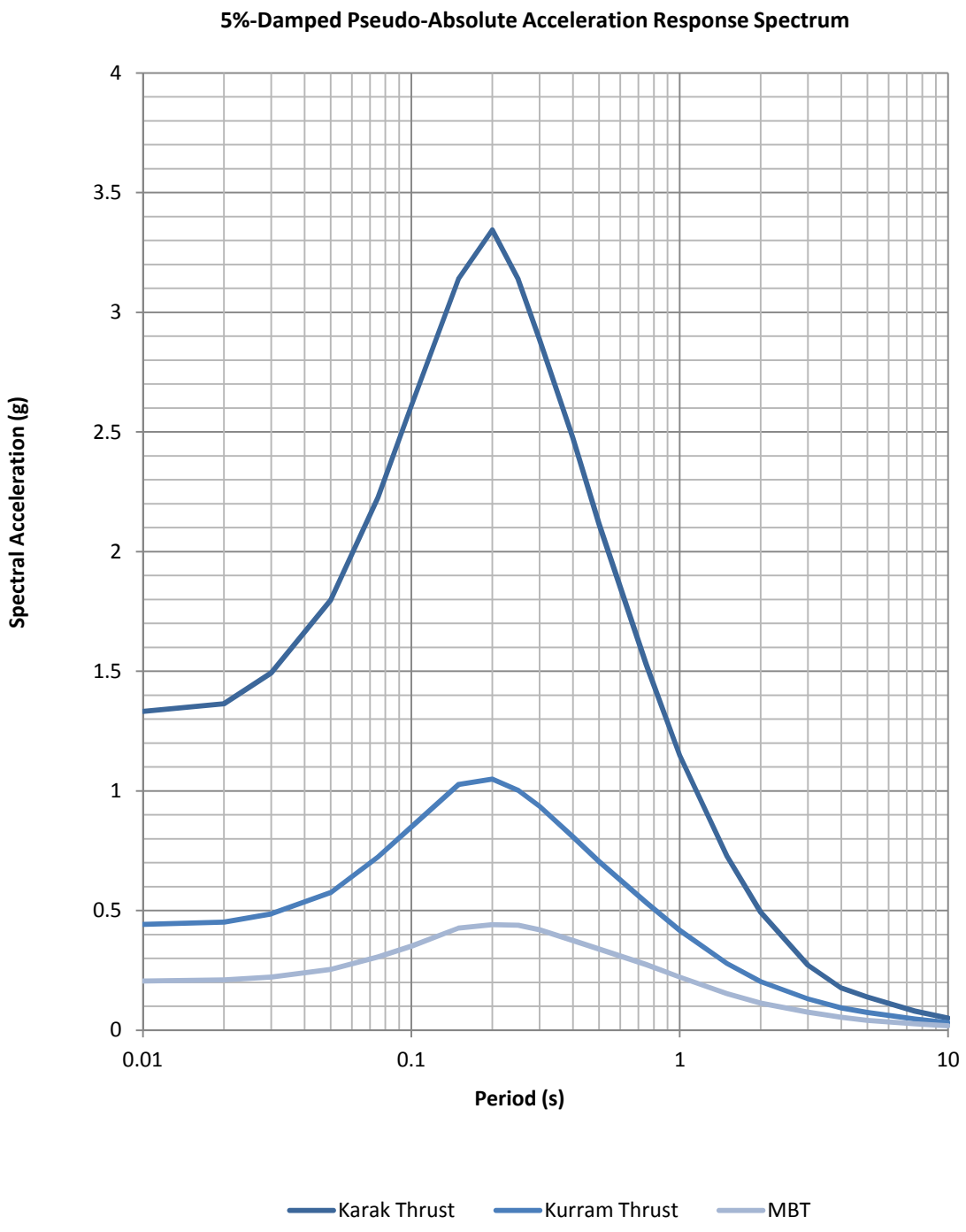

MWH®	Weir III - Deterministic Hazard Results Response Spectrum - 84th Percentile	Figure 71

This Page Left Blank Intentionally

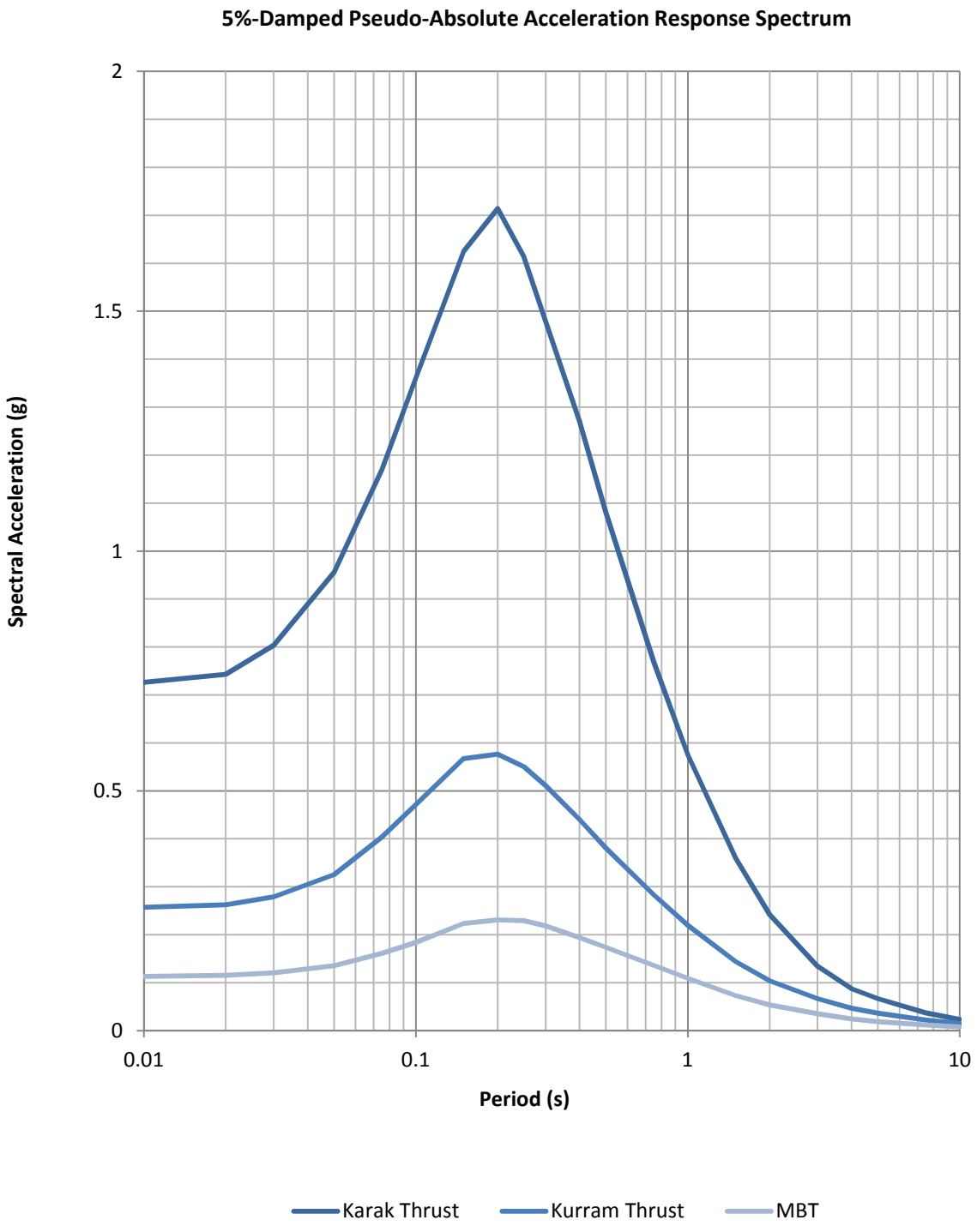

MWH®	Weir III - Deterministic Hazard Results Response Spectrum - 50th Percentile	Figure 72

This Page Left Blank Intentionally

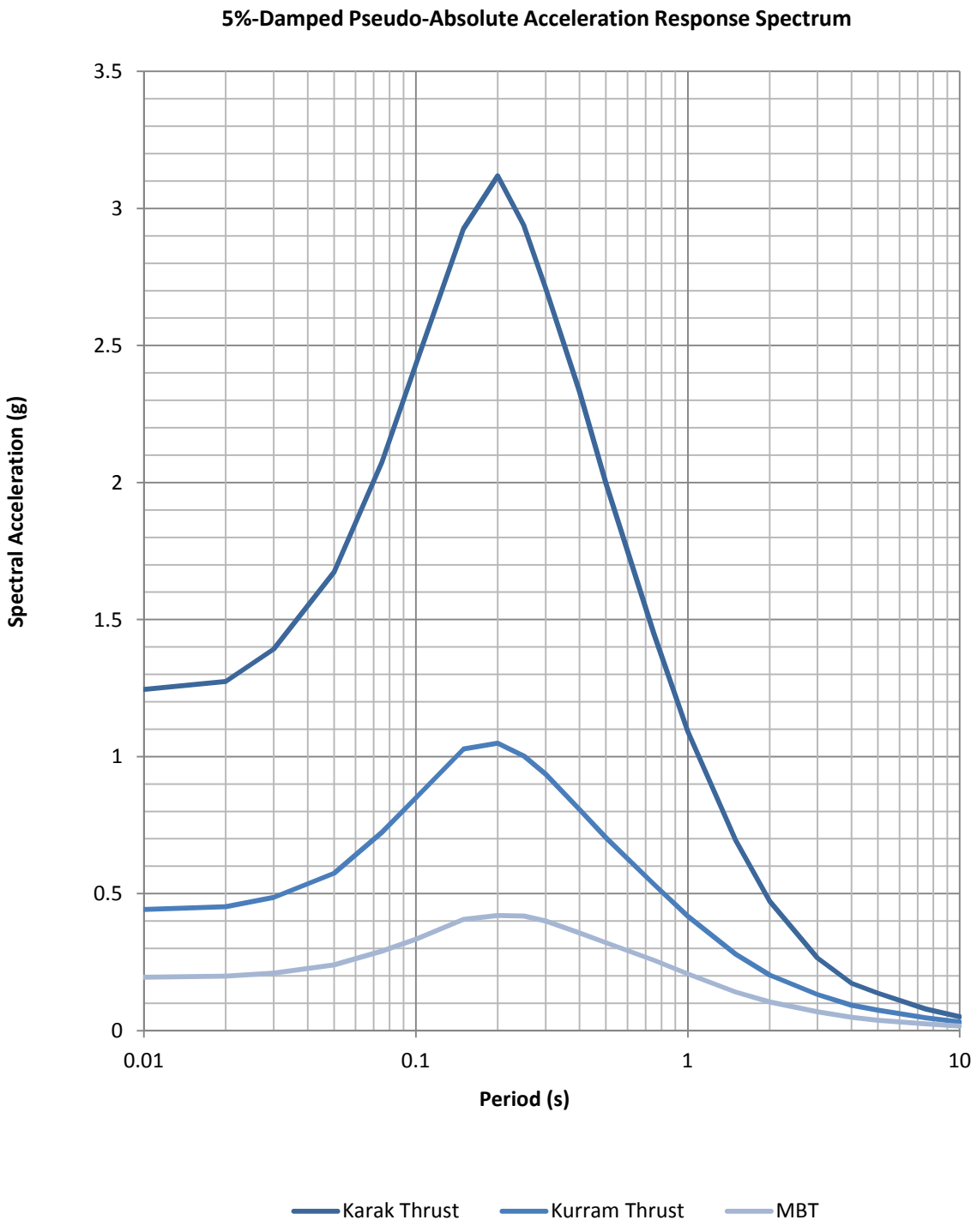

MWH®	Weir III - Deterministic Hazard Results Response Spectrum - 84th Percentile	Figure 73

This Page Left Blank Intentionally

Annexure – A Chronological Catalogue of Non-Instrumental (Intensity) Data

This Page Left Blank Intentionally

CHRONOLOGICAL CATALOGUE OF NON-INSTRUMENTAL (INTENSITY) DATA

Sr. No.	Year	Date	Description	Estimated Intensity MM	Source
1	4	BC	Aristobulus of Cassandreia, who accompanied Alexander on his expedition to India, points out that the country above the river Hydaspes (Jhelum) is subjected to earthquakes which cause the ground to open up so that even the beds of river are changed.	IX-X	Ambraseys
2	25	AD	A destructive earthquake in north-western Pakistan laid Taxila in ruins and caused wide spread havoc throughout the country side. The effects of this earthquake can still be seen among the excavated remains at Jandial, Sirkap and Dharmarajika. As a result of the earthquake new methods of buildings were introduced and the height of buildings was reduced from four to two storeys with special precautions to make the foundation secure.	IX-X	Q&J
3	50	AD	A destructive earthquake in north-central Afghanistan destroyed the city of Aikhanum on the east bank of the Oxus and the north bank of the Kokcha rivers.		Ambraseys
4	1505	Jul.06	The region north of Kabul was almost totally destroyed. In Kabul many houses collapsed and the walls and towers of the citadel as well as part of the city walls fell. Pagham was levelled to the ground and in Tibah most of the houses collapsed. The damage was particulalry severe along the foothills of Mount Raham, from Istarghij to Begtut. The earthquake was associted with large-scale faulting of the gorund running along the Pagham valley, with vertical displacements of many metres. Aftershocks continued for many months and the shock was felt as far as Agra. (Al-Asafi:934; Ferishta:183; Bada 'uni:i.319; Babar Nameh:170/247).		Ambraseys
5	1669	Jun.04	Strongly felt in Mandra	VI-X	Q&J
6	1669	Jun.23	An earthquake at Attock, a fissure 50 yards long was formed in the ground.	VIII-IX	Q&J
7	1831	Mar.	Peshawar & valley of Indus - Severe, extended from Peshawar to Dera Ghazi Khan, felt most at Dera band (Daraban) in the Suleiman range; men and camels unable to stand, rocks fell in many places, water forced from crevices in the plains.	Daraban VIII-IX Peshawar & D.G. Khan IV-VI	Q&J

CHRONOLOGICAL CATALOGUE OF NON-INSTRUMENTAL (INTENSITY) DATA

Sr. No.	Year	Date	Description	Estimated Intensity MM	Source
8	1832	Jan.22	Destructive, large-magnitude earthquake in Badakhshan; most of the villages and forts in the valleys of Kokcha, Sargolian and Varodj were destroyed and 50% of the inhabitants perished. The damae extended to Kalifgan and Jurm, where all houses were destroyed and many lives lost. The shock was felt in Lahore and Kabul where it caused panic. Radius of perceptibility about 1,000 km.		Ambraseys
9	1832	Feb. 21	Lahore, valley of Badakhshan, N.W. India huge masses of rock was thrown from the cliffs at many places chocking up valleys. Great part of population destroyed.	Lahore V-VI	
10	1842	Feb.19	Kabul, Peshawar At Kabul said to have lasted for 3 mts, several shocks, rocked the fouth in a frightful manner. At Peshawar very destructive, "earth-trembled like aspen leaf", several killed. At Ferozepur severe. At Ludhiyana north south, the hot springs of South (temp. 140 deg - 110 deg) become as cold as the ordinary wells, water diminished greatly and at times the springs were completely dry. These appearances continued for 25 days.	Kabul VI-VII Peshawar VI Ferozepur VI	Q&J
11	1853	Nov.	Strongly felt at Attock	VI	Q&J
12	1865	Jan.22	Slight damage and great panic in Peshawar; long duration.	V-VII	Q&J
13	1867	Nov.10	Damaging in Bannu	VII-VIII	Q&J
14	1868	Aug.11	Damaging in Peshawar; a portion of the fort was shaken down (official record).	VII-VIII	Q&J
15	1868	Nov.12	Violent shock felt in Lahore, Dera Ismail Khan and Attock, followed by many aftershocks which were felt throughout the Punjab.	Attock IV-VI & D.I. Khan IV-V	Q&J
16	1869	Mar.25	A large earthquake in the Hindukush, strongly felt at Kohat, Lahore, Peshawar and at Khojend and Tashkent; shock lasted 20 seconds.	Kohat, Lahore & Peshawar V	NESPAK
17	1869	Apr.	Peshawar - Part of fort shaken down (official record).	VII-VIII	Q&J

CHRONOLOGICAL CATALOGUE OF NON-INSTRUMENTAL (INTENSITY) DATA

Sr. No.	Year	Date	Description	Estimated Intensity MM	Source
18	1869	Dec.20	Rawalpindi - Shock said to have lasted for half a minute; cracked walls and caused all people to run out of houses. Attock - A series of shocks at intervals of about 20 sec. Lawrencepur - 1st shocks 15 sec others at 5 sec. interval. Campbellpur - For half an hour; buildings much damaged. Talagang - Not felt.	VII-VIII VII-VIII	Q&J
19	1874	Oct.18	Jabal al Siraj totally destroyed with heavy loss of life; Kuhistan and Golbahar ruined and many people killed. In Kabul 1,000 houses collapsed or damaged beyond repair; ground deformations at Kuhistan; many aftershocks; not widely felt.		
20	1875	Dec.12	Damaging in villages between Lahore and Peshawar where a number of people were killed.	VII-VIII	Q&J
21	1878	Mar.02	Damaging earthquake in the Punjab. At Kohat several houses, public buildings and portion of the wall of the fort fell. At Peshawar it caused damage to houses and city walls. Damaging at Attock, Abbottabad, Rawalpindi, Jhelum, Murree. Strongly felt at Bannu, Nowshera, Mardan, Lahore and Simla. Many aftershocks.	Peshawar, Kohat VII-VIII Attock VI-VII Lahore VI	Q&J
22	1883	Apr.	Damaging shock at Peshawar.	VI-VII	Q&J
23	1892	Dec.20	Chaman Earthquake: The greater portion of Baluchistan was shaken by this earthquake which did great damage to buildings, bridges, rail roads, and other structures. The earthquake was caused by movement of fault on the west flank of the Kohjak range of mountains passing along the North Western Railway between Shelabagh and Sanzal. The west or off valley side subsided about 8 -12 inches and shifted south- ward relatively to the east side a distance of 24 -28 inches as shown by the buck- ling and shortening of rails and pipes which crossed diagonally and by offsets of roads and irrigation channels. At Shelabagh, the damage to the railway buildings was very severe. Chaman town, which was on the fault line, was destroyed.	VIII-IX at Chaman, VII at Sanzal	Q & J

CHRONOLOGICAL CATALOGUE OF NON-INSTRUMENTAL (INTENSITY) DATA

Sr. No.	Year	Date	Description	Estimated Intensity MM	Source
24	1893	Nov.03	Slight damage at Peshawar, Nowshera, felt throughout the Punjab	VI-VII	Q&J
25	1924	Oct.13	Caused panic in Kabul, V+.		
26	1934	Jul.12	The district of Badlakohan in Afghanistan was heavily damaged and the Spin area was destroyed.		
27	1935	May. 30	The 1935 Quetta earthquake occurred on May 30, in Quetta, Pakistan. It is estimated that there were 30,000 fatalities (USGS, 2013). Ambrasey & Bilham (2009) estimate the magnitude of the event to be MS=7.7. The towns of Quetta and Mastung were totally destroyed along with 100 villages (Ambrasey & Bilham, 2009). It is believed that this rupture was associated with the zone of faults that lie along the east edge of the Chiltan range with extends to the south passing the towns of Mastung and Kalat. The mechanism was most-likely a left lateral strike-slip event (Ambrasey & Bilham, 2009).	Ms=7.7	Ambrasey & Bilham, 2009 / USGS, 2013
28	1940	March 19	Felt in Kabul, .	V+	
29	1940	May 27	Felt in Peshawar.		
30	1943	Feb.28	Widely-felt shock, in Kabul and in Samarkand and Bukhara.		
31	1945	Jun.27	Felt in Peshawar	IV	NESPAK
32	1953	Mar.01	Slight damage in Campbellpur.	VI-VII	Q&J
33	1955	23-Aug	Leiah Earthquake: An earthquake of moderate intensity shook all districts of Multan Division and Bahawalpur. Several houses in villages near Leiah were damaged. The buildings at Leiah also suffered damage. The epicenter was very close to Leiah.		
34	1956	July 14	Felt in Kabul and Jalalabad.		
35	1956	Sept.16	Destructive in the Ghazi district in Afghanistan where many villages were destroyed and animals lost. The damage was equally serious at Said Karem. Caused panic at Kohat Strongly felt at Parachinar, Parwan, Loger, Ghazi, Nazerajat, Beshud, Makur, Rawalpindi and Srinagar. Radius of perceptibility about 450 km.	Rawalpindi V	NESPAK

CHRONOLOGICAL CATALOGUE OF NON-INSTRUMENTAL (INTENSITY) DATA

Sr. No.	Year	Date	Description	Estimated Intensity MM	Source
36	1957	Apr.04	Damaging in Gorband and in the Panjshir valley in Afghanistan. Severe in Charikar, Jabal as-Siraj, Ghorband, Gulbahar, Saighan, Doab, Bamiyan and Kahmard; felt in Kabul.		
37	1960	Feb.18	Felt in Kabul, and caused damage at Appsigh. (35.8 N - 71.3 E)		
38	1962	Aug.02	Felt at Rawalpindi	IV-VI	Q&J
39	1963	Jul.14	Felt strongly, without damage at Kabul, Jalalabad and Parwan.	IV+	
40	1966	Jan.11	Felt at Risalpur	IV	NESPAK
41	1966	Jan.19	Damaging in the Bashgal valley; at Bargematal and Patsigram houses cracked and a number of houses were ruined mainly from rockfalls. Further north at Panigir the shock was severe with rockfalls (35.5 N - 71.4 E) VI. Strongly felt at Appsigh, Kabul and Munjan as well as in Peshawar.		
42	1966	Feb.02	Strongly felt around Abbottabad and caused minar damage at Havelian. Felt at Rawalpindi, Islamabad. Abbottabad, Taxila. The shock was also felt at Muzaffarabad and Gujar Khan.	Abbottabad VI Islamabad V Taxila VI	Q&J
43	1966	May 11	Felt in Kabul.		
44	1971	May 09	Felt in Kabul and North Pakistan.		
45	1972	Jan 20	Widely felt in NWFP and at Warsak.		
46	1972	Jan. 28	Strongly felt at Kabut	V	
47	1972	Feb. 21	Widely felt in Kabul , Mangla .	Kabul V, Mangla III	
48	1972	Mar. 10	Felt in Kagan valley and at Rawalpindi.		
49	1972	Apr. 17	Felt at Rawalpindi		
50	1972	May 17	Felt at Peshawar and Rawalpindi.		
51	1972	July 24	Destructive shock in Afghanistan; in the region of Ishkamish 11 killed, 15 injured; major property damage; stronly felt in the Bashgal and Shukurigal valleys. Many aftershocks.		
52	1972	Sep. 27	Felt at Abbottabad and Rawlapindi.		
53	1972	Oct. 01	Felt at Rawalpindi.		
54	1972	Nov. 03	Felt in Kabul	V.	
55	1972	Dec. 28	Felt at Warsak	V.	
56	1973	Jun. 06	Felt in Kohat	III	
57	1973	Sep. 27	Felt at Kohat	III	
58	1973	Oct. 17	Felt at Risalpur, Rawalpindi, Peshawar	II	

CHRONOLOGICAL CATALOGUE OF NON-INSTRUMENTAL (INTENSITY) DATA

Sr. No.	Year	Date	Description	Estimated Intensity MM	Source
59	1974	May13	Felt at Warsak, Peshawar, Sargodha, Landikotal, Kohat , Rawalpindi, Lahore.	Kohat IV	
60	1974	July30	Felt at Peshawar, Warsak , Lahore, Mirpur	Warsak III, Mirpur II	
61	1978	May 07	Felt widely in Punjab and NWFP provinces. Some damage at Peshawar and Chitral.	Mangla IV Tarbela VI	WAPDA
62	1980	Feb.12	Felt widely in the areas of Punjab and NWFP.	Mangla IV Tarbela V	WAPDA
63	1983	Dec 31	Felt widely in the areas of Punjab and NWFP. Damages at Peshawar, Chitral and many northern areas. Some damage near Tarbela also. Felt in parts of Afghanistan also.	Chitral VII Peshawar VI Rawalpindi V, Tarbela V Mangla III	WAPDA
64	1996	Apr.04	Felt widely in the areas of Punjab and NWFP. Some damages at Peshawar, Chitral and northern areas. Some damage near Tarbela also. Felt also in parts of Afghanistan.	Chitral VI Peshawar V Rawalpindi IV Mangla III Lahore & Jhelum III	WAPDA
65	2005	Oct.08	Kashmir Earthquake: Epicenter near Muzaffarabad, most destructive earthquake, killed more than 80,000 people in Kashmir, Balako and Batagram.	Balakot XI Muzaffarabad IX-X Mansehra VIII Islamabad VII	NESPAK

Q&J - Quittmeyer & Jacob (1979), Historical and modern seismicity of Pakistan, Afghanistan, northwestern India and southeastern Iran, BSSA, Vol. 69, No 3.

Ambraseys N, Lensen G. and Monifer A. (1975), The Patan earthquake of 28 December 1974, UNESCO Technical Report.

NESPAK - National Engineering Services Pakistan (Pvt.) Ltd.Various Reports.

Ambraseys, N., & Bilham, R. (2000). *A note on the Kangra Ms = 7.8 earthquake of 4 April 1905.* Current Science 79.

US Geological Survey. (2013, March 6). Historic World Earthquakes. Retrieved July 9, 2013, from US Geological Survey: http://earthquake.usgs.gov/earthquakes/world/historical_country.php

WAPDA - Water and Power Development Authority-Mangla Seismicity Progress Reports.